KAUNAS UNIVERSITY OF TECHNOLOGY PANEVEZYS INSTITUTE
PANEVEZYS TECHNOLOGY AND SCIENCE PARK
WARSAW MOTOR TRANSPORT INSTITUTE
TALLINN UNIVERSITY OF TECHNOLOGY
RIGA TECHNICAL UNIVERSITY

INTELLIGENT TECHNOLOGIES IN LOGISTICS AND MECHATRONICS SYSTEMS

ITELMS'2010

PROCEEDINGS OF THE 5TH INTERNATIONAL CONFERENCE

EDITED BY Z. BAZARAS AND V. KLEIZA

June 03-04, 2010
Panevėžys, Lithuania

TECHNOLOGIJA
KAUNAS • 2010

CONFERENCE IS ORGANIZED BY

Kaunas University of Technology Panevezys Institute
Panevezys Technology and Science Park
Warsaw Motor Transport Institute
Tallinn University of Technology
Riga Technical University

CONFERENCE IS SUPPORTED BY

State Fund of Science and Study of Lithuania

The proceedings of the 5th International Conference INTELLIGENT TECHNOLOGIES IN LOGISTICS AND MECHATRONICS SYSTEMS contain selected papers.

All papers were reviewed.

The style and language of authors were not corrected. Only minor editorial corrections have been carried out by the Publisher.

CONFERENCE SCIENTIFIC COMMITTEE

CHAIRMAN
Prof. Z. Bazaras, Kaunas University of Technology, Lithuania

SCIENTIFIC SECRETARY
Prof. V. Kleiza, Kaunas University of Technology, Lithuania

MEMBERS
Dr. G. Badenes, Institute of Photonic Sciences, Spain
Prof. P. Balckars, Riga Technical University, Latvia
Prof. J. Bareišis, Kaunas University of Technology, Lithuania
Prof. P. Castro, Porto University, Portugal
Prof. J. Furch, Brno University of Defense, Czech Republic
Dr. V. Hutsaylyuk, Military University of Technology, Poland
Prof. I. Karabegović, Bosnia and Herzegovina
Prof. J. Laugis, Tallinn University of Technology, Estonia
Prof. A. Levchenkov, Riga Technical University, Latvia
Dr. M. Litwin, Motor Transport Institute, Poland
Prof. V. Ostasevicius, Lithuania
Prof. Ribickis, Riga Technical University, Latvia
Prof. M. Sitarz, Silezian Technical University, TRANSMEC, Poland
Prof. A. Sladkowsky, Silezian Technical University, Poland
Prof. D. Sprečić, Bosnia and Herzegovina
Dr. Ch. Tatkeu, Transport Electronics and Signal Processing Laboratory, France
Prof. V. Tilipalov, Kaliningrad State Technical University, Russia
Prof. B. Timofeev, St. Petersburg State Polytechnic Institute, Russia
Dr. D. Vinnikov, Tallinn University of Technology, Estonia

LOCAL ORGANIZING COMMITTEE
R. Bukėnas
V. Narbutas
E. Patapienė
Dr. D. Susnienė
Dr. A. Tautkus
Dr. D. Vaičiulis

PREFACE

The first (2006) and second International Workshops “Intelligent Technologies in Logistics and Mechatronics Systems ITELMS” were held at Riga Technical University. The 3rd international workshop ITELMS'2008 was held at Kaunas University of Technology Panevezys Institute on 22 - 23 May, 2008. The international conferences ITELMS'2009 and ITELMS'2010 continues three year tradition and takes place at Kaunas University of Technology Panevezys Institute.

The aims of the Conference are to share the latest topical information on the issues of intelligent technologies in logistics and mechatronics Systems. The papers in the Proceedings presented the following areas:

Intelligent Logistics Systems
Multi Criteria Decision Making
Composites in Infrastructures
Automotive Transport
Intelligent applications of solid state physics
Intelligent Mechatronics Systems
Mechanisms of Transport Means and their Diagnostics
Railway Transport
Transport Technologies
Modern Building Technologies

In the invitations to Conference, sent year before the Conference starts, the instructions how to prepare reports and manuscripts provided as well as the deadlines for the reports are indicated.

A primary goal of Conference is to present the highest quality research results. A key element in attiring goal is the evolution and selection procedure developed by the Conference Scientific Committee.

All papers presented in Conference and published in Proceedings undergo this procedure. Instruction for submitting proposals, including requirements and deadlines, are published in Call for Papers in the http://www.ktu.lt/lt/apie_renginius/konferencijos/2010/meniu.asp. Paper proposals must contain sufficient information for a trough review. All submissions to determine topic areas are directed to appropriate Topic Coordinators. The Topic Coordinators review the submissions much them to the expertise according to the interests and forward them to selected reviewers. At least two reviewers examine each submission in details.

Selection of papers for the Conference is highly competitive, so authors should assure their submissions to meet all Conference Scientific Committee’s requirements and to be of the highest possible quality.

All Conference participants prepare manuscripts according to the requirements that make our Proceedings to be valuable recourse of new information which allows evaluating investigations of the scientists from different countries.

Prof. Z. Bazaras
Prof. V. Kleiza

Contents

Proceedings of 5th International Conference ITELMS'2010

Comparison of Five National Noise Emission Calculation Methods for Rail Traffic

A. Baranovskii

Institute of railway transport, Riga technical university, Indrika street 8a, Riga, Latvia, LV-1004, email: andrejs.baranovskis@rtu.lv

Abstract

This paper contains comparison of five European national noise emission calculation methods for rail traffic, including RMR – interim calculation method for EU.
KEY WORDS: *railway, rolling stock, noise, level, measurement, calculation, prediction method.*

1. Introduction

During last few decades the development of surface transport has lead to rapid increase of noise level, especially in the areas of high-speed motorways and railways.

Accordingly to the results of French, Dutch and German scientist estimation (Lambert and others, 1998) around 120 million people in Europe (more than 30% of total population) incur the influence of louder than 55 dBA (equivalent A-weighted) transport noise, and 50 million people incur the influence of louder than 65 dBA transport noise. Thereby, significant part of Europe's population suffers from transport noise which affects people's health and life quality.

Therefore, during last years European Union has paid big attention to the problems of noise and vibration experimental investigation on railway transport, railway noise propagation prediction, noise mapping and development of noise and noise source reduction methods.

In many European countries national methods for railway rolling stock noise propagation prediction were developed already. Yet, many countries still don't have their own national methods.

Before development of new method for railway rolling stock noise propagation prediction it is useful to try to adopt and use one of the existing ones.

This paper provides description and comparison of the following national railway rolling stock noise propagation prediction methods:

RMR (the Netherlands, interim model for EU), Schall 03 (Germany), ON S5011 (Austria), NMT (Nordic countries), CRN (United Kingdom).

In general, the calculation procedure can be divided into the following parts: train category description, location of source(s), basic sound parameters, reference distance, speed influence, track conditions.

2. Train Categories

2.1. RMR

In RMR trains are divided into the following railway vehicles categories (these are primarily differentiated on the basis of drive unit and wheel brake system):

2.1.1. Brake-padded passenger trains (also electrical motor mail vehicle).
2.1.2. Disk-braked and brake-padded passenger trains.
2.1.3. Disk-braked passenger trains.
2.1.4. Brake-padded freight trains.
2.1.5. Brake-padded diesel trains.
2.1.6. Diesel trains with disk-brakes.
2.1.7. Disk – braked urban subway and rapid tram trains.
2.1.8. Disk-braked Inter City and slow trains.
2.1.9. Disk-braked and brake-padded high speed trains.
2.1.10. Provisionally reserved for high speed trains of the ICE-3(M) (HAST East) type.

Vehicles not mentioned here are allocated to the next appropriate category based on their drive unit, wheel brake system or maximum speed.

2.2. ON S5011

In ON S5011 four train categories are considered: Intercity trains with block brakes, disc brakes, combinations; railcar fast trains 4010; tandem railcars 4020; goods trains with 2 locomotive types (electric, diesel).

No further specifications of train length or brake types.

2.3. SCHALL 03

In SCHALL 03 are considered 14 train categories: ICE, EC/IC, IR, D/FD-Zug, Eilzug, Nahverkehrszug, S-Bahn (Triebzug), S-Bahn (Berlin), S-Bahn (Hamburg), S-Bahn (Rhein-Ruhr), Guterzug (Fernv.), Guterzug (Nahv.),

U-Bahn, Strasenbahn/Stadtbahn with specific values of maximum speed, average train length and percentage of wagons with disc brakes in the train.

2.4. NMT

In NMT typical trains from Norway, Sweden and Finland are considered.

Norway: standard passenger train, B 65 (passenger), B 69 (passenger), B 70 (passenger), standard goods train all with electric engines.

Sweden: standard passenger train, fast passenger train X2, passenger train X10, standard goods train, standard goods train with diesel engine, if nothing specified, with electric engines.

Finland: passenger train Sm, Passenger train Sr1, standard goods train.

2.5. CRN

Passenger trains with tread brakes, disc brakes, 2, 4, 6 or 8 axles; freight trains with tread brakes, disc brakes, 2 or 4 axles; diesel locomotive with steady speed, under full power; electric locomotives.

Location of sources:

RMR: In RMR up to four different sources are considered. There are two different sources for train categories 1 to 8:

At the level of the railhead and 0.5 m above railhead.

The source heights for category 9 are 0.5 m, 2.0 m, 4 m and 5 m above railhead.

SCHALL03: the source height is assumed to be at the level of the railhead.

ON S5011: the source height is assumed to be 0.3 m at the level of the railhead.

NMT: each octave band has its own individual source height as shown in the following table:

Table 1

Location of sources NMT

Octave band, Hz	Source height, m
63	2
125	1.5
250	0.8
500	0.3
1000	0.4
2000	0.5
4000	0.6

CRN: the source height is assumed to be at the level of the railhead [1].

3. Basic Sound Parameter, Reference Distance, Speed Influence

3.1. RMR

For the RMR the basis of the calculation is the sound power level per meter rail length for each source and each octave band between 63 Hz and 8 kHz as logarithmic function of train speed. For emission measurements the microphone distance is 7.5 m and 1.2 m above railhead. If sources above 0.5 m height have to be considered a second microphone height at 3.5 m must be added. The time signal is registered as an equivalent unweighted octave spectrum and third-octave spectrum, total A-weighted and unweighted levels. The measurement time T is also registered, which is the passage time including the 10 dB-down flanks. For a group of wagons within a train, the buffer-to-buffer time (speed/length) is taken.

The train speed is measured and must be within 5 km/h of the nominal speed for speeds below 100 km/h and 10 km/h for speeds above 100 km/h.

For vehicles with traction or aerodynamic sources at heights of 2 m and above, such as locomotives and high speed trains, additional measurements are carried out at 4 m of the track axis at a height of 1.2 and 4.5 m (± 0.2 m); only at one cross-section.

The condition of the track should be as good as possible to minimise its influence.

The emission is calculated from these measurement results for each noise source and each octave band. In this step also the A-weighting is applied. The emission results are then approximated by logarithmic speed functions of the form

$$E = a + b \log(v/v_0), \tag{1}$$

where a and b are correction coefficients; v is train speed, km/h; v_0 is reference speed, 1 km/h.

The emission represents the sound power of the considered source for one train per hour under reference track conditions. In cases where the deviations of the measurement results are higher than 1 dB, the speed range is split into different ranges and the regression calculation is done for each range separately.

To calculate the emission that is representative for the considered time interval “corrections” for the number of trains, type of locomotive (electric or diesel), the brake, the rail roughness, the wheel roughness and the type of superstructure have to be applied to the basic speed dependent emissions.

RMR provides also a simplified calculation method for the overall A-weighted emission. The basic formula is as follows:

$$E = 10 \lg\left(\sum_{c=1}^{y} 10^{E_{nr,c}/10} + \sum_{c=1}^{y} 10^{E_{r,c}/10} \right) \tag{2}$$

where $E_{r,c}$ is emission term for braking trains; c is train category; $E_{nr,c}$ is emission term for non braking trains; y is total number of categories present.

The emission values per rail vehicle category are determined from:

$$E_{nr,c} = a_c + b_c \lg(v_c / v_0) + 10 \lg(Q_c / Q_0) + C_{b,c} \tag{3}$$

$$E_{r,c} = a_{r,c} + b_{r,c} \lg(v_c / v_0) + 10 \lg(Q_{r,c} / Q_0) + C_{b,c} \tag{4}$$

where Q_c is average quantity of non braking trains of the considered rail vehicle category, h^{-1}; $Q_{r,c}$ is average quantity of braking trains of the considered rail vehicle category, h^{-1}; Q_0 is reference value, 1 h^{-1}; v_c is average speed of rail cars, km/h; v_0 is reference speed, 1 km/h; b is track type.

The standard regression coefficients are given in table 3.

Trains are considered "braking" when the brake system is active.

To determine the emission value E, the defined train categories are used, distinguishing between braking and non-braking trains.

3.2. SCHALL03

The basic emission value is the equivalent noise level per train per hour at a distance of 25 m and a height of 4 m above railhead. 25 m is also the distance for measurements. To get the equivalent sound level for the reference time intervals (day/night) corrections have to be added to consider different train classes, train length and superstructure. Rail or wheel roughness or brake influence is not taken into account.

The basis emission is given by the following formula:

$$L_m = 10 \log(l / l_0) + 10 \log(5 - 4\,p) + 20 \log(v / v_0) - 9 \tag{5}$$

where l is the length of the train, m; p is the percentage of wagons with disk brakes in fractions of 1; v is train speed, km/h; v_0 is reference speed, 1 km/h; l_0 is reference train length, 1 m.

The superstructure is ballast with wooden sleepers. No spectral calculation is foreseen.

In contradiction to the other calculation methods no individual speed influence is considered.

Table 2

Standard regression line coefficients as function of railway category c (RMR)

Category	Non-braking trains		Braking trains	
	a_c	b_c	$a_{r,c}$	$b_{r,c}$
1	14.9	23.6	16.4	25.3
2	18.8	22.3	19.6	23.9
3	20.5	19.6	20.5	19.6
4	24.3	20.0	23.8	22.4
5	46.0	10.0	47.0	10.0
6	20.5	19.6	20.5	19.6
7	18.0	22.0	18.0	22.0
8	25.7	16.1	25.7	16.1
9	22.0	18.3	22.0	18.3

3.3. ON S5011

The basic emission parameter is the sound power level per meter rail. As for the RMR method the calculation is executed for octave bands separately using the same frequency range (63Hz to 8kHz).

Measurements are carried out in 7.5 m and 15 m distance from the source (straight line between source and microphone) and 4 different heights.

The emission values are related to a ballast superstructure with wooden or concrete sleepers and rails in good conditions. A correction for rail or wheel roughness is not foreseen.

The approach is similar to the RMR but there is only one source considered and no other influencing parameter.

3.4. NMT

Also the NMT is based on the sound power levels per meter track in octave bands between 63 Hz and 4000.

The sound power levels are calculated from measurements of sound exposure levels (SEL) for a given train type and track type. The measurements have to be carried out in different speed intervals and octave bands between 63 and 4000 Hz. The measurement distance is between 7.5 m and 30 m from the track centre line. The full height of both rails must be visible from the measuring position, the elevation angle should be less than 20°.

The measurement results are then normalised to a reference distance of 10 m and a height of 2 m. Corrections for ground effects (in octave bands), train length and A-weighting have to be applied during this normalisation process. The sound power levels per meter track can then be calculated by adding 16 dB to the SEL.

Then approximation functions for the results at different speeds are calculated using logarithmic speed function of the following form:

$$L_w = a + b \log(v / v_0), \tag{6}$$

where v is the train speed, km/h; v_0 is reference speed, 100 km/h; a and b coefficients are tabled for each train and each octave band.

Finally L_w will be corrected for track conditions. The 24 h energy equivalent noise level L_{eq}, which is one of the noise indicators of the NMT is then calculated by summarising the contributions of each train during the 24 h time period and by applying all the corrections necessary to consider the propagation from the source to the receiver.

Besides the equivalent noise level a second noise indicator for the maximum noise level at a given receiver is calculated. This indicator is based on the energy average over the maximum range of the instant noise level signal during the passage of a train. This value is then transformed into a power level per meter track in an analogue way as for the equivalent noise level.

3.5. CRN

CRN aims to predict either daytime or night time equivalent A-weighted noise level. CRN mainly works with the sound exposure level for each train which is converted, after allowances for distance, ground effect, reflections, gradient, source enhancements (e.g. by bridges), angle of view, screening and the number of trains, into the required A-weighted equivalent sound level.

The reference SEL for a train depends on its speed and is predicted by:

$$\mathrm{SEL}_{ref} = 31.2 + 20 \log(v / v_0) + 10 \log(N), \tag{7}$$

where v is the train speed, km/h; v_0 is reference speed, 1 km/h; N is the number of vehicles in the train.

The distance correction is given by:

$$C_{dist} = -10 \lg(d / (25\, d_0)), \tag{8}$$

where d is the normal distance from the track segment to the observer, m ($d > 10$ m); d_0 is reference distance, 1 m.

The railway noise scheme also has an explicit allowance for air absorption given by:

$$C_{abs} = 0.2 - 0.008\ (d / 25), \tag{9}$$

where d is the normal distance from the track segment to the observer, m.

The ground effect correction for propagation over acoustically soft ground is given by:

$$\left.\begin{aligned} C_{ground} &= -3\, P_d \lg\left(\frac{d}{25\, d_0}\right), \quad \text{then } H \le 1\ \text{m}; \\ C_{ground} &= -0.6\, P_d \left(6 - \frac{H}{h_0}\right) \lg\left(\frac{d}{25\, d_0}\right), \quad \text{then } 1\ \text{m} < H \le 6\ \text{m}; \\ C_{ground} &= 0, \quad \text{then } H > 6\ \text{m} \quad \text{or} \quad 10\ \text{m} < d < 25\ \text{m}; \end{aligned}\right\} \tag{10}$$

where d is the normal distance from the track segment to the observer, m; d_0 is reference distance, 1 m; H is the mean propagation height, m; P_d is the fraction of absorbing ground between the source and receiver.

If the required measurement conditions are fulfilled, then the barrier correction $C_{barrier}$, reflection related correction $C_{reflection}$ and view correction C_{view} are equal to zero.

The corrected SEL value at the receiver point is:

$$\mathrm{SEL}_{tot} = \mathrm{SEL}_{ref} + C_{dist} + C_{abs} + \max(C_{ground}, C_{barrier}) + C_{view} + C_{reflection} \tag{11}$$

The next step is calculation of component $L_{A\,eq}$ levels for each train type on each track segment using:

$$L_{A\,eq\,c\,night} = \mathrm{SEL}_{tot} - 43.3 + 10 \lg Q_{NIGHT}$$
$$L_{A\,eq\,c\,day} = \mathrm{SEL}_{tot} - 48.1 + 10 \lg Q_{DAY}, \tag{12}$$

where Q_{NIGHT} is the number of each train type passing the receiver in the period midnight to 6am; Q_{DAY} is the number of each train type passing the receiver in the period 6am to midnight.

The overall $L_{A\,eq\,tot}$ level is calculated by combining component $L_{A\,eq}$ values for each track segment and train type using the logarithmic summation equation [2]:

$$L_{A\,eq\,tot} = 10 \lg\left(\sum_i 10^{L_{A\,eq\,c(i)}/10}\right) \tag{13}$$

4. Track Influence

4.1. RMR uses the following track classification:
1. Railway tracks with single block or double block (concrete) sleepers, in ballast bed (index code *bb* = 1).
2. Railway tracks with wooden or zigzag concrete sleepers, in ballast bed (index code *bb* = 2).
3. Railway tracks in ballast bed with non-welded tracks, tracks with joints or switches (index code *bb* = 3).
4. Railway tracks with blocks (index code *bb* = 4).
5. Railway tracks with blocks and ballast bed (index code *bb* = 5).
6. Railway tracks with adjustable rail fixation (index code *bb* = 6).
7. Railway tracks with adjustable rail fixation and ballast bed (index code *bb* = 7).
8. Railway tracks with poured in railway lines (index code *bb* = 8).
9. Railway tracks with level crossing.

Furthermore distinctions are also made, according to how many track disconnections occur on the emission route concerned:
1. Jointless rails (fully welded tracks) with or without jointless switches or crossings (index code *m* = 1).
2. Rails with joints (= tracks with joints) or an isolated switch (index code *m* = 2).
3. Switches and crossings with joints, 2 per 100 meters (index code *m* = 3).
4. More than 2 switches per 100 meters (index code *m* = 4).

For jointless rails (*m* = 1) the track correction $C_{bb,m}$ can be taken from the following table.

Table 3

Correction factor $C_{bb,i}$ as a function of structures above station compounds/railway track condition (*bb*) and octave band (*i*)

band	$C_{bb,i}$							
i	*bb* = 1	*bb* = 2	*bb* = 3	*bb* = 4	*bb* = 5	*bb* = 6	*bb* = 7	*bb* = 8
1	0	1	1	6	6	-	6	5
2	0	1	3	8	8	-	1	4
3	0	1	3	7	8	-	0	3
4	0	5	7	10	9	-	0	6
5	0	2	4	8	2	-	0	2
6	0	1	2	5	1	-	0	1
7	0	1	3	4	1	-	0	0
8	0	1	4	0	1	-	0	0

Furthermore, special corrections for other track disconnection classes and bridges are provided. In addition RMR offers the possibility to consider the influence of local rail and wheel roughness in relation to average values for the whole country.

4.2. SCHALL03 distinguishes between the following track classes: grass covered superstructure (– 2 dBA), ballast with wooden sleepers (0 dBA), ballast with concrete sleepers (2 dBA), hard ground (5 dBA).

4.3. ON S5011 uses the same track classes and correction values as SCHALL 03 except class 1.

4.4. NMT: the correction for track conditions is less specific than for the other methods. The correction is zero for ballasted tracks with continuously welded rails on concrete or wooden sleepers and typical maintenance procedures for the considered country.

If the rail or wheel surface is somewhat rougher than normal + 1 to + 3 dB should be used as correction. For very rough rails and/or wheels + 4 to + 6 dB should be used.

For particularly well maintained tracks – 1 to – 3 dB may be used. When the track and the wheels permanently have very smooth running surfaces larger negative values up to – 6 dB may be used. The use of negative values must be based on well documented and appropriate field measurements.

In addition the following corrections have to be applied to consider the influence of joints, switches, crossings or bridges: rails with joints + 3 dB; 10 m track length for each unit of switches and crossings + 6 dB; partial track length on a bridge without ballast + 6 dB; partial track length on a bridge with ballast + 3 dB.

4.5. CRN specifies the following track correction: jointed track (2.5 dBA), points and crossings (2.5 dBA), slab track (2.0 dBA), concrete bridges and viaducts (2.0 dBA), steel bridges (4.0 dBA), box girder with rails fitted directly to it (9.0 dBA).

5. Summary and Assessment

The by far most detailed and specific emission calculation method is provided by RMR, followed by NMT. Compared with these methods the emission modeling of SCHALL 03 can only be considered as a survey method, whereas the differentiation of this method is lower than that of the simplified option (dB(A)-option) of the RMR. The CRN and ON S5011 are ranked between the NMT and SCHALL 03. In detail the differences between the emission calculations of the 5 methods are summarised in table 4.

Table 4

Methods differences

Characteristics	Method				
	RMR	SCHALL03	ONS5011	NMT	CRN
Basic noise parameter	Octave band sound power level, calculated from measurements at different distances and heights, the emission is a function of train category and speed, locomotive and brake influences are considered separately	LAeq at reference distance 25 m and 4 m height, based on measurements, the emission is a function of train category, length, percentage of disc wheels and speed	Octave band sound power level, calculated from measurements at different distances and heights, the emission is a function of train category and speed	Octave band sound power level, calculated from measurements at different distances and heights, the emission is a function of train category and speed	LAeq at reference distance 25 m and 1,2 to 4 m height, calculated based on SEL levels, the emission is a function of train category, speed and number of vehicles in the train
Frequency range	From 63 Hz to 8000 Hz	-	From 63 Hz to 8000 Hz	From 63 Hz to 8000 Hz	-
Location of source	Up to 4 sources with different heights, at railhead, 0,5 m, 2 m, 4 m, 5 m above railhead, representing different mechanisms	One source at railhead level	One source 0,3 m above railhead	One source for each octave band with its specific source height	One source at railhead level
Speed dependency	For each octave band and source	For A-weighted levels	For each octave band	For each octave band	For SEL and A-weighted levels
Track influence	9 different classes, corrections are frequency dependent	4 different classes, no frequency dependency	3 different classes, no frequency dependency	Corrections from – 6 dB to + 6dB, but no specific classification, no frequency dependency	6 different classes, no frequency dependency
Influence of joints, switches, crossings and bridges	Correction table, correction are frequency dependent	–	–	Correction table, correction are not frequency dependent	Correction table, correction are not frequency dependent
Specific parameter	Local rail and wheel roughness consideration	–	–	–	–

References

1. **Attenborough K., Li K. M., Horoshenkov K.** Predicting outdoor sound. NY: Taylor and Francis, 2007.
2. **Meehan P. A.** Railway noise and control. The workbook for the course in engineering acoustics. Queensland: The University of Queensland, 2006.
3. **Wolfel Messysteme.** Software GmbH & Co, Adaptation and revision of the interim noise computation methods for the purpose of strategic noise mapping. The project report, unpublished.
4. **Baranovskis A., Balckars P., Popovs V.** Railway rolling stock CRN mathematical model. RTU proceedings, vol. 6, pp. 21-28, Riga: RTU institute of railway transport, December 2008.

Proceedings of 5th International Conference ITELMS'2010

Fracture Toughness of 10MNNI2MOVA Steel Welded Joints

Z. Bazaras*, B. Timofeev, N. Vasilieva****

** Kaunas University of Technology, Panevėžys Institute, Kalipėdos 1,44309 Panevėžys, Lithuania, E-mail: zilvinas.bazaras@ktu.lt*
*** Central Research Institute of Structural Materials "Prometey", 49 Shpalernaya str., St. Petersburg, Russia. E-mail: prometey@pop3.rcom.ru*

Abstract

The experimental results on fracture toughness crack initiation for 10MnNi2MoVA steel and its weldments are presented. The data array containing more than 200 test results has been obtained for various products (plate, forging, tube) steel and welds, produced by SAW and MAW.
KEY WORDS: *Fracture toughness; Base and weld metal; Crack initiation.*

1. Introduction

Low alloy steel of the type 10MnNi2MoVA is widely used in nuclear power plant equipment. It is used for the manufacture of steam generator cases, collectors and piping of NPPs with WWER-1000 reactors. Forgings and 200 mm thick plates, as well as cold-drawn pipes having a thickness to 100 mm are used for the manufacture of these components. Considering the different conditions of plastic deformation involve in the manufacture of these products (rolled stock, forgings, pipe) their mechanical properties, as well as their characteristics of fracture resistance, may differ considerably. Experimental data on such mechanical properties were presented in some publications [1-4].

The aim of the present study is to summarise experimental data on the brittle fracture resistance of 10MnNi2MoVA steel, obtained by different laboratories in Russia and Ukraine (ZNIITMash, CRISM "Prometey", SPI) with the use of various criteria. Beside the linear elastic fracture mechanics parameter K_{1C}, the parameter J_{1C} hand J_R curves were used in the determination of the fracture resistance of this steel. These latter parameters are useful for the "Leak-Before-Break" concept in the assessment of piping.

2. Investigated Materials

Nine heats of steel in the form of forgings (including 4 forgings, applied for collectors), three heats of steel in the form of plates, intended for steam generator cases and four heats in the form of tubes, were used as test materials. The presented information shows that this steel is used both after quenching with tempering and after normalization with tempering. The highest temperature for heat treatment of products is used for tube samples (quenching at 970°C). Besides the forging of 10MnNi2MoVA steel were melted by open-hearth furnace and electroslag re-melting.

The range of experiments on the brittle fracture resistance of welded joints is considerably less than for base metal. In all 5 welded samples were tested, having a thickness to 120 mm (4 samples were fabricated by submerged arc welding with Sv-10GN1MA wire and one sample by manual electric arc welding with type PT-30 electrodes (Table 1). All of the welded samples were heat treated in the tempering regime. The production method for the welded samples was consistent with the welding process of the PGV-1000 pressure vessel (mechanized welding) as well as the Du-850 piping (manual electric arc welding) in the assembly.

The chemical composition and mechanical properties of the materials investigated are given in Tables 2 and 3, respectively.

Compact specimens having 25, 50 and 75 mm thickness and also three point bend specimens of 50×100×450mm, 40×80×360mm and 25×50×300mm were fabricated from the materials investigated.

Table 1

Types of investigated materials

Prod No	Heat Nr	Product	Thickness	Heat treatment of products
GN1	118902.	Forging	200.	Quenching 920 C, 5h, water; tempering 660 C, 8h, air; 650 C, 45h,air
GN1.1	118902.	Forging	200.	Quenching 920 C, 5h, water; quenching 910 C, 4h, air; tempering 660 C, 75h, air
GN2	129554.	Forging	185.	Quenching 920 C, 4h, water; tempering 650 C, 8h, air; 650 C, 45h,air
GN4	132288.	Forging	180.	Quenching 920 C, 5h, water; tempering 660 C, 7h, air, 650 C, 45h,air
GN3	131630.	Plate	120.	Quenching 920 C, 4h, water; quenching 910 C, 4h, air; tempering 650 C, 45h,air
GN5	119516.	Forging	200.	Quenching 920 C, 5h, water; tempering 660 C, 8h, air; 650 C, 45h,air
GN6	129574.	Plate	150.	Quenching 920 C, 6h, water; tempering 660 C, 9h, air; 640 C, 45h,air

Sequel of Table 1

Prod No	Heat Nr	Product	Thickness	Heat treatment of products
GN7	110096.	Plate	185.	Quenching 920 C, 5h, water; tempering 660 C, 8h, air; 650 C, 45h,air
GN8	T51879	Tube	80.	Quenching 970 C, 3h, air; tempering 630 C, 10h, air; 650 C, 30h,air; 620 C,10h,air
GN9	T23574	Tube	40.	Quenching 970 C, 3h, air; tempering 620 C, 10h, air; 650 C, 30h,air; 620 C,10h,air
GN10	133737.	Tube	85.	Quenching 970 C, 2h, air; tempering 620 C, 10h, air; 650 C, 30h,air; 620 C,10h,air
GN11	120254.	Tube	70.	Quenching 970 C, 3h, air; tempering 620 C, 10h, air; 650 C, 30h,air; 620 C,10h,air
GN12	190276.	Forging	160.	Quenching 920 C, 5h, water; tempering 660 C, 8h, air; 650 C, 45h,air
GN13	161184.	Forging	160.	Quenching 920 C, 8h, water; tempering 650 C, 28h, air; 620 C, 25h, air;650 C, 20h, air
GN14	11699ESM	Forging	160.	Quenching 900 C, 9h, air; tempering 660 C,38h, air; quenching 910 C, 9h,water; 650,25h, air
GN15	11843ESM	Forging	160.	Quenching 910 C,18h, air; tempering 650 C,45h, air; quenching 920 C,10h,water; 660,24h, air
GNW1		Plate	120.	Tempering 650 C,10h, air;
GNW2		Plate	120.	Tempering 650 C,15h, air; tempering 620 C ,15h,air
GNW3	191659.	Plate	100.	Tempering 650 C,8h, air; tempering 620 C ,10h,air; 650 C, 30h, air;
GNW4		Plate	80.	Tempering 650 C,15h, air; tempering 620 C ,15h,air
GNWM1	35.	Plate	80.	Tempering 650 C, 7h, air;

Table 2

Chemical composition of investigated materials

Prod.No.	No. heat	C	Si	Mn	S	P	Ni	Mo	V	Cr	Cu
GN1	118902.	0.11	0.33	1.08.	0.012	0.011	2.16	0.55	0.06	0.15	0.14
GN2	129554.	0.10	0.23	0.82	0.015	0.010	1.82	0.50	0.03	0.12	0.16
GN3	131630.	0.12	0.26	0.98	0.014	0.012	2.18	0.55	0.07	0.18	0.14
GN4	132288.	0.12	0.27	0.82	0.011	0.010	1.72	0.45	0.04	0.22	0.20
GN5	119516.	0.09	0.28	0.70	0.016	0.013	1.79	0.40	0.03	0.13	0.09
GN6	129574.	0.10	0.30	0.76	0.010	0.010	1.97	0.45	0.03	0.12	0.15
GN7	110096.	0.12	0.25	0.65	0.013	0.008	2.50	0.55	0.03	0.12	0.12
GN8	T51879	0.09	0.25	0.74	0.010	0.011	1.94	0.49	0.04	0.06	0.06
GN9	T23574	0.11	0.33	0.97	0.019	0.015	2.35	0.58	0.07	0.18	0.08
GN10	133737	0.10	0.26	0.75	0.020	0.017	2.05	0.46	0.06	0.20	0.12
GN11	120254.	0.12	0.34	0.90	0.013	0.010	1.79	0.48	0.04	0.13	0.13
GN12	190276.	0.10	0.35	0.75	0.015	0.012	1.85	0.51	0.06	–	–
GN13	161184.	0.10	0.30	0.91	0.012	0.012	2.15	0.58	0.03	0.12	0.17
GN14	11699.	0.10	0.24	0.76	0.017	0.010	1.97	0.44	0.04	0.21	0.14
GN15	11843.	0.10	0.33	0.87	0.011	0.005	2.08	0.43	0.06	0.18	0.12
GNW1	Weld	0.06	0.30	0.75	0.010	0.015	1.62	0.67	–	0.12	–
GNW2	Weld	0.06	0.36	0.79	0.009	0.014	1.63	0.71	–	0.17	–
GNW3	Weld.	0.08	0.27	1.40	0.010	0.008	1.70	0.60	–	0.16	0.06
GNW4	Weld	0.08	0.32	0.80	0.010	0.012	1.65	0.68	–	–	–
GNWM1	Weld	0.07	0.17	0.99	0.011	0.007	1.50	0.65	–	0.14	–

Table 3

Mechanical properties of 10GN2MFA steel and its weldments at 20°C

Prod No	*UTS*, MPa	*YS*, MPa	*A*, %	*Z*, %	*DBTT*, °C
GN1	653	504	24.5	71.3	-10
GN1.1	653	465	21.4	65.0	10
GN2	585	508	27.4	74.9	-50
GN3	633	536	27.3	75.5	-60
GN4	609	448	25.0	74.2	0

Sequel of Table 3

Prod No	*UTS*, MPa	*YS*, MPa	*A*, %	*Z*, %	*DBTT*, °C
GN5	552	436	25.7	65.9	-25
GN6	555	410	22.7	67.7	-10
GN7	627	517	24.0	70.3	-45
GN8	550	410	28.7	77.1	-55
GN9	710	590	17.5	60.0	-10
GN10	600	461	26.1	70.4	-10
GN11	670	550	23.5	71.0	-30
GN12	651	407	24.8	75.6	-10
GN13	630	510	23.5	71.5	-20
GN14	600	500	25.7	77.5	-25
GN15	570	436	25.6	78.0	-40
GNW1	587	495	23.1	67.2	-10
GNW2	532	417	19.7	70.3	0
GNW3	586	492	25.4	73.9	-20
GNW4	613	490	25.2	64.4	0
GNWM1	659	591	20.9	71.4	-20

3. Investigation Procedure and Test Results

The determination of the fracture toughness parameter K_{1C} was carried out on specimens of Type 3 (compact specimens) and Type 4 (three point bend specimens) according to the requirements of GOST25.506-85 [5]. The requirements to specimen sizes and test procedure were in detail described in Ref. [4].

The summarized experimental data on the brittle fracture resistance of type 10MnNi2MoVA steel and its welded joints are given in Fig. 1, where 191 plotted points correspond to fracture toughness of base metal, 28 points from submerged arc welds and only 5 points from manual electric arc welds.

As there are not many experimental points the spread of fracture toughness values is quite small. Nevertheless, it should be noted that practically all data from welds are in the lower half of the scatter band of all experimental data. This applies both to weld fabricated by manual arc welding with the type PT-30 electrodes and to weld fabricated by submerged arc welding, using Sv-10MnNi1MoA wire and the types AH-17M or FZ-16 flux. The limited scatter of K_{1C} values for weld metal is associated with the limited number of experimental data, as well as with the fact that the selected welded samples have quite similar thicknesses (80-120 mm) and similar heat treatment regimes (tempering at 650°C), though the exposure time at this temperature varied from 7 to 38 hrs. It should also be mentioned that the scatter in *DBTT* for welds was also small.

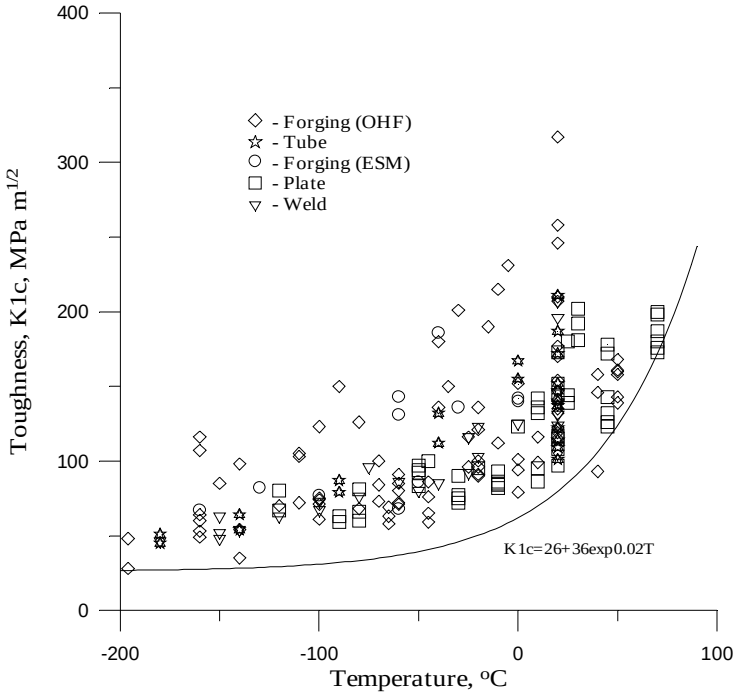

Fig. 1. Fracture toughness of 10GN2MFA steel and its weldments

A greater scatter of experimental data was observed for base metal. In this case, (as stated above) various types of product were tested (plates, forgings, tubes) and the heats were produced by both open-hearth furnaces (OHF) and electroslag re-melting. This factor and the various thicknesses of products (from 40 mm to 200 mm) were the main causes of the considerable scatter in K_{1C} values at a given test temperature. As the results obtained show, the spread of K_{1C} values occurs in both the brittle area (temperature – 160°C) and in the ductile-brittle transition zone (temperature +20°C). It should be noted that the *DBTT* for the steel heats investigated also varied within wide limits, from +10°C to – 60°C), i.e. it varied to a greater extent than in the welds. The greatest difference of minimum and maximum values of fracture toughness is observed for forgings and the smallest for tubes.

As for the main circulating circuit piping of NPPs which contain the type WWER-1000 reactors and are made of 10MnNi2MoVA steel, the LBB concept is used in calculations J_R the criterion of safety, it is necessary to determine the J_R of the elastic-plastic fracture mechanics for this material. For this purpose the criterion of the resistance to a stable growth of crack is used (J_R curves). The paper presents investigations of this steel at 20 and 270°C in the range of crack increment to 3.0 mm. J_R curves were constructed on the basis of test results from compact specimens having a having a thickness of 25 mm. The results are given in Fig. 2. For heat number 133737, of 10MnNi2MoVA steel with $T_{KO} = -10$°C, compact specimens were machined in two mutually perpendicular directions, which corresponded to crack growth along the tube axis orientation (direction TL) and in the circumferential direction (TS). It can be seen, from the results presented, that the J-integral value in the TL direction is higher. The difference at room temperature is small, but at the operating temperature of 270°C, this difference is considerable. The data presented show that a stable crack growth resistance is higher at room temperature, than at 270°C. The exception is the data on heat 133737 in the direction TL, for which the J_R curve is located higher at the elevated temperature.

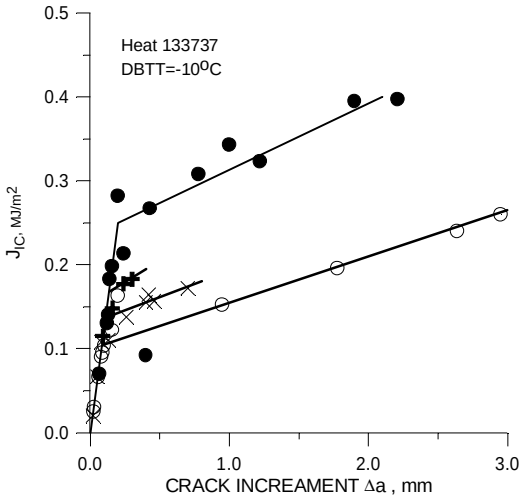

Fig. 2. Fracture toughness $J_R - \Delta a$ curve of 10MnNi2MoVA steel (tube): ˜ – TL at 270°C; š – TS at 270°C; É – TL at 20°C; ï – TS at 20°C

Apparently, this difference is associated with strain ageing, since the content of harmful impurities (0.020%S and 0.017%P) in this heat is higher in comparison with the other investigated heats of Type 10MnNi2MoVA steel (see Table 2 and the caption of Fig. 2). The *J*-integral value of the steel with $T_{KO} = -55$°C is higher than that for the same steel grade with a higher *DBTT*. This difference is greater at the 20°C test temperature. The permissible J_{1C} values for forgings from ferritic steel for Sizewell [6] were 156 kJ/m^2 at 43°C and 136 kJ/m^2 at 293°C and it is more or less consistent with the data obtained from 10GN2MFA steel. In the case of a 2 mm crack increment, $J_{a\,2} = 720$ kJ/m^2 at 43°C and $J_{a\,2} = 400$ kJ/m^2 at 293°C. As can be seen from Fig. 2, these values are between 200 and 800 kJ/m^2 for the 10MnNi2MoVA steel heats investigated.

The above-stated experimental data on fracture toughness of steel and its welds, as well as J_R curves were obtained from standard specimens and standard crack sizes. This information is usually used in failure calculations for components and piping. Under real conditions, the crack shape and size can differ considerably from these idealised ones. Therefore, it is of interest to compare the characteristics on the basis of test results from specimens having surface and through cracks. The authors of the present article did not carry out such experiments for this type of steel and in the analysis data have been used that were obtained in ZNIITMash [7, 8] by testing large scale segment specimens (70×250 mm), which contained through and surface cracks. The specimens were loaded in tension at 20°C. The test material was a PGV-1000 steam generator collector sample. The test results (Fig. 3) show clearly that, by testing compact specimens, a more conservative result was obtained than by testing large scale specimens with through central and surface cracks. To assess the specimens that are most appropriate for evaluating *J-R* curves, it is also necessary to take into consideration the influence of the compact specimen size on the form of $J_R = f(\Delta a)$ curves. According to Ref. [9], the most conservative results were obtained on 1/2CT specimens, in comparison with 1CT and 3CT specimens, although this would not normally be expected. Thus, fracture toughness test results for 10GN2MFA steel, obtained on compact specimens, are quite conservative.

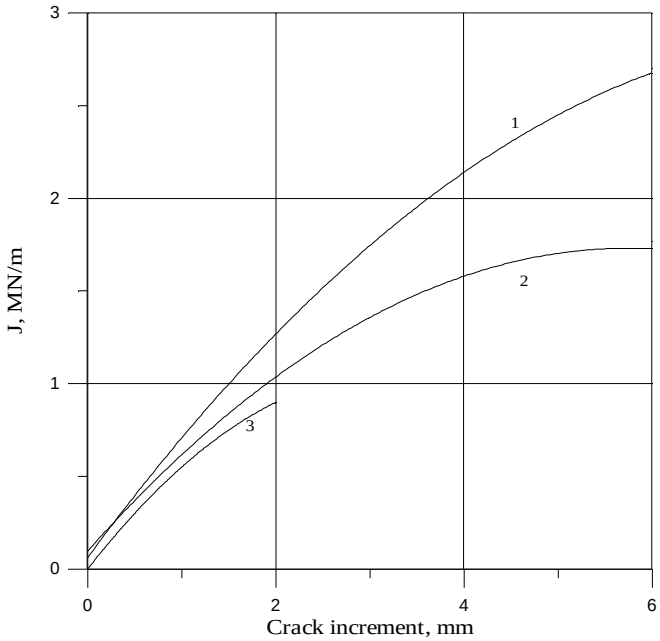

Fig. 3. Calculated *J-R* curves plotted on the base of test results of various specimens: 1 – with central through crack; 2 – with surface crack; 3 – compact specimen

4. Conclusion

For the first time a generalised study has been made of experimental data on brittle fracture resistance, using the criteria of linear and non-linear fracture mechanics for low alloy steel of the type 10MnNi2MoVA. This steel is widely used in nuclear power engineering for pressure vessels, steam generators, collectors and the piping of the main coolant circuit of NPP with WWER-1000 reactors. These data can be used in failure calculations of the above-stated items carried out for both brittle fracture and LBB concepts. It has been shown that the fracture toughness depends considerably on the type of base metal (forging, plate, tube) and the steel melting process (OHF, ESM). Welded joints do not posses an inferior brittle fracture resistance compared base metal. However, there are few experimental data for welds and it will be necessary to continue the accumulation of experimental data.

The experimental data presented demonstrate that, for 10MnNi2MoVA steel and its welded joints, it is possible to offer a new temperature dependence $K_{IC} = f(T - T_K)$ instead of the presently recommended dependence $[K_I]_3 = 26 + 36 \exp[0.02\ (T - T_K)]$ (in accordance with the Russian Strength Norms [10]).

References

1. **Zherebenkov A. S., Timofeev B. T., Chernaenko T. A.** Statistical anslysis of mechanical properties and technological damages for welded joints of steam generators from 10GN2MFA steel. Voprosy Sudostroeniya, Seriya Svarka, 33, 1982, pp. 30-38.
2. **Daunis M. A., Matrosova E. G., Pimenov V. N., Rasskazov M. A., Timofeev B. T.** Fatigue strength of welded joints from low alloy steel. Voprosy Sudostroeniya, Seriya Svarka, 24, 1977, pp. 3-8.
3. **Bobrov V. I., Grekova I. I., Zvezdin Yu. I., Rasskazov M. A., Timofeev B. T.** Properties of large sizes semi-products from Ni-Mo-V steel. Voprosy Sudostroenija. Serija Metallovedenie, issue 29, 1979, pp. 32-38.
4. **Timofeev B. T., Blumin A. A., Anikovsky V. V.** Fracture toughness of 10GN2MFA steel and its welds. International Journal Pressure Vessel and Piping, 2000, No.4.
5. GOST25.506-85. Design, calculation and strength testing. Methods of mechanical testing of metals. Determination on fracture toughness characteristics under static loading. Moscow. Standard Publish House, 1985, 61 p.
6. **Sharples J. K. & Hooton D. G.** Comparative review of defect assessment requirements (France, Germany, US and UK). Nuclear Energy, 1995, 34, No.4, Aug., pp. 238-248.
7. **Vasilchenko G. S., Artemyev V. I., Merinov G. N.** The investigation of resistance fracture characteristics of pipe weld metal by means of testof large-scale thickness specimens with cracks.
8. **Vasilchenko G. S., Vasnin A. M., Getmanchuk A. V., Rivkin E. Yu.** Investigation of fracture toughness characteristics of 10GN2MFA steel weld metal. Tjazheloe mashinostroenie, 1994, No.11-12, pp. 19-22.
9. **Rice J. R. & Johnson M. A.** In M.F.Kanninen "Inelastic Behaviour of Solids". New York, 1970, pp. 641-672.
10. PNAE G-7-002. Strength Calculation Norms for Nuclear Power Plant Equipment and Piping. Energoatomizdat, Moscow, 1989, 525 p.

Proceedings of 5th International Conference ITELMS'2010

Plastic Strain Effect on Fatigue Growth Crack Rate for 10MnNi2MoVA Steel

Z. Bazaras*, B. Timofeev, N. Vasilieva****

** Kaunas University of Technology, Kestucio 27, 44312, Kaunas, Lithuania, E-mail: Zilvinas.Bazaras@ktu.lt*
*** Central Research Institute of Structural Materials "Prometey", 49 Shpalernaya str., St. Petersburg, Russia. E-mail :prometey@pop3.rcom.ru*

Abstract

At connection heat-exchanging tubes and the wall of header metal of the ligament between tubes is exposed to influence of the plastic strain approximately equal of 5% that causes appreciable change of a macrostructure. The influence of plastic strain of such level at the static and dynamic loading on fatigue crack growth rate of the low alloyed steel type 10MnNi2MoVA was submitted.
KEY WORDS: *plastic strain effect, fatigue crack growth rate, low alloyed steel, tube.*

1. Introduction

During manufacturing materials of separate units of the power equipment are exposed to influence of plastic strains, for example, cold and hot a rolling , drilling, a bend and other operations. So, for connection heat-exchanging tube in a wall of steam generator header or a trumpet lattice explosive processing which causes appreciable plastic strains in a material with high speed of deformation is used. Besides while in service the material in separate zones can be subjected to a unilateral overload at static strain. Preliminary static and high-speed deformation of a material leads to change of characteristics of strength ($s_в$ and $s_{0,2}$), plasticity (δ and y) and microstructures. It has been reflected in a number of publications [1-3]. Unitary plastic deformation is known, that both at room, and at the elevated temperature, on the one hand, reduces relative elongation a sample after destruction, and with another - increases the yield strength of structural materials. Though this law is conventional, features of the mechanism of reduction of relative elongation in interrelation with characteristics of mechanical properties of a material are still investigated a little.

In the end of 1987 year when in operation there were already 7 units with WWER-1000 reactors on "cold" collectors of steam generators of the Southern - Ukrainian NPP cracks have been found out. The circuit of origin and development of a crack in ligament of a collector has been considered earlier in Ref. [4] and also shown on Fig. 1.

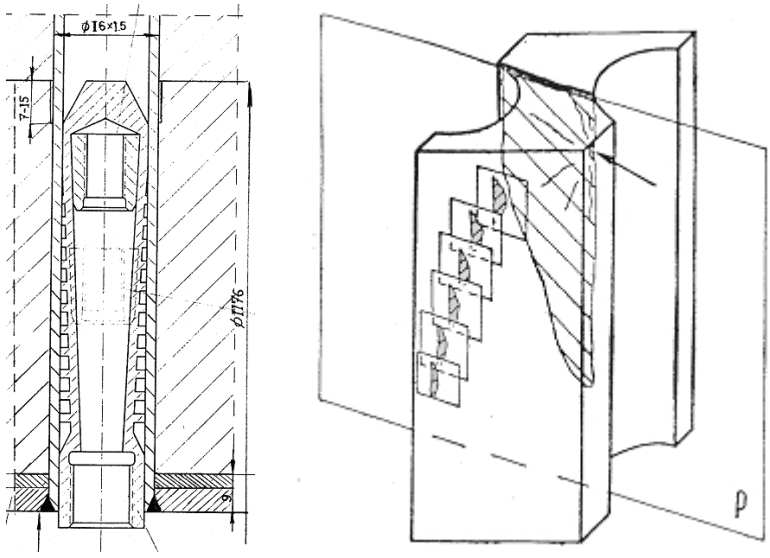

Fig. 1. Scheme for initiation and propagation of crack in ligament of header

Subsequently such damages on similar sites of collectors have been found out on 25 steam generators PGV-1000. As a result of research of the reasons and the mechanism of damage of collectors which have been carried out by the various organizations during the 1987-1991 year, it has been established, that one of the reasons were the big plastic strains of a wall of the collector made of steel 10MnNi2MoVA as a result of accepted technology [4]. Originally the technology provided connection the heat-exchanging tubes in a wall of a collector with the help of explosion that led to to appreciable plastic strains of a wall of a collector in ligament. Character of distribution of stresses and strains in this area is submitted on Fig. 2.

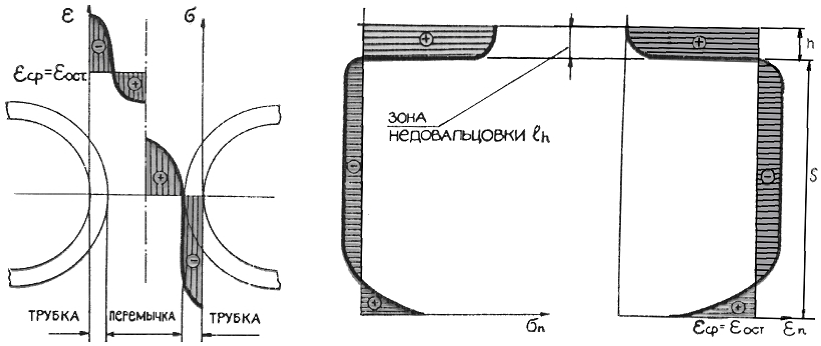

Fig. 2. Stress and strain level in ligament: on wide (left) and on high (right)

In connection with the found out damages investigations on influence of plastic strains on properties of 10MnNI2MoVA steel which results are submitted below have been executed.

That similar damages did not appear further, the technology connection tubes and the header wall has been changed. So, rolling by explosion has been replaced on hydraulic rolling pipes with the subsequent mechanical procedure target sites (5-10 mm) with the purpose of full elimination narrow gaps between a wall of a pipe and an aperture in a wall of a collector. The circuit of this operation is resulted in the left part of Fig. 1. Besides the special technology of drilling of apertures in a wall of a collector which provided expansion for removal plastic strain drilling of a layer of metal has been applied.

As in operation were collectors PGV-1000, executed on former technology, it was necessary to estimate influence of preliminary strain on characteristics of a material of a header. In this connection researches after preliminary static and dynamic strain on mechanical properties of 10MnNi2MoVA steel have been carried out.

2. Technique of Carrying out of Modeling

Preliminary deformation spent on special preparations of the cylindrical form at unitary loading and the conic form at dynamic loading (Fig. 3) from 10MnNi2MoVA steel a open-hearth furnace and electroslag re-melting [5, 6]. Both investigated materials were exposed thermal heat treatment on one mode: quenching at 920°C – 10 hours with cooling in water and to the subsequent tempering at 660°C – 20 hours with cooling on air. The chemical composition and mechanical properties of the investigated materials are submitted in Table 1.

Then of preliminary deformed metal made cylindrical samples for definition of standard mechanical properties and compact samples CT25 (Fig. 4) for definition of growth rate of a crack and fracture toughness.

Experimental results of influence of preliminary deformation on properties of 10MnNi2MoVA steel open-hearth furnace melt and electroslag re-melting are submitted in Table 2.

Table 1

Chemical composition and mechanical properties at 20°C of 10MnNI2MoVA steel

Melt	C	Mn	Si	Cr	Ni	Mo	V	S	P	Cu	*UTS*, MPa	*YS*, MPa	*A*, %	*Z*, %	Heat treatment
OHF	0.09	0.91	033	0.24	1.79	0.45	0.03	0.008	0.008	0.16	597	491	24.6	75.9	Quenching, tempering
ESR	0.10	0.87	0.33	0.18	2.08	0.43	0.06	0.011	0.005	0.12	570	436	25.6	78.0	Quenching, tempering

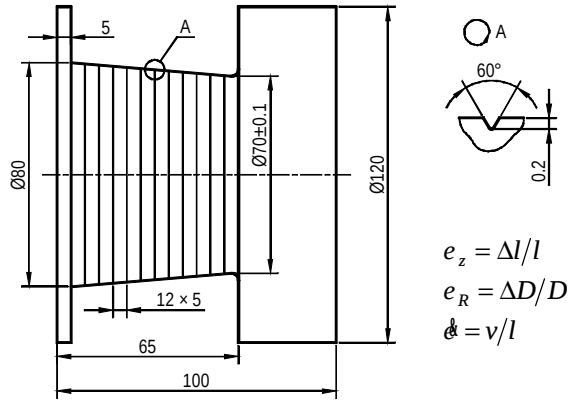

Fig. 3. Type of specimen for preliminary dynamic straining

The received data testify that after static deformation mechanical properties change insignificantly, however after dynamic influence characteristics of strength appreciably increase, and plastic – are reduced [5].

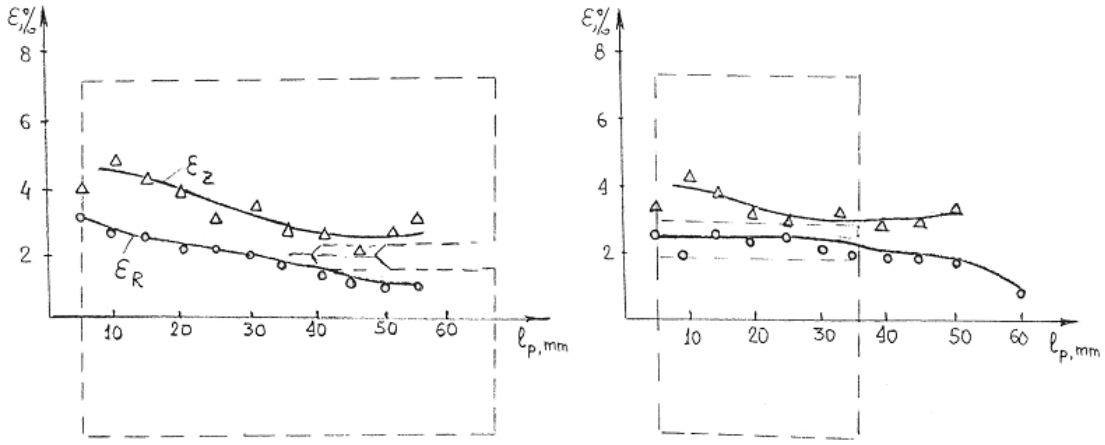

Fig. 4. Distribution of residual strain after preliminary dynamic (high rate) straining and scheme of cutting out compact specimens for determination FCGR

Table 2

Mechanical properties of 10MnNi2MoVA after preliminary static and dynamic straining

Melt	T, °C	$\dot{\varepsilon}$, s^{-1}	ε_R, %	*UTS*, MPa	*YS*, MPa	*A*, %	*Z*, %
OHF	20	0	0	597	491	24.6	75.9
		10^{-1}	5	644	528	27.5	65.7
		10^{4}	1	700	476	25.0	66.0
		10^{4}	2.5	707	644	14.5	67.2
	280	10^{-1}	5	490	401	18.4	77.5
		10^{4}	2.5	544	486	22.8	80.4
	-60	10^{4}	2.5	807	662	7.8	47.3
	-90	10^{-1}	5	792	713	17.9	66.0
	-140	10^{-1}	5	823	700	25.9	64.0
ESR	20	0	0	570	436	25.6	78.0
		10^{4}	2	648	550	23.5	76.2
		10^{4}	6.8	789	764	18.7	69.2
	280	10^{4}	6.8	523	495	11.6	25.3

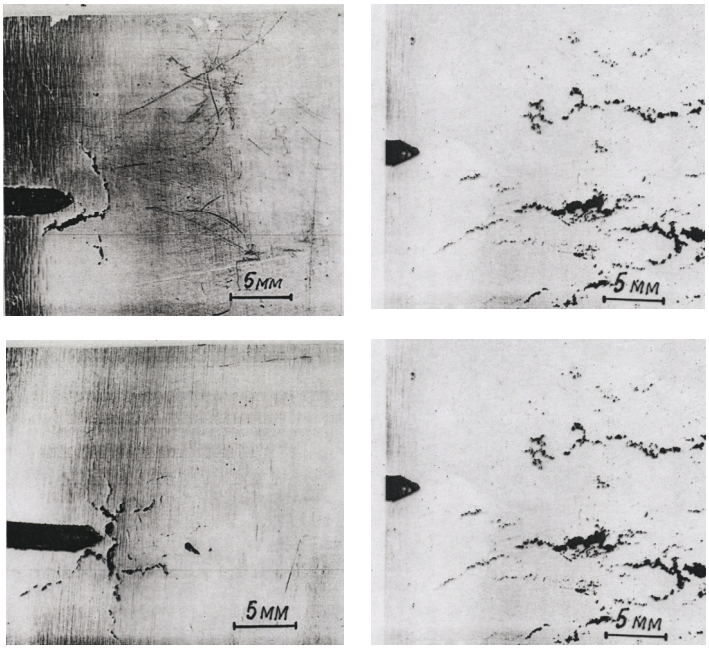

Fig.5. Various compact specimens CT1 for determination of fatigue crack growth rate after preliminary dynamic straining (e_R = 5 ... 6%) at speed $v \leq 300$ m/s

Samples CT25 cut out from preliminary statically and dynamically deformed preparations ∅120×100mm (Fig. 3) in two directions where alongside with an arrangement of a mechanical cut distribution of residual strains in a compact sample after preliminary dynamic loading (Fig. 4) in cross-section (R) and longitudinal (Z) a direction is submitted. High-speed dynamic loading with a speed it is brisk v = 260 ... 400 m/s leads to appreciable damages of a material of open-hearth furnace melt that is evidently visible from submitted on Fig. 5 (photos). For this mark of steel of electroslag melt the same deformation causes insignificant embrittlement preparations. At significant damages of test on FCGR a fatigue crack were not carried out.

3. Experimental Results

Results of tests of samples after preliminary static deformation on FCGR fatigue cracks at room and elevated (280°C) temperatures are submitted on Fig. 6.

Increase of temperature does not influence fatigue crack growth rate of a on middle area a peak site and increases it on threshold value of the diagram of fatigue failure both as-produced and the preliminary strained materials. High-speed dynamic and static preliminary deformation of 10MnNi2MoVA steel electroslag melt does not render influence on FCGR in the investigated range of stress intensity factor. The same effect can be noted and for steel of a open-hearth furnace melt, but only at static deformation. As to dynamic deformation, that, owing to appreciable embrittlement preparations after such processing, the similar conclusion is wrongful.

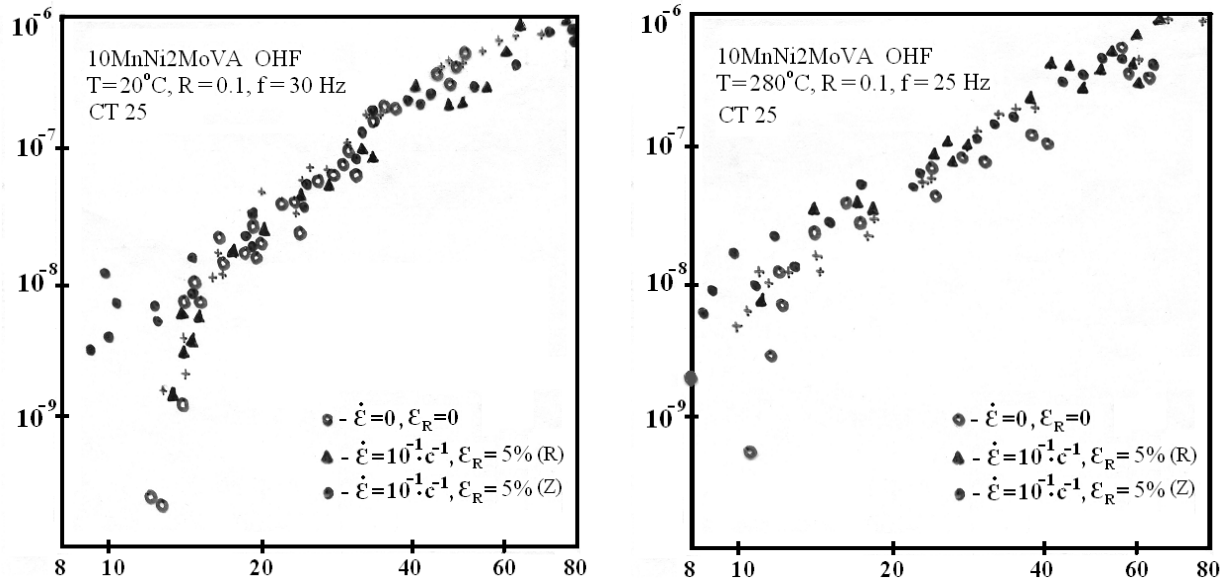

Fig. 6. Effect of preliminary static straining (e = 5%) on FCGR for 10MnNi2MoVA steel (OHF)

Thus, at the certain modes connection pipes in a wall of a collector of steam generator PGV-1000 in the ligament of material probably occurrence of absent-minded micro cracks, cracks or narrow zones plastic over deformed, being actually initial technological defects. The specified technological defects reduce a service life of the header ligament by the size required for origin a crack in the size of 0.1 ... 3 mm. From here follows, that the service life of the ligament (crosspiece of a wall of a collector) of steam generator PGV-1000 at presence of initial absent-minded technological defects is determined only by a stage of development of a crack through the ligament. Results of tests on K_{IC} are submitted in Table 3.

Characteristics of K_{IC} for 10MnNi2MoVA steel in an initial condition and after preliminary plastic deformation of a material became received. It is shown, that K_{IC} at static loading for steel of this type electroslag re-melting became higher, than at steel open-hearth furnace melt, as an initial condition, and in a condition after preliminary plastic deformation. Preliminary high-speed deformation (ε = 2.5 ... 5%) and static deformation (e = 5%) cause decrease in static fracture toughness. And the cutting of compact samples in longitudinal direction Z causes more essential decrease K_{IC} of the deformed material, than in a material deformed with the same degree of residual deformation, but with a cutting on cross-section direction R.

Influence of preliminary plastic deformation on low cycle fatigue of this type steel carried out on a material melted in open-hearth furnace. Thus deformation carried out as a static loading, and dynamically with the help of explosive processing (it is similar connection pipes in trumpet boards at manufacturing collectors of steam generators PGV-1000). The degree of plastic deformation at static loading made e = 5% that was approximately equal to size of deformation at explosive expanding pipes in a wall of a collector. Results of tests of samples on low cycle fatigue at a symmetric cycle of the set deformation in conditions of the elevated temperature (275°C the most typical temperature of operation of cold collectors for which the greatest damageability while in service has been marked) have been submitted earlier in work [4]. From the submitted data absence of influence of preliminary strain on resistance low cycle fatigue of

this type steel follows, and also, as the subsequent after the rolling low temperature thermal processing does not influence on low cycle fatigue of steel 10MnNI2MoVA.

Table 3

Test results on K_{IC} for 10MnNI2MoVA steel in various states

Melt	$\dot{\varepsilon}$, s^{-1}	T, °C	Orientation	ε_R, %	K_{IC}, MPa $\cdot\sqrt{m}$
OHF	0	-140	R	0	53.5
		-90	R	0	55.6
	10^{-1}	-140	Z	5	41.5
			R	5	49.3
		-90	Z	5	46.5
			R	5	50.5
	10^{4}	-140	Z	2.5	53.5
			Z	3.0	42.8
		-90	Z	2.5	48.9
ESR	0	-140	R	0	62.5
		-90	R	0	74.0
		-60	R	0	115.0
		+20	R	0	93.7
	10^{4}	-140	R	3	68.8
			R	5	51.2
		-90	R	3	87.0
			R	5	94.4

4. Conclusions

1. At rolling tubes in a wall of a collector of steam generator PGV-1000 a method of explosion in a material of the crosspiece probably occurrence of absent-minded micro cracks and cracks which actually are initial technological defects. The specified technological defects reduce a service life of the crosspiece of a wall of a collector. In this case the resource is determined only by a stage of development of a crack through the crosspiece.
2. Process of formation of such technological defects in steel 10MnNi2MoVA electroslag re-melting at the accepted technology rolling tubes occurs less actively in comparison with this steel of open-heart furnace melt.
3. After unitary deformation on 5 % mechanical properties of steel 10MnNi2MoVA change insignificantly, however after dynamic influence of a similar level прочностные characteristics appreciably increase, and plastic – are reduced.
4. High-speed dynamic and static preliminary deformation of steel 10MnNi2MoVA electroslag melt does not render influence on growth rate of a fatigue crack in the investigated range of factors of stress intensity factor. The same effect can be noted and for steel of a open-heart furnace melt, but only at static deformation.

References

1. **Yasniy P. V., Pokrovsky V. V., Shtukaturova A. D., Krasiko V. N., Timofeev B. T.** Effect of preliminary plastic strain on mechanical properties and microstructure of structural steel. Problemy prochnosti, 1988, Nr.9, p. 41-45.
2. **Schulte K., Nowack H., Lutjering G.** Influence of monotonic and cyclic pre-strain of fatigue crack propagation of high-strength aluminum alloys. Engineering Fracture Mechanics. 1980, vol.13, Nr.4, p. 1009-1021.
3. **Lindigkeit J., Gysler a., Luftjering G.** The effects of pre-strain of fatigue crack propagation behavior of the Al-Zn-Mg-Cu alloys in inert and corrosive environment. Z. Metallkunde. 1981, 72, Nr.5, p. 322-328.
4. **Bazaras Z., Timofeev B., Vasilieva N.** Damages analysis of header for PGV-1000 steam generator. Proceedings of the Riga Technology University, 2009.
5. **Timofeev B. T., Fedorova V. A., Pokrovsky V. V.** Plastic strain effect on behavior of some steels used for manufacture NPP equipment and piping. Proceedings of the Sixth International Conference on "Material Issues in Design, Manufacturing and Operation of Nuclear Power Plants Equipment", Volume 1, 19-23 June 2000, St.Petersburg, p. 213-229.
6. **Troshchenko V. T., Yasniy P. V., Pokrovsky V. V., Timofeev B. T., Fedorova V. A.** Influence of static plastic strain of fatigue crack growth rate of the heat-resistant steel. Problemy prochnosti, 1988. Nr.12, p. 9-14.

Determination of Vehicle Durability Based on Life Cycle Costs and Failure Intensity

J. Furch

University of Defence, Kounicova 65, Brno, Czech Republic, E-mail: jan.furch@unob.cz

Abstract

The paper deals with the model for determination of optimal vehicle durability time depending on life cycle costs and failure intensity. This method adopts two separate approaches. The first approach is based on the life cycle costs calculation, and the second on the determination of failure intensity relation. The whole life cycle of vehicles is divided into particular stages that are characterized by the type and the amount of expended costs. The paper presents a general model of life cycle cost of vehicles. Life cycle cost of vehicles in the operation stage is the focus of special attention.
KEY WORDS: *vehicle durability time, vehicle life cycle costs, failure intensity, costs on maintenance, amortization vehicles.*

1. Introduction

The initial programme of the vehicle maintenance is often elaborated in cooperation between a supplier and a user, and is prepared before the vehicle is put into operation. However, this maintenance programme is not always optimal. Therefore, immediately after the commencement of operation it is very useful, to initiate data collection on the actual course of degradation and failure occurrence, including the cost demands, i.e. to create a dynamic maintenance programme. This programme makes possible to calculate the life cycle cost (LCC) and failure intensity, which can be used for the assessment of the vehicle durability life assuming that the recommended reliability is kept.

The primary guidance for vehicle life cycle cost evaluation is a standard. According to this standard the vehicle life cycle cost can be divided into these five periods:

- concept and demand determination period,
- design and development period, } purchase costs,
- manufacture period,
- operating state and maintenance period, – proprietary costs,
- disposal period, – liquidation costs.

2. Model Design for Vehicle Durability Time Determination Depending on Life Cycle Costs and Failure Intensity

For the optimal mean time determination of the vehicle durability time it is necessary Fig. 1:

1. to carry out the calculation of vehicle life cycle cost; for this purpose it is necessary to be familiar with
   - the purchase costs of the vehicle and its amortization,
   - costs on operating state,
   - vehicle maintenance costs,
     - ¢ corrective maintenance costs,
     - ¢ preventive maintenance costs,
   - liquidation costs.
2. to carry out failure intensity calculation.
3. to determine the vehicle mean time on the basis of the curve course of the vehicle life cycle cost and the curve course of failure intensity, so called vehicle durability [1].

3. Vehicle Durability Time Determination Depending on Vehicle Life Cycle Cost

3.1. *Calculation of selected life cycle costs*

$$C_{PAM} = C_{PA} + C_{OMC} + C_{OMP} \tag{1}$$

where C_{PAM} is life cycle costs; C_{PA} is costs on vehicle purchase and amortisation; C_{OMC} is corrective maintenance costs; C_{OMP} is preventive maintenance costs.

3.2. *Costs on vehicle purchase and its amortization*

The actual value of a vehicle during its operation shall be calculated from costs on vehicle purchase reduced by its amortisation. Costs on amortisation include the vehicle age and kilometrage.

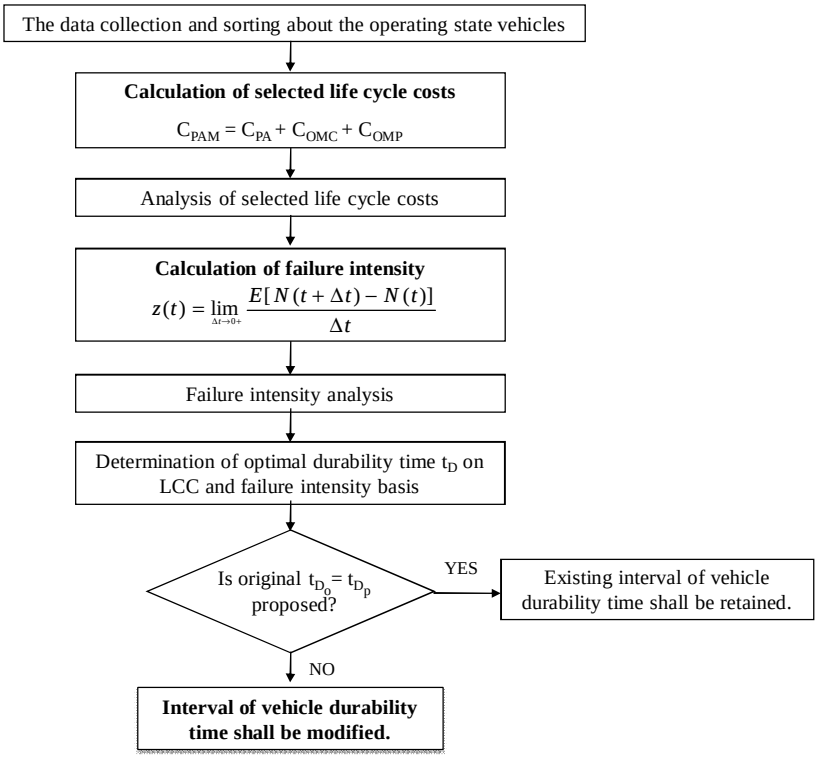

Fig. 1. Model for the determination of vehicle durability time

a) Costs on vehicle purchase. The vehicle purchase cost can be expressed by the following equation:

$$C_P = C_{CD} + C_{DD} + C_M + C_S + C_G \tag{2}$$

where C_{CD} is costs on concept and demand determination period; C_{DD} is costs on vehicle proposal and development period; C_M is costs on manufacture period; C_S is costs on vehicle sale period; C_{RG} is costs on repair during guarantee period.

b) Vehicle amortization calculation. Basic amortization (C_{PA}) is calculated as the arithmetic mean of a percent reduction for operating state time (C_{AT}) and percent reduction for a number of kilometres (C_{AO}) according to amortization scale [3].

$$C_{PA} = \left(C_{AT} + C_{AO}\right) / 2 \tag{3}$$

3.3. Costs on vehicle maintenance

a) Costs on corrective vehicle maintenance. The total cost amount necessary to expend on vehicle repairs during its operating state depends apparently on the number of failures which occur in the vehicle during its usage, and on the cost amount necessary to remove each failure. If the failure rate λ is regarded as a measure of reliability level, it is possible to use the following equation for repair support costs [2]:

$$C_{OMC_{(j)}} = \sum_{n=1}^{n=j} z_{(n)}\, i\, c_R, \text{ or} \tag{4}$$

$$f_{C_{OMC}} = c_R \int_{t_0}^{t_n} \frac{t}{E_t}\, \mathrm{d}t, \text{ or} \tag{5}$$

$$C_{OMC} = \frac{c_R}{f} t \tag{6}$$

where C_{OMC} is corrective maintenance costs during operating time t; t is operating time in kilometres; i is determined value of the interval in kilometres; j is number of determined intervals I; $z_{(n)}$ is failure intensity in interval n; $E_{(t)}$ is mean time between failures depending on mileage t, calculated with Weibull distribution; Φ is mean time between failures; c_R is average cost on one failure repair, consisting of costs on material and costs on work.

b) Costs on vehicle preventive maintenance. The costs include the scheduled costs of the maintenance which is done in accordance with the determined time plan for vehicle maintenance.

Total costs amount which will be necessary to spend on preventive maintenance during operating state apparently depends on the number of preventive maintenance actions which are necessary to be done on the object during its usage, and on the costs amount necessary to carry out these preventive maintenance actions. For the costs on preventive maintenance the following equation can be used:

$$C_{OMP} = t\,\hat{c}_M \tag{7}$$

where C_{OMP} is costs on preventive maintenance during operating time t; t is operating time in kilometres; $\hat{c}_M$ is average cost on ensuring preventive maintenance, consisting of costs on material and costs on work relating to an operation time unit.

c) Total costs on vehicle maintenance. The total costs on vehicle maintenance consist of preventive and corrective maintenance.

$$C_{OM} = C_{OMC} + C_{OMP} \tag{8}$$

3.4. Determination of vehicle durability time upon selected life cycle costs

This is one of possible methods employed for the determination of the vehicle life cycle. The determination of vehicle durability time based on LCC may be performed in two ways:

a) By deducing optimal life cycle costs directly from the graph.

b) By determining optimal life cycle costs using points of the elaborated graph through which a suitable regression curve shall be laid. This curve is expressed by an equation of function $f(x)$. For expressing the function equation, Matlab software may be used, or any other that meets required conditions. Calculation procedure:

- Finding a local extreme of the function within [0, T_D] domain, where T_D is vehicle durability time. The calculation is performed with the first derivation of function $f'(x)$, where the following applies:

$$f'(x_0) = 0. \tag{9}$$

The result is a local extreme within interval [0, T_D].

- Finding a strong local minimum of the function within [0, TD] domain:

$$f''(x_0) = 0, \tag{10}$$

After the function minimum within the searched interval [0, T_D] is determined, it is necessary to determine the value of vehicle durability time. It is recommended to determine optimal mileage interval which is 5 to 10 % higher than the calculated value of the minimal costs, see Fig. 2.

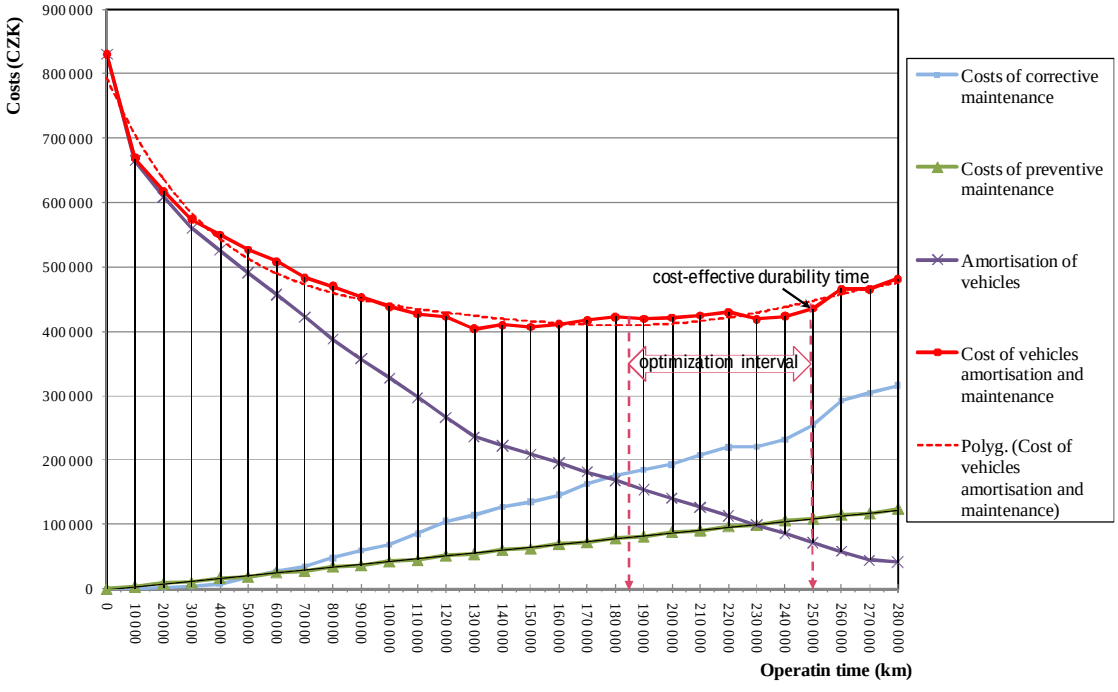

Fig. 2. Example determination of optimal durability time depending on costs for vehicle Land Rover Defender [2]

4. Vehicle Durability Determination Depending on Failure Intensity

The second method of determining optimal vehicle durability time is based on the calculation of failure intensity formula (11). Failure intensity $z(t)$ is the limit, if this exists, of the ratio of the mean number of failures of a repaired item in a time interval $(t, t + \Delta t)$, and the length of this interval Δt, when the length of the time interval tends to zero, given that the item is in an up state at the beginning of the time interval.

$$z(t) = \lim_{\Delta t \to 0+} \frac{E[N(t+\Delta t) - N(t)]}{\Delta t} \tag{11}$$

where $N_{(t)}$ is the number of failures in the interval $(0, t)$; E is denotes the expectation; $t + \Delta t$ is the time interval.

Generally we can divide failure intensity into three different stages:

- in the first stage of failure intensity there is a steep grow;
- in the second stage failure intensity oscillates around a constant value. The probability of failure occurrence in a random moment is practically the same. Periodical oscillation $z(t)$ is caused by periodical maintenance;
- in the third stage there is a rapid grow in failure intensity and further usage of the vehicle becomes uneconomic, and therefore it is necessary to consider vehicle liquidation or to carry out so called overhaul.

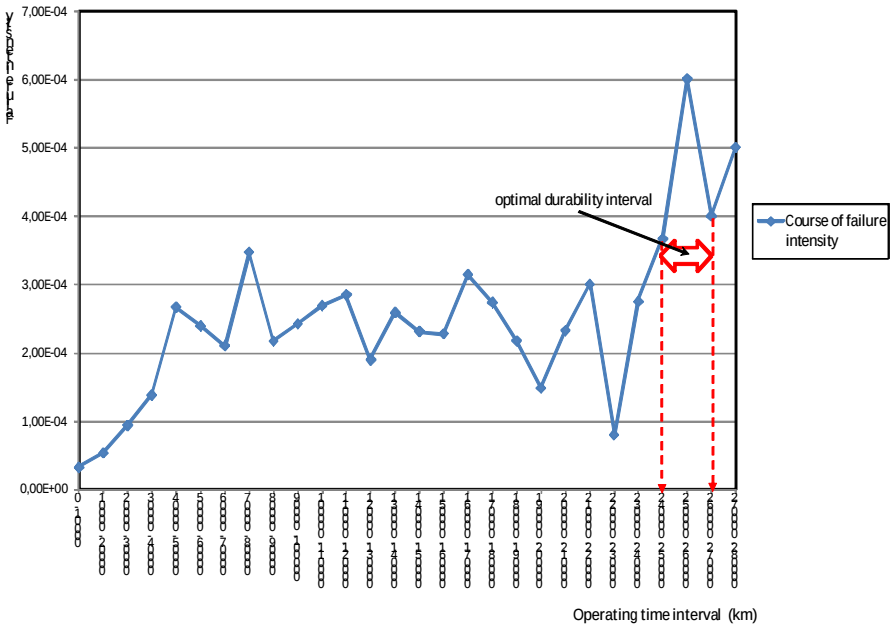

Fig. 3. Example expression of failure intensity-kilometrage dependency for vehicle Land Rover Defender [2]

5. Conclusion

The article describes two possible approaches to the determination of optimal vehicle durability time. To carry out this task successfully, it is necessary to collect and sort data on the occurrence and relevancy of failures, costs on failures removal, preventative maintenance costs and costs on operating state. The article shows two separate approaches to the determination of vehicle durability time. The first solution is based on the vehicle life cycle cost calculation. In the second case, the failure intensity calculation has been used. In this case, the vehicle durability time for the Land Rover Defender was calculated at 250000 km. This results from the calculation using both abovementioned independent methods.

References

1. **Furch J.** Dependence of Vehicles Life Cycle Costs and Failure Intensity on the Vehicles Durability. “Machines, Technologies, Materials”, volume 2-3/2007, p. 17-19.
2. **Furch J.** Design of Operational Vehicle Maintenance Programme Based on Life Cycle Cost and Reliability Centred Maintenance. Advances in Military Technology. 2009, vol. 4, no. 2, p. 37-54.
3. Znalecký standart č. I/2005. Oceňování motorových vozidel. Akademické nakladatelství CERM, s.r.o. Brno: 2005.

Acknowledgement

The work presented in this paper has been supported by the Ministry of Defence of the Czech Republic (research project No. MO0FVT0000401).

Proceedings of 5th International Conference ITELMS'2010

Non-Destructive Analysis of Heat-Resistant Steel Applied to Continuous Caster Roll after Plastic Deformation

P. Yasniy*, P. Maruschak*, V. Hlado*, V. Hutsaylyuk, R. Bishchak***

** Ternopil Ivan Pul'uj National Technical University, Ruska 56 str., 46001, Ternopil, Ukraine, E-mail: Maruschak.tu.edu@gmail.com*
*** Military University of Technology, Kaliskiego str. 2, 00-908, Warsaw, Poland, E-mail: v.hutsaylyuk@ wat.edu.pl*

Abstract

The hardness, microhardness and microstructure of steel 25Kh1M1F after tensile plastic deformation are studied in this paper. Using the statistical analysis of the data on the microhardness, the effect of the deformation temperature on the microhardness variation coefficient, which is one of the numerical characteristics of the material damageability, has been established. The microstructure of the specimens was investigated by SEM and TEM microscopy.
KEY WORDS: *Hardness, surface, deformation, defects, damage, anisotropy.*

1. Introduction

Up to now a great number of the methods to control the physico-mechanical parameters of a plastically deformed material have been known. The choice of the method of investigation is usually caused by the sensitivity of the material under study to variations in the material damage [1]. The hardness and microhardness are among the parameters characterizing the mechanical properties of structural materials. The statistical analysis of the hardness and microhardness makes it possible to explain the basic mechanisms of damage accumulations after exposure to different modes of deformation and to assess the degree of their spread. The scattering parameters depend, to a great extent, on the conditions of deformation as well [3-5]. In particular, the temperature that increases the deformability of the material and homogenizes the microstructure is one of the most important influencing factors [6].

2. Testing Procedures

The aim of the present work is to establish main regularities of the temperature effect on the micromechanisms of deformation and ferritic-pearlitic steels and to estimate the material hardening based on the equation:

$$\tilde{y} = \ln(F_0 / F) \tag{1}$$

where F_0, F are the initial and current cross-section areas, respectively.

The hardness was measured using a Super Rockwell hardness meter at an indentation load of 150 N. The microhardness was measured on a PMT-3-type device at an indentation load of 1.0 N. The microstructure of specimens from steel 25Kh1M1F in their initial state and after tensile deformation was studied using a transmission electron microscope type TEM-125K and scanning electron microscope SEM-106I.

The material hardening as a function of the test temperature and plastic strain value was determined from the hardness and microhardness, whereas the nonuniformity of the material hardening (inhomogeneity) by the method of the statistical processing of the results of the microhardness measurements [4]. The coefficient of variation of the studied parameter was determined by the formula:

$$n_H = \frac{s_H}{\overline{H}} \tag{2}$$

where $\overline{H}$ is the mean value of the studied parameter, $\overline{H} = \frac{1}{n}\sum_{i=1}^{n} H_i$; n is the number of measurements; H_i – is the current value of the studied parameter; s_H is the mean-square deviation, $s_H = \sqrt{\frac{1}{n-1}\sum_{i=1}^{n}\left(H_i - \overline{H}\right)^2}$.

3. Plastic Strain Effect on the Change in the Dislocation Structure of Steel

All the 25Kh1M1F steel specimens have been prepared for microstructure analysis using standard metallographic practice 5% nital is used as etchant. Volume fraction of pearlite is measured by point counting method and grain size is measured. Scanning microscope micrograph of as-received 25Kh1M1F steel specimens at

magnification ×100 is shown in Fig. 1. Here black region depicts pearlite and «white» region is ferrite. The average grain size is 30 ... 40 μm.

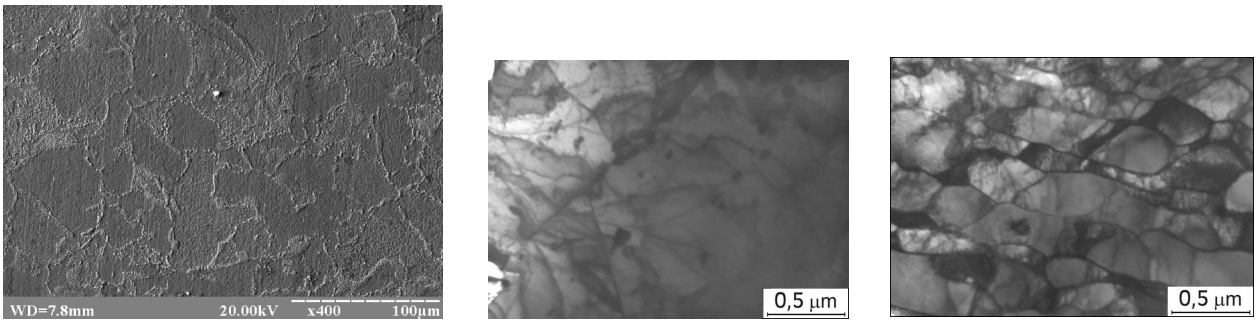

a b c

Fig. 1. SEM (a) and TEM (b) micrograph of ferrite-pearlite structure of 25Kh1M1F steel in the initial state and structure after maximum plastic deformation

Steel 25Kh1M1F of the load-bearing layer belongs to steels of the ferritic-pearlitic class (Fig. 1, a). In the nondeformed material, there was revealed the presence of structurally free ferrite, pearlitic colonies situated in different parts of ferritic grains and carbide inclusions of an elongated and globular shape. The dislocation microstructure of steel 25Kh1M1F in its initial state has a reticular and partially cellular dislocation structure (Fig. 1, b).

After plastic deformation of the ferritic-pearlitic steel 25Kh1M1F, at a temperature of 600°C, with an increase in the strain, the reticular and partially cellular dislocation structure is transformed into the following structures: the tangle and cellular nondisoriented structure; the cellular disoriented and partially fragmented structure; the areas of the completely fragmented dislocation structure are formed (Fig. 1, c). The character of the processes involved in the formation of dislocation substructures is indicative of the processes of self-organization of the deformed material. To every substructure of the material there corresponds a proper range of the dislocation density [7].

4. Effect of Temperature on Hardening of the Deformed Steel

In this paper the influence of temperature of deformation on microstructure and hardness of heat resistance steel (25Kh1M1F) was investigated. The dependence of the hardness and microhardness of steel 25Kh1M1F upon the actual necking was studied after tensile deformation at temperatures of 20°C, 375°C, 600°C (Fig. 2).

The intensity of hardening is governed by the initial hardness (microhardness) of the material and its microstructure, which determines the magnitude of the hardness (microhardness) increment at various degrees of deformation. The material properties after plastic deformation depend on the changes in its microstructure. As is seen from Fig. 2, a considerable reduction in the rate of increase in the hardness (microhardness) is observed in steel 25Kh1M1F at a temperature of 600°C, which is likely to be associated with the effect of thermal change at this temperature. High temperatures are responsible for the increase in the plasticity of materials, which contributes to their self-acting reorganization, with the result that a free energy of grains is lowered. Thus, as a result of the thermal change, the dislocation density decreases, and the remaining dislocations form stable configurations in the form of low-angle boundaries [6]. Thus, it is seen from Fig. 2 that the hardness (microhardness) of deformed steel 25Kh1M1F at all the temperatures studied (20°C, 375°C, 600°C), depends on the actual necking linearly. The slope angle of the rectilinear dependence is defined by the intensity of the material hardening at different temperatures.

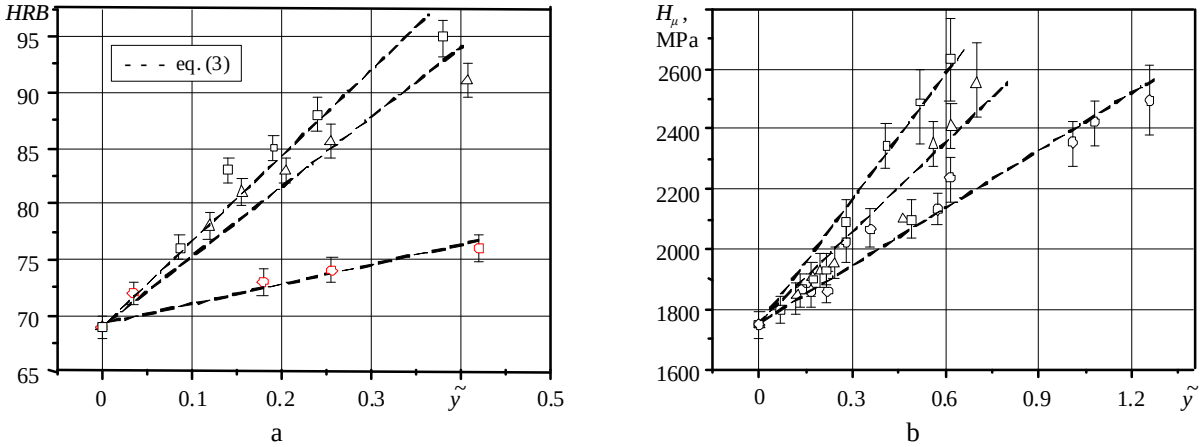

a b

Fig. 2. Dependence of the hardness (a) and microhardness (b) of steel 25Kh1M1F on the actual necking at temperatures of 20, 375, 600°C (The symbols are given in the Table 1, calculations are made by equation (3))

In accordance with the experimental data obtained, the interrelation between the hardeness (microhardness) parameters and actual necking at different test temperatures can be described by the linear dependence:

$$H = H_0 + k\tilde{y} \tag{3}$$

where H_0 is the initial hardness (microhardness) of the material; ΔH is the increment of the material hardness (microhardness) after deformation; k is the coefficient characterizing the intensity of hardening.

The values of the parameters of equation (3) for steel and 25Kh1M1F at the test temperatures under study are given in the Table 1 below.

Table 1

The parameters of equation (3)

Steel	Symbol	Test temperature, °C	H_0		k
			H_μ, MPa	*HRB*	
25Kh1M1F	□	20	1750	68	1359 / 75.3
	△	375			1028 / 61.0
	○	600			646 / 18.3

* the values of the coefficient for the hardness are presented in the numerator and those for the microhardness are presented in the denominator.

5. Effect of the Plastic Strain on the Change in the Coefficient of Variation in the Microhardness

It has been revealed that at the initial stage of the material deformation, the coefficient of variation in the microhardness increases with various intensity at different test temperatures (Fig. 3), which is caused by the different plasticity at different temperatures (different intensity of hardening). With the increase in the deformation temperature, the rate of increase in the coefficient of variation diminishes (Fig. 3).

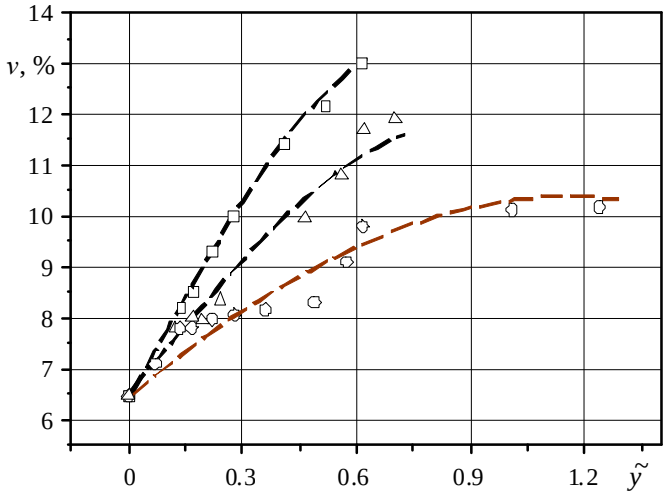

Fig. 3. Dependence of the change in the coefficient of variation of the microhardness of steel 25Kh1M1F (on the plastic strain value at temperatures of 20 °C, 375 °C, 600 °C (The symbols are given in the Table 1.)

Under plastic deformation, the hardening – the transformation of the dislocation structure – occurs. At the initial stage of deformation, the material hardening occurs at the local areas, which reveals itself in the considerable increase in the coefficient of variation. At this stage, in the majority of cases, individual grains of the material are subjected to deformation, that is to say, the nonuniformity of deformation of the adjacent grains and their groups is the cause for the internal nonuniformity and localization of the plastic deformation. With the increase in the plastic strain, the rate of increase in the coefficient of variation diminishes. Under further deformation, when the plastic deformation gradually occupies the entire volume of the material, the material hardening is continued (both the hardness and microhardness are increased). However, the coefficient of variation is stabilized since the hardening in the material occurs more uniformly (Fig. 3). Further loading is accompanied by the increase in the microhardness but the rate of increase in the material nonuniformity during deformation is reduced due to the mutual adaptation of structural elements and their self-organization. Figure 4 shows the magnified SEM images of the surfaces with normal stress fracture. The fracture surfaces of the specimens at 600°C were found to be covered with dimples. On the other hand, the fracture surfaces of the specimens investigated at 20°C were covered with the quasi-cleavage zones and dimples.

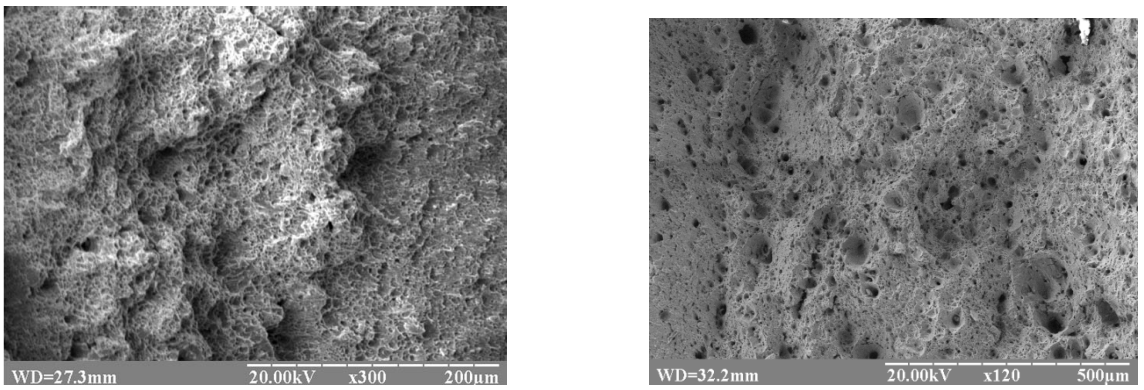

a b

Fig. 4. Fracture surfaces of the ruptured at 20°C and 600°C specimens after the tensile test

However, the low ductility fracture surfaces here at 20°C contained shallow and small size of dimple compared at 600°C. Generally, ductile fracture in 25Kh1M1F steel is frequently initiated by the fracture of precipitates of inclusions or by their parting from the metal matrix, final failure then arises as a consequence of the coalescence of voids formed in this way.

6. Conclusions

With increasing strain under conditions of plastic deformation of ferritic-pearlitic steel 25Kh1M1F, the reticular and partially cellular dislocation structure is transformed into the tangle, cellular and fragmented dislocation structures. The mean value of the hardness and microhardness of the steel 25Kh1M1F under study increases linearly with the increase in the plastic strain value. With the increase in the test temperature, the rate of increase is diminished for the steel 25Kh1M1F. It has been found that with the increase in the plastic strain value, the coefficient of variation in the microhardness of the plastically deformed steel 25Kh1M1F increases and reaches a plateau at certain values of the strain. This is caused by more uniform structural changes and the decrease in the degree of localization of the plastic deformation.

References

1. **Lebedev A. A., Chausov N. G.** Advanced methods for assessing the degradation of the mechanical properties of structural metal during the operating time. - Kyiv, G.S. Pisarenko Inst. for Problems of Strength, Nat. Ac. Sci. of Ukraine, 2004. – 133p.
2. **Lebedev A. A., Muzyka N. R., Volchek N. L.** Determination of damage accumulated in structural materials from the parameters of scatter of their hardness characteristics.- Strength of Mat., 2002, Vol. 34, p. 317-321.
3. **Lebedev A. A., Makovetskii I. V., Muzyka N. R.** et al. Estimation of material damage level by scatter of characteristics of elasticity and static strength.- Strength of Mat., 2006, Vol. 38, p. 109-116.
4. **Yasniy P., Maruschak P.,** and **Hlado V.** Hardening of heat-resistant steels under conditions of plastic deformation at different temperatures. In: Pavlou D.G., editor. Computational & Experimental Analysis of Damaged Materials, Transworld Research Network, 2007, p. 167-182.
5. **Yasniy P., Hlado V., Maruschak P., Baran D.** Evaluation of hardening of plastically deformed steels. - Proc. XIII Int. Conf. on Experimental Analysis of Nano and Engineering Materials and Structures. Alexandroupolis, July 1-6, 2007, p. 147-148.
6. **Yasniy P., Maruschak P., Hlado V., Baran D.** Correlation of the microdislocation parameters with the hardness of plastically deformed heat-resistant steels.- Materials Science, 2008, Vol. 44, p. 194-200.
7. **Keh A. S., Weissmann S.** Deformation Substructure in Body-Centered Metals, in Electron Microscopy and Strength of Crystals, Ed. by G. Thomas and J. Washburn. - Interscience, New York, 1963, p. 231–300.

Proceedings of 5th International Conference ITELMS'2010

The Monitoring and Control System of the Intrapipe Sealer

Y. Kryshneu, L. Zakharanka, E.Vinagradau, A. Khramau, A. Sakharuk, M. Stalbou, V. Starastsenka

Pavel Sukhoi State Technical University of Gomel, Pr.Octiabria., 48 , 246746, Gomel, Belarus, E-mail: kyuri73@tut.by

Abstract

In the paper the monitoring and control system of the intrapipe sealer, intended for carrying out repair work on the oil pipelines, is considered. The system structure, its general work principle, data transmission and reception algorithms and the results of the experimental researches are presented.
KEY WORDS: *intrapipe sealer, monitoring and control system, inlet flap, rod movement sensor, signal attenuation, information signal transmission, data transmission algorithm.*

1. The Structure and Designation of the Monitoring and Control System of the Intrapipe Sealer

Intrapipe sealers are applied on oil pipelines for the performance of repair work. They are equipped by the gaskets moved by the pressure of oil, what allows the shell to be fixed in the pipeline.

Standard sequence of performance of operations at repair work with the sealer use is the following.

1. As sealer approaches the repair place, it is detected by the «beacon» signal.
2. A command to stop the pumps is given.
3. A latch of the pipeline is closed below the sealer position.
4. The pressure in the pipeline is rises until the entrance membrane of the hydrocylinder is destroyed. The hydrocylinder piston moves and through the system of levers unclenches sealer gaskets. On the piston there is a rod with grooves into which the mechanical clamps keeping the final position of the piston enter, and, hence, and the pressure of the gaskets upon pipeline walls. At the expense of this the sealer stops and keeps the hydrostatic pressure of the column of oil.
5. Repair work on the pipeline is carried out.
6. After the end of the works the latches open, at inclusion of the pumps the pressure in the pipeline rises, the sealer moves from its place and is carried away by an oil stream.

At present time for tracing and detection of the sealer location is used the CD–42 system, which consists of a transmitting part («the beacon»), mounted on the sealer, and a receiving part ("the locator").

The experience of use of the intrapipe sealer at the RUE "Gomeltransoil Druzhba" together with the CD–42 system has revealed its essential lacks:

1. Absence of the information on the real position of the piston of the hydrocylinder, and, hence, and about position of the sealer gaskets.
2. A weak «beacon» signal owing to what on some sites of the pipeline it is impossible to define the sealer location.

For sealer operation the pressure in the pipeline rises. As on many sites the pipeline is considerably worn out, a large increase of the pressure can lead to its damage. One more lack of the given way of control is the impossibility of the exact assignment of the sealer operation moment.

The monitoring and control system of the intrapipe sealer is intended for simplification of the search of the intrapipe sealer, oil pipeline sealing process automation and monitoring.

Technical requirements for the monitoring and control system of the intrapipe sealer are the following:

- The detection device should duplicate functionally the basic functions of regular system of detection of CD–42.
- The control unit should open the inlet flap to start the sealing process on the command given from the land device.
- The rod moving measuring instrument should be mounted on the intrapipe sealer of the standard design or with its insignificant adaption. Inaccuracy of the rod movement measuring should not exceed 10% from the rod full movement.

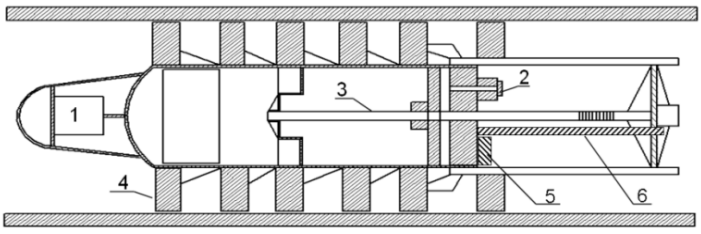

Fig.1. The sealer schematics: 1 – the CD–42 system beacon; 2 – the membrane; 3 – the rod; 4 – the gaskets; 5 – the antenna unit; 6 – the measuring unit

- The device should provide the measuring information transmission from the pipe line for spacing interval not less than 3 m.
- The device should keep its functionality at the pressure levels of 5MPa in the environment of oil.

2. The Monitoring and Control System of the Intrapipe Sealer Block Ddiagramme

The monitoring and control system of the intrapipe sealer block diagramme is presented on fig.2, and functional diagrammes of the land transceiving unit (LTU) and the intrapipe unit (IU) is presented on fig.3.

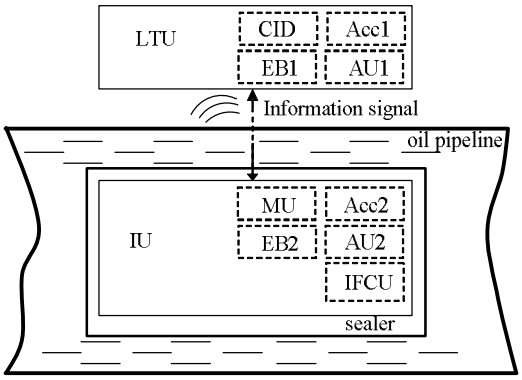

Fig.2. The monitoring and control system of the intrapipe sealer block diagramme: LTU – the land transceiving unit; CID – the control and indication desk; EB – the electronics block; Acc – the accumulator; AU – the antenna unit; IU – the intrapipe unit; MU – the measuring unit; IFCU – the inlet flap control unit

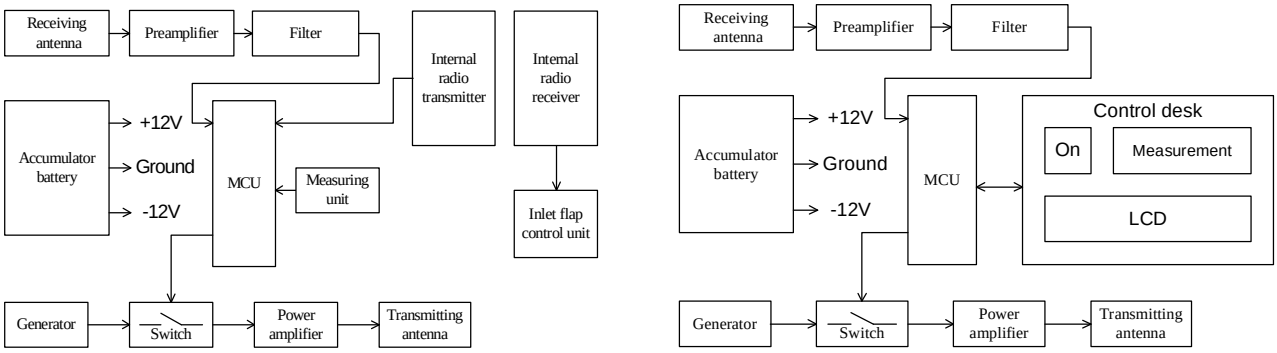

Fig.3. Functional diagramme: a – IU; b – LTU

3. Calculation of the Signal Attenuation by the Pipe Walls

To define the requirements to the parameters of the transceivers transmitting signal into the pipe line and reverse, it is necessary to calculate the signal attenuation in the environments "air–soil–pipe line". Passing each of the environments will result in signal attenuation, however 90 ... 95% of attenuation will be determined by the pipe line steel. As a matter of fact, the pipe line is the shield for magnetic fields. We will estimate the influence of this shield on magnetic field attenuation in the pipe. The attenuation coefficient can be determined approximately [1] on the equation:

$$K = 1 + \frac{m_r \, d}{D} \tag{1}$$

where: μ_r is the relative magnetic conductivity of the shield material (steel); d is the shield walls thickness; D is the diameter of the equivalent spherical shield close to the cubical shield wall length.

Taking into account that the magnetized steel has $\mu_r = 100 \ldots 1000$, the attenuation coefficient will be:

$$K = 1 + \frac{(100...1000) \cdot 10 \text{ mm}}{800 \text{ mm}} = 1.75 ... 17.5$$

Let's simulate the magnetic field allocation in Elcut software. For this purpose we will build a project in which the conductor with a current is disposed on certain distance from a pipe and compare values of a magnetic induction with and without the tube in the same point. The simulation results are presented on Fig. 4.

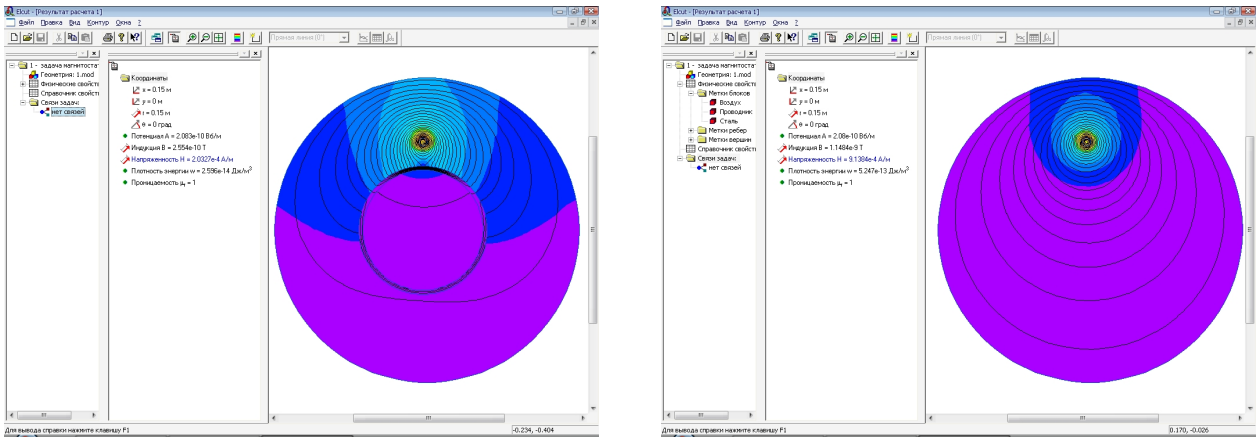

a b

Fig. 4. The simulation results of the magnetic field allocation in Elcut software: a– magnetic field allocation with the shield; b – magnetic field allocation without the shield

From results of simulation it is clear, that a magnetic induction in the point x = 0.15 m; y = 0 m is equal to:

- without the pipe: B = 1.1484 nT;
- with the pipe: B = 0.2554 nT.

Let's calculate the attenuation coefficient:

$$K = \frac{1.1484}{0.2554} = 4.496$$

According to [2], it is possible to apply the following method of the signal attenuation calculation.

Let's suppose that it is necessary to shield some field of room in an uniform magnetic field with intensity H_0, for example cylindrical, so that field intensity in it was many times less, than intensity of an exterior field.

The cylindrical shield with the internal radius a, external radius b has the relative magnetic conductivity μ_{2r}, (see Fig. 5).

Let's mark the internal area as I, area of the shield body as II, area outside the shield as III.

Areas I and III has a relative magnetic conductivity equal to 1. As in all three areas there is no current the magnetic field in them is described by the Laplace equation $\nabla^2 j_m = 0$. Let's suppose the shield to be stretched enough along the z axis (the z axis is perpendicular to the Fig. plane); j_m depends only on co–ordinates r and a of the cylindrical system. Let's open the equation $\nabla^2 j_m = 0$ in the cylindrical system:

$$\nabla^2 j_m = \frac{1}{r}\frac{\partial}{\partial r}\left(r\frac{\partial j_m}{\partial r}\right) + \frac{\partial^2 j_m}{r^2 \partial a^2} = 0$$

Solving it by the method of Fourier – Bernoulli gives the following:

$$\text{for the first area } \; j_m{}^I = \left(C_1 r + \frac{C_2}{r}\right)\cos a$$

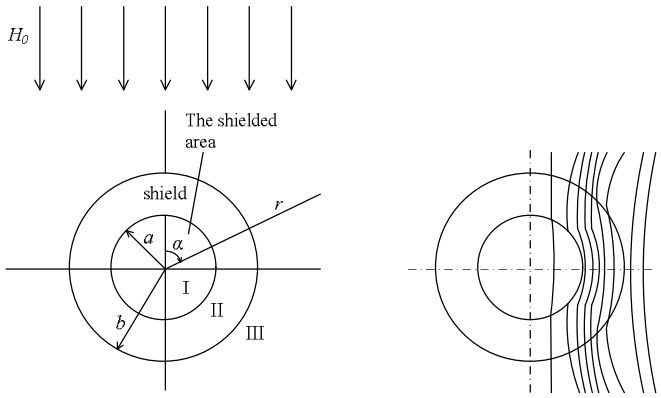

Fig. 5. To the calculation of the signal attenuation by the pipe wall

for the second area $j_m^{II} = \left(C_3\, r + \frac{C_4}{r}\right)\cos a$

for the third area $j_m^{III} = \left(C_5\, r + \frac{C_6}{r}\right)\cos a$

The joint solution of all equations results in the potential expression in the first area:

$$j_m^{I} = H_0 \frac{2\, q\, b^2}{\Delta} r\cos(a)$$

or passing to the Cartesian reference system (the x axis is directed upwards, $x = r\cos a$)

$$j_m^{I} = H_0 \frac{2\, q\, b^2}{\Delta} x$$

where $q = \frac{2m_{2r}}{(1+m_{2r})^2} \approx \frac{2}{m_{2r}}$; $\Delta = b^2 - b^2 a^2$; $b = \frac{m_{2r}-1}{m_{2r}+1} \approx 1$.

Field intensity in the first area (modulo):

$$H^I = \frac{\partial j_m^I}{\partial x} = H_0 \frac{2\, q\, b^2}{\Delta}$$

The relation of field intensity inside the shield to the intensity of exterior field H_0:

$$\frac{H^I}{H_0} = \frac{2\, q\, b^2}{\Delta} \approx \frac{4}{m_{2r}} \frac{b^2}{b^2 - a^2} \qquad (2)$$

Calculation under the formula (2) for the given geometrical sizes gives the following result: $\frac{H^I}{H_0} = \frac{4}{m_{2r}} \frac{b^2}{b^2 - a^2} = 0.81$ or, at m_{2r} = 100 ... 1000, the attenuation coefficient is equal to 1.24 ... 12.4.

Apparently, calculation under formulas (1) and (2) gives values of the same order.

At any m values the signal attenuation increases with frequency magnification and that faster, than steel magnetization is less. The maximum level of the transmitted signal will be observed in the field of low frequencies. However it is necessary to notice, that build-up of the communication channel in the field of very low frequencies is problematic for the reason of unreal big required dimensions of the receiving and transmitting inductors (antennas). The conciliatory proposal is the work in a range of frequencies 20 ... 25 Hz when the transmission factor is about the level of 0.1 at the medial value of the pipe line steel magnetization.

For the operation of the monitoring and control system of the intrapipe sealer transceiver the frequency of 22 Hz is selected, considering the following:

- the operation frequency must not be multiple to the cathodic protect stations pulsations frequency (100 Hz) and to the network frequency 50 Hz;
- compatibility with the locator of the regular CD–42 system;
- sufficient speed of information exchange between land and intrapipe units.

4. Experimental Research of the Conditions of the Signal Transmission Between IU and LTU

Experiment № 1. The research of impulse attenuation by the magnetic shield. For the experiment realization a special steel container with the wall thickness of 12 mm. was made, into which the IU transceiver circuit was put. The scheme of experiment is demonstrated on Fig. 6, and the digital results of the experiment are presented in table 1.

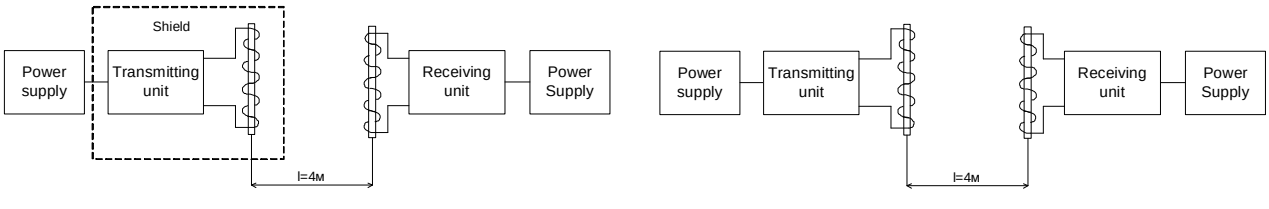

a b

Fig. 6. The scheme of experiment № 1: a – IU is not placed into the shield; b – IU is placed into the shield

Table 1

The results of the experiment: the research of impulse attenuation by the magnetic shield

The experiment conditions	The amplitude value, V
IU is not placed into the magnetic shield	3.5
IU is placed into the magnetic shield	0.23

Experiment № 2. The dependence of the signal amplitude on spacing interval to the receiver (the transmitter is inside the shield).

The scheme of experiment is demonstrated on fig.7, the digital results of experiments received at various values of spacing interval between LTU and IU, placed inside the shield, are presented in tab. 2 and on fig. 8.

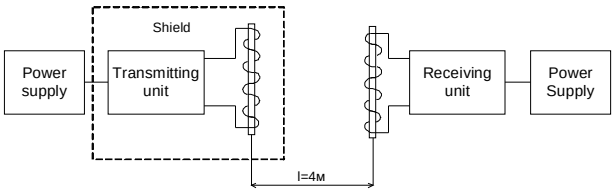

Fig. 7. The scheme of the experiment № 2

Table 2

Results of experiment: dependence of amplitude of a signal on spacing interval to the recipient (the transmitter is inside the shield)

Length *l*, m	The amplitude value, V
1	9
1.6	3.3
2.3	1
3	0.85
3.5	0.47

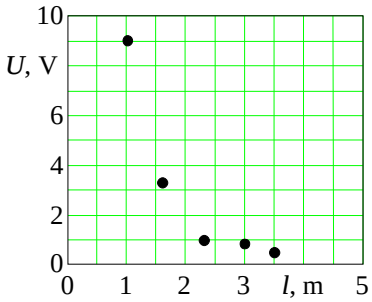

Fig. 8. The experimental dependence of the signal amplitude on spacing interval between the receiver and the transmitter

5. Algorithms of the Data Transmission and Rreception

IU in a regular mode works in the «beacon» mode, i.e. it produces packs of impulses with the duration of 0.36 s and the following phase of 1.45 s. (for the compatibility of the device with the CD–42 locator system), as is shown in Fig. 9. In the time interval when impulses are not transmitted, IU is tuned on reception.

If IU detects the beginning of the request signal, the «beacon» signal is not sent. After the request reception IU shapes a code sending (Figs 11, 12), containing the measuring information, and begins its transmitting.

Launching bit S corresponds to the logic «1», and the data bits D0–D3 encode the measuring information in the binary code. The parity bit P supplements the data code to parity.

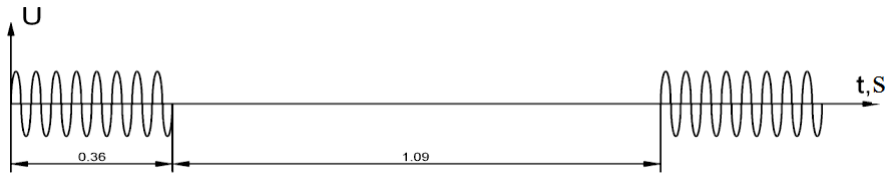

Fig. 9. Time charts of the «beacon» signals

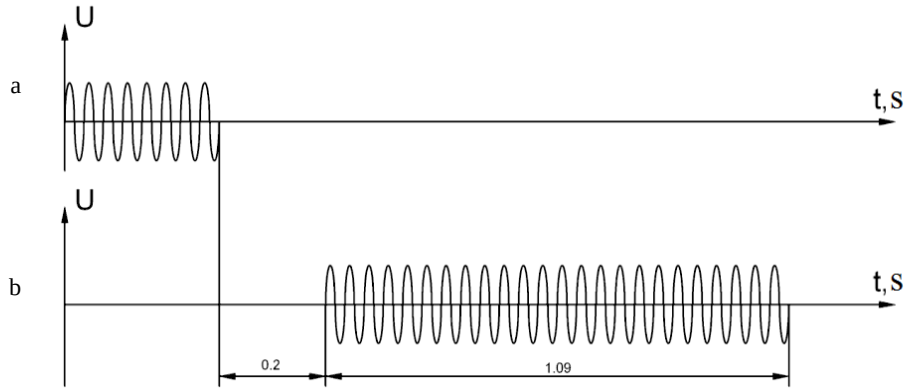

Fig. 10. The request sending: a – the «beacon» signal from IU; b – the request signal from LTU

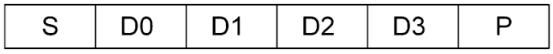

Fig. 11. The format of data sending: S – launching bit; D0–D3 – data; P – parity bit

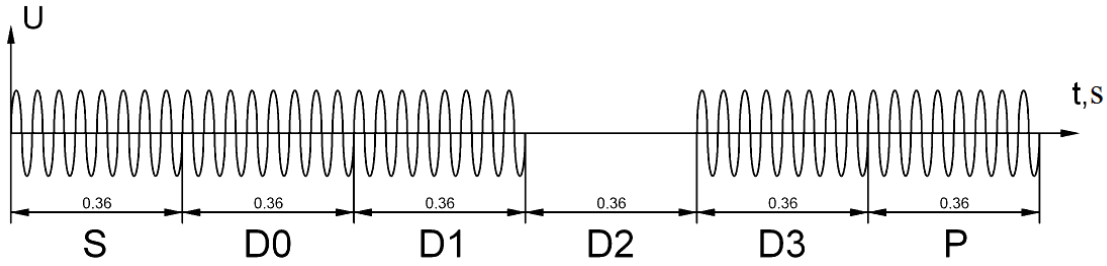

Fig. 12. The example of sending «1011» code

6. Conclusions

1. The structure and the working principle of the monitoring and control system of the intrapipe sealer have been determined. Taking into account the conditions of its operation the optimum transmission frequency of the operating and measuring information (22 Hz) have been determined.
2. All electronic blocks of the intrapipe and land transceiving units are designed, produced and experimentally verified. The IU «beacon» operating mode is provided so that its signal is detected by the regular CD–42 locator system.
3. Experimental verification of the information signal transmission conditions from IU to LTU and reverse has been carried out with the change of various affecting factors: spacing intervals, complementary shielding of the environment, voltage level of the self-contained supply. The results of the experiments indicate the correspondence of the designed device to the requirement specification.

References

1. **Каден Г.** Электромагнитные волны в высокочастотной технике и технике связи. – М.: Госэнергоиздат, 1946. – Т.1.–р. 20-25.
2. **Бессонов Л. А.** Теоретические основы электротехники. – 1964. –р. 637-639.

Modeling of Embedded Intelligent Device for Control of City Electric Transport

A. Potapovs*, M. Gorobetz, A. Levchenkov**, L. Ribickis****

** Faculty of Power and Electrical Engineering, Riga Technical University, 1, Kalku Street, LV-1658, Riga, Latvia, E-mail: Andrejs.Potapovs@rtu.lv*
*** Institute of Industrial Electronics and Electrical Engineering, Riga Technical University, 1, Kalku Street, LV-1658, Riga, Latvia, E-mail: mihails.gorobecs@rtu.lv; anatolijs.levcenkovs@rtu.lv; leonids.ribickis@rtu.lv*

Abstract

In this day's the permanent increase of traffic in urban areas becomes a topical issue related to public transport routing accuracy and accurate performance of following the schedule. These problems often caused traffic jams and other unforeseen stopping reasons, but sometimes this reason of such delays is behavior of urban public transport drivers. Therefore, it is proposed to develop a control system and its operational algorithm, which helps the driver to follow the timetable with maximum precision and increased quality service for the passengers.
KEY WORDS: *electric transport; embedded systems; intelligent control; control algorithm.*

1. Introduction

The offer system will significantly increase electric transportation routing accuracy (at the time), helping the driver to drive a tram directly to the driving speed, which will guarantee the exact arrival passenger stop.

The system also allows more efficient use of electricity, since often the driver's actions contribute to the fact that there is no maximum saving in electrical consumption (improperly giving unnecessary acceleration and then braking sharply, respectively). All of this leads to the excess power consumption, both- at different electric transport (in our case, the tram) and node excess wear and tear. Under these circumstances, suffering the passengers travel comfort.

In the real system would need to equipped tram with a controller, transmitter, through which the control center could receive data on their location and various sensors, which supply the controller with a control program of the requested data.

View topic is chosen because the automatically controlled systems are large development opportunities in the future.

2. Purpose and Tasks

The authors aim to design an algorithm and implement an accurate guidance system for electric transport.

The main tasks are:

- Analyze the intelligent transport system and define its objects;
- Define the activities in the system and interactions between its objects;
- Develop the electric transport control algorithm;
- Implement the algorithm in "Step-7" programming environment.

Realization of the program using computer software, controllers and stalls equipped with two traffic lights and low power DC motor.

3. System Description

One of the main hubs of the proposed control system is controller C that is installed in the tram, and processing all the information necessary to regulate the movement of the tram by control of tram electric engine E. This operation requires a controller program, after which it also will make all necessary calculations.

As we already known, before beginning any program of writing is required of the program algorithm development. The algorithm is a precise prescription of a task. In other words, the algorithm tells the programmer how to program a given controller, providing every possible situation and error, without any diversion of the set operating principle.

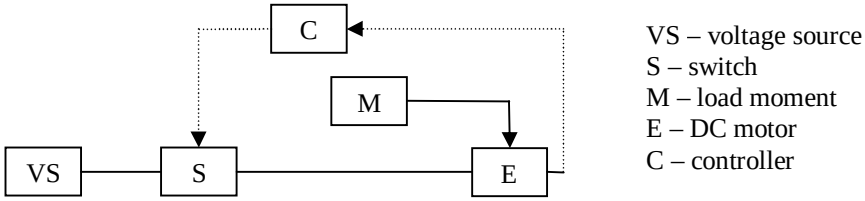

Fig. 1. Engine control systems principle scheme

Be described in electrical control system of operation will be as follows. Tram will take a particular route (Fig. 2.), which will cross over a number of passenger stops, arrival in the exact time specified.

Passenger stop coordinates, or distance from the route to the departure station and arrival time of those programs will be entered into the table, which can provide a large enough number of stops on the data storage, allowing it to enter the whole movement stops on the route list. Each road section between points will be used directly to stop the upcoming data.

Fig. 2. Motion routing scheme

The program allows driving the tram without unnecessary additional equipment, since it is sufficient that the tram will be equipped with a positioning sensor, but the known coordinates of the stops will be given the same program before starting the movement along the route, which will be dispensed without any data exchange between trams and passenger stops. The respective data flow directions between the master control program and data table shown in the 3nd figure, which shows that the main program receiving data from the data tables, send them to the processing of the sub, which also performs all the required tram traffic management functions. Passengers stop coordinates, or time of arrival changes the case, there is always a possibility to effectively implement the necessary adjustments to the data table.

Tram management program using the data to meet the approaching stop activities that one way or another be related to the movement of the tram ride in the required speed or stopping exactly stop.

The required speed of calculation principle will be as follows. Knowing the time at which the tram is due to arrive on the bus, and the rest of the way to stop this will be calculated for average speed, which should take the remaining road section. In case of unexpected stops (stopper, the barrier material or delays in the stop, etc) needed to be converted into speed and movement will take place with this new highest speed. This required the speed calculation will keep the program at each processing cycle, which will provide fast and precise speed needed for a change.

Stopping or slow downing will simulate a supply of specially intended for the controller input signal, which will drop the engine revolutions, after which can be observed as the speed increases when compared with the speed, which has previously been unexpected braking.

The stopping principle will be that, if fulfilled the condition that the distance to the passenger stop is less than the distance by tram traveled slowing it to a certain braking acceleration (which is suitable for passenger convenience and safety), then the signal is fed to the fact that the voltage pulse width is reduced by one percent. This operation will result in the cyclical performance of the tram stop directly in the desired route.

Stopping in the passengers stop (raising the level of automation control algorithm) will be provided a specific tram waiting time, which is required for passenger service. The real world this waiting time, passenger security interests can be controlled by the driver, since the main objective of the algorithm, however, follow the schedule associated with the arrival of stops.

In the next step we can see all the objects and components that will be involved in the control system, as well as the variables that characterize these objects.

1) The main objects that will be used for our tram management model:

- Tram (T);
- Passenger stop Nr. 1;
- Passenger stop Nr. 2;
- Passenger stop Nr. 3.

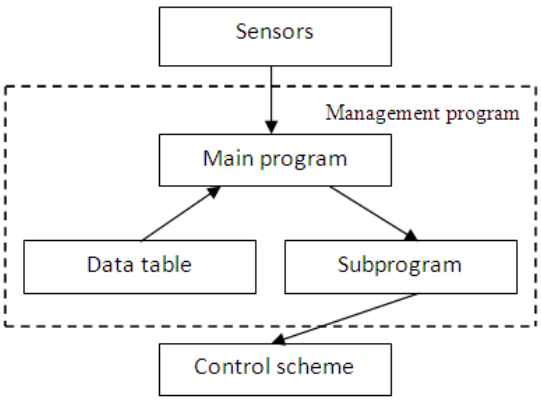

Fig. 3. Data flow chart of management program

2) Components of tram which includes the above-mentioned principal objects:

- Positioning sensor (P_d);
- Rotation speed sensor (A_d);
- Speed sensor (A_{ad});
- Completed road sensor (V_{cd});
- Braking distance sensor (B_{cd});
- Transmitter (R).

3) Variables of tram corresponding to the above attractions:

- Coordinate X_T;
- Engine speed w;
- Speed V;
- The completed road S_T;
- Stopping distance at the current speed S_{br}.

Passenger stop:

- Coordinate X_P.

Formula's whose used in the calculation algorithm. Tram completed road:

$$S_T = X_T \text{ , m} \tag{1}$$

Tram breaking distance

$$S_{br} = \frac{V_T^{\,2}}{2\,a} \text{ , m} \tag{2}$$

The distance from the tram, to the passenger's stop

$$S_{TP} = X_P - X_T \text{ , m} \tag{3}$$

Breaking time

$$t_{br} = \frac{V_T}{a} \text{ , s} \tag{4}$$

Time to stop the motion at constant speed V_T:

$$t_{kust} = \frac{S_{TP}}{V_T} \text{ , s} \tag{5}$$

Braking distance and the distance to the stop the comparison:

$$S_{br} \le S_{TP} \tag{6}$$

The remaining travel time to the next stop

$$t_{atl} = t_P - t_{tekošais} \text{ , s} \tag{7}$$

Required speed

$$V_{nepiec} = \frac{S_{TP}}{t_{atl}} \text{ , m/s} \tag{8}$$

Formula for obtaining the required parameters of the tram. Engine speed

$$w = (U_{imp} - 40)\,70 \text{ , min}^{-1} \tag{9}$$

Simplify the calculation it is assumed that at 40% pulse width of the engine speed is already equal to zero, but at 100% of the voltage pulse width speed is 4200 min $^{-1}$. Tram speed:

$$V_T = \frac{2\,p\;w\;R}{R_p} \text{ , m/min} \tag{10}$$

where R – the tram wheel radius, m; R_p = 7.36 – reducer gear ratio.

Tram speed

$$V_{T\ \mathrm{m/s}} = k\, V_{T\ \mathrm{km/h}}\ ,\ \mathrm{m/s} \tag{11}$$

where $k = 0.27777$ – the calculated ratio.

Formulas for calculating the parameters of trams require full algorithm development. In reality, these parameters can be obtained from the relevant employers, to which will need to calculate these values management program.

4. Algorithm for Task Solution

After all the necessary ingredients of the preparation can begin to draw up the algorithm, after which will be built above the control program, and will be implemented in a programmable controller.

Operational algorithm:

Step 0: Initialization: $U_{imp} = 41\%$; $i = 1$.
Step 1. Read data from the sensors V_T and S_{nobr}.
Step 2. If M0.1 ≠ 1, start timer T38 to time the time the route will be enough to complete rout.
Step 4. Read next stop data from data base X_{Pi}, t_{Pi}.
Step 5. If VW1998 < VW998 and if $S_{nobr} \geq X_P$, then $i = i + 1$ VW1998 = VW1998 + 1.
Step 6. Call *Tram control subroutine*.
Step 7. Return to Step 1.

Tram control subroutine

Step 1. Calculate remaining distance between vehicle and passenger stop on route S_{TP}.
Step 2. Calculate remaining time for arriving in passenger stop – t_{atl}.
Step 3. Calculate necessary vehicle speed – V_{nepiec}.
Step 4. Calculate necessary breaking time t_{br}.
Step 5. Calculate necessary breaking distance between vehicle and passenger stop according current speed – S_{br}.
Step 6. If M0.3 ≠ 1, then start timer T34 to 3 s.
Step 7. If timer is overflow, then set address M0.3 = 1.
Step 8. If M5.3 ≠ 1 and if $S_{br} > S_{TP}$, then $U_{imp} = U_{imp} - 1$.
Step 9. If M5.3 ≠ 1and if $V_T = 0$, then M5.3 = 1 Set.
Step 10. If M5.3 = 1, then start timer T201.
Step 11. If T201 = 1 and if M5.3 = 1, then $U_{imp} = U_{imp} + 1$.
Step 12. If $V_T \geq 0$, then M5.3 = 1 Reset.
Step 13. If address and M1.3 ≠ 1 and vehicle moving speed is smaller then necessary speed for vehicle and smaller then 20, then increase $U_{imp} = U_{imp} + 1$ (speed increasing).
Step 14. END of subroutine.

5. Numerical Example

For example, you can view the following situation. Tram begins route movement from the starting point, or end-stops and starts to approach the station P1. Immediately after the departure of the route from the departure stop coordinates and arrival time tables are read first stop data, which will be used for future management of the tram.

The motion changed during the tram traveled path (coordinates), respectively, decreasing the distance between tram stops and in front of the S_{TP}.

The motion at the start of the distance to the next stop is 1000 m and the arrival time of it after 80 s. Followed by the first moment of the required speed will be calculated as:

$$V_{nepiec} = \frac{S_{TP}}{t_{atl}} = \frac{1000}{80} = 12.5\ \mathrm{m/s}$$

Next, assuming that the motion at $t_1 = 20$ s since the beginning has been a driving need to stop, $t_2 = 5$ s, since that time have the necessary speed will be:

$$V_{nepiec2} = \frac{S_{TP} - V_{nepiec1} \cdot t_1}{t_{atl} - t_1 - t_2} = \frac{750}{55} = 13.63\ \mathrm{m/s}$$

Here the example of simplification is not respected the time that is lost during braking and make speed up (up algorithm it is observed).

6. Testing

The real algorithm for checking equipment was involved in bench (fig. 4.) situated in the industrial programmable controller for Simatic 224 xp (1),, “Ethernet” block (2), the power supply unit (3), fuse (4), router (5) through which only made wireless connections to computers, two traffic lights, (6) DC motor (7).

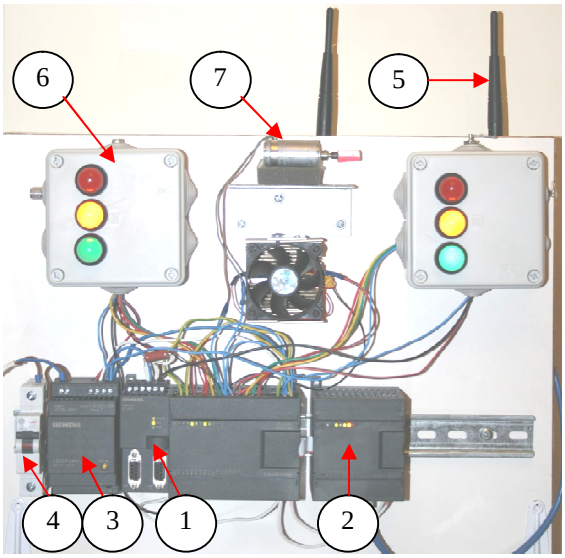

Fig. 4. Stand

When starts running “Step-7” program, was connected to the controller and loaded up the program. “Simulink” medium was prepared by the open model, which graphically depicted the different parameters.

This model was connected to the controller with the program “PC Access” assistance, which provided continuous exchange of data between the controller and the model.

Traffic signal lights were used at the control system controller 24 V output.

Engine control was used in the controller output, which generates a voltage with variable pulse width. It was practically the only size that was controlled and enrolled in reality, in other calculations required values were obtained by leaving them directly from this parameter.

When you run the program where simulated tram movement initiation, which could be inferred from the engine speed climb. "Simulink" environment was admitted to the tram model of speed traveled path versus time (Fig. 5.), who moved after the passenger stop time and the coordinate list, which is depicted in the Table 1.

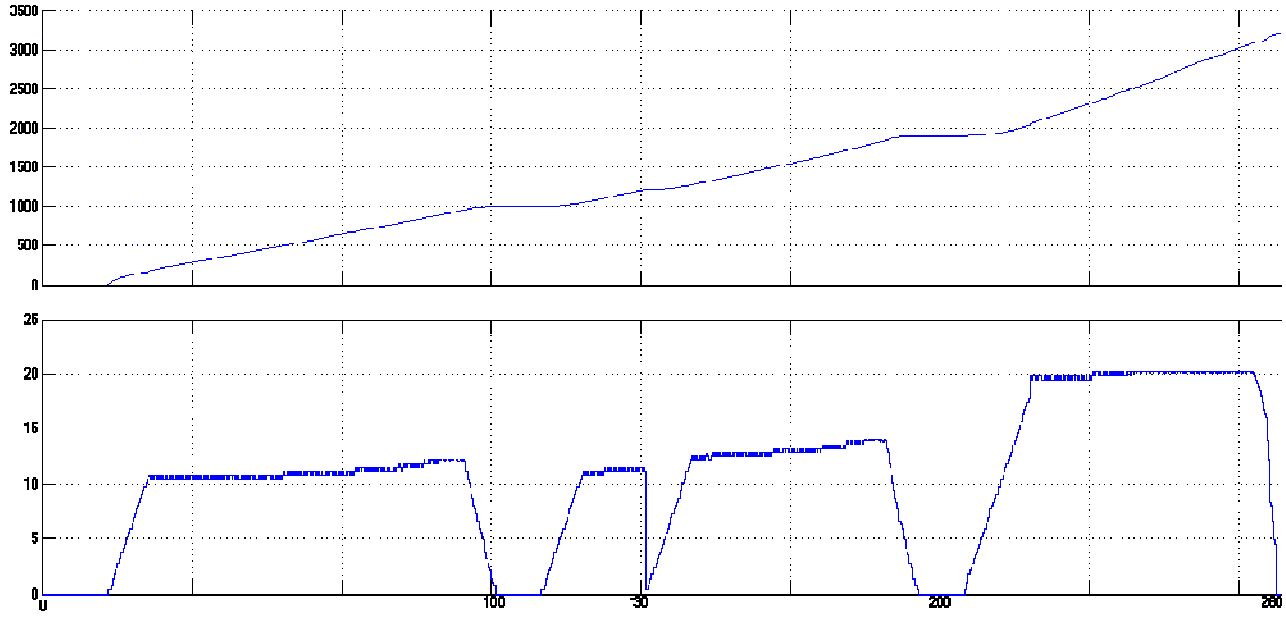

Fig. 5. Tram speed and traveled path dependence of the time

Table 1

Passengers stops data

Nr.	Coordinate X, m	Arrival time t_P, s
1	1000	100
2	1900	200
3	3200	290

From the results, tram is running directly, to the required speed and arrive at exactly the passenger stop time specified, in addition, shows how breaking at path point between the first and second passenger stops, on the road below is increased speed due to lost time.

7. Conclusions

From given results it is impossible to conclude, that the established electric tram control algorithm provides accurate tracking of stops on the schedule time, when driving the tram directly to the speed of what is necessary to the timely arrival of the stop (with some seconds accuracy).

The developed control algorithm also ensures the brake before the tram stops with a specific set an acceleration.

Experimental works with stand where was obtained results confirmed the quality of algorithm and written program.

The topics, for the development is to create the algorithm, involving a real device such as sensors that simulate the occurrence of an obstacle.

The program can create in order to notice the traffic lights, who would also direct make a stop at them, dividing the total route into the smaller pieces, which increase the overall accuracy of the program.

References

1. **Ribickis L., Valeinis J.** Elektriskā piedziņa mehatronikas sistēmās. – Rīga, 2008. – 287 lpp.
2. **Ribickis L., Ļevčenkovs A., Gorobecs M.** Sistēmu teorijas pamati industriālās elektronikas modelēšanā. – Rīga, 2008. – 95 lpp.
3. **Levčenkovs A., Gorobecs M., Ribickis L.** Programmēšanas tehnoloģijas industriālā elektronikā. – Rīga, 2009. – 72 lpp.
4. **Ribickis L., Raņķis I., Ļevčenkovs A., Gorobecs M.** Programmēšanas valodas industriālā elektronikā. – Rīga, 2007. – 69 lpp.
5. **Колесов Ю. Б.** Объектно-ориентированное моделирование сложных динамических систем. – Санкт-Петербург, 2004. – 232 с.
6. **Hunt B. R., Lipsman R. L., Janathan M., Rosenberg A.** Guide to Matlab for beginners and experienced users. University Of Cambridge, 2008. – 351 p.

Proceedings of 5th International Conference ITELMS'2010

Environmental-Economic Analysis of Engine-Driven CHP Plant Running on Liquid Biofuels

L. Raslavičius, A. Strakšas

Lithuanian University of Agriculture, Institute of Agro-Engineering, Instituto g. 20, LT–54132, Raudondvaris, Kaunas region, Lithuania, E–mail: Laurencas.Raslavicius@gmail.com; Anicetas@mei.lt

Abstract

This paper was conducted to forward a plan related to utilization of the first generation biofuels in cogeneration output cycle in Lithuania and to serve as a reference for other researchers working in the field of combined energy production. The first part of the report focuses on existing pecularities of the diesel engine performance and evaluation of obtained results. The second part focuses on economical criterions specific to the Republic of Lithuania and their implemetation following the up–to–date practice in other countries.
KEY WORDS: *CHP, combined energy, energetic independence, first-generation biofuels, liquid biofuels.*

1. Introduction

Liquid biofuels are increasingly being put forward as a renewable fuel for Combined Heat and Power (CHP) plants [1, 2]. Many CHP systems involve heat transmission through distances of 10 ... 50 km (decentralised and centralised CHP plants). In some regions, pure heating plants are attached to a district heating grid [3].

CHP uses fuel to provide all or a part of the electric energy and thermal energy output to a facility at an overall energy efficiency that is greater than what would be required if the electricity and thermal energy were being provided separately. CHP systems use fuels, both fossil and renewable, to produce electricity or mechanical power and useful thermal (heating and cooling) energy far more efficiently and with lower emissions than conventional separate heat and centralized power systems [4].

CHP systems need a balanced relationship between the thermal energy supplied and the electric power produced that depends on the type of CHP system being used. It is also normally important to have thermal loads that are coincidental with the electrical load to make CHP cost effective. The use of thermal energy storage is not typically economic unless the electrical rate structure has a heavy demand charge. Hence, most CHP facilities use the thermal energy at the time it is produced and so thermal energy demand should match the time that electrical energy is needed. A facility can be designed to match either the thermal or electrical load of the facility. If a facility is designed to meet the thermal load, the difference between the electrical power produced by the CHP system and the power required by the facility must either be sold to others or purchased from the grid. Conversely, if the facility is designed to meet the electrical load, energy to meet the thermal load will either need to be supplemented or disposed of [4]. CHP technology should be considered in geographical areas where electricity rates are high, fuel costs are low, and for applications with a requirement for both electricity and thermal energy.

Need to admit, that the nature of the fuel itself has a great influence on combustion–generated emissions [5-8]. By the method of data collation an important details and peculiarities about the exploitation properties of the liquid biofuels and derived blends were spotlighted.

The aim of the present work: to examine the use of first-generation biofuels for stationary decentralized energy generation under conditions in Lithuania, focusing on both environmental and economic aspects.

2. Material and Methods

2.1. The Electromechanical System and Load Performance

The electromechanical system is composed of a 4.2L T40M tractor diesel engine D–144 with mechanical power of 37 kW at 1600 rpm, coupled with an asynchronous generator AKB–82–4UZ of 55 kW. Specifications for the natural aspirated, direct injection, four–cylinder engine are as follows: bore/stroke – 110/120 mm; compression ratio 16.5; piston bowl shape – dished piston; No. of fuel injector holes – 3; initial fuel delivery starting – 25±1° before top dead center; needle valve lifting pressure for all injectors – 17.5 ± 0.5 MPa. The crankcase was fulfilled with 11L of motor oil M–10G_2K.

D–144 engine torque measured via dynamometer with ±2% accuracy. The revolution frequency of the crankshaft measured with a digital tachometer Tessa–1 (accuracy: ±1%). The engine speed was kept constant at 1600 rpm. High load mode (0.650 MPa) related to those applied in cogeneration plants has been selected to discuss the results of engine brake test.

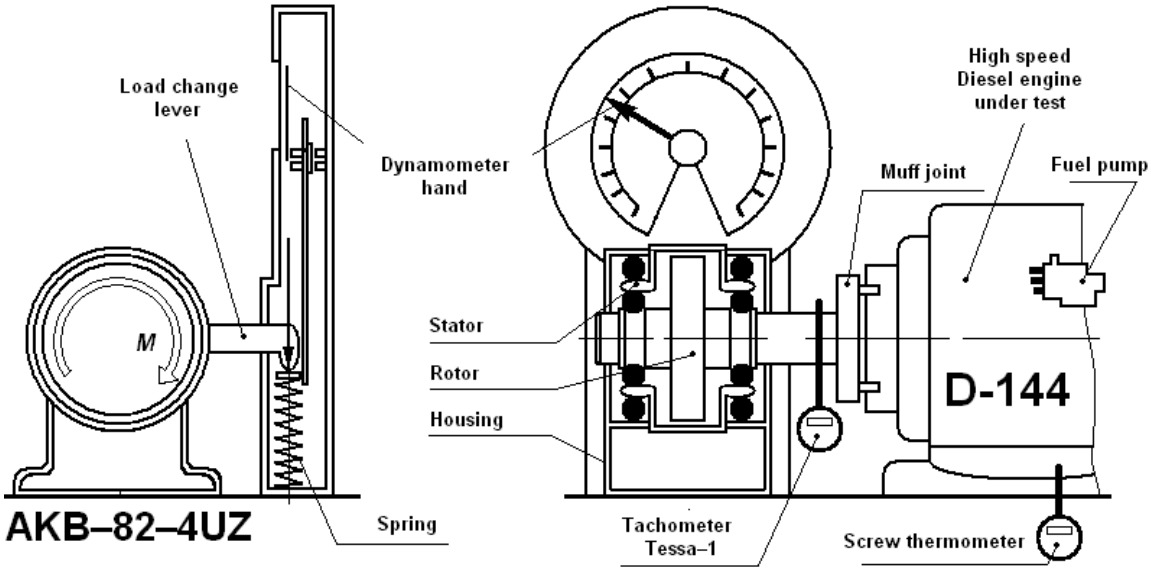

Fig. 1. The electromechanical system applied for establishment of engine performance characteristics

2.2. Tested Fuels (Abbreviations, Acquisition)

- Diesel fuel (DF) / Dyed diesel fuel (dDF) produced by SC "Mažeikių nafta" refinery;
- Rapeseed oil (RO) produced by JSC "Rapsoila" as a raw material for biodiesel production;
- Rapeseed oil methyl ester (hereinafter RME, biodiesel, B100) produced by JSC "Rapsoila";
- B50/dB50 biodiesel blends (50% RME + 50% DF (or 50% dDF)).

2.3. The Gas Analysis System

Analyzers of gases manufactured by Instruments Techno Test Inc., models Technotest 481 (CO: 0 – 9.99%, accuracy: ±0.01%; HC: 0 – 1995 ppm, accuracy: ±2%) and Technotest 490 (Smoke opacity: 0 – 100%, accuracy: ±0.2%) were used. Before carrying out of the experiments Technotest equipment was calibrated at State Metrology Service, established under the resolution of the Government of Republic of Lithuania. The level of nitrogen oxides was measured using an analyzer manufactured by Bacharach, Inc., model PCA–65 (NO_x: 0 – 1000 ppm; accuracy: ±2%).

2.4. Diagnosis of the Economical Situation

Economical calculations and arrived suggestions related to utilization of the renewable types of liquid fuel in cogeneration output cycle providing a reliable, rational guide to action were obtained following Department of Statistics to the Government of the Republic of Lithuania, PSRC Resolution No. 206 N [9], Schneider [10] and Law on Energy of the Republic of Lithuania [11].

3. Results and Discussion

3.1. Engine Performance (BSFC Rates and Exhaust Emission)

Table 1 shows the brake specific fuel consumption (BSFC) for the three fuel groups at the full load engine condition. Since the energy per unit mass of B100, B50/dB50 and rapeseed oil was lower than diesel fuel, the fuel consumption had to be higher to maintain the same brake power. At high load condition 0.650 MPa, the torque and the RPM were kept constant, so the brake power was also constant. There was a 15% higher BSFC rates measured for the B100 than both, the fossil diesel fuel and dDF. Brake specific fuel consumption rates for rapeseed oil and B50/dB50 blends seems to be increased for 5% and 8% respectively, while comparing to conventional diesel.

In general, the replacement of pure DF/dDF by RME causes a decrease in emission level of carbon monoxide dramatically, by 54.1%. Must to admit, the emission of carbon monoxide diminishes when operating high–speed diesel engine at overloaded mode conditions. Under given testing condition the biggest CO emission was generated by diesel fuel whereas pure RO exhibited by 49% lower emission. While compounding DF with biodiesel fuel in equal proportions (v/v), the mentioned above emission changes remain in good agreement with higher combustion efficiency obtained for pure biofuels of first generation.

Table 1

BSFC rates and exhaust emission changes in comparison to diesel fuel

Type of fuel / Measured parameter	B100	B50	RO
BSFC	+15%	+8%	+5%
CO	-54.1%	-19.4%	-49%
Smoke Opacity	-42.5%	-25%	-55%
NO_X	+10.4%	+4.6%	+11.6%
HC	-25.3%	-17.7%	-35.3%

The results of the selected engine smoke opacity level subjected to the type of fuel differ widely. The significant decrease in smoke opacity for biological origin based combustible compounds fuelled engine is explained by the oxygen content of the fuel. It enhances the oxygen availability within the cylinder during combustion and thus reduces pyrolisis of unburned and partly burnt compounds, which would lead formation of soot. In general, total smoke opacity from B100 and rapeseed oil combustion was lower than that for conventional diesel (DF/dDF), in 42.5% and 55% respectively. All three groups of fuels, the fossil diesels, the B50/dB50 blends, and the rapeseed oil were significantly different from each other. The RO had an even greater reduction in smoke opacity than pure B100.

Obtained level of NO_X emissions for all tested pure biofuels (B100 and RO) or compounded blends (B50/dB50) average from 4.6% to 11.6% higher than those of diesel fuel. Analysis of the test results shows, that the maximum NO_X emissions increase proportionally with the mass percent of oxygen in the fuel.

Unburned hydrocarbons (HC) generally stem from the regions in the combustion chamber in which the fuel is diluted with air to such a high extent that it is past the combustion limit. The concentration of unburned HC emitted from these over–lean regions depends on the amount of fuel injected during the ignition delay period. As this period is shorter for RME due its higher Cetane number, hydrocarbon emissions decrease correspondingly.

The rapeseed oil methyl ester operation produced the lowest HC emission. Need to admit, that at high loading and combustion temperature (typical to cogeneration plant's operating mode), the unheated RO better suits in the case of the reduction of HC emission compared to the heated rapeseed oil (because of the decreased fuel viscosity).

3.2. Borrowing Capacity Provided by the Banking System

For the economic analysis, some assumptions have been made about the investment and operational costs involved in utilization of the first generation biofuels. These costs change depending on technologies used, plant size, management organization, contractual relations and others. Production costs for RME have not been estimated due to the fact that there are many big–sized enterprises in local market able fully satisfy a demand for Lithuania as well as the wholesale prices cannot be diminished by farm–scaled plants.

Lithuanian banks aggregating activities to many borrowers having an intend to apply any biomass as a renewable type of fuel. The long term bank credit for buisiness purpose have time horizon of 7 years with the interest rate of 10% per year giving a vision to the companies development.

3.3. Rapeseed Oil Production-Based Costing

Activity–based costing provides an enhanced means for the owners of cogeneration plants to assess the cost–versus–benefits of such activity. The following assumptions are made:

- Prices are referred to the year 2010;
- The farm is a dairy farm of large size, situated in Lithuania.

For the technical–economical evaluation of using of rapeseed oil as a fuel we choose an oil–mill of the 500 t capacity subjected to utilization of rapeseed grown in the area of 750 ha. It is recommendable that the oil–mill must be founded on the cooperation basis. A rapeseed yield of 1500 t will yield approximately 500 t of oil per annum. Expenses for rapeseed oil production are presented in Table 2.

A cost price for rapeseed oil has been evaluated as the difference between total expenses and total earned incomes obtained for the sold oilcake to the stockbreeders.

According Table 2, a prime cost for 1 kg of rapeseed oil comprises of 1.523 LTL or 1.39 LTL per litre. Estimated price is 2.53 times lower than the wholesale price for conventional diesel fuel and about 45% less than the price of dyed diesel used by farmers.

Table 2

Cost price for ready production

Name of materials and expenditure	Amount	Cost (LTL/yeardstick)	Overall (thousand LTL/year)
(1) Rapeseed, t	1500	900	1350.000
(2) Electricity, MWh	95	400	38.000

Sequel of Table 2

Name of materials and expenditure	Amount	Cost (LTL/yeardstick)	Overall (thousand LTL/year)
(3) Depreciation expenses: 10%		150100 (7 year bank credit)	36.450
(4) Deduction for maintenance: • rapeseed oil press: 5% • other equipment: 2%		 37.000 114.800	 1.850 2.300
(5) Rapeseed preparation and storage, t	1500	10	15.000
(6) Transportation			5.300
(7) Expenses for factory, marketing, etc.			62.800
(8) Total (1) + (2) + ... + (7)	1511.700		
(9) Rapeseed oilcake, t	1000	750	750.000
(10) Rapeseed oil cost price, t (8)–(9)	500	1.523	761.700

3.4. Cost Prices for "Thermal Energy Produced–Versus– Type of Fuel"

The modulus of cogeneration plant of the capacity of 340 (kW) has been selected to evaluate the economic feasibility to utilize first–generation biofuels in cogeneration output cycle (Table 3) under conditions in Lithuania.

The economic attractiveness of cogeneration plants for consumers largely rests on a number of regulatory advantages. These include the exemption from electricity taxation, the payment of a bonus for generated electricity fed into the grid and the avoidance of concession levies and grid charges for electricity generated on–site. Unfortunately, the mentioned above initiatives are at the initial stage of development in Lithuania.

Table 3

Economic indicators of 340 kW capacity cogeneration plant

	DF	dDF	B100	B50	dB50	RO
Cogeneration plant, LTL	448500					
Building works, LTL	30000					
Working hours, h/year	8500					
(1) Depreciation expenses, LTL/year	116200					
(2) Maitenance, LTL/year	24000					
(3) Incidental expenses, LTL/year	20000					
(4) Fuel, LTL/year	2273920	1627920	2793304	2540174	2191249	942837
• consumption, l/h	76.0	76.0	87.4	82.1	82.1	79.8
• market cost, LTL/l	3.52	2.52	3.76*	3.64	3.14	1.390
(5) **Total** (1)+(2)+(3)+(4), LTL/year	2434120	1788120	2953504	2700374	2191249	1103037
Price for „Green electricity" sold to the grid, LTL/kWh	0.30					
„Green electricity" produced, kWh/year	2890000					
(6) Incomes from „Green electricity" produced, LTL/year	867000					
(7) Deficit spending (5)–(6), LTL/year	1567120	921120	2086504	1833374	1324249	236037
Thermal energy produced, kWh/year	4188406					
Cost price for thermal energy produced, LTL/kWh	0.374	0.22	0.498	0.437	0.316	0.056

*wholesale price + profit mark-up on cost of 30%.

The most significant barrier to the use of B100 for stationary energy generation is represented by economic issues: the biodiesel cost is the most critical element in a decentralized and liberalized energy market, where fossil fuel prices do not act in favor of RME, unless externalities are not taken into account. Analogous could be said about the compounding fossil diesel with rapeseed oil methyl ester to obtain B50. Taking into account an expectative increase of prices for fuel oil in near future, the biodiesel can be utilized only as a compounding additive to the dyed diesel fuel, if no subsidies be foreseen.

In fact cogeneration plants working on rapeseed oil has the biggest potential to strongly modify the electricity industry in Lithuania (see Table 3). It is a cost–effective method of generating electricity and thermal energy with an estimated high potential. It can be economically viable for the end–user even without any form of subsidy.

4. Conclusions

With the integrated energy production system in the co–generative farm, a possibility is demonstrated of improving their economic, energetic and ecological balances. The farmers are playing a new role as producers and sellers of different form of energy (fuel, heating, electricity). These results obtained are quite positive when compared

with other arm activities and justify the higher investments and management skills required to manage this complex production system. On the basis of discussed above, following could be said:

- The use of the first generation biofuels for decentralized energy generation is not really limited by technological constraints;
- Explored above type of the co–generated energy production allows a remarkable increase in the total output of primary energy exploitation;
- dB50 and rapeseed oil (especially) have the biggest potential to be used as a fuel for engine-driven cogeneration plants in Lithuania. Both types of fuels indicated the low emission levels, brake specific fuel consumption rates as well as cost per 1 MWh of thermal energy produced.

References

1. **Wang Y., Huang Y., Roskilly A.P., Ding Y., Hewitt N.** Trigeneration running with raw jatropha oil**.** Fuel Processing Technology.-Elsevier B.V., 2010, vol. 91(3), p. 348-353.
2. **Wärtsilä.** Web site: <http://www.wartsila.com/,en,press,0,pressrelease,D2064F49-3205-4D4B-8228-684B7DEA2F32, 19C7C4 1C-F824-4125-A294-72DD17619D36,,.htm>.
3. **Sörensen B.** Renewable energy. Its physics, engineering, use, environmental impacts, economy and planning aspects, 3rd ed. Elsevier Academic Press, UK, 2004, 946 p.
4. Center of Energy Efficiency & Renewable Energy. Web site: <http://www.ceere.org/iac/iac_combined.html>.
5. **Raslavicius L., Bazaras Z.** Variations in oxygenated blend composition to meet energy and combustion characteristics very similar to the diesel fuel. Fuel Processing Technology.-Elsevier B.V., 2010, (accepted for publishing).
6. **Raslavicius L., Bazaras Z.** The possibility of increasing the quantity of oxygenates in fuel blends with no diesel engine modifications. Transport, 2010, vol. 25(1), p. 81-88.
7. **Raslavicius L., Bazaras Z.** Oxygenated diesel fuels: physical–chemical properties and exploitation characteristics, in Intelligent Technologies in Logistics and Mechatronics Systems (ITELMS) – 2009: Proceedings of the 4th International Conference, 4–5 June, 2009, Panevėžys, Lithuania, p.17–20.
8. **Kopeyka A. K., Golovko V. V., Zolotko A. N., Darakov D. S., Liubarskij V. M., Raslavicius L.** Inflammation and combustion of the multi–component biofuels [Воспламенение и горение мультикомпонентных биотоплив], in Proceedings of the 6th International Heat and Mass Transfer Forum, May 19–23, 2008. A.V. Luikov Heat and Mass Transfer Institute of the National Academy of Sciences of Belarus, Minsk, 2008 (in Russian). Web site: <www.itmo.by/forum/mif6/program(rus).pdf>.
9. Methodologies on calculation of tariffs for electric and thermal energy of cogeneration based on useful thermal demand: Attachment to the PSRC Resolution No. 206 N, May 4, 2007. Web site: <http://www.erranet.org/ index.php? name=OE-eLibrary&file=download&id=5667&keret=N&showheader =N>.
10. **Schneider L.** Economics of micro cogeneration. In: Pehnt M, Cames M, Fischer C, Praetorius B, Schneider L, Schumacher K, Voß J–P, editors. Microcogeneration. Towards decentralized energy systems. Berlin: Springer Berlin Heidelberg, 2006. p. 67–86.
11. Law on Energy No IX-884 of the Republic of Lithuania. Official Gazette (Valstybės Žinios) 2002, No 56–2224.

Spectral analysis of power quality of asynchronous thyristor loading device

M. Shchuplov*, I. Daroshchanka, V. Zakharenko*****

** Gomel State Technical University, Gaidara str. 4-57,246020,Gomel,Belarus, E-mail: shchuplov@gmail.com*
*** Gomel State Technical University, Ilicha str. 31,246020,Gomel,Belarus, E-mail: dr-acd@yandex.ru*
**** Gomel State Technical University, October av. 48a-141,246023,Gomel,Belarus, E-mail: zevs@gstu.by*

Abstract

The paper presents an investigation aimed at exploring the power quality of asynchronous thyristor loading device. In the process of work the simulation model of asynchronous thyristor cascade was created. Then software to calculate it was developed. Spectrogram of current for power quality analysis and three-dimensional dependencies diagram of distortion of the angle of opening thyristor and engine speed were built.
KEY WORDS: *asynchronous thyristor cascade, asynchronous thyristor loading device, energy consumption, asynchronous motor with slip-ring rotor.*

1. Introduction

To analyze the quality of energy consumption of asynchronous thyristor cascade (Fig. 1) is necessary to use a simulation model of the cascade with a real circuit including the windings of the stator and rotor. Existing development are based on a mathematical model of the engine in the coordinate system ABCabc (3.221) (3.222) [1], which is valid only for the wiring of the stator and rotor star with neutral. But there are also other disadvantages associated with a simplified model, for example, in [2] assumed that the phase windings of the induction motor and transformer have the same active resistance and inductance and the resistance of the valve in the forward and reverse direction does not depend on the value of current through it, that not quite adequately.

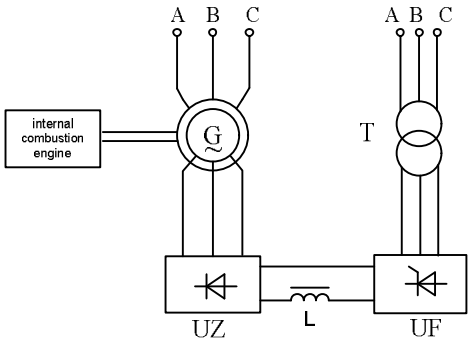

Fig. 1. Functional circuit of an asynchronous thyristor loading device: UZ – diode rectifier; UF – thyristor inverter; T – Transformer; L – smoothing choke; G – asynchronous motor with slip-ring rotors

2. Simulation Model

In connection with this simulation model of asynchronous thyristor cascade was developed, which is devoid of the above-mentioned shortcomings.

The result is a system of equations:

$$\left.\begin{aligned}
&(L_1+0{,}5L_{11})\cdot\frac{di_A}{dt}-(L_1+0{,}5L_{11})\cdot\frac{di_B}{dt}+\left(L_m\cos\gamma_{el.}-L_m\cos\left(\gamma_{el.}-\frac{2\pi}{3}\right)\right)\cdot\frac{di_a'}{dt}+\\
&+\left(L_m\cos\left(\gamma_{el.}+\frac{2\pi}{3}\right)-L_m\cos\gamma_{el.}\right)\cdot\frac{di_b'}{dt}+\left(L_m\cos\left(\gamma_{el.}-\frac{2\pi}{3}\right)-L_m\cos\left(\gamma_{el.}+\frac{2\pi}{3}\right)\right)\cdot\frac{di_c'}{dt}=\\
&=-R_1i_A+u_A+R_1i_B-u_B+\omega i_a'\left(L_m\sin\gamma_{el.}-L_m\sin\left(\gamma_{el.}-\frac{2\pi}{3}\right)\right)+\\
&+\omega i_b'\left(L_m\sin\left(\gamma_{el.}+\frac{2\pi}{3}\right)-L_m\sin\gamma_{el.}\right)+\omega i_c'\left(L_m\sin\left(\gamma_{el.}-\frac{2\pi}{3}\right)-L_m\sin\left(\gamma_{el.}+\frac{2\pi}{3}\right)\right);
\end{aligned}\right\}\qquad(1)$$

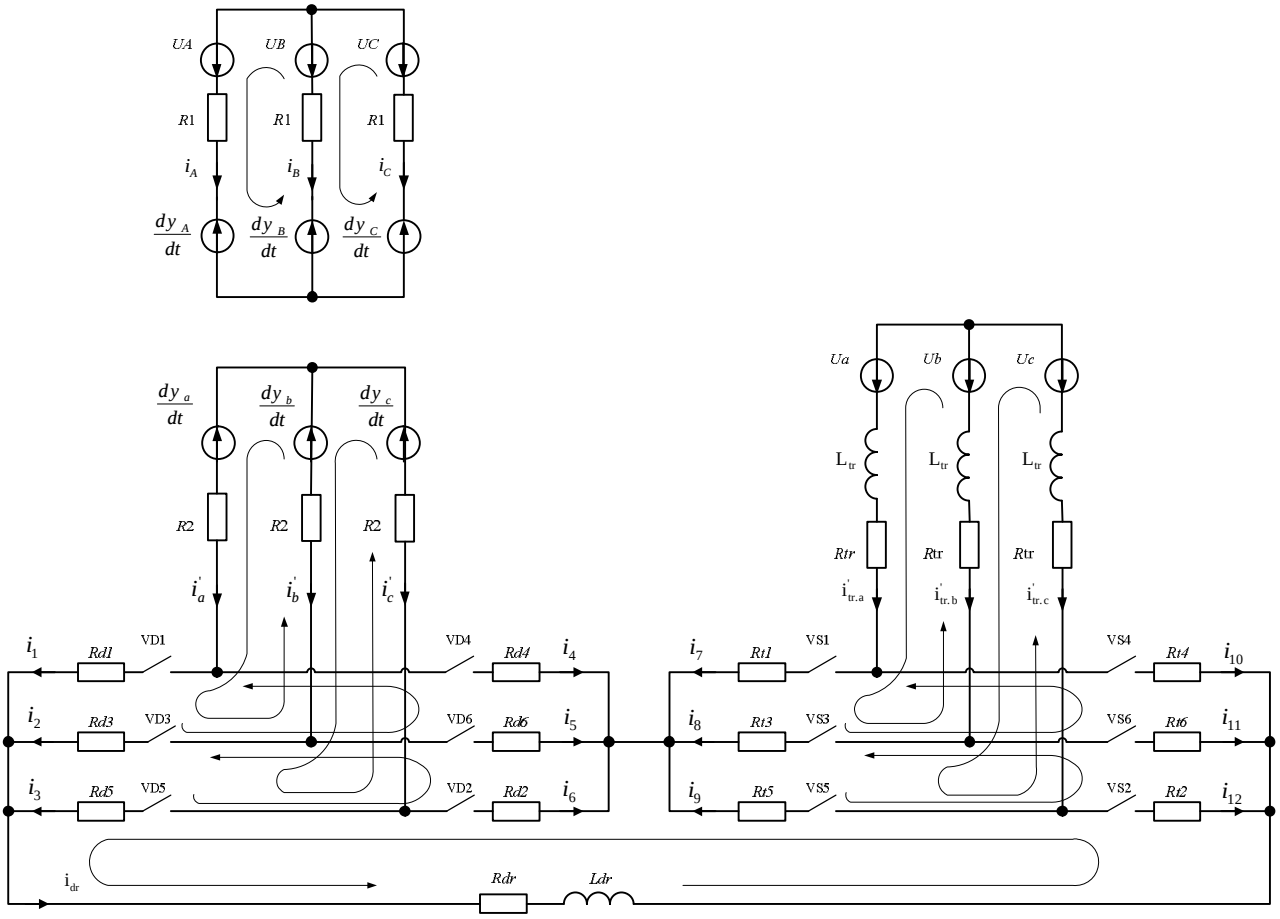

Fig. 2. Equivalent circuit of asynchronous thyristor loading device

$$
\left.
\begin{aligned}
&\left(L_1 + 0.5\,L_{11}\right)\cdot\frac{di_B}{dt} - \left(L_1 + 0.5\,L_{11}\right)\cdot\frac{di_C}{dt} + \left(L_m\cos\left(\gamma_{el.} - \frac{2\pi}{3}\right) - L_m\cos\left(\gamma_{el.} + \frac{2\pi}{3}\right)\right)\cdot\frac{di'_a}{dt} + \\
&+\left(L_m\cos\gamma_{el.} - L_m\cos\left(\gamma_{el.} - \frac{2\pi}{3}\right)\right)\cdot\frac{di'_b}{dt} + \left(L_m\cos\left(\gamma_{el.} + \frac{2\pi}{3}\right) - L_m\cos\gamma_{el.}\right)\cdot\frac{di'_c}{dt} = \\
&= -R_1 i_B + u_B + R_1 i_C - u_C + \omega i'_a\left(L_m\sin\left(\gamma_{el.} - \frac{2\pi}{3}\right) - L_m\sin\left(\gamma_{el.} + \frac{2\pi}{3}\right)\right) + \\
&+\omega i'_b\left(L_m\sin\gamma_{el.} - L_m\sin\left(\gamma_{el.} - \frac{2\pi}{3}\right)\right) + \omega i'_c\left(L_m\sin\left(\gamma_{el.} + \frac{2\pi}{3}\right) - L_m\sin\gamma_{el.}\right);
\end{aligned}
\right\}
$$

$$
\frac{di_A}{dt} + \frac{di_B}{dt} + \frac{di_C}{dt} = 0\,;
$$

(Sequal of Eq. 1)

$$
\left.
\begin{aligned}
&\left(L'_2 + 0.5\,L'_{22}\right)\cdot\frac{di'_a}{dt} - \left(L'_2 + 0.5\,L'_{22}\right)\cdot\frac{di'_b}{dt} + \left(L_m\cos\gamma_{el.} - L_m\cos\left(\gamma_{el.} + \frac{2\pi}{3}\right)\right)\cdot\frac{di_A}{dt} + \\
&+\left(L_m\cos\left(\gamma_{el.} - \frac{2\pi}{3}\right) - L_m\cos\gamma_{el.}\right)\cdot\frac{di_B}{dt} + \left(L_m\cos\left(\gamma_{el.} + \frac{2\pi}{3}\right) - L_m\cos\left(\gamma_{el.} - \frac{2\pi}{3}\right)\right)\cdot\frac{di_C}{dt} + \\
&+\frac{di_1}{dt}\cdot R_{d1} - \frac{di_2}{dt}\cdot R_{d3} = -R'_2 i'_a + R'_2 i'_b + \omega i_A\left(L_m\sin\gamma_{el.} - L_m\sin\left(\gamma_{el.} + \frac{2\pi}{3}\right)\right) + \\
&+\omega i_B\left(L_m\sin\left(\gamma_{el.} - \frac{2\pi}{3}\right) - L_m\sin\gamma_{эл.}\right) + \omega i_C\left(L_m\sin\left(\gamma_{el.} + \frac{2\pi}{3}\right) - L_m\sin\left(\gamma_{el.} - \frac{2\pi}{3}\right)\right);
\end{aligned}
\right\}
$$

$$\left(L_2^{'}+0.5\,L_{22}^{'}\right)\cdot\frac{di_b^{'}}{dt}-\left(L_2^{'}+0.5\,L_{22}^{'}\right)\cdot\frac{di_c^{'}}{dt}+\left(L_m\cos\left(\gamma_{el.}+\frac{2\pi}{3}\right)-L_m\cos\left(\gamma_{el.}-\frac{2\pi}{3}\right)\right)\cdot\frac{di_A}{dt}+$$

$$+\left(L_m\cos\gamma_{el.}-L_m\cos\left(\gamma_{el.}+\frac{2\pi}{3}\right)\right)\cdot\frac{di_B}{dt}+\left(L_m\cos\left(\gamma_{el.}-\frac{2\pi}{3}\right)-L_m\cos\gamma_{el.}\right)\cdot\frac{di_C}{dt}+$$

$$+\frac{di_2}{dt}\cdot R_{d3}-\frac{di_3}{dt}\cdot R_{d5}=-R_2^{'}i_b^{'}+R_2^{'}i_c^{'}+\omega i_A\left(L_m\sin\left(\gamma_{el.}+\frac{2\pi}{3}\right)-L_m\sin\left(\gamma_{el.}-\frac{2\pi}{3}\right)\right)+$$

$$+\omega i_B\left(L_m\sin\gamma_{el.}-L_m\sin\left(\gamma_{el.}+\frac{2\pi}{3}\right)\right)+\omega i_C\left(L_m\sin\left(\gamma_{el.}-\frac{2\pi}{3}\right)-L_m\sin\gamma_{el.}\right);$$

$$\frac{di_a^{'}}{dt}+\frac{di_b^{'}}{dt}+\frac{di_c^{'}}{dt}=0;$$

$$\frac{di_{tr.a}}{dt}\cdot L_{mp}-\frac{di_{tr.b}}{dt}\cdot L_{mp}+\frac{di_7}{dt}\cdot R_{t1}-\frac{di_8}{dt}\cdot R_{t3}=u_a-u_b-R_{tr}i_{tr.a}+R_{tr}i_{tr.b};$$

$$\frac{di_{tr.b}}{dt}\cdot L_{tr}-\frac{di_{tr.c}}{dt}\cdot L_{tr}+\frac{di_8}{dt}\cdot R_{t3}-\frac{di_9}{dt}\cdot R_{t5}=u_b-u_c-R_{tr}i_{tr.b}+R_{tr}i_{tr.c};$$

$$\frac{di_{tr.a}}{dt}+\frac{di_{tr.b}}{dt}+\frac{di_{tr.c}}{dt}=0;$$

$$\frac{di_{tr}}{dt}\cdot L_{tr}+\frac{di_3}{dt}\cdot R_{d5}-\frac{di_6}{dt}\cdot R_{d2}+\frac{di_9}{dt}\cdot R_{t5}-\frac{di_{12}}{dt}\cdot R_{t2}=-i_{tr}\cdot R_{tr};$$

$$\frac{di_1}{dt}\cdot R_{d1}-\frac{di_2}{dt}\cdot R_{d3}+\frac{di_5}{dt}\cdot R_{d6}-\frac{di_4}{dt}\cdot R_{d4}=0;$$

$$\frac{di_2}{dt}\cdot R_{d3}-\frac{di_3}{dt}\cdot R_{d5}+\frac{di_6}{dt}\cdot R_{d2}-\frac{di_5}{dt}\cdot R_{d6}=0;$$

$$\frac{di_{dr}}{dt}-\frac{di_1}{dt}-\frac{di_2}{dt}-\frac{di_3}{dt}=0;$$

$$\frac{di_1}{dt}-\frac{di_a^{'}}{dt}+\frac{di_4}{dt}=0;$$

$$\frac{di_2}{dt}-\frac{di_b^{'}}{dt}+\frac{di_5}{dt}=0;$$

$$\frac{di_3}{dt}-\frac{di_c^{'}}{dt}+\frac{di_6}{dt}=0;$$

$$\frac{di_7}{dt}-\frac{di_{tr.a}}{dt}+\frac{di_{10}}{dt}=0;$$

$$\frac{di_8}{dt}-\frac{di_{tr.b}}{dt}+\frac{di_{11}}{dt}=0;$$

(Sequal of Eq. 1)

$$\left.\begin{aligned}
&\frac{di_9}{dt}-\frac{di_{tr.c}}{dt}+\frac{di_{12}}{dt}=0;\\
&\frac{di_7}{dt}\cdot R_{t1}-\frac{di_8}{dt}\cdot R_{t3}+\frac{di_{11}}{dt}\cdot R_{t6}-\frac{di_{10}}{dt}\cdot R_{t4}=0;\\
&\frac{di_8}{dt}\cdot R_{t3}-\frac{di_9}{dt}\cdot R_{t5}+\frac{di_{12}}{dt}\cdot R_{t2}-\frac{di_{11}}{dt}\cdot R_{t6}=0;\\
&-\frac{di_{dr}}{dt}-\frac{di_{10}}{dt}-\frac{di_{11}}{dt}-\frac{di_{12}}{dt}=0
\end{aligned}\right\} \quad \text{(Sequal of Eq. 1)}$$

where: ψ_A, ψ_B, ψ_C, R_1, i_A, i_B, i_C, u_{fA}, u_{fB} and u_{fC} are flux linkage, active resistance, stator currents and voltages; ψ_a, ψ_b, ψ_c, $R_2^{'}$, $i_a^{'}$, $i_b^{'}$ and $i_c^{'}$ are flux linkage, referred to the stator resistance and rotor currents; R_{tr}, L_{tr}, $i_{tr.a}$, $i_{tr.b}$, $i_{tr.c}$, u_a, u_b and u_c are active resistance, inductance, current and voltage of transformer; $L_1 = L_{1s} + L_m$ is own inductance of stator phase winding; L_{1s} is inductance of stator phase windings (on the T-shaped pattern of substitution); L_m is primary mutual inductance between stator phase windings and the phase of the rotor; L_{11} is mutual inductance between the windings of stator phases; $g_{el.}$ is angle of the rotor in electrical radians; $L_2^{'} = L_{2\sigma}^{'} + L_m$ is reduced to the stator winding inductance own phase rotor; $L_{2\sigma}^{'}$ is reduced to the stator winding inductance of rotor phase (for T-shaped pattern of substitution); $L_{22}^{'}$ is reduced to the stator windings mutual inductance between phases of the rotor; i_{dr} is rectified current choke; i_1 ... i_6 are currents of the rectifier; i_7 ... i_{12} are currents of the inverter; R_{d1} ... R_{d6} are resistance diode rectifier, changing depending on its condition; R_{t1} ... R_{t6} are resistance thyristor inverter, changing depending on its condition; R_{dr} and L_{dr} is active resistance and inductance of the choke.

The equations of mechanical parts for the study of the generator mode the engine look like:

$$\left.\begin{aligned}
&w_{\text{el.}} = const\\
&\frac{dg_{\text{el.}}}{dt} = w_{\text{el.}}
\end{aligned}\right\} \quad (2)$$

where $w_{el.}$ is speed of the rotor in electric, rad/s.

Electromagnetic moment is given by:

$$\begin{aligned}
M = -L_m p i_A\Bigg[&\left(i_a^{'}\sin\gamma_{el.}+i_b^{'}\sin\left(\gamma_{el.}+\frac{2\pi}{3}\right)+i_c^{'}\sin\left(\gamma_{el.}-\frac{2\pi}{3}\right)\right)+\\
&+i_B\left(i_b^{'}\sin\gamma_{el.}+i_c^{'}\sin\left(\gamma_{эл.}+\frac{2\pi}{3}\right)+i_a^{'}\sin\left(\gamma_{el.}-\frac{2\pi}{3}\right)\right)+\\
&+i_C\left(i_c^{'}\sin\gamma_{el.}+i_a^{'}\sin\left(\gamma_{el.}+\frac{2\pi}{3}\right)+i_b^{'}\sin\left(\gamma_{el.}-\frac{2\pi}{3}\right)\right)\Bigg]
\end{aligned} \quad (3)$$

Based on this model was developed the software using language Free Pascal.

All processing of calculations were performed with the aid of software written in the language «python» and modules NumPy, SciPy, Matplotlib.

3. Spectral Analysis

With the help of the developed software we calculated different modes of operation of the device and made a spectral analysis of stator current (Fig. 3).

Fig. 4 shows the harmonic current spectrum at the frequency is 50 Hz and an angular velocity of rotation of the generator 570 rad/s.

For this signal the distortion factor is:

$$K_d = 19.7\%$$

During the spectral analysis of stator current has been hypothesized the existence of a definite relationship between the coefficient of distortion and proportion between rotor speed and the synchronous frequency.

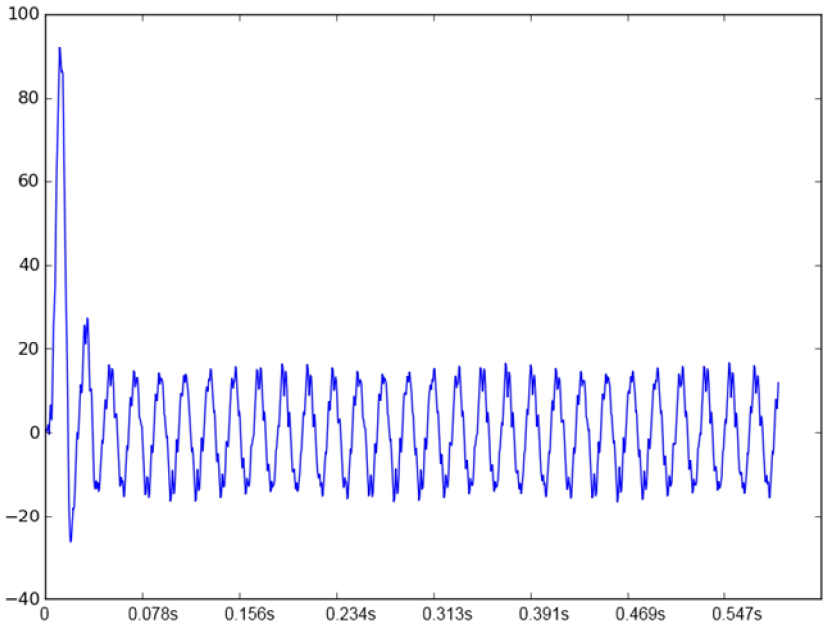

Fig. 3. Current of phase A stator of MTF112 BP-6. Rotation speed of the generator – 570 rad/s and β = 50

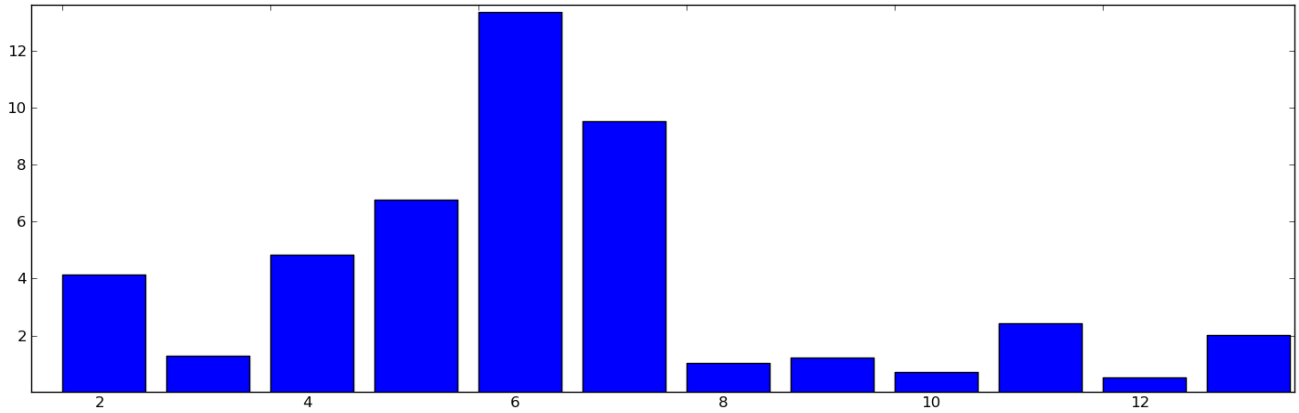

Fig. 4. Harmonic spectrum of current. Rotation speed of the generator – 570 rad/s and β = 50

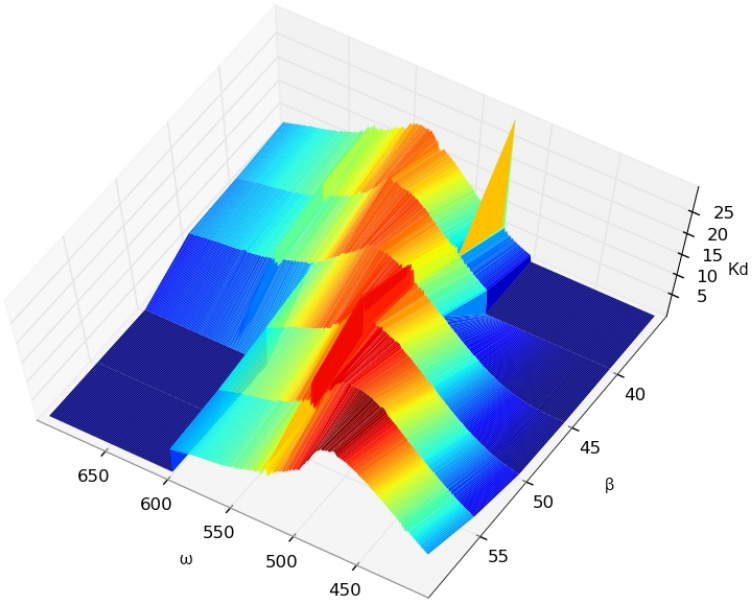

Fig. 5. Dependence of the coefficient of distortion of the angle of opening of the inverter β and the rotor speed ω for engine type – MTF112 BP-6 (range of values where the calculation was not made, supplemented by zeros)

To test this hypothesis, with help of GRID we calculated the modes of the machine at different angles of opening of the inverter and the rotor speed.

Three-dimensional plot of the coefficient of distortion depending on the angle of opening inverter β and the angular velocity of rotation of the rotor ω_{EL} shown in Fig. 5.

3. Conclusions

The graph shows that at an angle control β = 60 ° the worst value of the coefficient of distortion occurs when the frequency ratio $\omega_{EL} / \omega_{0EL} = 1.5$. While reducing the opening angle, the maximum of distortion factor is shifted to increasing speed.

Analysis of the graph allows to select modes with the lowest harmonic distortion, and improve the quality of power quality of test bench.

References

1. Asynchronously, the loading gate device / S.V. Khvatov, V. Titov and others. – M.: Energoatomizdat, 1986.
2. Asynchronous motors series 4A: Reference / A.E. Krawczyk and others. – M.: Energoatomizdat, 1982.
3. Complete thyristor electric drive: A Handbook. Ed. VM Perelmuter. – M.: Energoatomizdat, 1988.
4. Theory of electric drive: Proc. manual / BI Firagho, LB Pavlyachik. – Mn.: JSC Tehnoperspektiva, 2004. – 527 p.

Proceedings of 5th International Conference ITELMS'2010

On Surface Cross Curvature Influence for Heat Transfer in Laminar Liquid Film

S. Šinkūnas*, A. Kiela**

** Kaunas University of Technology, Donelaičio str. 20, 44239, Kaunas, Lithuania, E-mail: stasys.sinkunas@ktu.lt*
*** Kaunas College, Pramones av. 22, 50468, Kaunas, Lithuania, E-mail: algimantas.kiela@kauko.lt*

Abstract

The objective of present paper is to obtain comprehension for heat transfer developments in gravity driven liquid fil9m flow. Heat transfer in laminar film flow is influenced by the cross curvature of the wetted surface, heat flux on the film surface and boundary conditions on the wetted wall. The analytical study evaluating the influence of cross curvature on heat transfer in laminar film has been carried out. Equations using correction factors for the calculation of heat transfer to laminar liquid film with respect to the cross curvature for different boundary conditions were established. Theoretical analysis of the temperature field change due to heat flux variation in the liquid film was performed as well. An equation allowing determining the temperature profiles in laminar film was established. The results of calculations are discussed with respect to the temperature gradient dependence on the film relative cross curvature and the ratio of heat flux densities on the film surface and the wetted surface respectively.
KEY WORDS: *cross curvature, heat transfer, laminar film, heat flux, temperature field.*

1. Introduction

Thin liquid films occur in many industrial processes, but perhaps the most challenging application is in engine design. Liquid fuel wall films form in diesel and gasoline engines due to impingement of injected fuel sprays on pistons and intake valves and on the surfaces of ports and cylinders. Fuel film develops dynamically under the influence of gas flow and wall movement. At the same time, heat exchange with walls and the surroundings gas leads to evaporation, affecting the composition of the mixture and hence increasing the complexity of the flow and combustion process. Therefore, a complete knowledge of falling film flow can help engineers understand and optimise these highly complex processes, providing a powerful tool for improving efficiency and reducing pollutant emission in internal combustion engines. The film flow was the subject of numerous researches [1-3] in recent years.

In paper [4] was researched the influence of fuel spray impact on fuel/air mixture for combustion in port fuel injection engines. Analysis shows that during engine warm up, the heat transfer over entire valve surface occurs within the vaporization nucleate boiling regime and the local instantaneous surface temperature correlates with the dynamics of droplets impacting at the same point. A functional relation is found for the heat transfer coefficient, which also describes other experiments reported in the literature.

In contrast, in internal engines, the fuel jet generally impinges on a curved wall rather than on a flat wall. The theoretical analysis of the liquid flow on the curved wall was performed in [5]. The measurements of the film thickness on the curved wall were carried out, while varying the impingement angle, the curvature of the concave wall, the distance between the measurement point and the impingement point, and the jet Reynolds number.

An experimentally study [6] was performed to research the nonlinear flow and heat transfer characteristics for a slot-jet impinging on slightly curved surfaces. The effects of curved surface geometry and jet Reynolds number on the jet velocity distribution and circumferential Nusselt numbers were examined. Two different slightly curved surface geometries of convex and concave were used as target surfaces. New correlations for local, stagnation point and average Nusselt numbers as a function of jet Reynolds number and dimensionless circumferential distance were reported. The correlations revealed that the impinging cooling rate is higher with the concave surface and increase with increasing Reynolds number.

The paper [7] have investigated the flow and heat transfer characteristics in laminar flows with pressure gradients, streamwise distance Reynolds number and wall curvature. Results were compared with analytical solutions and numerical prediction and a new empirical equation was established. It was found that Stanton numbers augmentation with Reynolds number became more pronounced than concave curvature. Favourable pressure gradients caused heat transfer to increase and adverse pressure gradients to decrease.

Study [8] developed a mathematical model predicting evaporation and fluid flow in evaporating film region on a curved film to determine the interface temperature, heat flux distribution and film profile in the film region. The numerical results showed that temperature of an equilibrium film on the curved surface of solid wire is larger than on a flat surface and equilibrium film thickness formed on the curved surface of solid wire is smaller than the one on the flat surface if the bulk fluid curvature of both evaporating film regions is the same. The rate of increase of the magnitude of total heat transfer through the evaporating thin film region per unit length begins to decrease with larger superheat temperature due to the effect of a decreasing evaporating film region length.

2. Heat Transfer in Laminar Film Flow on a Surface of Vertical Tube

In study [9] was obtained that for the case of film flow on outside surface of vertical tube the modified Nusselt number Nu_M can be calculated by the following equation:

$$Nu_M = \frac{0.5\left\{(1+e_R)^4\left[\ln(1+e_R)-0.75\right]+(1+e_R)^2-0.25\right\}^{4/3}R_e^{-1/3}}{e_R^2\int_0^1(1+e_Rz)\left\{(1+e_R)^2\ln(1+e_Rz)-0.5\left[(1+e_Rz)^2\right]\right\}\frac{y}{h_d}dz} \tag{1}$$

For the case of film flow on an inside surface of vertical tube, this expression can be defined in the following way:

$$Nu_M = \frac{0.5\left\{(1-e_R)^4\left[0.75-\ln(1-e_R)\right]-(1-e_R)^2+0.25\right\}^{4/3}R_e^{-1/3}}{e_R^2\int_0^1(1-e_Rz)\left\{(1-e_R)^2\ln(1-e_Rz)+0.5\left[1-(1-e_Rz)^2\right]\right\}\frac{y}{h_d}dz} \tag{2}$$

where $e_R = d/R$ is relative cross curvature of the film; R is cross curvature of wetted surface (tube external radius), m; $R_e = 4\,\Gamma(r\,n)$ is Reynolds number; Γ is wetting density, kg/(m·s); n is kinematic viscosity, m^2/s; $z = y/d$ is dimensionless distance from the wetted surface; y is distance from the wetted surface, m; d is liquid film thickness, m; $h_d = v^* d/n$ is dimensionless film thickness; $v^* = (t_w/r)^{1/2}$ is dynamic velocity of the film, m/s; r is liquid density, kg/m^3; t_w is shear stress on the wetted surface, Pa.

The parameter ψ may be expressed as follows:

$$y = \int_0^z \frac{q/q_w}{1+e_R\,z}\,dz \tag{4}$$

where q is heat flux density across the film, W/m^2; q_w is represents the wall heat flux density, W/m^2.

When calculating the modified Nusselt number Nu_M according the Eqs. (1) and (2), it is necessary to know the parameter ψ, which could be found by using the ratio q/q_w. The regularity $q/q_w = f(z)$ can be determined only for two boundary conditions: $q_w = const$ and $T_w = const$.

At first case the ratio of heat flux densities in the liquid film can be defined as follows:

$$\frac{q}{q_w} = 1-(1-e_q)\frac{\int_0^z(1+e_R\,z)\,j\;dz}{\int_0^1(1+e_R\,z)\,j\;dz} \tag{5}$$

and at second case:

$$\frac{q}{q_w} = 1-(1-e_q)\frac{\int_0^z(1+e_Rz)\,j\;y\;dz}{\int_0^1(1+e_Rz)\,j\;y\;dz} \tag{6}$$

where $e_q = q_s/q_w$ is represents the ratio between the heat flux densities on the film surface and the wetted surface, respectively.

As can it be seen from above-mentioned equations, the result of calculations is the following function:

$$Nu_M = R_e^{-1/3} f(e_R, e_q) \tag{7}$$

It can also be seen from these equations, that for the boundary condition $q_w = const$, it is possible to solve the problem without difficulty by the method of direct numerical integration. However, for the boundary condition $T_w = const$, it is necessary to use the method of consecutive approximations, because $q/q_w = f(y)$ and $y = f(q/q_w)$. At first approximation, the ratio q/q_w may be calculated from the Eq. (5).

For both the plane film flow and the film flow on a vertical surface cylindrical surface, evaluating the variability of liquid physical properties in the film, the modified Nusselt number Nu_M can be written as follows:

$$Nu_M = K\, R_e^{-1/3}\, C_{Rq}\, e_{Pr} \tag{8}$$

where e_{Pr} is the multiplier, evaluating the liquid physical properties.

The correction factor C_{Rq}, evaluating curvature of the film and heat transfer between the film surface and surrounding medium of gas or vapour may be defined as:

$$C_{Rq} = \frac{f(e_R, e_q)}{K} \tag{9}$$

where $K = 2.27$ for $q_w = const$ and $K = 2.07$ for $T_w = const$. When $e_R = 0$ and $e_q = 0$, $C_{Rq} = 1$.

In case of external film flow, the correction factor C_{Rq} (with calculation error less than 1%) can be determined by equations: when $q_w = const$

$$C_{Rq} = \frac{136}{136 + 39\, e_R} + (0.52 - 0.03\, e_q)\, e_R \tag{10}$$

and when $T_w = const$

$$C_{Rq} = \frac{136}{56 + 10\, e_R} + (0.58 - 0.05\, e_q)\, e_R \tag{11}$$

In case of internal film flow, the correction factor C_{Rq} can be determined by equations: when $q_w = const$:

$$C_{Rq} = \exp(-0.56\, e_R) - \frac{39\, e_q}{136 + 39\, e_q} \tag{12}$$

and when $T_w = const$

$$C_{Rq} = \exp(-0.61\, e_R) - \frac{10\, e_q}{56 + 10\, e_q} \tag{13}$$

The results of calculations, using above-mentioned method, are shown in Fig. 1 and 2. As can it be seen from these figures, with increasing the parameter e_R, for the case of film flow on outside surface of vertical tube, the value

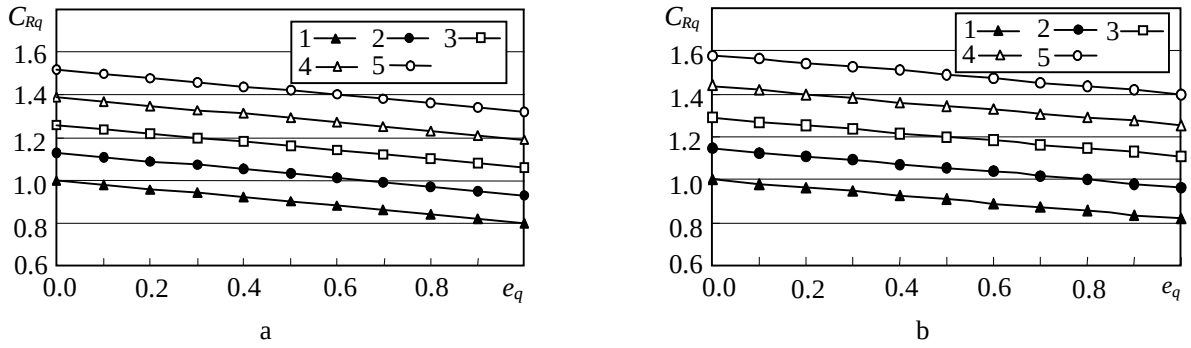

Fig. 1. Variations of correction factor on film cross curvature and external heat transfer in case of external film flow: a – boundary condition $q_w = const$; b – boundary condition $T_w = const$. Curves 1 ... 5 correspond $e_R = 0$; 0.25; 0.50; 0.75 and 1.0

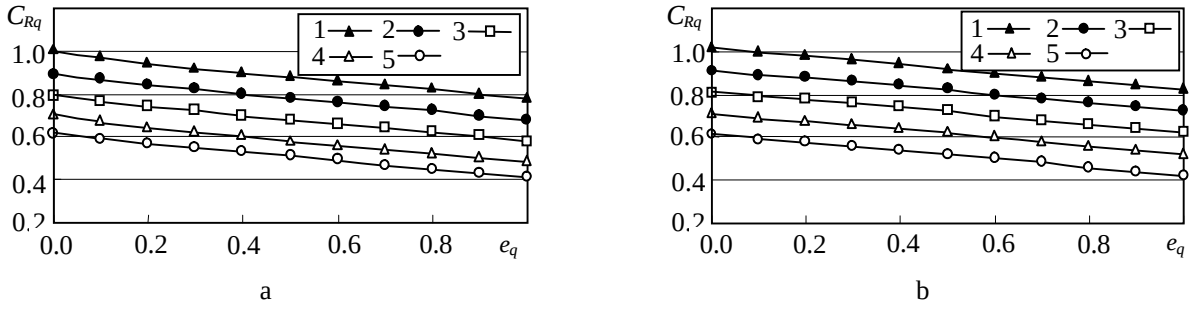

Fig. 2. Variations of correction factor on film cross curvature and external heat transfer in case of internal film flow: a – boundary condition $q_w = const$; b – boundary condition $T_w = const$. Curves 1 ... 5 correspond $e_R = 0$; 0.20; 0.40; 0.60 and 0.80

of heat transfer coefficient increases and it decreases, when the film flows down an internal surface of a tube. For both cases, the increase of parameter e_q diminishes the heat transfer intensity from the wetted surface.

The variation of physical properties of the liquid across the film must be taken into account in a case of high value of temperature difference. The multiplier e_{Pr} in Eq. (8) can be determined as an exponential function of the following ratio Pr_f / Pr_w or m_f / m_w. The results of numerical calculations showed that ratio Pr_f / Pr_w unambiguously does not evaluate the influence of physical properties variation for different liquids and the character of this influence practically is not dependent upon the values of e_q and e_R. This research showed that for $-0.5 \le e_R \le -1$ and $0.4 \le Pr_f / Pr_w \le 2$ the multiplier $\left(Pr_f / Pr_w\right)^{0.25}$ can be used. For more accurate evaluation of liquid physical properties variation, the multiplier e_{Pr} must be determined as a function of parameters m_f / m_w. This parameter evaluates practically the influence of physical properties variation for water, transformer oil and compressor oil. The multiplier e_{Pr} in such case can be calculated by the following equation:

$$e_{Pr} = \left(m_f / m_w\right)^n \tag{14}$$

where $n = 0.315\left(2 + e_R\right)^{-0.49}$, for $0.1 \le m_f / m_w \le 1$ and $n = 0.325\left(2 + e_R\right)^{-0.24}$, for $1 \le m_f / m_w \le 10$; m_f and m_w – dynamic viscosity referred to the film and wetted surface, respectively.

3. Temperature Field Alteration in the Case of Heat Flux Density Variation in the Film

As can it be seen from Eqs. (10) – (13), that the heat transfer intensity increases with increasing of the film curvature parameter e_R, however it decreases with increasing of external heat exchange parameter e_q. It occurs due to the different influence of these parameters on the film temperature profile and the temperature gradient on the wetted surface. The latter is augmenting with increasing of e_R and decreasing of e_q respectively. It evidently can be seen by depicting the temperature profile graphically. For this purpose, it is convenient to use a function $q = f(z)$.

This function can be obtained from the heat flux density equation:

$$q = -\left(1 + e_R \frac{y}{d}\right) l \frac{dT}{dy} \tag{15}$$

where l is thermal conductivity, W/(m·K).

It follows from Eq. (15) that:

$$T_w - T = \frac{q_w}{l} \int_0^y \frac{q/q_w}{1 + e_R\, y/d}\, dy \tag{16}$$

and respectively:

$$T_w - T_s = \frac{q_w}{l} \int_0^y \frac{q/q_w}{1 + e_R\, y/d}\, dy \tag{17}$$

where T_w, T and T_s represents the wetted wall, liquid film and film surface temperature, respectively.

Then, temperature field in the film can be defined by the following expression:

$$q = \frac{T_w - T}{T_w - T_s} = \frac{\int_0^y \frac{q/q_w}{1 + e_R\, y/d}\, dy}{\int_0^d \frac{q/q_w}{1 + e_R\, y/d}\, dy} \tag{18}$$

or, using the dimensionless distance from the wetted surface z, this equation takes the form as:

$$q = \frac{T_w - T}{T_w - T_s} = \frac{\int_0^z \frac{q/q_w}{1 + e_R z}\, dz}{\int_0^1 \frac{q/q_w}{1 + e_R z}\, dz} \tag{19}$$

Taking into account Eq. (5) and (6), from this expression can be calculated the film temperature profile. By employing the heat flux distribution in the film and Eq. (18), respectively, the temperature profiles in the laminar film were calculated. The calculation results are reported in Fig. 3.

As can it be seen from Fig. 3, that with increase of relative cross curvature of the film e_R, heat transfer intensity increases and with increase of the heat flux densities ratio e_q, heat transfer intensity decreases. This phenomenon takes place due to the different impact of these values on temperature gradient on the wetted surface.

The data presented in Fig. 3 demonstrate that temperature gradient on the wetted surface increases with increase of the parameter e_R and with decrease of the parameter e_q.

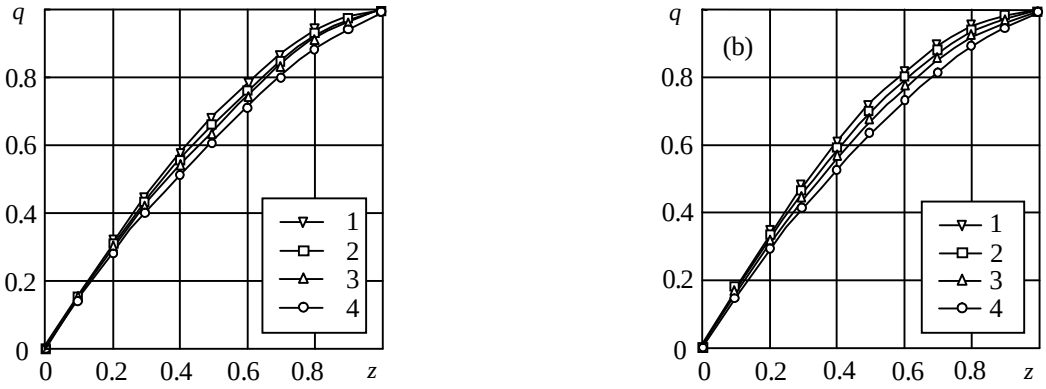

a b

Fig. 3. Temperature profiles in laminar film: a, b – relative cross curvature of the film respectively $e_R = 0$; 0.5, respectively; 1, 2, 3, 4 – $e_q = 0$; 0.2; 0.4 and 1.0, respectively

4. Conclusions

It was estimated that heat transfer in laminar film falling down an outside surface of vertical tube increases with increase of the film relative cross curvature, while it decreases in the case of film flow on an inside surface of vertical tube. For both cases, the presence of heat transfer between the film surface and surrounding medium of gas or vapour diminishes the value of heat transfer coefficient.

The temperature profiles in laminar film were calculated evaluating the heat transfer flux density distribution across the film. The results of calculations and equations analysis showed that temperature gradient on the wetted surface increases with increase of the film relative cross curvature and with decrease of the heat flux densities ratio on the film surface and wetted surface, respectively. Then, the value of heat transfer coefficient increases. In that way, the calculations results show the possibilities to intensify the heat transfer in gravity driven liquid laminar film flowing down a vertical surface.

References

1. **Benhamza M. E., Belaid F.** Computation of turbulent channel flow with variable spacing riblets. -Mechanika.- Kaunas: Technologija, 2009, no.5 (79), p.36-41.
2. **Deheri G. M., Nikhilkumar D., Abhangi D.** Magnetic fluid based squeeze film between curved rough circular plates. –Mechanika. - Kaunas: Technologija, 2008, no.4(72), p.34-40
3. **Zhurauski M. N., Dragasius E., Korobko E., Novikova Z. A.**. Mechanical properties of smart fluids under combined electrical and magnetic fields. – Mechanika. – Kaunas: Technologija, 2008, no.6 (74), p.21-24.
4. **Panaoand M. R. O., Moreira A. L. N.** Interpreting the influence of fuel spray impact on mixture preparation for HCCI combustion with port fuel injection. -Proc. of Combustion Institute, 2007, vol.31, no.2, p.2205-2213.
5. **Inamura T., Amagasaki S., Yanaoka H.** Thickness of liquid film formed by impinging jets on a concave wall. – J. of Propulsion and Power, 2007, vol.23, no.3, p.612-617.
6. **Eren H., Celik B. Y. N.** Nonlinear flow and heat transfer dynamics of impinging jets onto slightly-curved surfaces.- Applied Thermal Engineering, 2007, vol.27, no. 2, p.2600-2608.
7. **Umur H.** Flow and heat transfer with pressure gradients, Reynolds number and surface curvature. -Int. Communication. Heat Mass Transfer, 2000, vol. 27, no.2, 397-406.
8. **Demsky S. M., Ma H. B.** Thin film evaporation on a curved surface. -Microscale Thermophysic Engineering, 2004, vol.8, no.3, 285-299.
9. **Gimbutis G., Gimbutyte I., Sinkunas S.** Heat transfer in a falling liquid film with large curvature. – Heat Transfer Research, 1993, v.25, p.216-219.

Proceedings of 5th International Conference ITELMS'2010

Analysis of Stress and Deformations the Rotating Platform Structure of the Bucket-Wheel Excavator Srs (H) 220 9.5/0.5

D. Sprečić, F. Mrkaljević, F. Mulahalilović

University of Tuzla, Faculty of Mechanical Engineering, Univerzitetska 4, 75000 Tuzla, Bosnia and Herzegovina
E-mail: esprecic@bih.net.ba

Abstract

In the paper are shown strees and deformations of the upper rotating platform of the bucket-wheel excavator due to the moved location of any upper part of the bucket-wheel excavator (rotating, hoisting, lowering), as well as owing to the changed digging resistance, leaning of rotor against the base, wind action or plane inclination. Using the results of the in situ researches carried out on the bucket-wheel excavator SRs (H) 220 9.5/0.5, and applying the appropriate software for modeling and simulation, the identification of stress and deformations of the bucket-wheel excavator rotating platform structure was carried out, the aim being to reconstruct and find a higher quality solution for the rotating platform.
KEY WORDS: *bucket-wheel excavator, rotating platform, 3D model.*

1. Introduction

Bucket-wheel excavators, as mining machines, are the most frequently used machines in open pit mines worldwide at the present time. Continuous progress achieved in the construction technology provides greater possibilities of using theses excavators in the mining of very hard rocks under extreme weather conditions. Basically, the bucket-wheel excavators are divided into bucket-wheel excavators with one working cell – cyclic (discontinuous) and bucket-wheel excavators with multiple working cells – continuous [1]. Both types of bucket-wheel excavators can work with high (upper) digging and deep (lower) digging. The working cell of continuous bucket-wheel excavators consists of a few buckets which move along the closed trajectory and provide continuous digging, transfer and shaking out of rock masses [2]. With these bucket-wheel excavators there is no rotating operation unlike with the cyclic bucket-wheel excavators. Regardless to a great number of bucket-wheel excavators constructed so far, there is always an option for further advancements and improvements referring to the construction and performances.

Fig. 1. Illustration of the bucket-wheel excavator SRs (H) 220 9.5/0.5

The bucket-wheel excavator SRs(H) 220 9.5/0.5 (Fig. 1) is a medium size bucket-wheel excavator with electro-mechanic drive, while the manipulation of hoisting and lowering of the operating wheel and of the hoisting and lowering of the discharge boom is carried out hydraulically [3, 4]. The above mentioned bucket-wheel excavator is equipped with a discharge boom to perform loading to conveyer systems. Theoretical working capacities amount to 770 m^3h^{-1} of loose material at the working specific force of 220 $kpcm^{-1}$ of the tooth width. The working height amounts to 9.5 m. In the case of decreased efficiency, the working height of up to 10 m is achieved. The power is supplied through a cable approximately 250 m long which is wound on a drum located on the lower structure of the bucket-wheel excavator.

As regards the balancing of the rotor boom and of the discharge boom, the bucket-wheel excavators can be divided into the bucket-wheel excavators with:

- the balancing of the rotor boom,
- the balancing of the rotor and of the discharge booms,
- balancing of the rotor boom and hanging of the discharge boom to a special support,
- mutual balancing of the rotor and the discharge booms placed on the same bearing structure.

According to the placement of the discharge boom receiving part:

- with the placement of the discharge boom receiving part to the rotating platform,
- with the placement of the discharge boom receiving part to the lower facility,
- with the placement of the discharge boom receiving part to the central intermediate platform.

According to the structure of the lower facility - moving mechanism:

- on caterpillars,
- on railway rails,
- moving bucket-wheel excavators.

Compact bucket-wheel excavators have been developed over the last 30 years. A compact bucket-wheel excavator can be defined as an active space mechanism, a mechanically multivariable system of a rather complex structure of a locomotors-handling type [5, 6]. The cutting process makes the kinematic configuration of the bucket-wheel excavator changing during the working cycle.

2. Research Polygon

The bucket-wheel excavators represent the skeleton of the mechanization system in the open pit mines. Their exploitation under extremely heavy conditions result in failures of parts of the bearing structure (plastic deformations, splits, cracks, breaks and the like). The polygon of the research in this paper is the bucket-wheel excavator SRs (H) 220 9.5/0.5 (Fig. 1). In situ researches on the bucket-wheel excavator were carried out, while an appropriate software was used to carry out other researches referring to the modeling and the simulation of the load of the structure of the bucket-wheel excavator rotating platform.

Fig. 2. Structure of the rotating platform of the bucket-wheel excavator

Fig. 3. Damages on the structure of the rotating platform of the bucket-wheel excavator

The rotating platform (Fig. 2) represents the base part of the superstructure of the bucket-wheel excavator which supports a tower with the counterweight arrow, a boom with the operating wheel and drive and the loading boom. The rotating platform takes the total superstructure load and transmits it to the lower machine with a caterpillar moving mechanism. Splits and cracks have appeared on the rotating platform structure over many years of the exploitation of the bucker-wheel excavator SRs (H) 220 9.5/0.5 (Fig. 3). For this reason the reconstruction of the bucket-wheel excavator rotating platform was proceeded to.

3. Computer 3D Model of the Rotating Platform Structure

Computer 3D model of the rotating platform structure (Fig. 4) is formed based upon the original technical documentation. The computer model makes possible a higher number of simulations, faster estimation and analysis of the rotating platform structure stress, taking into consideration the set limitations and different values for the input parameters (loads). The computer 3D model of the rotating platform structure is formed in such a way that it corresponds to the actual structure in all the details. The rotating platform structure is shaped in accordance with its purpose (load transmission) and comprises two basic sub-domains:

- cylinder beam supported by a radiaxial bearing,

- two cantilever beams elastically fixed into the cylinder beam, to which the latticed structure of a tower with the counterweight arrow is linked by means of corresponding eyes.

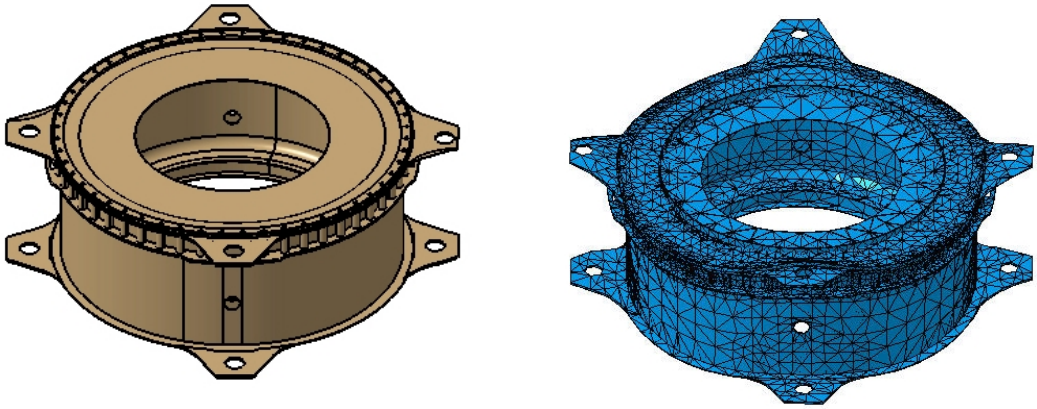

Fig. 4. 3D model of the rotating platform structure

The analysis of the rotating platform structure stress was performed in accordance with the regulations of the standards DIN 22261-2 for the case of the action of the main loads - H. This case comprises the combinations of loads acting constantly during the bucket-wheel excavators operation. These are: constant load resulting from their own weights (E), the weight of the transported material (F), the weight of the crust - pasted soil material (V), loads resulting from the action of the wind (W), loads owing to the slope (N), large force on the rotor (U), lateral force (S) and dynamic loads (D). It is interesting to mention that, when identifying the large and lateral forces on the rotor, according to the standard DIN 22261-2, the influences of their eccentricities in relation to the system lines of the arrow and of the incline with respect to the horizontal and vertical plane, are neglected. The changed position of the rotor arrow results in the change of:

- the position of the centre of the masses located on it,
- the position of the lines of the action of the external loads caused by the working resistance, which conditions the dependence of the loads of the tower and of the counterweight arrow upon the rotor angle of incline with respect to the horizontal line.

The identification the stress-deformations condition of the original rotating platform structure was carried out for the case of load which most frequently occurs during the working process of the mining machine - the bucket-wheel excavator. In order to recognize more clearly the nature of the structure movement, Fig. 5. shows the appearance of the deformed rotating platform structure in different planes. The maximum stress value of 23.5 kN/cm^2 occurs on the lower board in the internal part of the rotating platform structure.

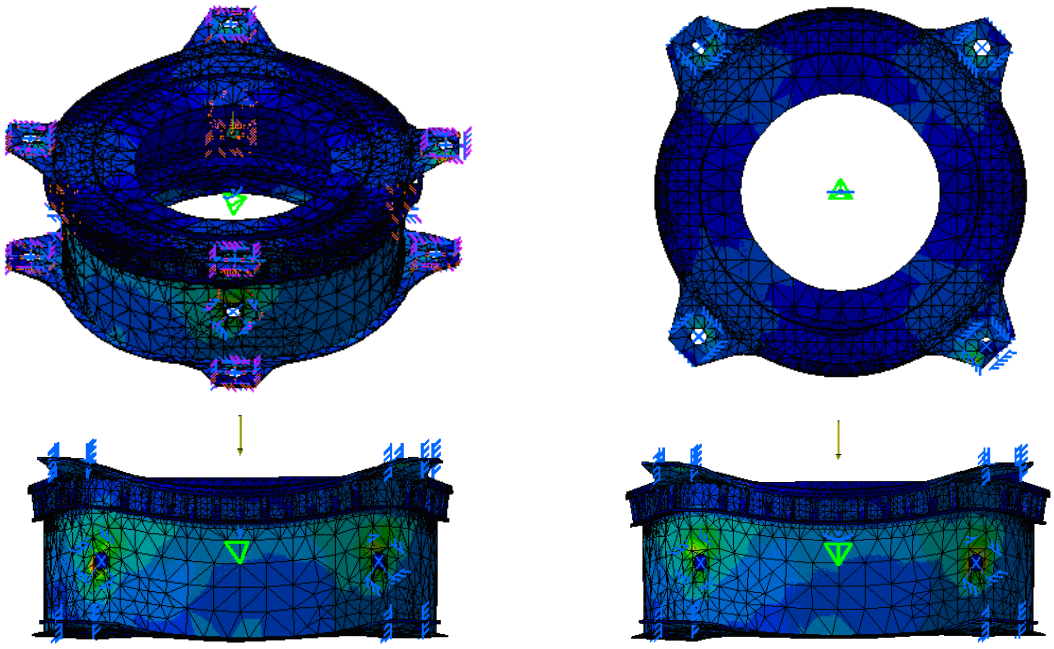

Fig. 5. Results of the performed simulations on the computer 3D model of the rotating platform structure the bucket-wheel excavator SRs (H) 220 9.5/0.5

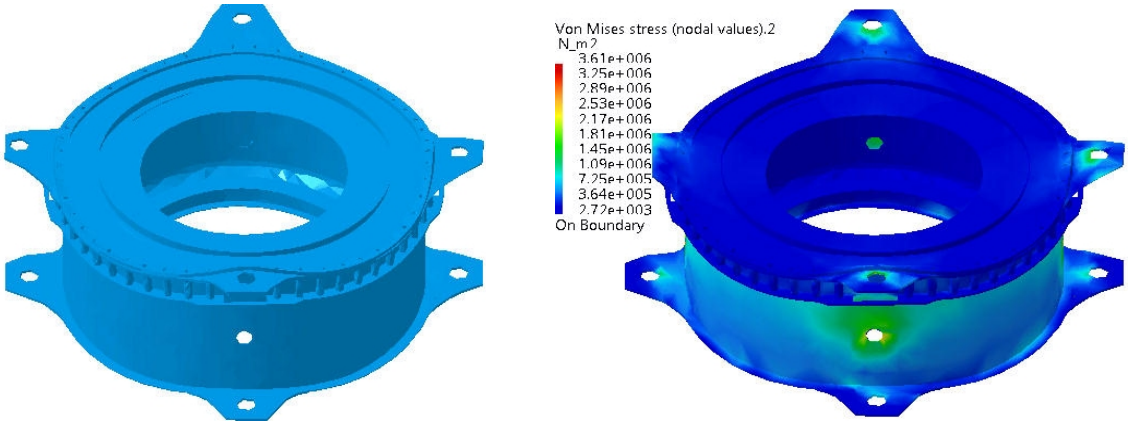

Fig. 6. The illustration of the stress on the computer 3D model of the rotating platform structure

The appearance of the rotating platform structure and of the zone of the occurrence of splits and cracks is shown on the Fig. 6. Here are clearly evident distinct changes in the movement field. The clear illustration of the stress distribution is also presented. Using corresponding results of the in situ measurements and performing a greater number of simulations on the 3D model of the rotating platform structure, the conditions for the reclamation and the reconstruction of the rotating platform structure of the bucket-wheel excavator SRs (H) 220 9.5/0.5, were created.

4. Conclusions

Based upon the created 3D model and the executed in situ measurements on the actual structure, the items of information were acquired which refer to the occurrence of stress and deformations of the structure of the rotating platform of the bucket-wheel excavator SRs (H) 220 9.5/5.0. This information was used to reconstruct the rotating platform structure of the bucket-wheel excavator. When doing this, it was necessary to notice the weak points in the existing solution of the rotating platform structure and then to study and analyze the existing similar solution, aiming at finding such a solution which will secure more reliable and safer operation of the bucket-wheel excavator. In order to achieve this, corresponding software's for the stress modeling and simulation were used on the created 3D model of the rotating platform of the bucket-wheel excavator. Contemporary approach based upon the application of appropriate software's, modeling process, considerably facilitates simulations and shortens the time required to carry out optimization and to find the most favorable solution which will providing increased reliability in operation and lower costs. By performing the visual control of the reconstructed rotating platform, after the bucket-wheel excavator had worked under actual conditions, no occurrences of splits or cracks on the rotating platform were found.

References

1. **Grathof H.** Design (Constructional Characteristics) of Large Bucket Wheel Excavators. Journal of Mines, Metals, and Fuels, 34(4), 204-213. 1986.
2. **Durst W., Vogt W.** Bucket wheel excavator, Trans. Tech. Publications, Series of Mining Engineering, vol. 7, 1988.
3. **Jevtović B., Mataušek M.** Bucket-Wheel Excavator: Theory and Experimental Results, Elec. Energ. vol. 18, no. 3, December 2005.
4. **Marinković Z., Petrović G.** Processing the lifetime of bucket wheel excavator parts in strip mine technologies, Mechanical Engineering Vol. 2, No 1, 2004.
5. **Schlecht B.** Simulation of the Bucket Wheel Drive of a Compact Bucket Wheel Excavator, Krupp Foerdertechnik GmbH, Germany.
6. **Chironis N.** Bucket Wheel Excavators of Compact Design Growing Popular. Coal Age, 84(10), 84-91. 1984.

Identification the Stress on the Working Wheel Carrier of the Loading System the Bucket-Wheel Excavator SRs (H) 220 9.5/0.5

D. Sprečić, F. Mulahalilović, F. Mrkaljević

University of Tuzla, Faculty of Mechanical Engineering, Univerzitetska 4, 75000 Tuzla, Bosnia and Herzegovina
E-mail: esprecic@bih.net.ba

Abstract

In the paper was carried out the research, the aim of which was to optimize the working wheel carrier of the loading system the bucket-wheel excavator applying contemporary methods based upon the computer modeling and simulation. The existing solution of the loading system was executed based upon the components which are obsolete and no longer in use. Some of the components have not even longer been manufactured. Therefore, the aim of the reconstruction of the loading system of he bucket-wheel excavator, i.e., of the working wheel carrier, is to obtain a more contemporary, more functional and more reliable loading system. With the reconstruction of the loading system support and the building-in of the contemporary components, the working reliability of the loading system will be increased and the costs of its maintenance will be lowered.
KEY WORDS: *bucket-wheel excavator, working wheel carrier, 3D model.*

1. Introduction

Bucket-wheel excavators represent complex mechatronic systems. Generally speaking, they can be divided according to their purpose or according to the working technology [1,2]. According to their purpose, the bucket-wheel excavator are divided into:

- bucket-wheel excavators used for overburden;
- bucket-wheel excavators used for mineral raw material;

and according to the method of working:

- bucket-wheel excavators used for high digging;
- bucket-wheel excavators used for high and deep digging.

Compact bucket-wheel excavators have been developed over the last 30 years. The difference between the compact bucket-wheel excavators and the classical ones is as follows:

- classical structures have mostly multi-caterpillar moving mechanism, high-placed counterweight and very long working wheel carrier in relation to the diameter of the working wheel ($L_k / D > 3$);
- compact bucket-wheel excavators have double-caterpillar moving system, low-placed counterweight in the platform extension and relatively short working wheel carrier ($L_k / D > 2$).

Nowadays intensive efforts have been done to develop a new family of baggers which would unite good features of the classical and the compact bucket-wheel excavators under the name of semi-compact baggers with the ratio of $L_k / D = 3$. Many researchers and manufacturers of the bucket-wheel excavators are involved in the researches connected with the improvement of the characteristics working wheel carrier of the loading system [7]. This refers particularly to the location of the working wheel in relation to the geometry of the carrier, because the efficiency operation of the total system mostly depends of the location of the working wheel.

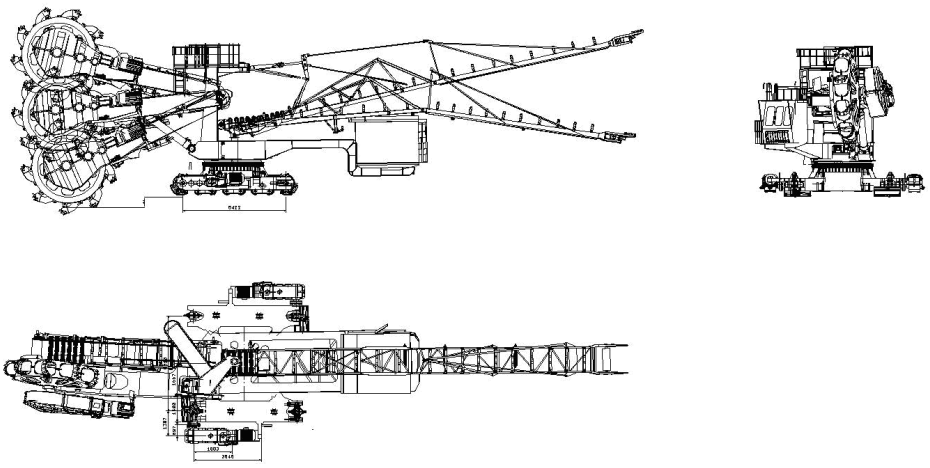

Fig. 1. Illustration of the bucket-wheel excavator SRs (H) 220 9.5/0.5

Under the improvement of the characteristics of the loading system mechanism the optimization of the working wheel support (cantilever, boom) is generally understood. This requires to:

- improve power efficiency (reduction of losses resulting from the shut-downs which are most frequent if the appropriate sliding plane is not achieved);
- increase the resistance moment of the working wheel carrier;
- improvement of the angles of sliding of materials and cutting.

2. Research Polygon

The bucket-wheel excavator SRs (H) 220 9.5/5.0 (Fig.1.) represents the research polygon. In situ researches on the bucket-wheel excavator were carried out, while the other researches referring to the modelling, simulation and optimization of the loading system were carried out by means of the application of corresponding software's [6]. Over several years of the exploitation of the bucket-wheel excavator SRs (H) 220 9.5/5.0 in an open pit mine, numerous defects have been noticed on the loading system (particularly damages of the working wheel carrier) which were partly eliminated during the course of the work, i.e., during the course of the bucket-wheel excavators exploitation. The growing unreliability and frequent shut-downs and, consequently, the capacity drop, impose the necessity to reconstruct the unreliable and obsolete loading system. For this reason it was necessary to execute the reconstruction of the working wheel carrier, taking into account, when doing this, the possibility to purchase new equipment and the economic aspect of the reconstruction [5].

Fig. 2. The working wheel carrier of the loading system of the bucket-wheel excavator SRs (H) 220 9.5/0.5

3. Basic Parameters for the Determination of the Length of the Working Wheel Carrier

In order to carry out the reconstruction of the working wheel of the existing loading system of the bucket-wheel excavator, it was necessary to perform corresponding researches and experimental measurements on the support (boom) of the loading system of the bucket-wheel excavator according to a clearly defined methodology [3,4]. To this effect, the planned researches were implemented through theoretical and experimental parts of the research. Within the framework of the theoretical part, the basic parameters and elements of the estimate for the determination of the length of the working wheel carrier were presented. The length of the working wheel carrier, among other things, can be determined based upon the following expression:

$$L_k = \frac{(H - h_n)\operatorname{ctg} a_b - (X + r)(\sin b_u - \sin b_d)}{\cos d_u \sin b_u - \cos d_d \sin b_d} \tag{1}$$

This is possible in the case when the incline angles of the working wheel carrier are known. In the expression (1) it is:

H = 9.5 m	bench height,
H_n = 4.4 m	the last bench height,
X = 0.723 m	the distance of the attachement point of the working wheel carrier from the axis of the bucket-wheel excavator,
r = 2.6 m	diameter of the working wheel,
d_u = 27°	incline angle of the working wheel carrier at the overcut,
d_d = 22°	incline angle of the working wheel carrier at the undercut,
b_u = 85°	inner angle of the working wheel carrier rotation at the upercut,
b_d = 45°	inner angle of the working wheel carrier rotation at the undercut,
a_b = 60°	incline angle of the lateral slope.

4. Computer 3D Model of the Working Wheel Carrier of the Loading System

In order to execute a greater number of simulations and to analyze the results, the computer 3D model of the working wheel carrier of the loading system of the bucket-wheel excavator, was formed. The computer 3D model makes possible a greater number of simulations, quicker estimation and analysis of the stress on the working wheel carrier of the loading system taking into account the set limitations and different values of the input parameters (loads).

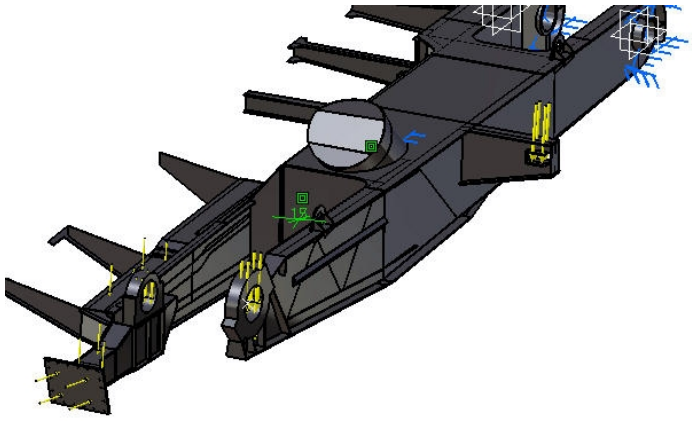

Fig. 3. The computer 3D model of the working wheel carrier of the loading system the bucket-wheel excavator SRs (H) 220 9.5/0.5

5. Results of the Load Analysis on the 3D Model

After the appropriate experimental researches had been done and the results of the measurements on the working wheel carrier had been obtained, the results of the measurements and the results obtained on the basis of a greater number of executed simulations on the created 3D model were compared. The coincidence of the results confirmed the validity of the created 3D model of the working wheel carrier of the loading system the bucket-wheel excavator.

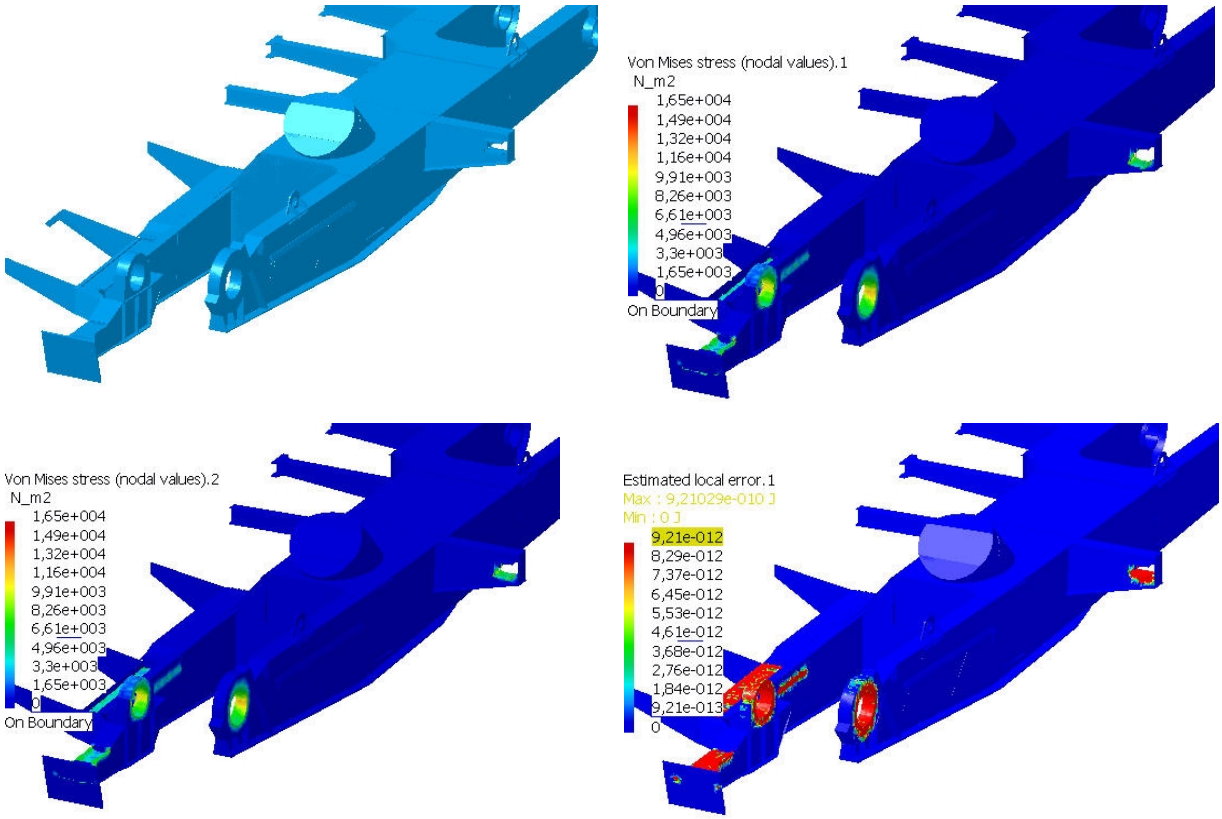

Fig. 4. The results of the performed simulations on the computer 3D model of the working wheel carrier of the loading system the bucket-wheel excavator SRs (H) 220 9.5/0.5

The analysis of the tension-deformation condition of the structure of the working wheel carrier of the loading system of the bucket-wheel excavator was performed in accordance with the regulations of the standards DIN 22261-2 for the case of the action of the main loads – *H*. This case comprises the combinations of loads acting constantly during the bucket-wheel excavators operation. These are: constant load resulting from their own weights (*E*), the weight of the transported material (*F*), the weight of the crust – pasted soil material (*V*), loads resulting from the action of the wind (*W*), loads owing to the slope (*N*), large force on the rotor (*U*), lateral force (*S*) and dynamic loads (*D*). It is interesting to mention that, when identifying the large and lateral forces upon the working wheel, according to the standard DIN 22261-2, the influences of their eccentricities in relation to the system lines of the arrow and of the incline with respect to the horizontal and vertical plane, are neglected.

The identification of the transmitted main loads from the working wheel (rotor) to the loading boom structure is carried out on the basis of the created 3D model for different values of loads which occur during the exploitation and the work of the bucket-wheel excavator. For each of the analyzed variants, the estimate of the relevant values for the whole range of the changes in the incline angle of the loading boom and of the intensity of the forces which load the loading boom structure was done.

The external load of the loading boom structure was introduced by means of the joint links with the tower superstructure. The reaction of the support of the loading boom structure were introduced as the external load of the structure of the slide bearing of the loading boom, with the sinus spreading (distribution) across the contact surfaces of axes and eyes.

When analyzing the deformations of the loading boom structure, it was noted that the greatest movement occurred in the zone of the front right eye and it amounted to 45 mm. The highest value of the tension on the working wheel carrier structure amounts to 33.5 kN/cm^2. The maximum value of the stress on the front board of stator on the working wheel carrier is 23.5 kN/cm^2, while the maximum value of the stress in the zone in which splits occur is 20.0 kN/cm^2.

After the performed analysis of the tension-deformation condition of the working wheel carrier and the determination of the weak points on the support structure, the support reclamation and reconstruction were executed in order to eliminate damages and secure safe working of the bucket-wheel excavator.

6. Conclusions

Analyzing the load on the computer created 3D model of the working wheel carrier the loading system, and performed in situ measurements in real-loading system, we created the conditions for reconstruction working wheel carrier of the loading system the bucket-wheel excavator SRs (H) 220 9.5/0.5. When doing this, it was necessary to notice the defects of the existing system and then to study and analyze the existing similar solutions, aiming at finding such a solution which will secure more reliable and safer operation of the bucket-wheel excavator. In order to achieve this, corresponding software's for the modeling and simulation of the load of the loading system structure were used. Contemporary approach based upon the application of appropriate software's, modeling process, considerably facilitates the simulations and the analysis of the load of the loading system elements and shortens the time required to carry out optimization and to find the most favorable solution which will provide increased reliability in operation and lower costs.

References

1. **Bošnjak S., Zrnić N.** On the dynamic modeling of bucket wheel excavators, Faculty of Mechanical Engineering, Belgrade, FME Transactions, 2006.
2. **Durst W., Vogt W.** Bucket wheel excavator, Trans. Tech. Publications, Series of Mining Engineering, vol. 7, 1988.
3. **Jevtovic B., Mataušek M.** Bucket-Wheel Excavator: Theory and Experimental Results, Elec. Energ. vol. 18, no. 3, December 2005.
4. **Marinković Z., Petrović G.** Processing the lifetime of bucket wheel excavator parts in strip mine technologies, Mechanical Engineering Vol. 2, No 1, 2004.
5. **Schröder D.** Economic and technologic aspects of Bucket-wheel Excavator – and Crusher/Conveyor-Systems, Krupp Fördertechnik GmbH, Essen, Germany
6. **Schlecht B.** Simulation of the Bucket Wheel Drive of a Compact Bucket Wheel Excavator, Krupp Foerdertechnik GmbH, Germany.
7. **Tanasijević M., Ivezić D.** Quality of Service Evaluation for Bucket Wheel Excavator, Monography Machine Design, Faculty of Technical Sciences, Novi Sad, 2007.

Proceedings of 5th International Conference ITELMS'2010

Sustainable Development Approach to Mobility Management

D. Susnienė

Kaunas University of Technology Panevežys Institute, Klaipėdos str. 1, 35209 Panevėžys; e-mail: dalia.susniene@ktu.lt

Abstract

The public organizations that are responsible for the delivery of a large share of transportation facilities need to become more flexible and adaptive in response to increasingly uncertain and unpredictable external conditions, on the one hand, and to become more creative in enhancing the capability of the facilities they operate. Involvement of stakeholders in supply of public transport services, i.e. what level of relationships are needed between a transportation company and its various stakeholders is necessary in order to meet the main stakeholder – passenger – needs. Consequently, as to supply the passenger with best service, relationships between different stakeholders (municipality. public transport company. state. road maintenance service. etc.) are of vital importance. Helping stakeholders to set up transport policies effective in making travel behaviors more sustainable is one of the central issues in making urban travel greener, better organized and more user-friendly.
KEY WORDS: *mobility, sustainable development, public transport, management, stakeholders.*

1. Introduction

Urban mobility is recognized as an important facilitator of growth and employment with a strong impact on sustainable development in the EU. Addressing market needs forms is essential component of success for public transport in all countries. Effective development of public transport systems requires involvement of the many stakeholders who form part of the public transport industry. Most of these have a direct or indirect interest in the systems either in terms of systems to manage service operations or systems to inform customers.

2. Negative Aspects of Urban Mobility

European cities increasingly face problems caused by transport and traffic. The question of how to enhance mobility while at the same time reducing congestion, accidents and pollution is a common challenge to all major cities in Europe. Congestion in the EU is often located in and around urban areas and costs nearly 100 billion Euro, or 1% of the EU's GDP, annually [1], see Fig. 1, Table 1.

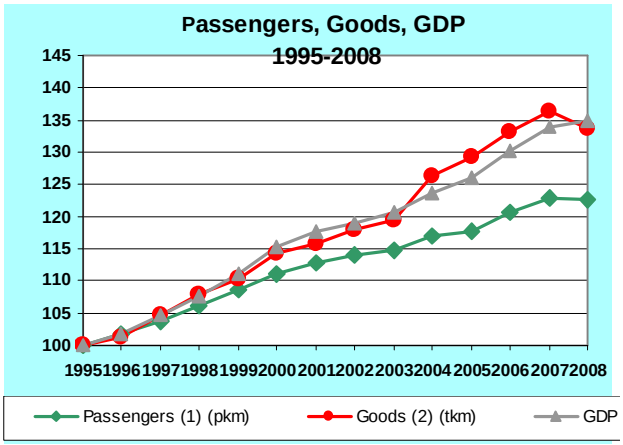

Notes:

(1) – passenger cars, powered two-wheelers, buses & coaches, tram & metro, railways, intra-EU air, intra-EU sea

(2) – road, rail, inland waterways, oil pipelines, intra-EU air, intra-EU sea

GDP – at constant year 2000 prices and exchange rates

Fig. 1. Transport growth EU 27 (Source: <http://epp.eurostat.ec.europa.eu/>)

A large majority of European citizens live in an urban environment, with over 60% living in urban areas of over 10.000 inhabitants. They live their daily lives in the same space, and for their mobility share the same infrastructure. Urban mobility accounts for 40% of all CO_2 emissions of road transport and up to 70% of other pollutants from transport. Negative aspects of urban living include traffic congestions, noise, poor public transport, urban sprawl, air pollution, a lack of easily accessible shops and services, and a host of other daily conveniences. Many bigger cities are reaching crisis point. Choked roads, overburdened public transport systems, pollution, noise and poorly serviced neighbourhoods are making life increasingly unbearable for more and more citizens. Urban congestion, road accidents, air pollution and energy consumption all have a negative impact on country's economy and the welfare of all its citizens. More than 70% of the EU population lives in urban areas while about 85% of the EU's GDP is generated in

cities. Some 40% of CO_2 emissions and 70% of emissions of other air pollutants from road transport are due to urban traffic. In addition one in every three fatal road traffic accidents happens in urban areas [2].

Table 1

Annual growth rates EU 27

GDP at year 2000 prices and exchange rates	1995-2008 p.a.	2,3%	2000-2008	2,0%	2007-2008	0,7%
Passenger transport pkm	1995-2008 p.a.	1,6%	2000-2008 p.a.	1,2%	2007-2008	-0,3%
Freight transport tkm	1995-2008 p.a.	2,3%	2000-2008 p.a.	2,0%	2007-2008	-2,1%

The number of road traffic accidents in towns and cities is growing each year: one in three fatal accidents now happen in urban areas, and it is the most vulnerable people, namely pedestrians and cyclists, who are the main victims (Table 2). While it is true to say that these problems occur on a local level, their impact is felt on a continental scale: climate change/global warming, increased health problems, bottlenecks in the logistics chain, etc.

Table 2

Road fatalities country rankings
(Source: <http://epp.eurostat.ec.europa.eu/>)

Fatalities 2008					
per million inhabitants		per 10 billion pkm		per million passenger cars	
MT	36	UK	39	MT	66
NL	41	SE	40	UK	91
SE	43	NL	45	NL	91
UK	43	LU	51	SE	93
DE	55	DE	51	LU	108
IE	63	FI	53	DE	109
FI	65	IE	56	FI	131
ES	68	FR	58	IT	132
FR	69	IT	59	FR	137
LU	72	MT	68	ES	141
DK	74	DK	75	IE	144
EU27	**78**	**EU27**	**80**	AT	159
IT	79	BE	84	**EU27**	**168**
AT	81	SI	85	BE	185
PT	83	ES	89	CY	192
BE	88	AT	91	DK	195
EE	98	PT	99	PT	201
HU	99	EE	124	SI	208
SK	103	**LT**	**129**	EE	245
CZ	103	CY	139	CZ	247
CY	103	CZ	142	**LT**	**306**
SI	106	EL	147	EL	317
EL	138	LV	181	HU	328
BG	139	PL	196	LV	344
LV	139	SK	206	PL	355
RO	142	HU	230	SK	375
PL	143	BG	241	BG	477
LT	**148**	RO	420	RO	809

Notes:

Fatalities: all fatalities on the road: car drivers and passengers, bus and coach occupants, powered two-wheelers' riders and passengers, cyclists, pedestrians, commercial vehicle drivers, etc. indicated in table 3.7.1 for 2008

pkm: indicator of traffic volume (in the absence of consistent vehicle-kilometre data); passenger-kilometres of cars indicated in table 3.3.4 for 2008 plus (mostly estimated) passenger-kilometres of motorised two-wheelers

inhabitants: the sum of the population indicated in table 1.5 at 1 January 2008 and 1 January 2009 divided by two

passenger cars: the sum of the stock of vehicles indicated in table 3.6.2 for 2007 and 2008 divided by two.

BE: Belgium
BG: Bulgaria
CZ: Czech Republic
DK: Denmark
DE: Germany
EE: Estonia
IE: Ireland
GR: Greece
ES: Spain
FR: France
IT: Italy
CY: Cyprus
LV: Latvia
LT: Lithuania
LU: Luxembourg
HU: Hungary
MT: Malta
NL: Netherlands
AT: Austria
PL: Poland
PT :Portugal
RO: Romania
SI: Slovenia
SK: Slovakia
FI: Finland
SE: Sweden
UK: United Kingdom

Local authorities cannot face all these issues on their own; there is a need for cooperation and coordination at all stakeholder levels. The vital issue of urban mobility needs to be addressed as part of a collective effort involving different stakeholders: local, regional, national and European. The European Union must play a leading role in order to focus attention on this issue (2, 3).

3. Sustainable Development and Mobility Management

However, there is one overriding idea that constantly recurs: to be effective, urban mobility policies need to be based on an approach which is as integrated as possible, combining the most appropriate responses to each individual problem: technological innovation, the development of clean, safe and intelligent transport systems, economics incentives and amendments to legislation.

Efficient urban transport systems are critical elements of the sustainable development of urban areas. They ensure that:

- people have access to employment, education and recreation facilities, goods & services;
- the risk of social exclusion is minimized (people without car, young, elderly, unemployed and disabled people);
- the distribution of goods is properly achieved.

Efficient and effective urban transport can significantly contribute to achieving objectives in a wide range of policy domains concerning sustainable development. The success of policies and policy objectives that have been agreed at EU level, for example on the efficiency of the EU transport system, socio-economic objectives, energy dependency, or climate change, partly depends on actions taken by national, regional and local authorities. Mobility in urban areas is also an important facilitator for growth and employment and for sustainable development in the EU areas. Tackling these challenges will address citizens' concerns.

4. Stakeholder Approach in Management of Public Transport Services

How carefully do public transport organizations listen to its customers and other stakeholders? Everyone says they listen but do they actually hear what the customer is saying? Or do they tend to filter customer needs and expectations through old paradigms, twisting what customers say they want to fit what you thought they wanted, or what you hoped they wanted, or perhaps what you already provide? The only reasonable way in which to reconcile individual aspirations and the will of all stakeholders in public transport, is to provide public transport services of the highest possible quality in a way that will persuade a large number of inhabitants to resist the temptation to use individual modes, to resist the temptation to use individual modes, to give public transport a try and become regular public transport users. The improvement of quality presents positive stakes for all the stakeholders concerned: the public authority, the clients, the operators, the community and others. Any such action to improve quality naturally comes at a price of all stakeholders. However, it must be seen as an investment whose beneficial spin-offs for the community, passengers and operators will easily justify the commitment. Competing with other modes of transportation, especially the personal car, requires understanding what good public transport service is and why it is important [4, 5]. The first question is, “What is customer service and how can public transport service meet customers’ and other stakeholders’ needs? Clearly, customer service means more than putting vehicles on the street. In the broadest sense, customer service is doing whatever it takes to satisfy passengers. Service quality is more elusive than product quality. Because human behavior plays such an important role in service quality, it cannot be dealt with as much rigor and precision as one would engineer a manufacturing process so as to produce consistent products [6, 7]. However, as consumers and users of both products and services, we have no trouble identifying what is important to us. Customer satisfaction or the lack thereof, is the difference between the services customer expect from public transport system and the services they perceive they are getting, all the time comparing public transport services to alternative modes of travel. While most passengers do not expect public transport services to be as convenient as a personal car, they often expect them to be more affordable. They have every right to expect that buses will arrive on time, be clean, comfortable, safe, and that the whole process of using public transport will be understandable and responsive to them as users.

A tool which takes stakeholder demands as its energy source, and focusing those demands so intently that it can cut through old modes of thinking and operating, to pinpoint a product or level of service that truly will satisfy your customer [8, 9]. Stakeholder can be a good source of information and finding solutions. For example, experiences from stakeholders show that there is no single solution to reduce congestion. However, alternatives to private car use, such as walking, cycling, collective transport or the use of the motorbike and scooter should be made attractive and safe. Citizens should be able to optimize their travel through efficient links between the different modes of transport. Authorities should promote co-modality and reallocate space that becomes available after congestion mitigation measures. Intelligent and adaptive traffic management systems have also proven their efficiency in reducing congestion.

Involvement of stakeholders into provision of public transport services is necessary to assure that a passenger as an important stakeholder would be satisfied [10, 11]. Therefore, it is necessary to implement new management models in order to achieve good results and create value to stakeholders. It is necessary to identify and structure the criteria of meeting stakeholder needs, and to adapt them to organizational management and activity processes. Thereby the issue of satisfaction of stakeholder needs is viewed from organizational aspect and is confined to organizational management and activity processes. The position is taken up that in order to create value for stakeholders it is necessary to identify criteria that organization could follow in its activity and consequently generate premises for efficient management of stakeholder relationships and for satisfaction of stakeholder needs.

Particular stakeholders or their groups could be distinguished in public transport enterprises. A very large impact on the decisions of the public transport enterprises has not only typical stakeholders (customers and end users, employees, owners and investors, suppliers and partners, community) but state institutions and local authorities (municipalities) as well. Unlike other organizations public transport enterprises experience great influence from state institutions and local authorities in their decision taking, organizational management and performance. Therefore, public transport enterprises have particular stakeholders with the specific relationships and influence, and it is important to know how to align and satisfy their interests. Consequently, the research carried out on the example of public transport enterprises will help to solve the analogical problems of other organizations, which have smaller number of stakeholders and their groups.

5. Challenges for Public Transport (PT)

Existing urban public transport must improve and develop their activity in many aspects:

- ***Improving PT attractiveness.*** Public transport is considered key to the policy objectives of achieving an integrated and sustainable transport system. Improvements to public transport operations alone will not necessarily persuade people to forego the use of their cars and make use of public transport modes. Improvements to public transport operations alone will not necessarily persuade people to change mode. Intending travelers need to be informed of what is available [12]. Existing urban public transport systems must improve their travel speed, reliability and quality. New organizations and wider application of new PT systems based on existing new technologies with lower cost must be investigated.

  Taking care of innovation and optimization. New innovative public transport services should be developed, in terms of development and applications of public transport organization in areas with low population density and in times with low demand. New sources and forms of innovation need to be identified and legally facilitated to provide additional development means for public transport infrastructure and services: expansion of research on fresh concepts in urban buses systems in towns in relationship with new mobility culture, such as new modular vehicles offering dedicated wagonloads to major roads or to secondary roads or to different uses; new optimization of the multi-modals systems of transport including buses, trains, bikes and so on.

  New technologies: driven by industry and in response to the European emissions thresholds, conventional combustion engine technology is becoming cleaner. Catalytic converters and particulate filters will yield significant improvements in reduction of pollutant emissions in the future. Research and technological development co-funded by the EU has had a strong focus on clean and energy efficient vehicle technologies and alternative fuels, such as biofuels, hydrogen and fuel cells[1] [2, 13]. The environmental performance of the existing vehicle fleet could be further improved by setting harmonised minimum performance standards for the operation of vehicles. A gradual tightening of these standards over time could lead to a continuous process of upgrading or phasing out of old heavily polluting vehicles. Such a general approach could help to increase the use of clean and energy efficient vehicles in urban transport and on the longer term prevent a fragmented patchwork of different low-emission zones.

  Further promotion of a broad market introduction of new technologies could be achieved through economic instruments, such as incentives for the purchase and operation of clean and energy efficient vehicles by public authorities, and non-economic instruments, such as restrictions for heavy polluters and privileged access for low-emitting vehicles in sensitive areas, provided they do not distort the internal market rules.

- ***Involvement of all stakeholders.*** According to all the stakeholders, the new economic context justifies a pursuit of efficiency effort in transport with a new urban mobility culture. New technology to improve BHLS (Bus with High Level Services) and BRT (Bus Rapid Transit) new solutions are concerned as well as fresh concepts for organizing urban transport.

  Some strong recommendations must be welcomed by all the stakeholders:

  - Urban mobility must be taken in a very large sense of the term including persons and goods, cities and inter-cities management, public transport and new public or private solutions, new urban mobility policies.
  - Partnership between transport research institutions and city authorities has to be most often develop in different fields.
  - Towns and cities policy makers and citizens are now aware of the very important role of urban mobility management on different scales levels and with an open-minded intermodal way of thinking.
  - It is time for the research to make a bigger step in many topics related to urban mobility (from citizens' behavior to high tech traffic management or information, related to new transport systems).
  - European specificities in transport system must be analyzed and taken into account in relationship with the European harmonization closely linked with economic development and public transport management.

- ***Sustainable development.*** The demographic developments that are considered to have the highest impact on public transport are the continuous decline in birth rate and the ever-increasing life expectancy of the European population. Both trends lead to a significant shift in the age structure towards higher ages. Yet, elderly are expected to be more active in future with new mobility needs, but ageing will generate new transport needs.

  Major lifestyle changes will continue in future with the increase of new forms of work, changed consumption behavior and diversified leisure activities. An accompanying development will be the increasing wish of most customers to get individualized products and services. Public schedules will become less important. Travel patterns will become more individual and complex over distance and time. Traditional public transport services will have to be adapted accordingly.

  On the other hand, it has to be taken into account that a growing part of the society might not be able to adapt to the new technologies of information and communication proposed in PT. Many users are afraid of using high-tech devices (e.g. ticket machines or fully automatic transport systems). Automotive industry experience in that regard has to be used as a reference. Specific approaches have to be developed:

---

[1] See for example the Communication from the Commission to the European Parliament, the Council, the European Economic and Social Committee and the Committee of the Regions - Towards Europe-wide Safer, Cleaner and Efficient Mobility: The First Intelligent Car Report - COM(2007) 541, 17.9.2007.

- Development of physical implementations and major demonstration programs in the main big European cities according to the sustainable development aim (such as new bus station, implementation of system and demonstration sites, test of second generation hybrids, full electric, travelers information.
- Development and generalization of tools such as sustainable urban transport planning (including buses) as a contribution to sustainable urban mobility linked with city planning [13, 14].

- ***More customer-oriented services.*** In order to deliver more tailor-made yet efficient public transport services, travel patterns need to be analyzed as detailed as possible. The public transport providers have to respond to varying mobility needs of the different customer groups across distance and time (including at night). Assurance of easy access to PT use is also of great importance. Increasingly complex travel services and devices require public transport systems to be easy to understand before and during use, and to reduce inhibition thresholds [15, 16]. Ticketing and information systems will need to respond to the desired door-to-door service approach and be as simple as possible. For public transport infrastructure and rolling stock a higher level of accessibility is needed to respond to all travelers' demands.

  For the customer, service quality is everything. Approaches in the past that entailed (even opposing) one particular aspect of service quality to another – punctuality, safety, and customer service – overlooked this basic overall customer expectation. In the public transport sphere like any other, quality has to take account of service's every dimension [4].

  When faced with the necessity to travel, an individual's natural desire is for a personal mode of transport that is flexible, independent and that is perceived as fast. The only reasonable way in which to reconcile individual aspirations and the will of all stakeholders in public transport, is to provide public transport services of the highest possible quality in a way that will persuade a large number of inhabitants to resist the temptation to use individual modes, to resist the temptation to use individual modes, to give public transport a try and become regular public transport users [7]. It is important to finding way to enable the use of urban buses by giving the customers the possibility to use the trip time for work, information or leisure; to change the image of the bus in citizen's minds.

  The improvement of quality presents positive stakes for all the stakeholders concerned: the public authority, the clients, the operators, the community and others. Any such action to improve quality naturally comes at a price of all stakeholders. However, it must be seen as an investment whose beneficial spin-offs for the community, passengers and operators will easily justify the commitment.
- ***Creating a new urban mobility culture.*** The challenge facing urban areas in the context of sustainable development is immense: that of reconciling the economic development of towns and cities and accessibility with improving the quality of life and with environmental protection, on the other [13]. In order to address these issues, which have many and varied implications, a joint effort will make it possible to encourage the search for innovative and ambitious urban transport solutions with a view to arriving at a situation where towns and cities are less polluted and more accessible and where traffic within them flows more freely. Working together, we must seek ways of achieving better urban and suburban mobility, sustainable mobility, and mobility for all the inhabitants of Europe, while allowing economic operators to play their role in our towns and cities.
- ***Optimizing the use of private cars.*** Less car-dependent life-styles can be promoted through new solutions like car-sharing. More sustainable use of the private car should be encouraged for example by carpooling, which will lead to roads with fewer cars each of them carrying more people. Other options may also include "virtual mobility": tele-working, tele-shopping, etc.

  As suggested during the consultation, adequate parking policy is also necessary to reduce the use of cars in the centre of the cities. Providing more parking spaces may, in the long term, encourage car transport, in particular if they are free of charge. Parking fees can be used as an economic instrument. Differentiated fees can be considered to reflect the limited availability of public space and create incentives (e.g. free parking spaces at the periphery and high fees in the centre).
- ***Better information for better mobility.*** One of the critical success factors for mobility in urban networks is, for travelers, to be able to make informed choice on mode and time for travel. This relies on availability of user-friendly, adequate and interoperable multi-modal trip information for planning a journey.

  Stakeholders indicate that ITS allows a dynamic management of existing infrastructure. Additional capacity in excess of 20-30% or more can be gained by more effective use of road space [17]. This is particularly important since there is usually little scope to provide additional road space in urban areas. The active management of urban transport infrastructures can also have a positive impact on safety and the environment. A particular area for ITS could be the management of seamless connections between networks at the urban-interurban interface. Local authorities and private stakeholders should be fully engaged in the implementation and operation of these applications and services from the early stages onwards. Stakeholders will include technology providers, transport and infrastructure operators, industry, value-added service providers, digital mapmakers, enforcement agencies and infrastructure users.

6. Findings and Conclusions

Public Transport is in the front line, certainly for a long time, in regards to the sustainable development necessities and the new economic context. Therefore, there is a strong demand on research efforts in the medium term, demanding ambitious research programs [3, 12].

A quality approach cannot be implemented without knowing the quality expected by the customers; not the utopian quality that might dream outside the specific context, nor contrarily the quality that expect to encounter objectively during the next journey, but the service that customers see as legitimate and normal. The expression of this expected quality means that all the stakeholders have to view the services through customer's eyes [8]. This can be achieved mainly through the provision of improved services and performing research in the most important fields:

- ***Information management.*** Traditionally, public transport companies issued information on times and fares of their services, primarily through timetables and fares tables; these were generally complemented with marketing initiatives, including special offers. Provision of this core information remains fundamental at least as a foundation to gaining – and keeping – travellers. However, simply providing the information will not of itself suffice to persuade habitual car users that they should consider public transport as an alternative: in many cases they will not even think of accessing information sources to see what options exist. To attract their interest, it is essential that the extent and scope of information provision should be substantially widened so that they become aware of the opportunity. Effective development of public transport information systems requires involvement of the many organizations and stakeholders.
- ***Quality management.*** Quality objectives expressed in terms of results for the customer and assessment by detailed criteria, e.g. timeliness measured by the number of affected customers rather than by the number of trains delayed; harmonization of the methods used to check passenger numbers and deviations to time-tables; benchmarking studies on PT costs and PT efficiency. Efficient public transport system and its management play a very important role in increasing safety, improving network efficiency and stimulating intermodality which reduces transport impact on environment and makes cities more attractive. Even with the constantly increasing number of private cars public transport can play a very important role as efficient management of public transport system is vital to rapid economic growth and people welfare.
- ***Innovative operation methods and tools.*** Research on innovative organization and communications structures for PT undertakings, on optimization of fleet and operating systems under consideration of interfaces with other modes/companies as part of an integrated network at the entire city and hinterland level; on integrated technical platforms for intermodal communication and real-time "rendez-vouz" between vehicles (different lines, different modes, different operators, different authorities); on the development on the basis for an efficient PT supply chain management; on new operation methods to better answer a flexible demand (flexible working time for staff, new skills, etc.), on innovative tools for managing PT companies and innovative marketing techniques. Continued progress in meeting the needs of the mobility problem in developing cities will focus on: (a) highway building, hopefully used as an opportunity to rationalize access, (b) public transport management improvements, (c) pricing improvements, (d) traffic management, and (e) possibly an emphasis on rail rapid transit based on new revenue techniques.

References

1. Commission of the European communities. Communication from the commission to the European parliament, the council, the European economic and social committee and the committee of the regions , Brussels, 30.9.2009. Web site: <http://ec.europa.eu/transport/urban/urban_mobility/urban_mobility_en.htm>.
2. Green Paper: Towards a new culture for urban mobility [COM(2007)55]. Web site: <http://eur-lex.europa.eu/LexUriServ/LexUriServ.do?uri=CELEX:52007DC0551:EN:HTML:NOT>.
3. Commission of the European communities. The Citizens' Network – fulfilling the potential of public passenger transport [COM(95)601]. Web site: <http://eur-lex.europa.eu/LexUriServ/LexUriServ.do?uri=CELEX:51995DC0601:EN:HTML:NOT>.
4. **Kennedy C. A.** A comparison of the sustainability of public transport and private transport systems. Transportation, 29 (4), 2002, p. 459-493.
5. **Richard M.** Quality and customer's satisfaction. 52 nd International Congress, Stuttgart 1997.
6. **Eden C.** Making strategy: The Journey of Strategic Management / C. Eden,.F. Ackermann. – London: Sage Publications, 1998, 117p.
7. **Mopin P.** Customer Defined Quality Standards. Presentation to Union of Public Transport International Conference. 2000. Web site: <www.publ./lit45_html>.
8. **2Elias A. A.** Stakeholder analysis for systems thinking and modelling / A.A.Elias, R.Y.Cavana. 2000. Web site: <www.esc.auckland.ac.nz/organizations/ORSNZ/conf35/paper/BobCavana.pdf>.
9. **Fley J. K.** From quality management to organization excellence: Don't throw the baby out with the bath water // Proceedings of the fourth international and seventh national research conference on quality management. – Sydney, 2001. p. 154-177.
10. **Viegas J. M.** Public transport in the sustainable urban transport policy package: taking an integral policy approach. ECMT/OECD Workshop on implementing strategies to improve public transport for sustainable urban travel. Athens, Greece, 1999.
11. **Carnell Don. S.** Performance Excellence System at Public Transport Companies. 2003. Web site: <www.atco.org>.
12. **Vinck S.** Quality and Customer Satisfaction in Public Transport – 52nd International Congress Stuttgart'2000. Web site: < www.art.man.ac./transres/lect6.htm>.

13. Commission of the European communities. Developing the Citizens' Network [COM(1998)431]. Web site: <http://eur-lex.europa.eu/LexUriServ/LexUriServ.do?uri=CELEX:51998DC0431:EN:HTML:NOT>.
14. Commission of the European communities. Keep Europe moving - Sustainable mobility for our continent [COM(2006)314]. Web site: <http://eur-lex.europa.eu/LexUriServ/LexUriServ.do?uri=CELEX:52006DC0314:EN:HTML:NOT>.
15. **Gifford J. L., Stalebrink O. J.** Remaking transportation organizations for the 21st century: consortia and the value of organizational learning Transportation Research Part A 36 (2002) 645–657.
16. **Gakenheimer R.** Urban mobility in the developing world. Transportation Research Part A 33 1999, p. 671-689.
17. **Marco D., Mokhtarian P. L.** Grouping travelers on the basis of their different car and transit levels of use. Transportation Planning - Policy - Research - Practic , 2009, p. 645–657
18. **Lyons G., Harman R.** The UK public transport industry and provision of multi-modal traveler information / International Journal of Transport Management 1, 2002, p. 1–13.

Proceedings of 5th International Conference ITELMS'2010

Use of Co Nanoparticles in the Hydrogen Fuel Production

J. Tamuliene*, R. Vaisnoras, M. L. Balevicius*****

** Vilnius University, Institute of Theoretical Physics and Astronomy, A. Gostauto 12, 01108, Vilnius, Lithuania, E-mail: Jelena.Tamuliene@tfai.vu.lt*
*** Vilnius Pedagogical University, Studentu 39, 08106 Vilnius, E-mail:vaisnoras@vpu.lt*
**** University of Vilnius, Department of General Physics and Spectroscopy, Sauletekio al. 9, 10222 Vilnius, E-mail: Mindaugas.Balevicius@ff.vu.lt*

Abstract

The paper presents an investigation of compound consists of Co_2 nanoparticle and different number of water molecules. Presence of a solvent is accounted. Obtained results help us foresee possibility of the cobalt nanoparticle using to split hydrogen from water .
KEY WORDS: *Co nanoparticle, deprotonation, hydrogen, hydrogen molecule.*

1. Introduction

Today, climate change is one of the main problems that is related with carbon dioxide emissions. It is well known transport sector is dependent on fossil fuels and responsible for almost a quarter of the above emission. During several decades different technologies of the alternative fuels have been developed. One of them is hydrogen which is called a second-generation biofuel due to lack of harmful emissions in the use phase. It is quietly functioning and has increased efficiency of fuel cell vehicles when compared to internal combustion engines [1]. However, the technology is dependent on rare metals such as platinum and palladium that dramatically increase the cost of the hydrogen fuel. The using of the above metals may hinder hydrogen fuel to become more democratic, i.e. widely used. Hence, some issues have to be addressed in order to make hydrogen technology more promising.

One of the ways to make hydrogen fuel technology more attractive is to decrease its cost, i.e. in the above technology to use metals that are not so expensive as platinum and palladium. Recently, we have studied the geometrical and electronic structures of small Co_6O_m particles containing m = 1-9 Oxygen atoms applying density functional theory [2]. It has been pointed out, that the Oxygen atoms stabilize Co_6O_m (m = 0-9) particles. The results obtained indicate that stabilization effect is depended on a number of the Oxygen atoms and allows us to predict that starting with m = 7 (m is number of Oxygen atoms) further increasing the number of the atoms will not influence strongly the stability of Co_6O_m particles. The results obtained and the explanation presented allows us to foresee, that Oxygen atoms will stabilize Co_6 particles due to dissolution of Co-Co bonds that possess the antibonding character.

On the other hand, the above results allow us to predict that Co nanoparticle could deprotonate water, i.e. Co nanoparticles could be used in the hydrogen fuel technology instead platinum or palladium. Hence, the aim of research performed is to predict the above presumption.

2. Method of Investigations

The structural origin of clusters has been studied by using the generalized gradient approximation for the exchange-correlation potential in the density functional theory (DFT) as described by Becke's three-parameter hybrid functional, using the non-local correlation and provided by Lee, Yang, and Parr. The DFT methods is commonly referred to as B3LYP [3, 4] – a representative standard DFT method. The 6-31G basis set has been used as well [5].

The calculation s performed in the presence of a solvent by placing the solute in a cavity within the solvent reaction field applying the Polarizable Continuum Model using the integral equation formalism variant (IEFPCM model) . In this case the solute cavity is created via a set of overlapping spheres [6, 7]. The approach and basis set were chosen keeping in mind relatively minimum computational costs. The structures of the investigated nanoparticles have been optimized globally without any symmetry constraint and by starting from three initial geometries taking in account the temperature of the solvent. The number of water molecules and their displacement in respect of Co_2 particle taking in the account the properties of Co atom to form coordination complexes. The Gaussian program suite was used for all simulations here [8].

3. Results Obtained

The main results of the investigations of the systems consisting of Co_2 nanoparticle with 8, 12 and 16 water molecules indicate that in water the squar planar coordinated complexes of Co should be formed and at least one water molecule should be deprotonated. However, destroing of Co_2 nanoparticle is water molecule number dependen. In the compound consists of 8 water molecules the Co-Co bond is not destructed while in other compounds investigated this

bond is absent. Additionally, the above destruction of Co-Co bond is not temperature depended. It implies, that binding energy per atoms remains approximately the same with incresing the temperature, i.e. the energy of the compounds obtained in different temperature is equal to 0.02 eV or less that is too small to make conclusion in which case the compounds are more stable (Fig.1).

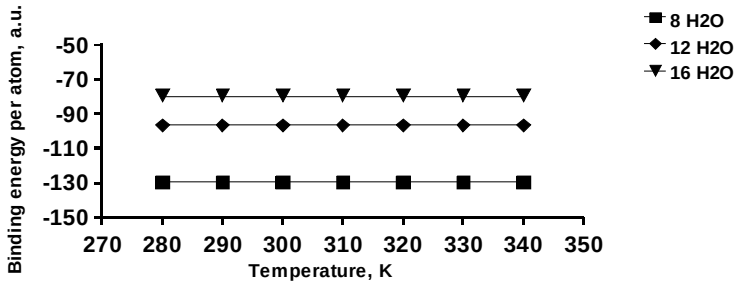

Fig. 1. Binding energy per atoms dependence on the temperature of the compaunds investigated consist of 8, 12 and 16 water molecules

It is not surprise, that compounds with non-destructed Co-Co bond is more stable than other. However, the larger number of water molecule not only destructed Co-Co bonds but decrease binding energy per atoms. It implies that the formed Co coordinated complexes should be more simple destructed when the Co nanoparticle concentration in the water will be as small as possible.

It is emphasized, the most important results are that in all our investigated cases one water molecule is deprotonated and hydrogen ion is present in the compounds investigated (Fig. 2).

It is necessary to pay attentions that different number of water molecules leads to formation of square planar Co coordinated compound with different ligands. It is interesting, that in case of 8 water molecules, the above coordinated complexes possesses ligands that are common for both Co atoms in spite of ligands sufficient. More probably that happens because the Co-Co bond is not destructed.

Moreover, in these compounds and in the compounds consist of 16 water molecules the OH^- and hydrogen atom are ligands, while in the cases of 12 water molecules the ligand is OH^- group only. It is prediction, that the above results are related with Co atom oxidation state.

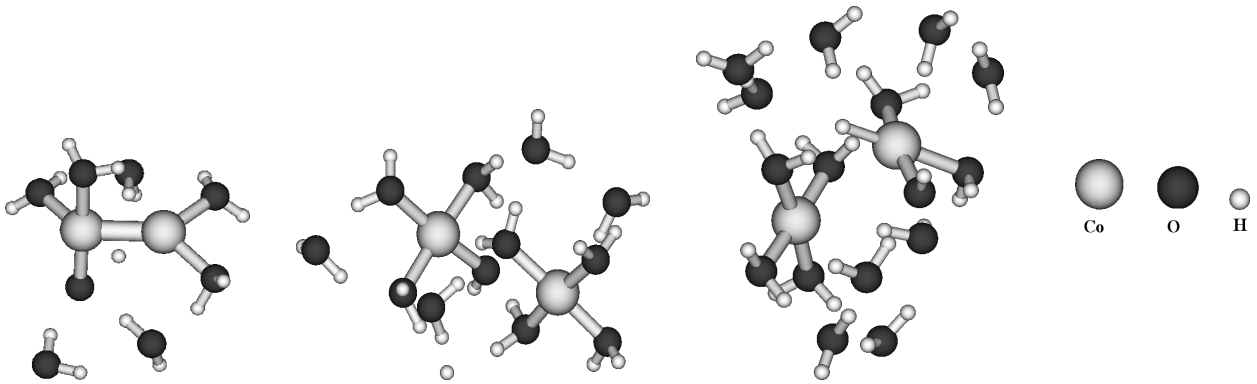

Fig. 2. An example of several results obtained to show that the water molecule is deprotonated if the Co_2 nanopaticle is in water

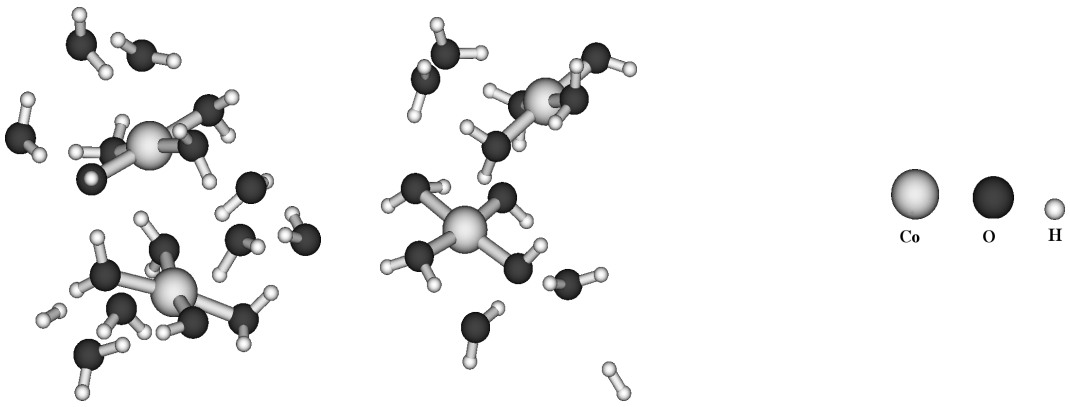

Fig. 3. Results indicated hydrogen molecule formed in the compounds with 12 and 16 water molecules when the temperature is 310 K in both cases

On the other hand, results of our investigation prove that the hydrogen molecule could be formed when the rate Co: water molecules are 2:12 or 2:16. In these cases the temperature is very important factor because the hydrogen molecules are formed only in certain temperature region. In the case of the 16 water molecules the temperature should be at 310 K, while in the case of 12 water molecule it is 310 – 320 K (Fig.3).

Hence, results obtained indicate, that Co nanoparticle could be used to split hydrogen from water. Moreover in some cases the Co nanoparticles may be used for hydrogen molecules formation. Additionally, we may speculate, that rate two Co atoms for 8water molecules could be the best choice in the fuel technology because the Co nanoparticle is not destructed. It implies that the Co particles could be used as catalyser in water deprotonation reaction. However, it is necessary to remember the stability of this compound which is the largest in the case of 8 water molecules than the stability of other compounds investigated. It implies that removing of the Hydrogen atom from the compound and forming of hydrogen molecule could be rather difficult.

4. Conclusions

Quantum mechanical investigations of Co_2 compounds consist of different number of water molecules exhibited that two coordinated Co complexes are formed. One of the ligands of these compounds could be hydrogen atom or OH^- groups and it is Co oxidation state dependent.

The investigations clearly indicate, that water molecule is deprotonated in the compound with Co nanoparticle. Basing on the results obtained it is possible foresee that rate two cobalt atoms and eight water molecules could be the best choice for hydrogen technology.

References

1. **Shehzad Ahmed, Marcos H. K. Conradt, Valeria DeFusco Pereir.** Alternative Fuels for Transportation - A Sustainability Assessment of Technologies within an International Energy Agency Scenario. Web site: <http://209.85.129.132/search?q=cache:6aQ97XR2yxEJ:www.bth.se/fou/cuppsats.nsf/all/a6f9c79df3672d60c12575ca004b1160/%24file/final_report_Alternative%2520fuels.pdf+Cobalt+%22Hydrogen+fuel+production%22&cd=50&hl=lt&ct=clnk&gl=lt>
2. **Tamulienė J., Vaišnoras R., Badenes G., Balevičius L. M.** Co_6O_m Nanoparticles Geometric and Electronic Structure Changes Within Increasing of Oxygen Number, Proceedings of 3rd International Workshop. ITELMS'2008, Panevezys.
3. **Becke A. D.** Density-functional thermochemistry. iii. The role of exact exchange, J. Chem. Phys., 98, 1993. p. 5648-5652.
4. **Gordon M. S., Binkley J. S., Pople J. A., Pietro W. J., HehreW. J.** Self-consistent molecular-orbital methods. 22. Small split-valence basis sets for second-row elements, J. Am. Chem. Soc., 104, 1982. p. 2797.
5. **Rassolov V. A., Ratner M. A., Pople J. A., Redfern P. C., Curtiss L. A.** 6-31G* Basis Set for Third-Row Atoms, J. Comp. Chem., 22 , p. 976-84.
6. **Cossi M., Rega N., Scalmani G., Barone V.** Energies, structures, and electronic properties of molecules in solution with the C-PCM solvation model, J. Comp. Chem., 24, p. 669-81.
7. **Cossi M., Scalmani G, Rega N., BaroneV.** New developments in the polarizable continuum model for quantum mechanical and classical calculations on molecules in solution, J. Chem. Phys., 117, p. 43-54.
8. **Frisch M. J., Trucks G. W., Schlegel H. B., Scuseria G. E., Robb M. A., Cheeseman J. R., Scalmani G., Barone V., Mennucci B., Petersson G. A., Nakatsuji H., Caricato M., Li X., Hratchian H. P., Izmaylov A. F., Bloino J., Zheng G., Sonnenberg J. L., Hada M., Ehara M., Toyota K., Fukuda R., Hasegawa J., Ishida M., Nakajima T., Honda Y., Kitao O., Nakai H., Vreven T., Montgomery Jr. J. A., Peralta J. E., Ogliaro F., Bearpark M., Heyd J. J., Brothers E., Kudin K. N., Staroverov V. N., Kobayashi R., Normand J., Raghavachari K., Rendell A., Burant J. C., Iyengar S. S., Tomasi J., Cossi M., Rega N., Millam N. J., Klene M., Knox J. E., Cross J. B., Bakken V., Adamo C., Jaramillo J., Gomperts R., Stratmann R. E., Yazyev O., Austin A. J., Cammi R., Pomelli C., Ochterski J. W., Martin R. L., Morokuma K., Zakrzewski V. G., Voth G. A., Salvador P., Dannenberg J. J., Dapprich S., Daniels A. D., Farkas Ö., Foresman J. B., Ortiz J. V., Cioslowski J., Fox D. J.** Gaussian, Inc., Gaussian 09, Revision A.1,Wallingford CT, 2009.

Proceedings of 5 rd International Workshop ITELMS'2010

Theoretical Study on Molecular Structures and Vibrational Spectra of Trinitrotoluene

S. Bekešienė*, V .Kleiza**

** Gen. J. Žemaitis Military Academy of Lithuania, Šilo 5A, LT-10322 Vilnius, Lithuania, E-mail: svajone.bekesiene@mil.lt;*
*** Kaunas University of Technology, Klaipedos str. 1, 35209 Panevezys, Lithuania, E-mail: vytautas.kleiza@ktu.lt*

Abstract

The article reviews and evaluates recent developments in methods and techniques for the analysis of explosives from the point of view of both experimental use of instrumentation and quality of the data obtained. Some current electronic structure calculations have concentrated on discussion of ab initio techniques, as these are the most accurate and, in principle, universal methods.
For the theoretical investigations of molecular electronic structure and geometrical data of 2,4,6-trinitrotoluene was used Hartree-Fock approximation with 6-31G* basis set (polarization *d* functions on second period elements; all in all 250 basis functions). Also 6-311G** basis set with two polarization *d* functions on second period elements, and plus one *f* function and diffuse *s* and *p* functions on second period atoms, and additionally diffuse functions on hydrogen atoms (all in all 770 basis functions). The basis functions used are necessary to achieve reliable results in such investigations.
Also this article analyses the multiconfigurational self consistent field (MCSCF) calculations performed for trinitrotoluene. In this theoretical investigations we left unfrozen 10 highest occupied MO's and 10 lowest unoccupied MO's from the Hartree-Fock Slater determinant. All configurations generated from unfrozen MO's with spin projection zero were included in the MCSCF procedure. In that case, we had more than 65000 configurations. All unfrozen MO's are π orbitals of the benzene ring and NO_2 groups.
All calculations were performed applying of *ab initio* quantum mechanical methods using the GAMESS computer code integrated under the SCore type PC cluster TAURAS [1, 2]. Obtained results show that the cluster is good device for such tasks. Also the electronic structure calculations provide useful estimates of the energetic properties of chemical systems, including preferred molecular structures, spectroscopic features and probable reaction paths.
KEY WORDS: *trinitrotoluene, electronic structure, spectroscopic features, parallel calculations, SCore cluster.*

1. Introduction

The intelligent technologies using parallel computing stimulated a fast growth of new ways of doing science. Computational quantum chemistry is the ground of molecular modeling and helps us simulate by supercomputers phenomena materials that are too complex to be reliably predicted by theory and too dangerous or expensive to be reproduced in the laboratory.

For these investigations was chosen explosive molecule such as trinitrotoluene ($C_7H_5N_3O_6$). This molecule can exist as different isomers such as: 2,3,4-, 2,4,5-, 2,4,6- and 2,5,6-TNT. The isomer that is used in the explosive industry is the symmetrical isomer 2,4,6-trinitrotoluene. The 2,4,6-trinitrotoluene – the most common nitro aromatic compound used to charge landmines and some of its physical constants. TNT is very stable, no hygroscopic, relative insensitive to affect friction, shock, and electrostatic energy. The trinitrotoluene molecule typical characteristics are: the molecular weight – 227.13; the density – 1.65 (g/mL); the melting point is 80.65 °C; the boiling point is 210 °C (10 torr); the flash point is 240 °C; the ignition point is 295 °C; the energy of formation – 184.8 kJ/kg; the enthalpy of formation – 261.5 kJ/kg. The precise computations of 2,4,6-trinitrotoluene molecule may be of interest for experimental spectroscopy, because the vibrational spectra are the fingerprints for molecular species identification.

For detection explosives from spectral characteristics can be used Infrared (IR) and Raman spectroscopy methods. The vibrational frequencies depend on interactions between atoms and groups of atoms. They tell us about intramolecular and intermolecular interactions. The vibrational modes vary with the nature of atoms in the bond and chemical environment. They give us information about chemical bonding and the chemical environment. Many bond types exhibit characteristic ("fingerprint") vibrational frequencies that allow us to establish the presence of certain functional groups, or products in a catalytic reaction.

In order to obtain the spectroscopic signature of the explosive molecules was performed frequency calculations for the different basis sets. The theoretical frequencies for 2,4,6-TNT was obtained. This work present the vibrational frequencies of the most stable geometry observed. These frequencies have to be real, or positive to consider that the geometry reach a minimum.

The purpose of our work was to investigate how strong calculated vibrational frequencies, infrared (IR) and Raman radiation intensities depend from the ab initio method used. We did not find in literature or in available databases the all results of analogous theoretical investigations for given molecules.

2. Optimization of TNT Molecular Structure

These investigations started at the geometry optimization of the 2,4,6-trinitrotoluene in order to determine the lowest energy conformation and the symmetry optimization. The energy of a molecular system varies with changes in its structure and it is specified by its potential energy surface. A potential energy surface is a mathematical relationship linking molecular structure and the resultant energy. The geometry optimizations usually attempt to achieve minimum potential energy surface, in that way predicting equilibrium structures of the molecular systems. To optimize the geometry was used the GAMESS computer code [2].

The calculated optimized energies of 2,4,6-trinitrotoluene at different basis sets, in hartrees are presented in Table 1. Among the several basis sets used for these calculations, the 6-311G** basis set provides the lower energy conformation. The most stable geometry obtained for the 2,4,6-trinitrotoluene is show in figure 1. This molecule has C_1 symmetry and consists of a phenyl ring with a methyl group and three nitro groups at positions 2, 4 and 6. Fig. 1 shows significant change of electronic charges of atoms and dipole momentum for trinitrotoluene molecule and significant influence of electron correlation and necessity of MCSCF method for investigated molecule multiconfigurational properties. The results in figure 1 where achieved by the cluster [1], and as visualization method was used the MOLDEN version 4.6.

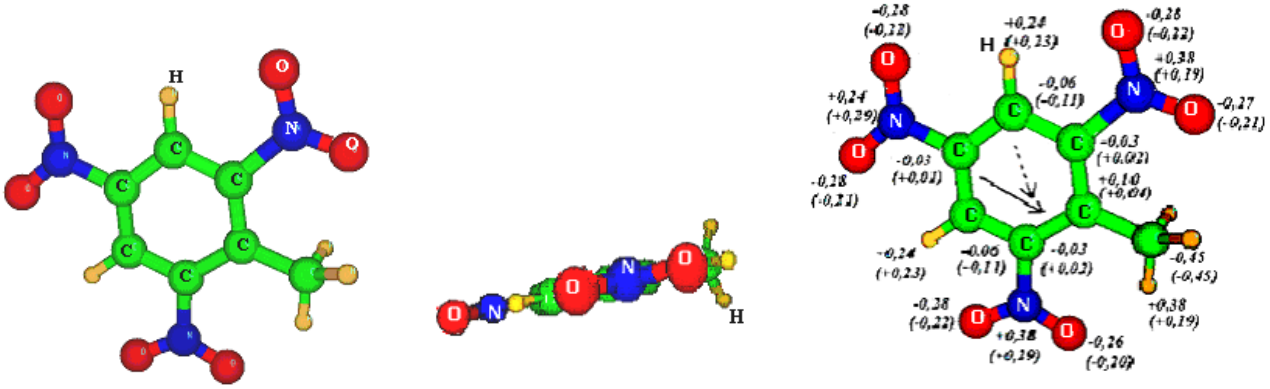

a b c

Fig. 1. The view of optimized 2,4,6-trinitrotoluene molecular structure: (a) top and (b) side; (c) the charges of the atoms in the trinitrotoluene molecule (in a. u.) calculated in the Hartree-Fock approximation in the 6-31G* basis set and by the MCSCF method (in parentheses). Arrows show approximate direction of the dipole moment calculated in the Hartree-Fock approximation (Dw = 1.759 D) and by the MCSCF method (DMCSCP - 1.444 D, dashed arrow)

All quantum mechanical calculations were performed using the Hartree-Fock approximation. The family of basis sets: 6-31G*(1d), 6-311G**(1d), 6-311G**(2d), 6-311G**(2d+1f), 6-311G**(3d+1f) and 6-311G**(3d+1f+3p) vas used. The investigations was done from 6-31 G* (with polarization d functions on second period elements; all in all 250 basis functions) to 6-311 G** (with two polarization d functions on second period elements). Additionally was used one f function and diffuse s and p functions on second period atoms and diffuse functions on hydrogen atoms (all in all 770 basis functions). The sets of basis functions were used to get a full optimization of 2,4,6-trinitrotoluene molecule with a C_1 symmetry.

Table 1

Geometry optimization results of trinitrotoluene molecule: basis sets and number of basis functions, total energy and dipole moment. Computations were performed in Hartree-Fock approximation. The cluster of 9 CPU's was *used.*

Basis set	Numb. of basis functions	$E_{tot.HF}$, a.u.	Dipole moment, *D*	Computational time, min (h)
6-31 G*(1d)	250	-880.117	1.759	146.9 (2.45)
6-311 G**(1d)	319	-880.326	1.785	247.4 (4.12)
6-311 G**(2d)	415	-880.365	1.702	555.0 (9.25)
6-311 G**(2d+1f)	575	-880.406	1.713	1511.7 (25.20)
6-311 G**(3d+1f)	671	-880.426	1.727	5349.8 (89.16)
6-311 G**(3d+1f+3p)	716	-880.432	1.716	6773.7 (112.9)

The basis functions used are necessary in order to achieve reliable results in such investigations During multiconfigurational self consistent field (MCSCF) calculations performed for trinitrotoluene was left unfrozen 10 highest occupied MO and 10 lowest unoccupied MO from HF Slater determinant [15, 16]. All configurations generated

from unfrozen MOs with spin projection zero were included in MCSCF procedure. Was used more than 65000 configurations.

Full geometry optimization was performed for trinitrotoluene molecule in Hartree-Fock and in MCSCF approximations. During investigation the C1 symmetry point group of the molecule was assumed. Figure 1 shows significant influence of electron correlation and necessity of MCSCF method for investigation of optical properties of investigated molecule multiconfigurational properties. Full geometry optimization was performed for the trinitrotoluene molecule in the Hartree-Fock and in MCSCF approximations. During investigation the C1 symmetry point group of the molecule was assumed.

The results of trinitrotoluene geometry optimization are presented in Table 1: basis sets and number of basis functions, total energy and dipole moment. Even with such comparatively small cluster TAURAS we can perform all necessary computations at Hartree-Fock level and some necessary computations at MCSCF. It can be stated that created PC's cluster allows solving of modern quantum chemical problems at necessary level.

Table 2

Bond lengths of the 2,4,6-trinitrotoluene

Bond(Å)	Basis sets				
	6-31G*(1d)	6-311 G**(1d)	6-311 G**(2d)	6-311 G**(2d+1f)	6-311G**(3d+1f)
C1-C2	1.413	1.409	1.412	1.409	1.408
C2-C3	1.382	1.385	1.380	1.385	1.377
C3-C4	1.373	1.370	1.372	1.370	1.369
C4-C5	1.371	1.371	1.370	1.372	1.366
C5-C6	1.386	1.380	1.385	1.380	1.382
C1-C6	1.410	1.412	1.409	1.412	1.406
C1-C7	1.518	1.518	1.518	1.518	1.515
C7-H8	1.067	1.066	1.066	1.066	1.065
C7-H9	1.080	1.080	1.080	1.080	1.080
C7-H10	1.080	1.080	1.080	1.080	1.080
C2-X1	1.474	1.489	1.482	1.482	1.480
X1-Y1	1.190	1.183	1.183	1.183	1.180
X1-Y2	1.193	1.185	1.186	1.186	1.183
C3-X2	1.068	1.068	1.068	1.068	1.066
C4-X3	1.456	1.463	1.463	1.463	1.461
X3-Y5	1.191	1.184	1.185	1.185	1.182
X3-Y6	1.191	1.185	1.184	1.184	1.182
C5-X4	1.068	1.068	1.068	1.068	1.066
C6-X5	1.481	1.482	1.489	1.489	1.487
X5-Y9	1.192	1.186	1.185	1.185	1.182
X5-Y10	1.190	1.183	1.183	1.183	1.180
Y1-H8	3.68622	3.51721	3.68959	3.68959	3.68715
Y1-H9	2.37672	2.01836	2.38180	2.38180	2.37886
Y10-H10	2.37672	3.51721	2.38180	2.38180	2.37886
Energy	-808.117	-808.326	-808.366	-808.407	-808.432
Dipole moment	1.702897	1.701599	1.701575	1.710988	1.716012

Table 3

Calculated dihedral angles (^{o}) of the 2,4,6-trinitrotoluene on cluster TAURAS

Dihedral angles	Basis sets				
	6-31G*(1d)	6-311 G**(1d)	6-31 G**(2d)	6-31 G**(2d+1f)	6-31G**(3d+1f)
C2-C1-C7-C6	180.0	180.0	180.0	180.0	180.0
C2-C1-C7-H8	180.0	121.6	180.0	180.0	180.0
X1-C2-C1-C3	180.0	180.0	180.0	180.0	180.0
Y1-X1-C2-C1	0.0	0.0	0.0	0.0	0.0
X2-C3-C2-C4	180.0	180.0	180.0	180.0	180.0
X3-C4-C3-C5	180.0	180.0	180.0	180.0	180.0
Y5-X3-C4-C3	0.0	0.0	0.0	0.0	0.0
X4-C5-C4-C6	180.0	180.0	180.0	180.0	180.0
X5-C6-C5-C1	180.0	180.0	180.0	180.0	180.0
Y9-X5-C6-C5	0.0	0.0	0.0	0.0	0.0

Table 4

Calculated angles (°) of the 2,4,6-trinitrotoluene on cluster TAURAS

Bond angles	Basis sets				
	6-31G*(1d)	6-311 G**(1d)	6-311 G**(2d)	6-311 G**(2d+1f)	6-311G**(3d+1f)
C1-C2-C3	123.8	123.1	123.8	123.8	123.8
C2-C3-C4	118.7	119.3	118.7	118.7	118.7
C3-C4-C5	121.1	121.1	121.1	121.1	121.1
C4-C5-C6	119.4	118.7	119.3	119.3	119.3
C1-C6-C5	123.0	123.8	123.1	123.1	123.1
C2-C1-C6	114.1	114.0	114.0	114.0	114.0
C2-C1-C7	121.3	124.6	121.4	121.4	121.4
C6-C1-C7	124.6	121.4	124.6	124.6	124.5
C1-C7-H8	111.9	109.5	112.0	112.0	111.8
H8-C7-H9	109.6	106.9	109.5	109.5	109.7
H8-C7-H10	109.6	109.5	109.5	109.5	109.7
C1-C2-X1	122.8	124.4	122.9	122.9	122.9
C2-X1-Y1	119.2	119.9	119.0	119.0	119.1
C2-X1-Y2	116.7	116.2	116.6	116.6	116.6
C2-C3-X2	120.4	120.4	120.5	120.5	120.4
C3-C4-X3	119.5	119.4	119.5	119.5	119.5
C4-X3-Y5	117.2	117.1	117.1	117.0	117.1
C4-X3-Y6	117.2	117.0	117.1	117.1	117.2
C4-C5-X4	120.3	120.8	120.3	120.3	120.4
C5-C6-X5	112.6	113.4	112.6	112.6	112.5
C6-X5-Y9	116.3	116.6	116.2	116.2	116.2
C6-X5-Y10	120.1	119.0	119.9	119.9	120.0

The calculated structural parameters (bond lengths, dihedral angles and angles) of the 2,4,6-trinitrotoluene are listed in Tables 2, 3 and 4, respectively. The labeling of the atoms in these tables is consistent with the labeling with the labeling model shown in Figure 1. The parameters were obtained using the Hartree-Fock method increasing the basis sets from 6-31G*(1d) to 6-31G**(3d+1f). Those tables also provide the parameters obtained from Chen and coworkers using the Hartree-Fock with the basis sets 6-31G* level.

The parameters obtained with the HF/6-31G*(1d) basis set are compared with the values obtained by Chen and coworkers using HF/6-31G*. The HF method used by P. C. Chen et al. (1997) underestimates the bond lengths of the 2,4,6-trinitrotoluene optimized compare structure to the DFT level of theory. The C-C, C-N, and N-O average bond lengths calculated by HF method has a lengths differences of -0.0085, -0.0170 and -0.0367 Å, respectively. However no significant differences where observed between the bound angles and dihedral angles (Table 3 and 4) calculated by cluster and obtained by Chen and coworkers [14].

3. The Vibrational Spectra Computations of 2,4,6-TNT

The geometrical conformation of the trinitrotoluene explosive molecule helps to understand the thermal decomposition mechanisms, and the vibrational frequencies depend on interactions between atoms and groups of atoms. They tell us about intramolecular and intermolecular interactions. The vibrational modes vary with the nature of atoms in the bond and chemical environment. They give us information about chemical bonding and the chemical environment. Many bond types exhibit characteristic (“fingerprint”) vibrational frequencies that allow us to establish the presence of certain functional groups, or products in a catalytic reaction.

In order to obtain the spectroscopic signature of the explosive molecules we performed frequency calculations for the different basis sets. The theoretical frequencies for 2,4,6-TNT was obtained. This work present the vibrational frequencies of the most stable geometry observed. These frequencies have to be real, or positive to consider that the geometry reach a minimum.

Trinitrotoluene molecule vibrational spectra computations were performed using computer code GAMESS [2]. For potential energy surface determination in Hartree-Fock (HF) approximation atomic orbital (AO) basis 6-31G* (total 250 basis functions) was used. Number of necessary to compute many center integrals was more than 10^9.

Though the bond length changes in the trinitrotoluene molecule were not large in HF and MCSCF methods, the change of vibrational frequencies and vibrational forms was significant (the changed molecular force field by the MSCSF method was the main cause). Most of the frequencies increased when the MCSCF method was used, all very low frequencies with out-of-benzene ring vibrational forms disappeared.

Table 5

Trinitrotoluene molecule harmonic vibrational frequencies, IR and Raman intensities and forms of vibrations calculated in the Hartree-Fock approximation in the 6-31 G* basis. Only the most significant intensities are shown

Frequency cm^{-1}	IR intensity, $D^2/(a.u.\ A^2)$	Raman intensity, A4/a.u.	Vibrational form
1306		16	Benzene ring in plane deformations
1623		37	Valence angle deformations in NO_2, CH_3 groups and benzene ring
1627	11	7	Valence angle deformations in NO_2, CH_3 groups and benzene ring
1639		40	Valence angle deformations in NO_2, CH_3 groups and benzene ring
1788		71	Benzene ring deformations
1885	14		NO_2 group stretching vibrations
3269		137	CH_3 valence angle deformations
3332		74	CH_3 group stretching vibrations
3467		36	CH_3 group stretching vibrations
3470		29	CH bond stretching vibrations
3496		29	CH group stretching vibrations

Table 6

Trinitrotoluene molecule harmonic vibrational frequencies, IR and Raman intensities and forms of vibrations calculated in the MCSCF approximation in the 6-31G* basis. Only the most significant intensities are shown

Frequency cm^{-1}	IR intensity, $D^2/(a.m.v.A^2)$	Raman intensity, A/a.m.v.	Vibrational form
849		145	Benzene ring deformations in the molecule plane
853		123	Benzene ring deformations in the molecule plane
1231		86	NO, CN bond stretching and benzene ring in the molecule plane deformations
1287		85	NO, C-CH_3 bond stretching and benzene ring in the molecule plane deformations
1478		286	NO, CN bond stretching and benzene ring in the molecule the molecule plane deformations
1520		156	Benzene ring deformations
1561	1.4	47	NO, CN bond stretching and benzene ring in the molecule the molecule plane deformations
1594	1.4	90	O, CN bond stretching and benzene ring in the molecule plane deformations
1708		158	Benzene ring in the molecule plane deformations
1789	2.7	82	NO bond stretching vibrations
1860	1.4	65	NO_2 group stretching vibrations
1903	3.3	81	NO_2 group stretching vibrations
2211		184	CH and CH_3 valence angle deformations
2889	1.5	233	CH and CH_3 valence angle deformations
2957		122	NO group stretching vibrations
2999		40	NO group stretching vibrations
3931		233	CH_3 group stretching vibrations
3504		25	CH bound stretching vibrations
3661		68	CH group stretching vibrations

The calculated by cluster TAURAS neat infrared spectrum corresponding to 2,4,6-TNT was visualized by MOLDEN 4.6 and presented in figure 2. The bands that allow identifying the neat TNT were obtained in the range of 350-3350 cm^{-1}. The vibrational signatures observed in the region of 3269-3496 cm^{-1} can be assigned to asymmetric and symmetric C-H stretch vibrations, respectively, belong to the alkyl CH_3 group and the aromatic ring. Other peaks of high intensity are 1885 cm^{-1} (NO_2 symmetric stretching vibration), in the region of 1623-1639cm^{-1} (Valence angle deformations in NO_2, CH_3 groups and benzene ring), 1306cm^{-1} (benzene ring in plane deformations).The assignments of the bands are summarized in the table 6.

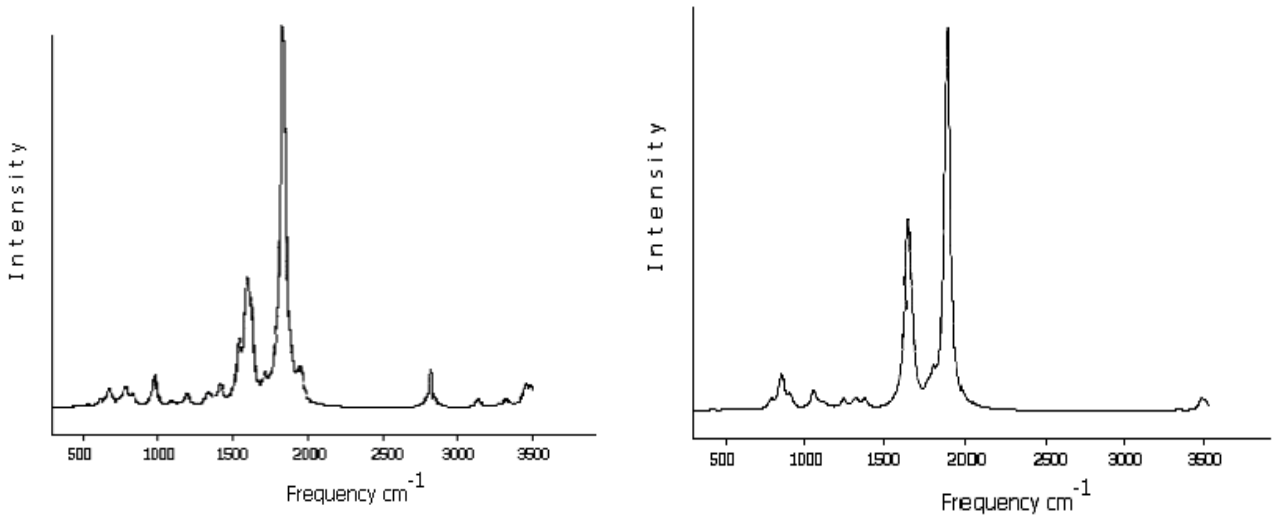

Fig. 2. Infrared spectrum of neat 2,4,6-TNT in the range of 300–3500 cm^{-1}: a)IR vibrations calculated in the Hartree-Fock approximation in the 6-G311 (1d) basis; b). IR vibrations calculated in the MCSCF approximation in the 6-31G* basis

The harmonic vibrational spectra of molecules (vibrational frequencies, IR and Raman intensities) were calculated in the HF approximation. The frequencies with greatest IR and Raman intensities only are summarized in the Tables 5 and 6. Very few frequencies retained the same form in HF and MCSCF approximations: 3496 cm^{-1} (HF) and 3661 cm^{-1} (MCSCF), 3470 cm^{-1} (HF) and 3504 cm^{-1} (MCSCF), 3467 cm^{-1} (HF) and 3931 cm^{-1} (MCSCF) – all CH bonds stretching vibrations; 3269 cm^{-1} (HF) and 2957 cm^{-1} (MCSCF), 3332 cm^{-1} (HF) and 2999 cm^{-1} (MCSCF) – CH_3 group CH bonds stretching vibrations; 1885 cm^{-1} (HF) and 1860 cm^{-1} (MCSCF) – NO_2 group stretching vibrations; 1788 cm^{-1} (HF) and 1520 cm^{-1} (MCSCF) – benzene ring deformations. Zero point energy for trinitrotoluene changes significantly: from 32572 cm^{-1}/molecules in the HF approximation to 44090 cm^{-1}/molecules in the MCSCH.

4. Spectra of TNT from IR Technique and Calculated in the MCSCF

In our investigations, as introduced above, was chosen the electronic structure calculations provide useful estimates of the energetic properties of chemical systems, including preferred molecular structures, spectroscopic features and probable reaction paths. These some current electronic structure calculations at first were concentrated on discussion of ab initio techniques, as these are the most accurate and, in principle, universal methods, because the achieved results with increasing the calculations of 2,4,6-trinitrotoluene molecule can help us better understand for whom belongs: the benzene ring and NO_2 group deformations, the frequencies of NO group and CH bonds stretching vibrations. This important information for TNT detection allows us more detail interpretation of experimental vibrational spectra get by experimenters [12], because infrared spectroscopy is a technique based on the vibrations of the atoms in molecules. The infrared spectrum is commonly obtained by passing infrared radiation through a sample and determining what fraction of the incident radiation is absorbed at a particular energy. The energy at which any peak in an absorption spectrum appears corresponds to the frequency of a vibration of a part of a sample molecule.

For experimental IR spectrum determination a standard solution of the explosive 2,4,6-trinitrotoluene (TNT) was prepared from a solid compound obtained from Chem Service, Inc. All standards were prepared in methanol (HPLC grade CH_3OH, 99.9%) solutions with a nominal concentration of 2,000 parts per million (ppm) and 4,000 ppm.

Stainless steel cylinders of dimensions 3 in. diam. × 1 in. height were used to contain and analyze the mixtures of explosive and soil particles in the Raman microscopy technique experiments. These cylinders were constructed at Añasco Precision Mechanical Shop, Añasco, PR. For FTIR plastic recipient were used to contain the mixture until analyzing. A sample holder of the FTIR instrument was used to place the pellet with the mixture of explosive and soil particles [12].

The samples analysis was carrying out by the using a Bruker Vector-22 spectrometer equipped with a DTGS infrared detector. The KBr pressed disc technique (3.0 mg of sample and 50.0 mg of KBr) was used for FTIR analysis. The sample was placed in the instrument on a sample holder and spectra were measured at a resolution of 4 cm^{-1} and 32 scans. The data was obtained using Opus V3.1 (Bruker Optics) Software [12]. IR absorption information is generally presented in the form of a spectrum with wavelength or wave number as the x-axis and absorption intensity as the y-axis. The experimental infrared spectrum corresponding to neat 2,4,6-trinitrotoluene are shown in Fig. 3, b [12]. The bands that allow identifying the neat TNT were obtained in the range of 350-3350 cm^{-1}.

The vibrational signatures (Fig. 3) observed in the region of 3000-3100 cm^{-1} can be analyzed and assigned to asymmetric and symmetric C-H stretch vibrations, respectively, belong to the alkyl CH_3 group and the aromatic ring.

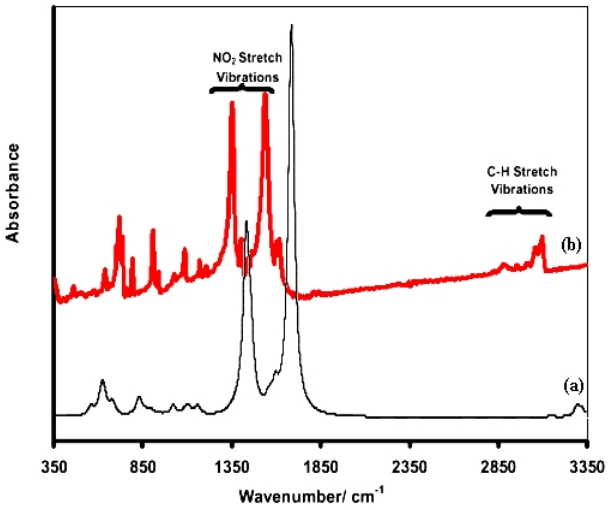

Fig. 3. The infrared spectrum corresponding to neat 2,4,6-trinitrotoluene in the range of 350-3350 cm^{-1}: (a) calculated in the MCSCF approximation in the 6-31G* basis; (b) experimental [12]

Other peaks of high intensity are 1355 cm^{-1} (NO_2 symmetric stretching vibration), 1540 cm^{-1} (asymmetric NO_2 stretching), 1025 cm^{-1} (CH_3 deformation), 1085 cm^{-1} (ring C-H in plane bend), at 909 cm^{-1} (methyl rock, C-N stretching band), at 794 cm^{-1} (ring in plane bend, C-CH_3 stretch) and at 720 cm^{-1} (C-N-O bend). The assignments of the bands are summarized in the Table 7.

5. Spectra of TNT from Raman Technique

The Raman spectroscopy is the alternative vibrational technique that can also provide a definitive spectral "fingerprint" that is unique to a specific molecule. Raman scattering was originally predicted by Ranais in 1924 and was first demonstrated in 1928 by C. V. Raman [18]. The characterization of explosives by Raman spectroscopy was first suggested in 1964 when it was used to investigate the processes involved in nitration reactions [20].

Table 8

Raman frequency assignment of TNT explosive

Experimental vibrational frequencies cm^{-1}	Assignments by theoretical investigations
326	2,4,6 C-N in plane torsion
366	Methyl group deformation
792	C-CH_3 stretch, 2,4,6-NO_2 scissors
822	2,4,6-NO_2 scissors
914	C-H (ring) out of plane bend
941	C-H (ring) out of plane bend
1091	C-H (ring) in plane bend
1175	Symmetric methyl C-C-H bend
1210	C-H (ring) in plane bend, ring breathing
1361	NO_2 symmetric, C-N stretching
1538	NO_2 asymmetric stretching
1616	2,6 NO_2 asymmetric stretching
2956	C-H asymmetric stretching
3016	Aromatic C-H stretching
3065	Aromatic C-H stretching
3102	Aromatic C-H stretching

Infrared spectroscopy is a technique based on the vibrations of the atoms in molecules, and the Raman spectroscopy is the study of a small portion of light scattered by a molecule, the light undergoing an exchange of energy with that molecule. Each Raman active bond in the molecule necessitates the emission of a different wavelength of light. Thus, while the light incident on the sample has one wavelength, the light scattered off the sample has many wavelength components, which take the information about the individuality of the sample.

The experimental sample we chose to analyze our calculated results was the experiment accomplished in the University of Puerto Rico Mayagüez Campus [12]. Where get vibrational spectroscopy measurements were employed for a Renishaw Raman Microspectrometer RM2000 system. The system was equipped with a Leica microscope and two

lasers: Spectra Physics Millennia laser and Renishaw, high power diode laser. The microscope contained objectives with magnifications of 5x, 10x, 20x and 50x. The Millennia laser had a monochromatic excitation source generated by a green diode laser of 532 nm with and a variable output power up to 1 W. The second laser was a Renishaw High Power 785 nm diode laser with a maximum power of 200 mW. The spectra were obtained in the 100-3800 cm $^{-1}$ range using 2 scans and 20 seconds of integration time. A multi channel Charge Coupled Device (CCD) detector and GRAMS software were used for data acquisition [12].

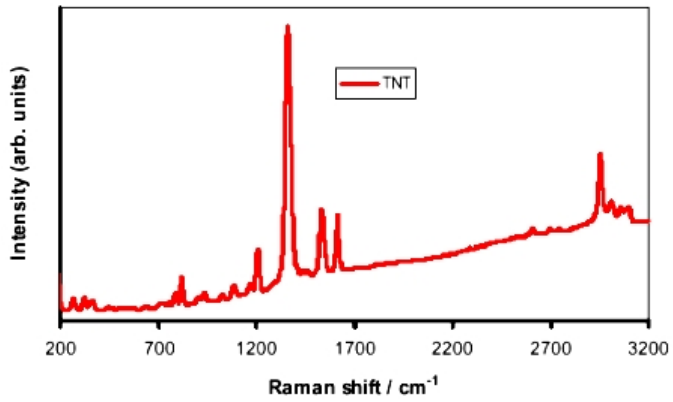

Fig. 4. The experimental Raman spectrum corresponding to neat 2,4,6-trinitrotoluene in the range of 200-3200 cm $^{-1}$ [12]

Raman Microscopy was used to identify the spectroscopic signatures of 2,4,6-trinitrotoluene in soil particles. In this step, the particles of soil used were sand and montmorillonite clay. The mixtures of TNT–soil were studied under different environmental conditions (pH, humidity, UV light exposure, temperature, concentration of explosive in the soil, and aging effect).

Figure 4 present the spectra of neat 2,4,6-trinitrotoluene. The peaks that permit identify compound can be observed. The major strong bands that allow identifying the TNT were observed in 3016 and 2955 cm $^{-1}$. These bands can be assigned to aromatic C-H stretch vibration and symmetric belong to the alkyl CH_3 group, respectively. The principal peaks of high intensity are 1365cm $^{-1}$ (NO_2 symmetric stretching vibration), 1535 cm^{-1} (asymmetric NO_2 stretching), 1617 cm $^{-1}$ (2,6-NO_2 asymmetric stretching vibration), 1210 cm $^{-1}$ (C-H (ring) in plane bend, ring breathing). Bands very weak too are observed at 822 cm $^{-1}$ (nitro-group scissoring mode), and 792 cm $^{-1}$ (C-CH_3 stretch, 2,4,6-NO_2 scissoring). Assignments of the bands are summarized in Table 8.

6. Conclusions

Calculations of 2,4,6-trinitrotoluene molecule optimization at Hartree-Fock level show the influence of NO_2 groups to electronic structure of TNT compounds. Results of this study provide valuably information in the field of aromatic nitro compounds.

Therefore, the calculations of 2,4,6-trinitrotoluene molecule by MCSCF method showed significant change of vibrational spectrum characteristics from those calculated at Hartree-Fock level. Achieved results with increasing the calculations can help us better understand for whom belongs: the benzene ring and NO_2 group deformations, the frequencies of NO group and CH bonds stretching vibrations. This information is important for detection and allows more detail interpretation of experimental vibrational spectra of investigated molecules and more accurate investigation of thermo chemical reactions dynamics.

Electronic structure calculations provide useful estimates of the energetic properties of chemical systems, including preferred molecular structures, spectroscopic features and probable reaction paths. This review of some current electronic structure calculations has concentrated on discussion of ab initio techniques, as these are the most accurate and, in principle, universal methods.

Rapid advances in computer technology are making computationally expensive ab initio methods increasingly more practical for use with realistic chemical systems. In particular, cheaper methods such as density functional calculations and, layered models are continually being refined, and show promise of providing consistent and accurate chemical predictions for most complex systems.

References

1. Basis of PC clusters. Web site: <http://clusters.top500.org/db>.
2. **Granovsky A. A.** Web site: <http://www.classic.chem.msu.su/gran/gamess/index.html>.
3. **Duesler E. N., Engelmann J. H., Curtin D. Y., Paul I. C.** Cryst. Strukt. Comm. 1978, 7, p 449-461.
4. **Dorsett H, White A.** Overview of molecular modelling and ab initio molecular orbital methods suitable for use with energetic materials. DSTO, 2000, p 1-35.
5. **Schmidt M. W.,** et al. J. Comput. Chem. 1993, V. 14, p. 1347.

6. **Schmidt M. W., Gordon M. S.,** Ann. Rev. Phys. Chem. 1998, V. 49, p. 233.
7. **Madejova J.** Review. FT –IR techniques in Clay Minerals Studies. Vibrational Spectroscopy, 2003, 31, p 1 – 10.
8. **Vošterienė S., Šulskus J.** GAMESS Calculations in Parallel Environment // Lithuanian Mathematical Journal. ISSN 0132-2818. 2005, 45 (spec. no.), p.190-193.
9. **Bekešienė S., Sėrikovienė S.** Quantum Chemical Calculations by Parallel Computer from Commodity PC Components // Nonlinear Analysis: Modelling and Control. ISSN 1392-5113. 2007, Vol. 12, No. 4, p. 461-468.
10. **Rakauskas R. J., Šulskus J., Vošterienė S.** Simulation of Vibrational Spectra Peculiarities of Trinitrotoluene Molecule Using Parallel Calculations // Материалы XV международного семинара "Лазеры и оптическая нелинейность" 6-8 июня 2002 г., Минск, Беларусь. с. 162-168.
11. **Šulskus J., Rakauskas R. J., Vošterienė S.** PC Cluster Possibilities in Mathematical Modeling in Quantum Mechanical Molecular Computations // Nonlinear analysis: Modelling and Control. ISSN 1392-5113. 2002, Vol.7, No.2, p. 113-121.
12. **Sandoval G. M. H.** Vibrational signatures of 2,4,6 - trinitrotoluene (TNT) in soil particles. Thesis for the degree of master of science in chemistry University of Puerto Rico Mayagüez campus, 2006.
13. **Šulskus J., Rakauskas R. J., Vošterienė S.** Parallel Algorithms for Solving of Multidimensional Vibrational Shrödinger Equation // Lithuanian Mathematical Journal. ISSN 0132-2818. 2002, 42, (spec. no.), p. 345–350.
14. **Chen P. C., Lo W.** Molecular orbital studies of the isomers of 2,4,6-trinitrotoluene and some of its thermal decomposition products. Journal of Molecular Structure (Theochem), 1997, 397, p 21-32.
15. **Ishikawa Y.** et al, In Proceedings of the 5th Annual Linux Expo.1999, p. 55-66.
16. **Canc`es E., H. Galicher H., Lewin M.** Computing electronic structures: a new multiconfiguration approach for excited states.// J. Comput. Phys. 2006, 212, p 73–98.
17. **Lewin M.** Solutions of the multiconfiguration equations in quantum chemistry. //Arch. Ration.Mech. Anal. 2004, 171, no. 1, p 83–114.
18. **Sands H. S., Hayward I. P., Kirkbride T. E., Bennett R., Lacey R. J., Batchelder D. N.** UV-excited resonance Raman spectroscopy of narcotics and explosives. J. Forensic Sci., 1998, vol. 43, p. 509–513.
19. **Bekešienė S., Kleiza V., Tamulienė J.** Theoretical Study on the Molecular Structures of Nitrophenols and Trinitrophenols. // Intelligent technologies in logistics and mechatronics systems ITELMS'2008: proceedings of the 3rd international workshop, May 22-23, 2008, Panevėžys, Lithuania/Kaunas University of Technology Panevėžys Institute, Warsaw Motor Transport Institute, Tallin University of Technology, Riga Technical University; edited by Ž. Bazaras, V. Kleiza. Kaunas: Technology, 2008. ISBN 978-955-25-531-4. p. 7-12.
20. **Urbanski T.** Chemistry and Technology of Explosives (I).// New York: Pergamon, 1964.

Proceedings of 5th International Workshop ITELMS'2010

Decision Support System in Career Counseling for Retired Military Officers

R. Smaliukienė, S. Bekešienė

Gen. J. Žemaitis Military Academy of Lithuania, Šilo 5A, LT-10322 Vilnius, Lithuania, E-mail: rasa.smaliukiene@mil.lt; svajone.bekesiene@mil.lt

Abstract

Civilian employment is reaming one of the most challenging steps after the end of the military career. Retired officers find them self in the situation when a complex strategic decision regarding their professional future needs to be made. There is not only a need to choose a new way for professional life, but also to integrate them into a civil life and reclaim the experience from a military. Such complex decision needs advanced IT methods to be involved [4]. Thus, the interest in decision support system (DSS) for decisions in counseling of retired officers is immediate and obvious. The application of DSS can reduce the risk in strategic decision making by optimizing the choice options.
This paper proposes decision support system guidance for retired military officers' career counseling. From a technical perspective we suggest that it is advisable to place a workflow engine at the core of the internet based e-decision making system. This will let to generate or manage personalized and adaptable individual recommendation assesses flows and during the processes of an individual recommendation culling grants the consumer access to subsequent databases of related resources or services. From a technical perspective the structure of DSS could be kept comparatively simple and self-controlled in process of logic analysis. The functions and subsystems reside on a networked multilevel infrastructure with strong internet connectivity and a number of databases. The internet portal systems could be used to provide different types of users by user's type specific and customized services. The databases are designed to collect and analyze data about a number of processes and entities.
KEY WORDS: *multidimensional database, professional counseling, DSS architecture.*

1. The Need for Decision Support System in the Professional Counseling for Retired Military Officers

Application of DSS is increasing in solving the issues of social security or people well-being (see for example Runner-up or Xiao et al.). The majority of these applications provide the support for policy decision makers; while the exploitation of DSS in decision making for personal goals is not a common case. Individuals are taking only few strategic decisions through their life; and choosing a profession is a major decision which will deeply affect person's life and well-being (Cheney et al.). Retired officers find them self in the situation when such decision needs to be made. Regardless the governmental program for the officers' integration into labor market is approved in 2005; only brief career counseling is designed for these people by the labor market training authority. Additionally, retired military officers can pursue the retraining courses, as it is available for all unemployed in Lithuania. These measures are not nearly enough. The proposed retraining courses do not guaranty the employment; there is no demand for people with military experience at the labor market – there is a general opinion that military officers are limited to leading and can not perform any other functions in the organization. Alongside all these obstacles, there is a strong impact of global economic crisis towards the access to the employment. According to Lithuanian statistics bureau, there are near to 1,000 officers and soldiers retiring every year; their average age is 47.5 years. It is most of the case these people are rich in experience and high in professional potential. Each of these individuals wants to continue their active life and needs for professional counseling for their future career and life.

One possible solution to the described situation is to encourage retired military officers for self-employment. This idea has its deep background. Firstly, military officers are trained to take a risk and to be responsible for the outcomes – these two competencies are most important for entrepreneurs in general and for business – starters in particular. Secondly, officers had not many opportunities for self-expressions during their military career; consequently majority of them involves themselves into the hobbies deeply and even professionally.

The application of DSS allows us to provide retired military officers with a powerful tool for self-evaluation and individual decision making. Additionally, DSS provides the possibility to utilize databases of more than thousand retired officers in systematical and highly targeted way by unlocking new opportunities for people. Two main stimuli encouraged us the development of decision support system guidance for retired military officers: the need to expend the impact of military conscription center on the activities related to the retired militaries' integration into social life, and to benefit from the favorable support conditions in the business-starters environment. Big variety of governmental initiatives can be identified as support conditions (see for example a governmental initiative Business Gateway Lithuania). However, utilization of these conditions in the career counseling needs to be expedient; and the DSS suites for this purpose.

The first step to this ambition goal is to create the architecture of decision support system for retired military officers' career counseling. The architecture allows us: (1) to systematically integrate all existing information that is already collected through the last years; (2) to add new information by even four groups of system stakeholders: system administrator, system developers, system experts and consumers; (3) to create internet delivery infrastructure.

2. The Architecture of Decision Support System for Retired Military Officers' Career Counseling

Application of DSS in retired military officers' career counseling can be interpreted as a flow of subsequent reclaim of experience that leads the individual person to a level of knowledge and competency in modified activities. DSS helps in solving such challenging question as how to resettle the military experience into civil activities. Moreover, it is capable to provide retired military officers with the decisions based on up-to date information form labor and business market that is changing constantly. The brainstorming on challenging ideas that we presented above and potential of contemporary IT provided us with new possibilities (Fig. 1):

- Possibility to get in touch with decision support system server in remote mode;
- The databases constantly are up to date with new and actual information;
- The users can connect at any time to the databases and receive expertise support for his decision;
- There is the possibility of multi-user connection at the same time.

All this possibilities ensure the simplicity of providing individualized decisions which includes the analysis of current situation in constantly changing economical conditions. All system is designed to take the individual recommendation how to start a new business or how to find the companions for new business.

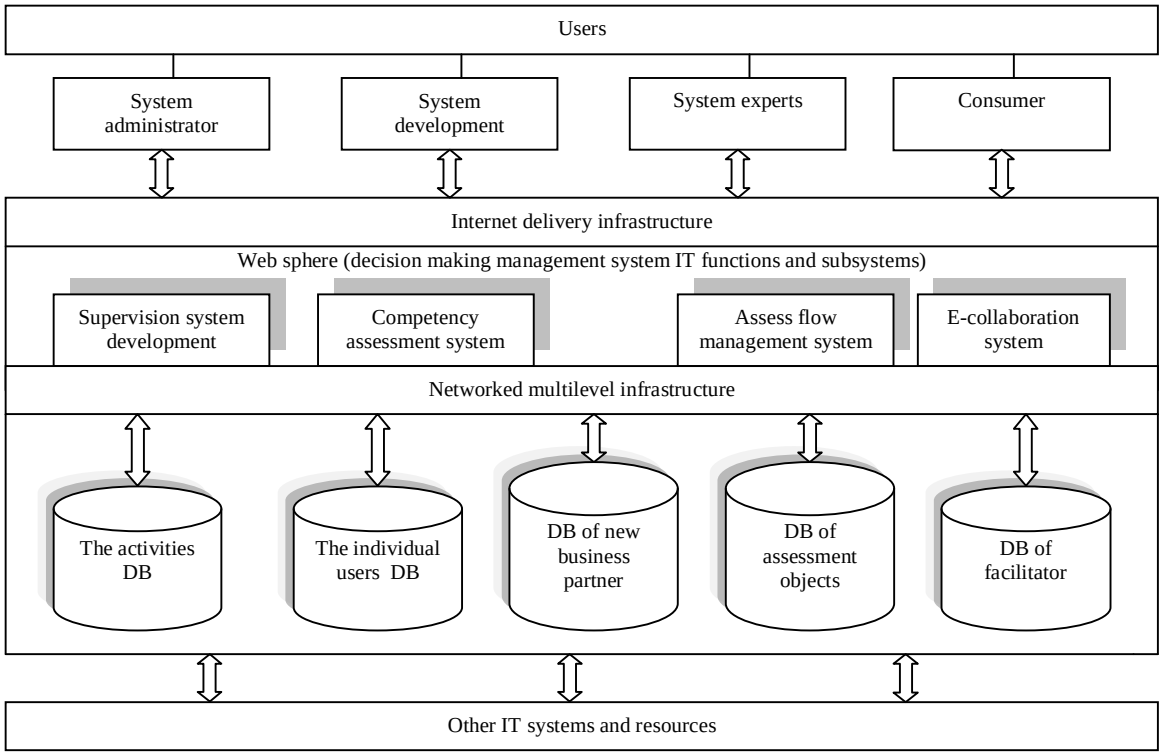

Fig. 1. The management of functions and subsystems information of the decision support system

Decision support system in accordance with input date (hobbies, activities, individual experiences, competence) culls necessary steps such as multilayer tests. The DSS proceeds in manner when consumer is registered and tested; he is integrated in the date base of system and all date are saving.

From a technical perspective we suggest that it is advisable to place a workflow engine at the core of the internet based e-decision making system [2]. This will let to generate or manage personalized and adaptable individual recommendation assesses flows and during the processes of an individual recommendation culling – grants the consumer access to subsequent databases of related resources or services. From a technical perspective the structure of decision support system could be kept comparatively simple and self-controlled in process of logic analysis. Figure 1 outlines DSS functions and subsystems.

The functions and subsystems reside on a networked multilevel infrastructure with strong internet connectivity and a number of databases [5]. The internet portal systems could be used to provide different types of users by user's type specific and customized services. The databases are designed to collect data about a number of processes and entities:

- The activities database – the consumer's readiness for the intended personalized integrating process needs to be evaluated; therefore his present knowledge and competency has to be evaluated and compared to his objective. The knowledge and competency have to be separated into standard role based competencies and associated knowledge requirements or patterns of behavior [2].
- Consumer database – individual user profiles, privileges, and data of the user's private information have to be stored. In addition the database contains personal curriculums, testing results, and individual recommendations.

- Facilitator database – this database contains the private environments data about user's activities searching history, and about his qualification.
- The assessment objects database – measurement objects including their metadata are stored in this db. These objects or "unit of tests" could be structured according to the proposed implementation concept and contain metadata (title, subtitle, creator, description, copyright, study-load), roles (system consumer, system expert), activities objectives, prerequisites, content (activity, environment – including knowledge object, announcement object, role information object etc.), method (activity structure, conditions). Therefore, knowledge and competency generating decision support system and the respective testing modules are assigned to this database [6].
- Business partner's databases – work flow systems usually use databases for the general definition of workflows (work flow templates) and databases which contain actual instances or work flow histories. The system's individual recommendation is attributed to assess the flow data.

As you can see the structure of DSS is very sophisticated. The multiplex date base system always gears up, so we must elaborate the system environment and structure. The important task is to create the Administrator subsystem, which leads to simplicity and integration of administration and author's subsystems to one application [8].

3. The Individual Recommendation Assesses Flow Algorithm

The individual recommendation assesses flow algorithm schema of decision support system, presented in blocs for test program of individually recommendation extraction (Fig. 2), was expanded by deep analyzing of get results and constructed to draw the individual recommendation for tested participant [2, 4, 5]. Equally we might say, that Figure 2 shows *a* decision support system assess flow which matches the ideas to support conditions in the business starter's environment process.

Traditionally existing tests are limited in first 10 blocs (1-10 blocs). The first bloc is constructed for the self containment as process logic and analysis of consumer objectives. After preliminary tasks evaluation the second bloc task is to search the possible behaviors for the tested person in the existing activities date base. The consumers that clearly cogitating their possibilities can get the help by 4-th bloc. The recommendation from 2-th bloc can be read and chosen as a test result. But there is foreseen the possibility to understand what really he needs after another deeper analyzing. If the dialogues in the 1-th section can not explicate the sphere of activities, because this procedure have not one step but are multilayer the consumer can continue with activities searching (6-th to 11 blocs). When the program user is tested by 7-th, 8-th, and 9-th blocs, then 10-th bloc analyzing and counting the answers and the selected result can be presented by 19-th bloc.

The test can inform participant about the get scores of tested factors, but to solve the problem in this easy way nowadays is not popular, because this type the get information is not easy to understand for user, and he can't correctly to form individual decisions for himself. So, for constructing the not ambiguity conclusion in this test program was realized multiplex intellectual task solving schema with the direct work of user and test program. This function is marked as the dotted lines, which including the 1-th, 4-th, 6-th and blocs from 13-th to 16-th.

The professional counseling system for retired military officers is based on three interlinked parts. The first part tests and represents the likes and hobbies of individual officer. At the traditional professional counseling the firs step is to test the persons' interests and competencies. The persons' interests are the main priority in the decision support system for self-employment. According to this approach, building a new career around the type of work that interests a person can bring additional efficiency and added value. The tests for preliminary tasks are constructed, that the person is asking to write up to 50 keywords, which describes his interests, hobbies and aptitudes, after that program analyzes input date and takes the recommendation of the possibility to start new action.

After testing the person's interests and hobbies program is testing its transferable competency, so the second step is the person's ability for entrepreneurship marking. The program is deeply analyzing and evaluating of overall motivation to start and operate own business. This part of program is designed for analyze: competence, decision making and innovative thinking. Where the competency testing is a measurement system that is capable of testing person's qualifications required for a particular job. In this case competency test is created according to Lithuanian Standard Classification of Occupations. The standard rubricates ten main groups and 5509 occupations, whereof 2876 occupations are directly related with the business activities and are used for our decision support system. Decision making is testing whether the person is decisive and can he able to successfully manage his favorite activities with risk associations. The innovative thinking is testing whether persons is innovative and can find a solution to challenges and problems.

The third part of the program creates the network of officers with complementary competencies for chosen business. The third level of this program is designed to help to start new business together with others. The system selects complementary profiles and created group of 2-5 retired officers - potential business network. This network we see as a business start-up meet up group. At the beginning this group needs for business-start consulting (system experts), while in the long period it can develop it self into the network where startups are learning from the experience of others on the basis of e-consultations. After consumers analyzing is done, person can make the decision by getting automated recommendations or can ask for help from experts. This possibility is intended in the DSS architecture, because there is not only a need to choose a new way for professional life, but also to integrate retired officers into civil life and reclaim the experience from military.

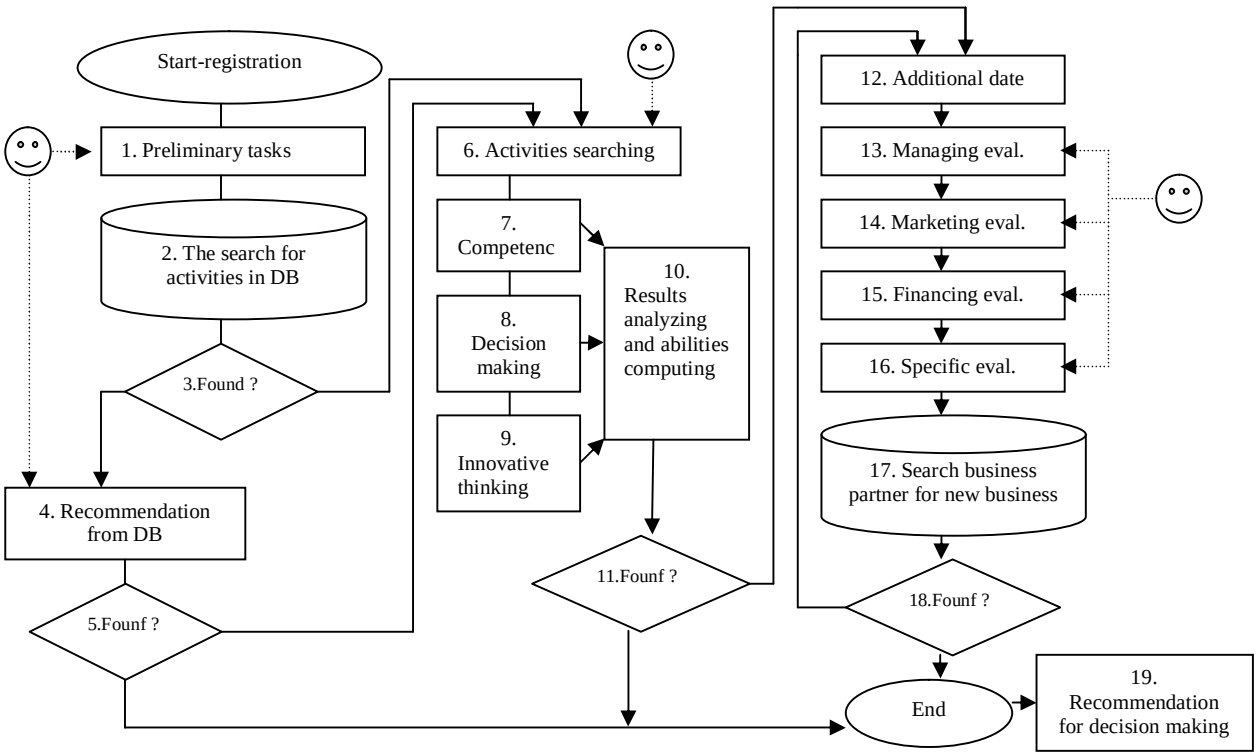

Fig. 2. The individual recommendation assesses flow in the decision support system

4. Conclusions

The integration into a labor market is an exceptionally complex decision for the retired military officers. In order to improve the quality of these individual decisions making, formal DSS was developed. By developing decision support system main challenges of retired military integration in to civil life was successfully tackled: convey of the experience from military to civil life of retired military officers; unlocking new business opportunities highly related with persons hobbies; and developing an expedient and complementary group of people of same interests and same positive attitudes towards entrepreneurship.

The first step to tacking these challenges is to create the architecture of DSS for retired military officers' career counseling. The architecture allows us: (1) to systematically integrate all existing information that is already collected through the last years; (2) to add new information by even four groups of system stakeholders: system administrator, system developers, system experts and consumers; (3) to create internet delivery infrastructure.

Decision support system in accordance with input date culls necessary steps such as multilayer tests. The functions and subsystems reside on a networked multilevel infrastructure with strong internet connectivity and a number of databases. The internet portal systems could be used to provide different types of users by user's type specific and customized services. The databases are designed to collect data about a number of processes and entities: the activities; consumer database; facilitator database; the assessment objects database; and business partner's databases. The multiplex date base system always gears up, so there is a need to elaborate the system environment and structure. The important task is to create the Administrator subsystem, which leads to simplicity and integration of administration and author's subsystems to one application.

The individual recommendation assesses flow algorithm schema of decision support system consist of three interconnected blocs: the first bloc is constructed for the self containment as process logic and analysis of consumer objectives; the second bloc analyses person's ability for entrepreneurship marking, it also evaluates individual's overall motivation to start and operate own business; the third bloc is provides with potential complementary business partners or business start-up meet up group.

By evaluating the architecture of decision support system for retired military officers' career counseling it is worth to stress on one changing point. The proposed DSS system is high in complexity, therefore the need to consider uncertainty at all stages becomes very important. Most important area that needs to be addressed in relation to the incorporation of uncertainty is related with human input.

References

1. **Lussato A.** Les tests de recrutement. Presses Universitaires de France, 1998. 127p.
2. **Izquierdo E., Deschoolmeester D.** What entrepreneurial competencies should be emphasized in entrepreneurship and innovation at the undergraduate level. //Proceedings of "Rencontres de St-Gall 2008", Fueglistaller, U., e.a., Innovation, Competitiveness, Growth and Tradition in SMEs, Verlag KMU, HSG. 2008.

3. **Baniulis K., Reklaitis V.** TestTool : Web-based Testing, Assessment, Learning. Informatics in Education, ISSN 1648-5831, Volume 1, 2002, Vilnius, Institute of Mathematics and Informatics, p.17-30.
4. **Butler J., Jia J., Dyer J.** Simulation techniques for the sensitivity analysis of multi-criteria decision models, European Journal of Operational Research, 1997. 103(3), 531-546.
5. **Jakeman A.J., Letcher R.A.** Integrated assessment and modelling: Features, principles and examples for catchment management, Environmental Modelling and Software, 2003,18, p.491-501.
6. **Hora S.C., Helton, J.C.** A distribution-free test for the relationship between model input and output when using latin hypercube sampling, Reliability Engineering and System Safety, 2003, 79(3), p.333–339.
7. Ranerup A. Decision Support Systems for Public Policy Implementation: The Case of Pension Reform. Social Science Computer Review, 2008, 26 (4), p.428-445.
8. **Xiao L., Lewis P., Gibb A.** Developing a security protocol for a distributed decision support system in a healthcare environment. ICSE'08. Proceedings of 30th International Conference on Software Engineering. Leipzig, 2008. p. 673-682.
9. **Cheney G., Zorn T.E., Planalp S., Lair D.J.** 4 Meaningful Work and Personal/Social Well-Being/ in Communication Yearbook 32. Ed. Ch.S.Beck. Routledge. 2008. p. 137-186.
10. Lietuvos Respublikos krašto apsaugos sistemos organizavimo ir karo tarnybos įstatymas. Vilnius: Žin., 1998, Nr. 49-1325.

Comparative Analysis of Vehicle Fleets of Panevezys and the Largest Cities of Lithuania

A. Demenienė *, D. Striukienė **

** Kaunas University of Technology, Panevezys Institute, Klaipėdos 3, LT – 35209, Panevezys, Lithuania, E-mail: alina.demeniene@ktu.lt*
*** Kaunas University of Technology, Panevezys Institute, S. Daukanto 12, LT - 35212, Panevezys, Lithuania, E-mail: danguole.striukiene@ktu.lt*

Abstract

The paper examines the economic phenomenon that has been little-studied in Lithuania – vehicle fleets of the largest cities of the country. The significance of this sector of economy as one of the parts of social infrastructure is emphasized.
A research was carried out applying comprehensive qualitative and quantitative data analysis.
This paper examines the scope and nature of the effects of regional vehicle population expansion, reflecting the economic structure and the homogeneity of the process while measuring it.
KEY WORDS: *transport, vehicle park, automobilization level.*

1. Introduction

Lately, a certain dynamic trend of the number of vehicles in the cities of the country has been observed [1, 2]. The expansion of vehicle fleets and the number of vehicles in use causes positive changes in economy growth and social infrastructure. However, the increasing number of vehicles affects the increase in the number of traffic accidents. It is noteworthy that transport sector is one of the largest polluters of the environment.

Scientific problem. The mentioned issues require comprehensive analysis and qualitative evaluation. The region of Panevezys is a part of central Lithuania with inherent specific characteristics of transport sector. Due to this it was important to analyze the vehicle fleet of Panevezys and Lithuania's cities.

Object of analysis in the paper. Evaluation of vehicle fleets of Panevezys and other largest cities of Lithuania.

Objective of the paper. To carry out a comparative analysis of vehicle fleets of Panevezys and other largest cities of Lithuania.

Tasks:

1. To present the dynamics of change in the number of vehicles in Panevezys and other largest cities of Lithuania.
2. To assess the structure of vehicle fleets of Panevezys and other largest cities of Lithuania.
3. To carry out an analysis of statistical data on the issue under consideration (2005- 2009).
4. The formulated tasks determined the structure of the paper.

Key methods of research:

1. Analysis the data of empirical research.
2. Analysis of secondary statistical data.

2. Investigations

Transport is one of the elements of economy and social infrastructure of the Republic of Lithuania. Its intended purpose is to carry passengers and consignments and to provide other transportation and associated services. In the Republic of Lithuania, there are the following branches of transport: railroad, automobile, marine, inland waters and air. Roads, vehicles, technological facilities, stations and other engineering structures fall under the vehicle transport category.

This paper reviews the population of road vehicles registered in 2005 – 2009 in Vilnius, Kaunas, Klaipeda, Siauliai and Panevezys, their types, the change in the number of vehicles and the most popular types of vehicles.

The change dynamics of the registered vehicles in Panevezys during 2005 -2009 is presented in Table 1 and Fig. 1.

The number of vehicles registered has been growing in Panevezys over the period of 2005 -2009, and as of 1 January 2010 there were 70988 road vehicles registered. In the total number, cars comprised 80 % (56932), cargo vehicles - 8 %, motorcycles - 2 %, busses - 1 % and trailers – 9 %. According to the statistical data of 2005 – 2009 [1], the number of registered trailers went up from 1097 (2 %) in 2005 to 6096 (9 %) in 2009. Based on the statistics, the number of vehicles annually grows by approximately 7 – 10 %. Over the last 5 years, the number of vehicles in Panevezys went up by 14753.

The given number of vehicles is an approximate figure, because in practice it is impossible to determine the number of vehicles registered elsewhere and driven in Panevezys as well as the number of vehicles registered in Panevezys, but driven elsewhere or just passing by. Nonetheless, these numbers are official and, in the opinion of road police officers, reflect the true situation [4].

Figure 1 depicts the number of registered new and used vehicles.

As the number of vehicles increases, relative ratios of automobilization are also going up. The automobilization level refers to the ratio of vehicles per 1000 of population.

Table 2 contains the numbers of road vehicles, comprising cars, busses, cargo vehicles, motorcycles, mopeds, trailers and semitrailers.

It can be seen from Fig. 2 that the relative automobilization level has been increasing in Panevezys as well as in Vilnius, Kaunas, Klaipeda and Siauliai. Klaipeda, Siauliai and Panevezys saw a very insignificant increase of automobilization level in 2006 – 2008. The vehicle to 1000 residents ratio in 2009 in Vilnius was 697, in Panevezys – 628, in Kaunas – 625, in Klaipeda – 576 and in Siauliai – 583.

Table 1

Composition of road vehicle population in Panevezys in 2005 – 2009

Year	Motor vehicles				Trailers	Other vehicles	Total	Vehicle to 1000 residents ratio
	Passenger	Cargo	Busses	Motorcycles				
2005	49 524	4059	435	390	1097	530	56235	502
2006	52 941	4298	447	652	1286	552	60176	537
2007	52 942	5140	431	880	1691	581	61215	546
2008	54 819	5240	441	1090	1843	624	64057	571
2009	56 932	5654	413	1393	6596		70988	633

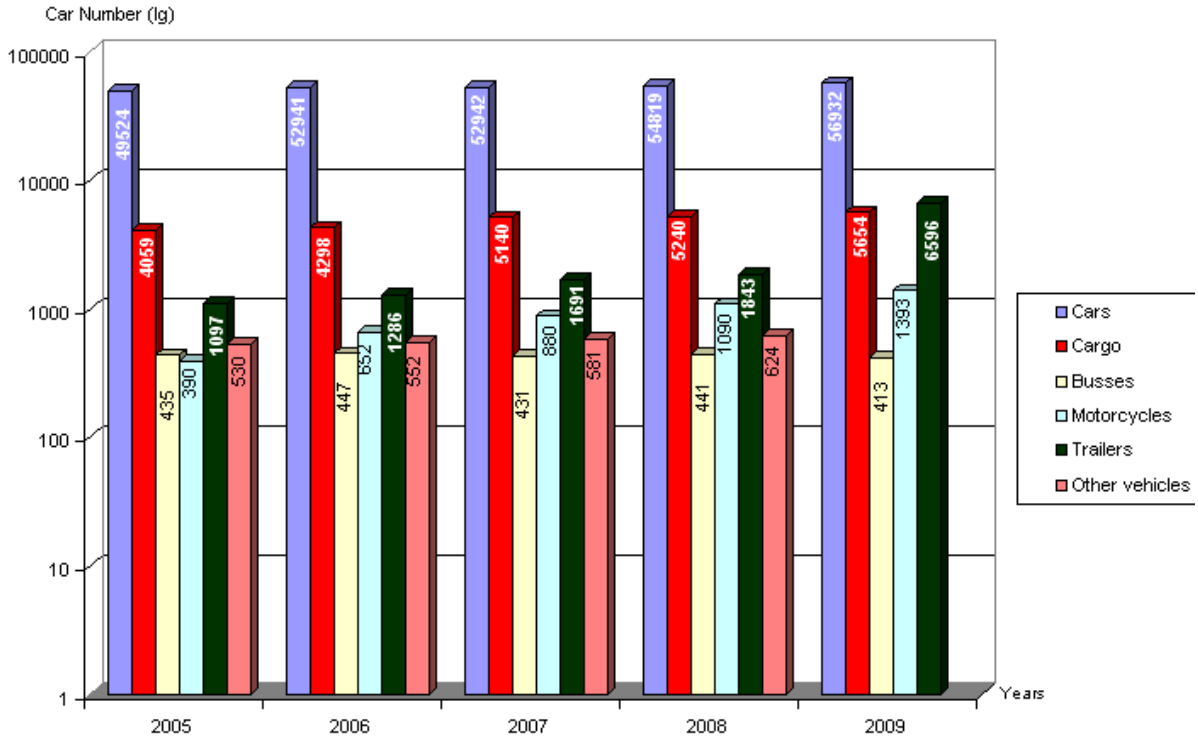

Fig. 1. Composition of road vehicle fleet in Panevezys in 2005 – 2009

Table 2

Change in the automobilization level in Vilnius, Kaunas, Klaipeda, Siauliai, Panevezys in 2005 – 2009

Cities	Number of road vehicles				
	2005	2006	2007	2008	2009
Vilnius	299103	326660	349292	370426	390069
Per 1000 residents	540	590	630	666	697
Kaunas	184602	197911	199798	206517	220001
Per 1000 residents	507	548	558	580	625
Klaipeda	93188	100762	100592	103093	105393
Per 1000 residents	498	538	540	557	576
Siauliai	62273	67909	67083	68097	72924
Per 1000 residents	479	526	524	536	583
Panevezys	56235	60176	61215	64057	70988
Per 1000 residents	484	523	532	561	628

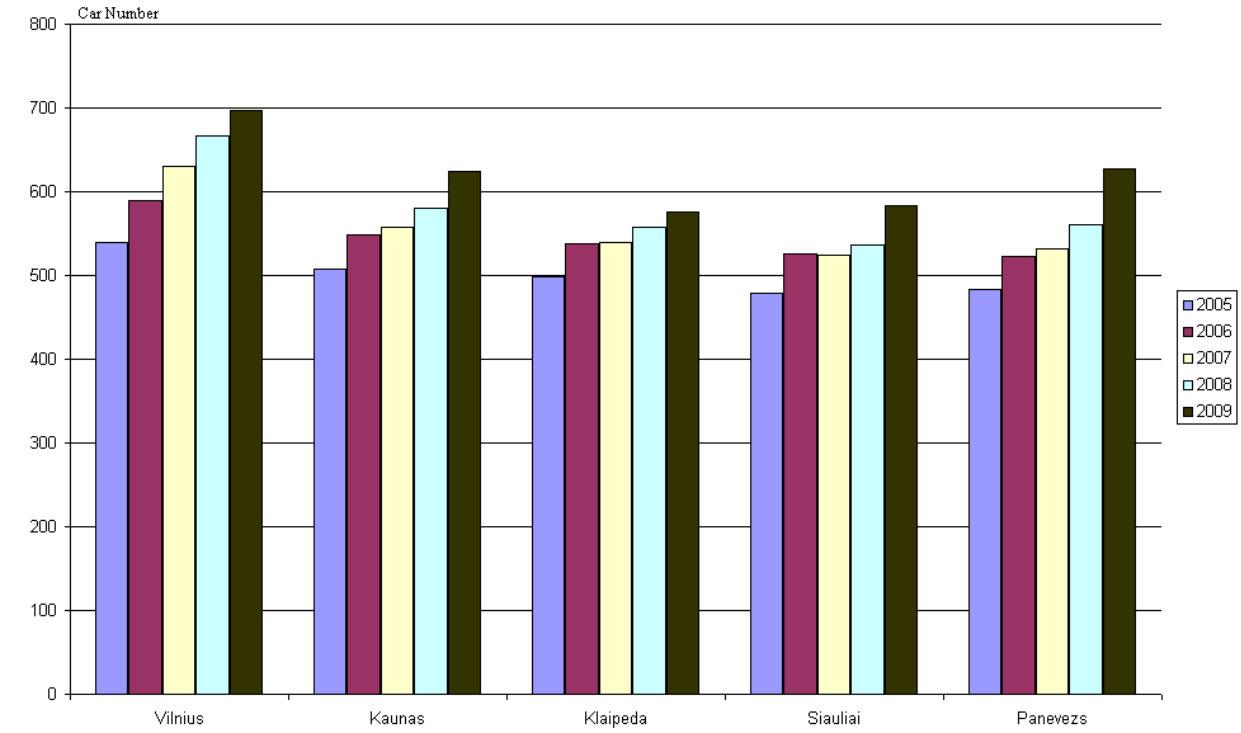

Fig. 2. Change in the automobilization level in Vilnius, Kaunas, Klaipeda, Siauliai, Panevezys in 2005 – 2009

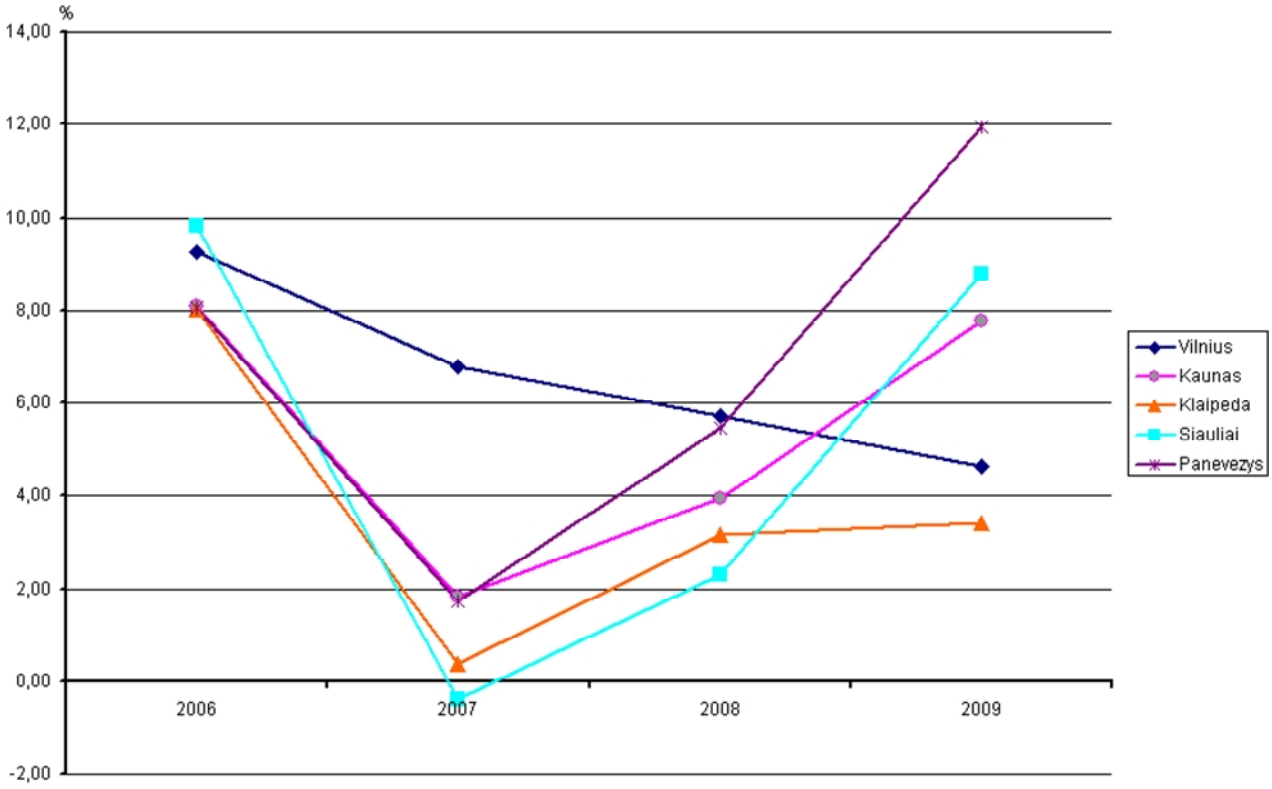

Fig.3. Vehicle number increase rates in per cent

After calculating the change in the number of vehicles (in per cent) compared to the last year, we obtain the following picture (Fig. 3).

The rates by which the numbers of vehicles have been increasing (each year is compared to the previous) in Panevezys, Kaunas and Siauliai were going up since 2007, whereas in Klaipeda, signs of a slow-down can be discerned. However, in Vilnius this indicator has been substantially slowing down since 2006. In future researches, a larger period should be examined in order to establish in which years Vilnius was ahead of other cities under consideration in the number of vehicles (per 1000 residents).

Seeing that individual cars comprise the largest share of vehicles, their distribution and the number of cars per 1000 residents in 2005 – 2009 in Vilnius, Kaunas, Klaipeda, Siauliai and Panevezys are presented in Table 4 and Fig. 4.

Bar chart in Fig. 4 shows the numbers individual cars per 1000 residents, while the line depicts the growth rates compared to the last year.

Table 4

Distribution and the number of individual cars per 1000 residents in 2005 – 2009 in Vilnius, Kaunas, Klaipeda, Siauliai and Panevezys

Cities	2005	2006	2007	2008	2009
Vilnius	249341	234858	235162	243258	321987
Per 1000 residents	396	424	424	436	579
Kaunas	150352	161240	158608	164366	182882
Per 1000 residents	417	450	446	467	519
Klaipeda	76931	81965	80495	82696	89153
Per 1000 residents	411	441	436	451	487
Siauliai	48972	52561	50734	51412	57753
Per 1000 residents	380	409	399	407	458
Panevezys	45699	48922	48303	50663	52063
Per 1000 residents	396	427	425	450	464

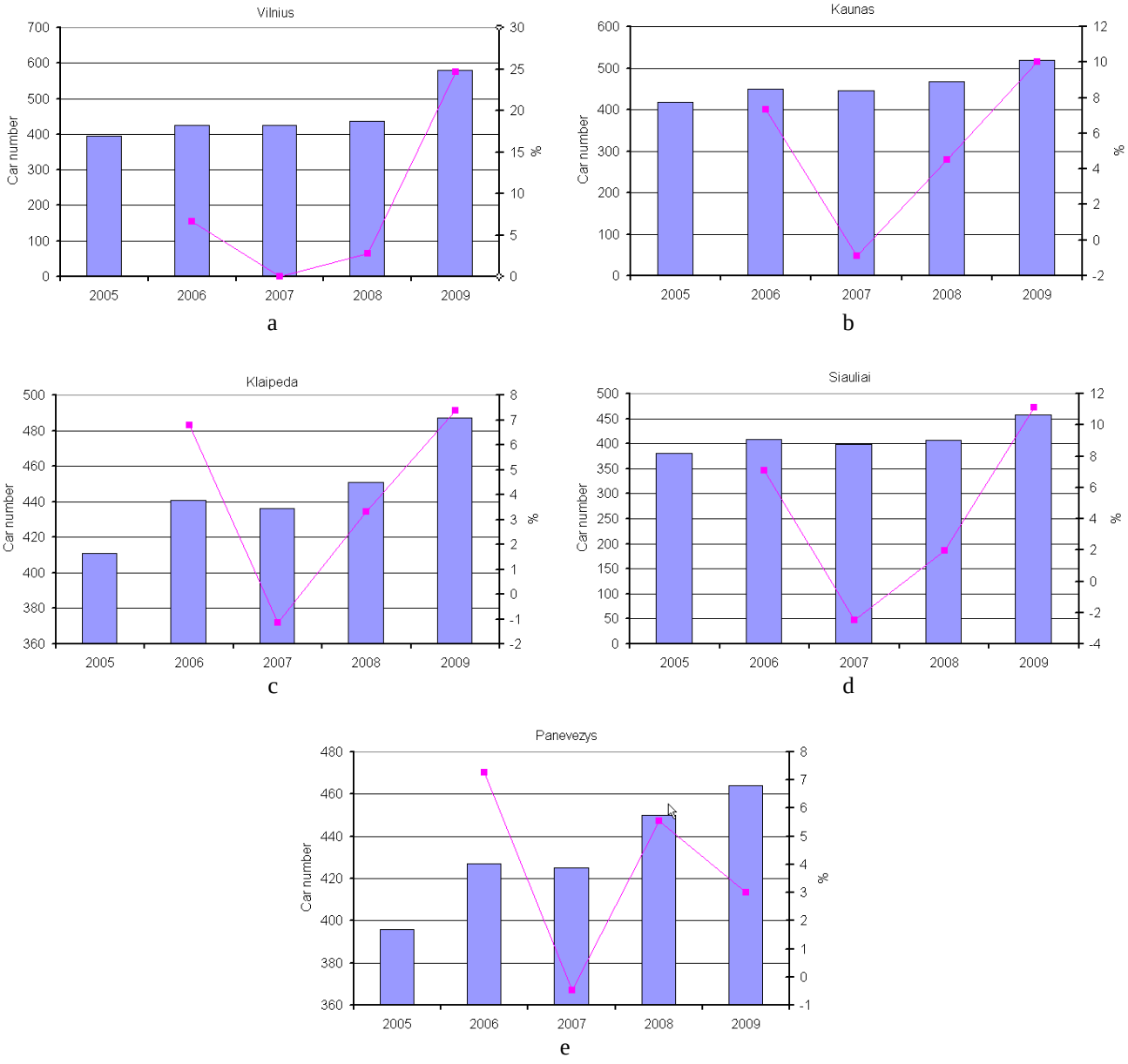

Fig. 4. The number of individual cars per 1000 residents and growth rates in per cent

In 2005-2006, the number of individual cars has been increasing, while in 2007 it sustained a small decrease and since 2007 started growing again. Comparing the vehicle number growth rates (Fig. 3) to the individual car number growth rates, a difference can be seen. In all cities, except Panevezys, it has been increasing, while in Panevezys it has been fluctuating.

3. Conclusions

1. After assessing the change dynamics of the number of vehicles in the largest cities of Lithuania, it was noted that:
   - transport sector represents one of the largest polluters of environment (holding the third place after energy and industry sectors) and, according to the statistics, its negative impact on the environment is increasing each year;
   - more attention should be devoted to safety and environmental protection.
1. Based on the analysis of data, it was determined that the growth of vehicle population increases the vehicle concentration, traffic intensity and traffic jams. This, in turn, causes the growing number of traffic accidents with more victims injured or killed. A negative social factor associated with the expansion of transport sector becomes obvious.
2. After carrying a quantitative analysis of presented statistical information (2005-2009), the necessity for deeper analysis of structure and change dynamics of vehicle population by different vehicle makes was noted.

References

1. Statistika (duomenų bazės) (2005-2009). Web site: <http://db1.stat.gov.lt/statbank/default.asp?w=1024> [visited at 2010 April 16].
2. Statistika (Transporto registravimo statistika) (2009-2010). Web site: <http://www.regitra.lt/index.php?Action=statist_reg_2010&node=40&node1=0&statid=menu1&s=0&f=0> [visited at 2010 May 16].
3. Eismo įvykių statistika (2009-2010). Web site: <http://www.lra.lt/lt.php/eismo_saugumas/eismo_ivykiu_ statistika/27> [visited at 2010 May 14].
4. Statistika (2005-2009). Web site: <http://www.lpept.lt/lt/statistika/index.php> [visited at 2010 May 14].

Intelligent Embedded Devices for Multistage Scheduling Tasks in Public Electric Transport

I. Alps, M. Gorobetz, A. Levchenkov

Riga Technical University, Riga, Latvia, E-mail: ivars.alps@rtu.lv; gorobetz@gmail.com; levas@gmail.com

Abstract

This paper describes the investigation of genetic algorithm using to control intelligent public electric transport in multistage scheduling tasks. Public electric transport in the city are influenced by several conditions, such as delaying in passengers stops and crossroads, whether conditions etc. All these conditions influence arriving time to next passengers stop on the route. On the other hands public transport units is obliged to arrive in stops according predefined schedule. Delaying is ultimate undesirable. Transport unit optimal motion speed is calculated using genetic algorithm to get next stop according schedule

KEY WORDS: *genetic algorithm, multistage tasks, intelligent electric transport, controller.*

1. Introduction

Nowadays in metropolis number of vehicles is increasing day by day. It is a reason for a lot of problems for public transport, causing traffic jams, schedule violation, etc. The tendency is to combine different transport types such as tram, trolleybus and bus in one stop. In city centre it causes scheduling conflicts in peak hours.

This is the cause for electric power overconsumption and public transport delay. To provide quick, cheap and comfortable passengers delivery with public electric transport in metropolis there was and will be topical problem. On the one hand, the amount of vehicles in the streets and electricity expenses are going up day by day, traffic jams become from bad to worse, public transport stays in traffic jams longer time and use electricity increasingly, but on the other hand the citizens require public transport as fast and as cheap as possible. To provide arriving public electric transport units at stops in time will help to solve this actual problem for any big city worldwide.

This paper describes a new application of genetic algorithm; to calculate optimal electric transport motion speed on the routes. Main goal of research is to found such motion speed, which provide transport unit arriving at stops exactly in time.

2. Problem Description

In the big cities public transport motion is influenced by several conditions, increasing number of vehicles and passengers, traffic jams, whether conditions. Today there is no any additional equipment in public electric transport units installed to immediate calculate motion speed considering into account possible delaying or staying on the crossroads.

In this paper as solution of public transport units delay eliminating authors proposed to use genetic algorithm and programmable industrial controller to calculate optimal motion speed and control electric transport DC drives.

Object of research is public electric transport system.

Main tasks of research are:

- to define structure of public electric transport with intelligent controller;
- to develop genetic algorithm of schedule fulfilment of public electric transport;
- to create computer model of proposed embedded control system;
- to create a functional model with real and virtual devices with realization of control algorithm in PLC.

Main tasks of research are to create programmable model for punctual predefined schedule consideration. Main goal of this research is to find out optimal motion speed on the route used immune algorithm and PLC. Purposed electric transport control system block diagram is shown in Fig. 1.

Electric transport control system consists of vehicle moving control scheme, programmable controller and DC drive model. Data block contains several data bases:

- data about distance between objects on the route, stops, traffic lights, curves;
- traffic lights operating schema und speed limits;
- public transport schedule.

Electric transport units receive GPS signal about current location, PLC calculate optimal current speed value according received signal and data from data block and send through transmitters relevant signal for DC drive control.

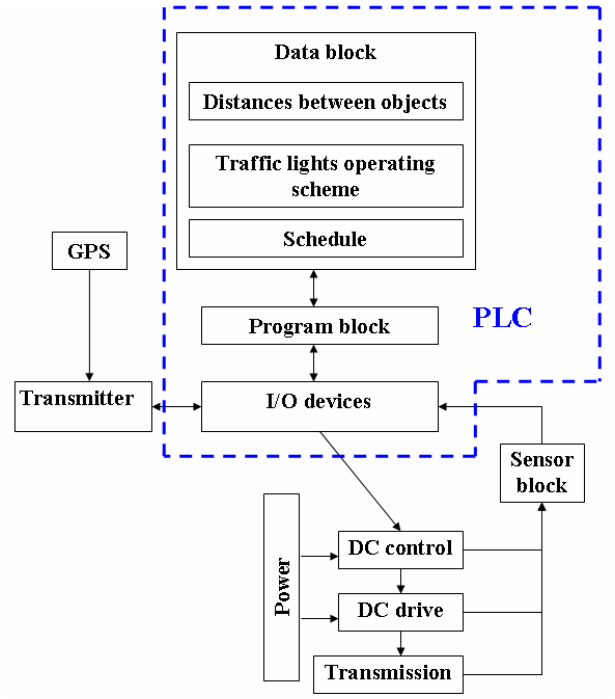

Fig. 1. Control system block diagram

3. The Mathematical Model for the Genetic Algorithm

Is given. The following definitions are proposed for mathematical model of genetic algorithm:

- Processors – $P = \{p_1, ..., p_n\}$ – crossroads, streets and passenger stops;
- Jobs – $TR = \{tr_1, ..., tr_m\}$ - vehicles;
- Set of sequences – $S = \{R_1, ..., R_b\}$ routes, where for each route $R \in S$, $R = \{o_1, ..., o_{k_r}\}$, where $k_R \le n$ – number of operations for route r; $o_i \in P$ – Processor to perform operation i;
- Set of prior operations of each route – $PR = \{0, o_1, o_2, ..., o_{k_r - 1}\}$, $PR \to R$;
- Each vehicle $t \in TR$ has a route R^t assigned to it, where $R^t \in S$;
- Duration for each operation $o \in R^t$ for each vehicle $t \in TR$, $D^t = \{d_1^t, ..., d_{k_{R^t}}^t\}$, $D^t \to R^t$, $d \in D^t$, $d \in \Re$.

Target function. Main goal of research is to create genetic algorithm fitness function for PLC for optimal DC drive control. Goal will achieve, when vehicle arrive in stops in time $t_p = t_{schedule} \pm 1 \to \min$

$$\begin{cases} \Delta t = f\left(v_1, ..., v_{(n-1)}, v_n\right) \to \min \\ 0 < v_1, ..., v_{n-1}, v_n \le v_{\max} \\ \Delta t = \left| t_{schedule} - t_p \right| \\ 0 \le \Delta t \le 1 \\ t_p = t_{p1} + ... + t_{p(n-1)} + t_{pn} \\ t_{p1} = f(v_1) \\ t_{p(n-1)} = f(v_{n-1}) \\ t_{pn} = f(v_n) \end{cases}$$

where: $v_1, ..., v_{n-1}, v_n$ – max motion speed on route; v_{max} – motion speed limit; Δt – fitness function; $t_{p1}, ..., t_{pn}$ – requiring time to complete each stage; $t_{schedule}$ – arriving time in stops according schedule.

4. Method of Solution

Authors offer use genetic algorithm as a method of problem solution.

Genetic algorithm – the searching algorithm used for optimization and simulation to solve the task with a random selection and combination. Genetic algorithm simulates biological evolution. Genetic algorithm is a kind of evolutionary

computing. It is adaptive search method, which can be used for optimization of functional tasks. This method is based on the genetic processes in biological systems: biological populations evolve over many generations under natural selection rules and the principle of the strongest survives (survival of the fittest – defined by Charles Darwin).

Genetic algorithms can be used almost everywhere; optimizing the various processes, such as treatment for reducing energy consumption etc.

The basic principles of Genetic algorithm were formulated by John Henry Holland. Evolution based on natural selection. The main principle for selection is that the best adapted individuals are more likely to survive and reproduce, so they make more offspring. Thanks to genetic inheritance, progeny obtained from parents' best qualities. Consequently, the stronger the individual offspring will be better prepared. Fitness value of individuals seriously increased after ten or a hundred generation's.

Genetic algorithm block diagram is presented in Fig. 2.

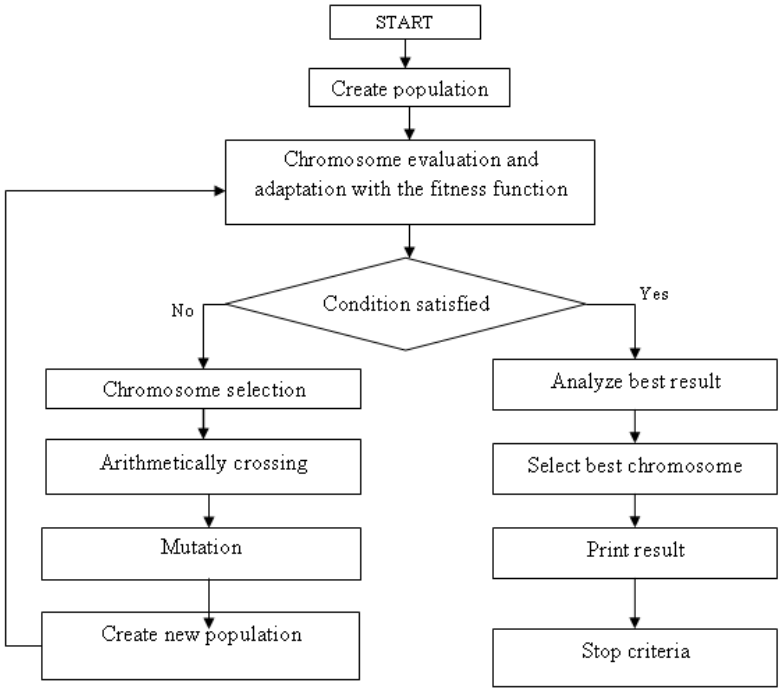

Fig. 2. Genetic algorithm block diagram

General steps for genetic algorithm:

- *Coding* – the genetic algorithm use the appropriate decimal or binary digital coding. Suppose that a genetic algorithm solution is expressed by the set of parameters. Set of parameter values are representing as chromosome. Chromosome containing the selected features variable called genes.
- *Initialization* – initialization phase formed a new population. Usually the population is formed from randomly created or already existed chromosomes. Set of chromosomes should be a diverse population to make algorithm more efficiently. If all chromosomes are identical, then result of genetic algorithm will be disappointing.
- *Evaluation* - in this stage algorithm decoding chromosomes and verify the results using the new parameters. Based on obtained results fitness function values are calculated.
- *Fitness function* – for each task should be create a fitness function. The fitness function give fitness value for each chromosome, which determines the (represented by a chromosome) suitability of the environment.
- *Selection* - in this stage chromosomes for next population will be selected.
- *Reproduction* – in this stage individuals from the populations are selected and combined. To combine individuals successors are formed. Successors will be entering in the new population. There already appears the statement "the strongest survives" (survival of the fittest), therefore, more suitable individuals will have more opportunities to be selected than a bad fit. Crossover or mutation function is used for combination.
- *Exposure and achievement the global maximum* – repeat previous stages in population individuals' value of fitness enlarge and exposure to global maximum. When program achieve global maximum, then next generation has value of solution (95% population has same value)

Operators of genetic algorithm:

- *Parents selection* – chromosome selection is choice of two parents, which will posterity next generation. Chromosome selection give opportunity for genetic algorithm to eliminate average fitness value for next generation over previous generation. Methods for chromosome selection:
  - roulette selection;

- tournament selection;
- ranking selection;
- random selection.

- *Crossover* – genetic algorithm one of the most important operator is crossover. Two parents are necessary to produce successors. Main required for crossover – successors obtain parental characteristics. Since parents are selected by one of the selections methods, thereby the strongest reproducing most often. There are three mode of crossover: binary crossover (one-point crossover, two-points crossover, multiple-point crossover), arithmetic crossover, mutation.
- *Inversion* – operating principle is similar mutations, but the inversion operator chooses two points to inverse.

5. Computer Experiment

As an example part of tram Route No.5 in Riga city centre is selected. As shown in Fig.3. there are three stops A,B and C "13.janvāra iela", "Grēcinieku iela" and "Valguma iela" and two traffic lights on the route No. 1 and No. 2, Fig. 3.

Transport units arriving in stops schedule are shown in table 1. In Fig.4 the Ghant chart shows time intervals of green/red lights for traffic lights No. 1 and No. 2.

Corresponding distance between start (stop "13.janvāra iela") and following traffic lights and stops are shown in Table 2.

Fig. 3. Part of tram Route No.5 in Riga city

Table 1

Arriving schedule

16	6	16	27	39	51	Stop 1
	9	19	30	42	54	Stop 2
	12	22	33	45	57	Stop 3
17	3	15	27	39	51	Stop 1
	6	18	30	42	54	Stop 2
	9	21	33	45	56	Stop 3
18	1	12	23	34	50	Stop 1
	4	15	26	37	53	Stop 2
	7	18	29	40	56	Stop 3

Table 2

Passengers stops and traffic lights location

	Stop1	TL 1	TL 2	Stop2	Stop3
Distance (m)	0	245	445	565	1335

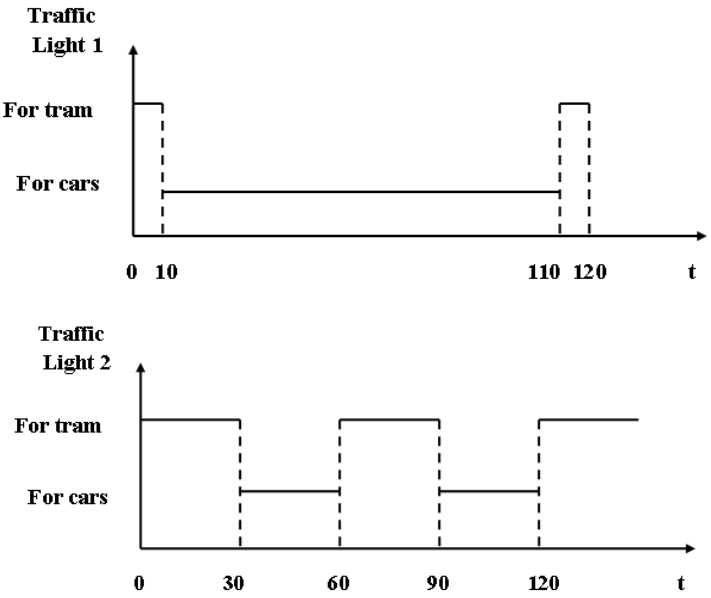

Fig. 4. The Ghant chart for traffic lights No. 1 and No. 2

Basic data was entered in SIEMENS SIMATIC S7-200 computer program Step7-Micro/Win. Part of programming code in Step7-Micro/Win environment is present in Fig. 5.

This part of program show calculation of several parameters.

```
Fitness function
Network 1   Calculate ta1 and Sa1 for first part of route
Network Comment
LD      SM0.0                   //nosacījums: jebkura gadijuma izpildit
MOVR    #v1:LD0, ta1:VD7020     //parvieto v1 atmina ta1:VD5020
AENO                            //
/R      1.0, ta1:VD7020         //dala vertibu ta1 ar 1
AENO                            //
MOVR    ta1:VD7020, AC0         //parvieto ta1:VD5020 akkumulatoras nulta
AENO                            //
*R      #v1:LD0, AC0            //reizina atrumu ar akumulatoru
AENO                            //un saglaba akkumulatoras atmina
MOVR    AC0, Sa1:VD7032         //dala vertibu akkumulatora uz 2 un sagla
/R      2.0, Sa1:VD7032         //un saglaba Sa1:VD5032 atmina
```

Symbol	Address	Comment
Sa1	VD7032	speed changes from v0 ==> v1
ta1	VD7020	speed or acceleration change

```
Network 2   Calculate accelerating distance and requesting time

LD      SM0.0                   //nosacījums: jebkura gadijuma izpildit
MOVR    SL1:VD7000, SL1a:VD7044 //SL1 parvieto atmina Sl1a
AENO                            //
-R      Sa1:VD7032, SL1a:VD7044 //no SL1a atnem Sa1
SUBROUTINE COMMENTS
Network 1   v1 gene crossover for first offspring
Network Comment
LD      SM0.0
MOVR    #v1_1:LD0, AC0
AENO
*R      #lamda1:LD24, AC0
AENO
MOVR    #v1_2:LD12, AC1
AENO
*R      #lamda2:LD28, AC1
AENO
MOVR    AC0, #v1_1n:LD32
+R      AC1, #v1_1n:LD32
Network 2   v1 gene crossover for second offspring

LD      SM0.0
MOVR    #v1_1:LD0, AC0
AENO
*R      #lamda2:LD28, AC0
AENO
MOVR    #v1_2:LD12, AC1
AENO
*R      #lamda1:LD24, AC1
AENO
MOVR    AC0, #v1_2n:LD44
+R      AC1, #v1_2n:LD44
Network 3   v2 gene crossover for first offspring

LD      SM0.0
MOVR    #v2_1:LD4, AC0
AENO
*R      #lamda1:LD24, AC0
```

```
PROGRAM COMMENTS
Network 1   Network Title
Network Comment
LD      SM0.0                       //iesacijums izpildas jebkura
CALL    ETH0_CTRL:SBR2, M6.0, VW10160, VW10162 //kontrolleru uzsta
```

Symbol	Address	Comment
ETH0_CTRL	SBR2	This POU was generated by the Ethernet Wizard for use with

```
Network 2

LD      SM0.1
MOVR    160.0, VD10184
AENO
MOVD    0, VD10180
AENO
MOVD    &VB8004, VD8000
AENO
MOVD    &VB8600, VD8996
AENO
CALL    fil_population:SBR12
```

Symbol	Address	Comment
fil_population	SBR12	SUBROUTINE COMMENTS

Fig. 5. Part of programming code in Step7-Micro/Win environment

All necessary assembled elements for computer experiment, controller, power supply, Ethernet block, installation elements and output device, are shown in the Fig. 6.

Computer experiment results can be seen on the output device display Fig. 7.

On the display are output following parameters:

- generation number of the genetic algorithm;
- three velocity values;
- target reaching time;
- the fitness function value.

Fig. 6. Model for computer experiment

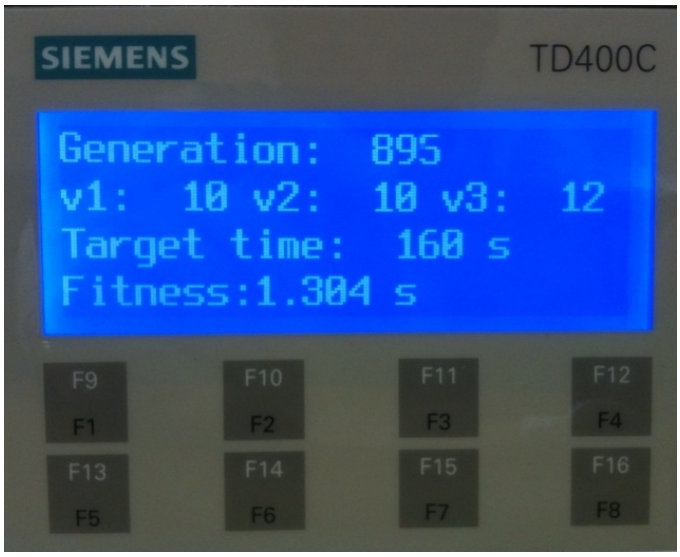

Fig. 7. Displaying experiment result on output device

6. Conclusions

To analyzed result of computer experiment the conclusions are:

- genetic algorithm for intelligent embedded devices can be used to solve public electric transport flow organization multistage tasks;
- the tram motion speed is control entire whole route with purpose consider predefined schedule;
- industrial controller can be used for intelligent public electric transport schedule control.

References

1. **Ribickis L., Gorobetz M., Levchenkov A.** Intelligent Electric Vehicle Motion And Crossroad Control. // In Proceedings of 12th International Power Electronics and Motion Control Conference. Portoroz, Slovenia, 2006 – 1239 - 1244 p.

2. **Rankis I., Gorobetz M., Levchenkov A.** Optimal Electric Vehicle Speed Control By Intelligent Devices. Rīgas Tehniskās universitātes raksti. Enerģētika un Elektrotehnika. Sērija 4, sējums 16. 2006. 127-137 p.
3. **Kuei-Hsiang Chao, Ren-Hao Lee, Meng-Hui Wang.** An Intelligent Traffic Light Control Based on Extension Neural Network// Department of Electrical Engineering, National Chin-Yi University of Technology, Taichung, Taiwan, R.O.C. Lecture Notes in Computer Science, Springer Berlin / Heidelberg, Germany, 2008.
4. **Gorobetz M., Levchenkov A.** Evolutionary Algorithms and Dynamic Parameters for Public Electric Transport Modeling //In Proceedings of 16th Mediterranean Conference on Control and Automation, Ajaccio, France, 25-27 June 2008, 215-219 p.
5. **Wiering M. A.** Multi-agent reinforcement learning for traffic light control. In Langley.// In Proceedings of the Seventeenth International Conference on Machine Learning (ICML'2000), Stanford University, June 29 to July 2 2000, USA, 1151–1158 p.
6. **Wiering M., van Veenen J., Vreeken J., Koopman A.** Intelligent Traffic Light Control. Institute of Information and Computing Sciences, Utrecht University. Padualaan 14, The Netherlands, 2004.
7. **Horyński M.** Intelligent Electric Systems in Urban Traffic Control. Department of Computer and Electrical Engineering, Lublin University of Technology, TEKA Kom. Mot. Energ. Roln. – OL PAN, Poland, 2007.
8. **Mitsuo Gen, Runwei Cheng.** Genetic Algorithms & Engineering design – EDA 1997.

Proceedings of 5th International Workshop ITELMS'2010

Data Clustering With Kohonen‘s Self-Organizing Networks at Production Evaluation Process

A. Česnulevičius, D. Garuckas, O. Purvinis

Kaunas University of Technology, S. Daukanto str. 12, 35212 Panevėžys, Lithuania, E-mail: aurimas.cesnulevicius@ktu.lt; danas.garuckas@ktu.lt; ojaras.purvinis@ktu.lt

Abstract

Kohonen self-organizing map (SOM) is very powerful method for cluster extraction and data mining. This is especially important for high-dimensional data sets analysis. This paper shows how to identify the relations between different parameters at production evaluation process.
KEY WORDS: *self organizing networks, Kohonen‘s SOM.*

1. Introduction

Production evaluation is related with establishment of different parameters. One of them is production cost. Calculation of production cost in early stages of design process is complicated task for lack of necessary information about different aspects of product design and production processes [1]. The initial stage of creation the production cost forecasting model was selection of the set of attributes as input vector for the problem‘s mathematical model. It appeared that these attributes should be selected from the set of product qualitative and quantitative parameters. Some of them may be necessary, a few may be sufficient. The next step were estimation of connections between selected attributes and production cost. The difficulty was that each sample were represented by vector of $N > 3$ attributes and the relations between them can be non-linear. To work around this difficulty and to visualize this high-dimensional data sample the data clustering was done. For that purpose the Kohonen‘s self-organizing maps were employed.

2. Self Organizing Networks

The self-organizing maps algorithm represents a variant of the multidimensional vectors clustering – the projection algorithm with maintenance of topological similarity.

A distinguishing feature of the SOM algorithm is that all the neurons in it are arranged in a two-dimensional grid. During training not only the best matching unit (the map neuron which better than others corresponds to the input vector and determines to what class he sample belongs) is modified, but its neighbors too, although in a smaller degree. Due to this the SOM can be considered as one of the methods of projecting a multi-dimensional space into a lower dimension space. This non-linear projection on two-dimensional grid is called a Kohonen map by the name of Finnish researcher Teuvo Kohonen who invented these SOM [2]. This map can serve as visual representation of high *n*-dimensional data set of points $P_i(x_1, x_2,.. x_n)$ or vectors, maintaining the structure of that data set, i.e. points that are close in *n*-dimensional space are also close on the map [3].

An example of Kohonen map built by selforganizing neural network and using 7-dimensional data (features or factors) is shown in the figure 1. The neural network algorithm discovered in the feature space four clusters, numbered them from 0 to 3 and projected them on 2-dimensional grid (the left picture).

On that grid there can be projected a separate layers cooresponding to each feature. The distribution of the feature‘s values on each layer are represented by diffrent colors or by shades of gray color ranging from black to white.

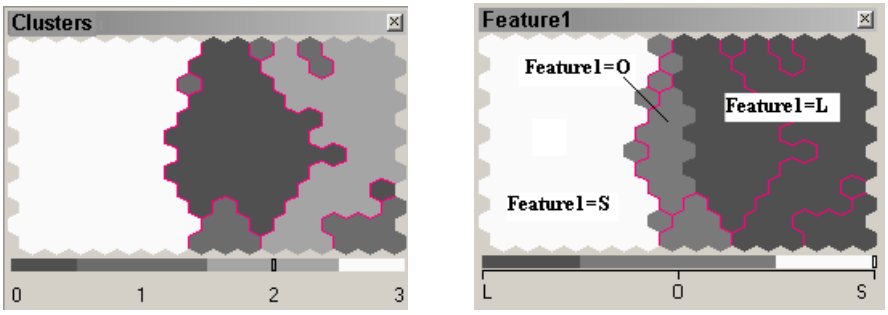

Fig. 1. Example of Kohonen map. Using seven different features there were recognized 4 clusters and every feature were projected on the 2-dimensional map

For instance, from the right picture of the figure 1 it is seen that the value *L* of the *feature*1 is distributed over the upper righ cluster and it partially occupies the middle cluster that is filled with black color in the left picture. On the other hand, the maps also indicate that the black cluster in the leftmost picture is formed taking into account another features not *Feature*1 only, while the white cluster depicts the value *S* of the *Feature*1.

3. Data Clustering with Kohonen Self Organizing Maps

The first stage in our research was composition the set of attributes. The set with seven attributes was chosen after discussions with production experts. These seven attributes are:

- relative cost of material;
- type of raw material;
- mass of the part;
- mass of the blank;
- minimal tolerance;
- minimal roughness of the part surface;
- number of machining features.

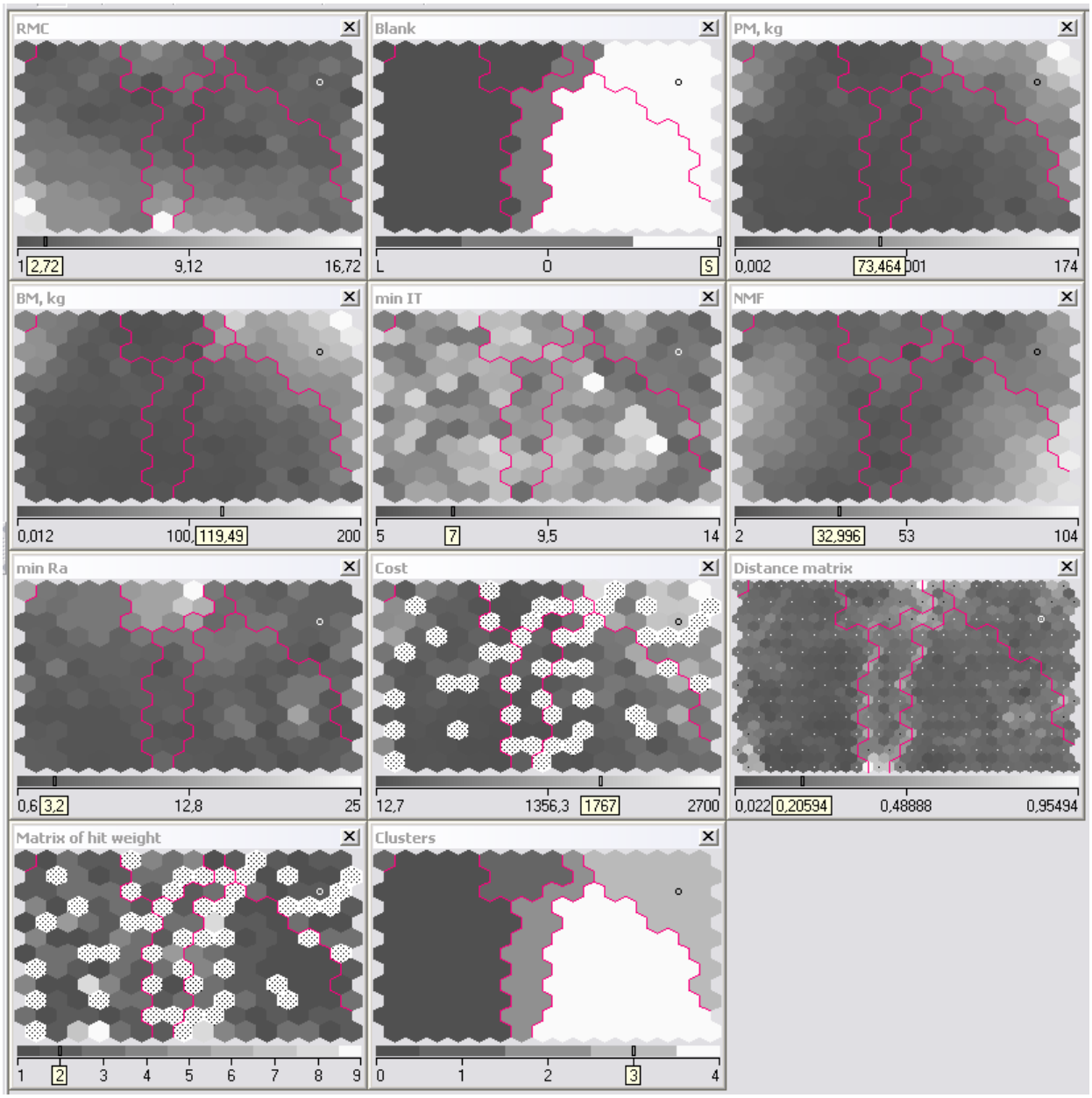

Fig. 2. The results of data clustering (RMC – relative cost of material; Blank – type of raw material; PM – mass of the part; BM – mass of the blank; minIT – minimal tolerance; NMF – number of machining features; minRa – minimal roughness of the part surface). Map initialization method: by random values; recognized – 80%

The clustering process starts with data initialization. Each attribute set is normalized to RMS = 1 (RMS – root mean square). This will prevent one attribute from overpowering in clustering. Two types of normalization were applied: linear normalization of the initial values and transformation of unique values to their indexes. The second type of normalization is applied only to attribute *type of raw material*. If the training set does not cover the entire range of the actual values it is possible to expand the range.

The next step is division of training sample in two sets – training and testing. The difference between these two sets is that testing set will be used for testing the results of the training, not for training the model. We have used 95% of samples for training and 5% for testing. Records for training process were selected randomly.

The training process of the map is iterational. Each iterational cycle is called an epoch. During each iterational cycle (epoch), the algorithm adjusts the weights of the Kohonen map neurons. The specification of how the initial weights of the map neurons will be set up calls initialization method. We have used two different initialization methods: by random values (Fig. 2) and using the training set (Fig. 3). The number of samples recognized in the training set and the testing set is approximately equal (accordingly 80 and 75 %) in both cases.

There were selected the representation of the data clustering results using Kohonen map according to eleven parameters (Fig. 2 and Fig. 3). All of them can be grouped into three categories:

- input parameters (*RMC* - relative cost of material; *Blank* - type of raw material; *PM* – mass of the part; *BM* – mass of the blank; *minIT* – minimal tolerance; *minRa* – minimal roughness of the part surface; *NMF* – number of machining features);
- output parameters (*Cost* – production cost);
- special parameters (*Clusters*; *Hit density matrix*; *Distance matrix*).

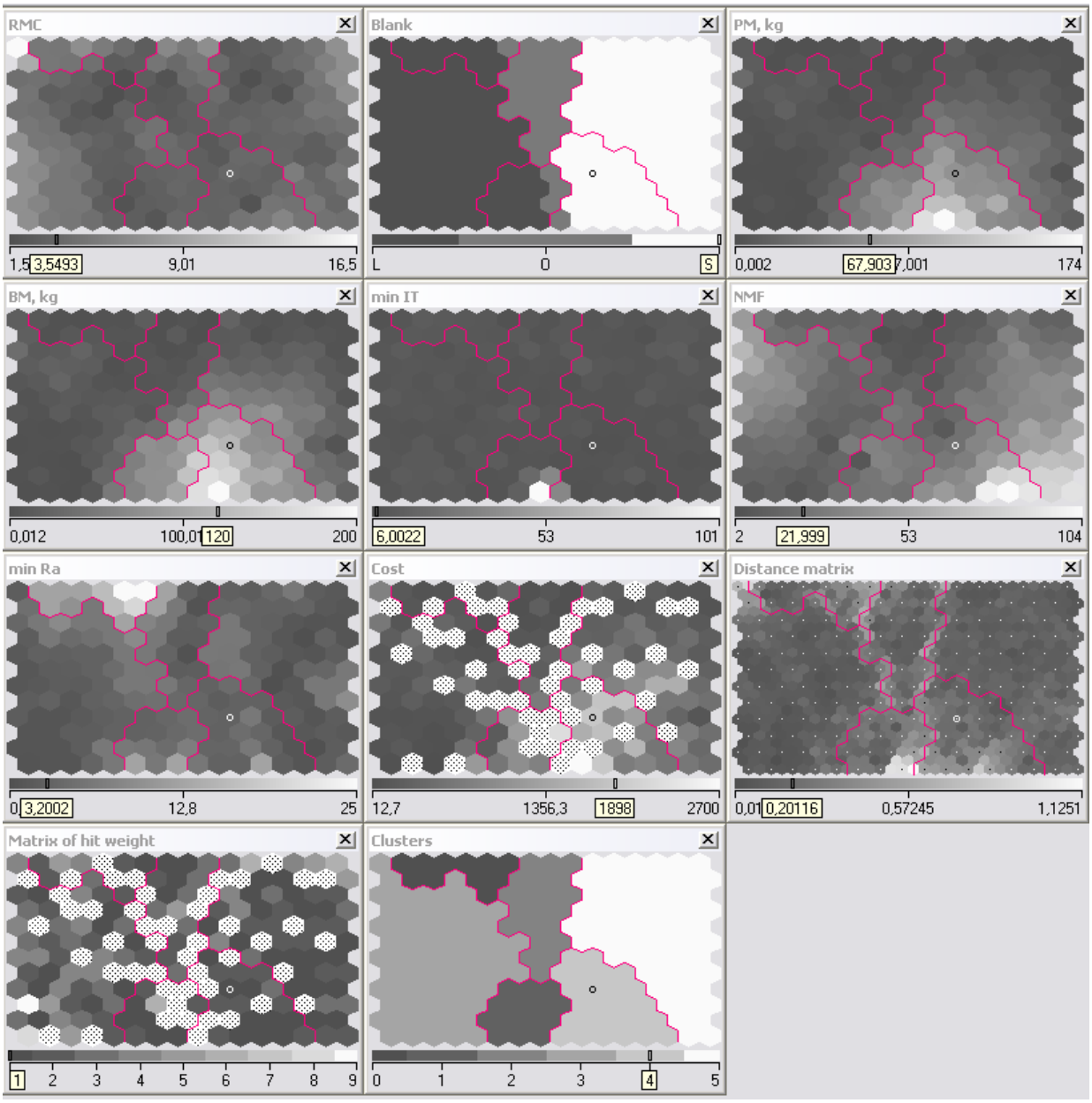

Fig. 3. The results of data clustering. Map initialization method: using training set; recognized – 75%

As it was mentioned before, clusters represent the groups of vectors the distance between which is smaller than to the adjacent groups. In other words, all the map elements which fall into the area of the same cluster are similar. Hit density matrix displays the number of samples that fall into the cell. Distance matrix (unified distance matrix, U-matrix) is used for visualizing the structure of the clusters obtained as a result of the map training. The matrix elements determine the distance between the neuron weight coefficients and its nearest neighbors. A large value indicates that this neuron considerably differs from the neighbors and belongs to another class.

Using map initialization method by random values were formed five clusters (Fig. 2, window "Clusters"). The analysis of the relations between clusters and input parameters shows that attribute *type of raw material* (Fig. 2, window "Blank") has the largest influence to clusters formation as well as attributes *mass of the part* and *mass of the blank* (Fig. 2, windows "PM" and "BM"). This relation is obvious analysing cluster 3. The attribute *minimal roughness of the part surface* has large impact on formation of the cluster 1. The minimum impact on clusters formation has attribute *minimal tolerance* as well as *relative cost of material* (Fig. 2, windows "minIT" and "RMC"). Analysis of connection between clusters and attribute *number of machining features* shows that the impact level of attribute is very low when NMF is less than 10 features and very high when NMF > 80 (Fig. 2, window "NMF"). Analysis of connection between output and input parameters denotes that the significant connection exists between *production cost* and *mass of the part* or *mass of the blank* (Fig. 2, windows "Cost", "PM" and "BM").

Figure 3 represents the results of clustering with another one map initialization method. Using training set for map initialization were formed six clusters (Fig. 3, window "Clusters"). The major attributes of clusters formation are *type of raw material* (Fig. 3, window "Blank"), *mass of the part* and *mass of the blank* (Fig. 3, windows "PM" and "BM") as well as at previous case (Fig. 2). It seems that the influence of other attributes on clustering process is practically the same as at previous case: the attribute *minimal roughness of the part surface* is responsible for formation of cluster 0 and influence of attribute *minimal tolerance* is negligible. The impact of attribute *number of machining features* (Fig. 3) is more or less identical to previous results (Fig. 2). The connection between output and input parameters is analogical using both map initialization methods (Fig. 2 and Fig. 3): the strongest connection noticed between *mass of the part* or *mass of the blank* and *production cost*.

4. Conclusions and Further Research

The results of clustering using Kohonen SOM revealed that a major influence on the cost have three attributes (*type of raw material, mass of the part, mass of the blank*). It is rational to eliminate one of the mass attribute, because the impact of these two attributes (*mass of the part* and *mass of the blank*) to clustering process is uniform (Fig. 2 and 3, windows "PM" and "BM"). The necessity of attribute *minimal tolerance* is also questionable. The strongest connection exists between *production cost* and *mass of the part* or *mass of the blank.*

The plan for further research:

- to compare clusters formed for separate type of raw material and estimate the correlation between input and output parameters;
- to compare clusters formed with various subsets of the possible input parameters.

References

1. **Česnulevičius A., Garuckas D., Purvinis O.** Artificial intelligent methods in production costs estimation // Proceedings of the 15th international conference "Mechanika 2010", 2010 April 8-9, Kaunas, Lithuania / Kaunas University of Technology, Lithuanian Academy of Science, IFTOMM National Committee of Lithuania, Baltic Association of Mechanical Engineering. – Kaunas: Technologija, 2010. ISSN 1822-2951. p. 112-115.
2. **Kohonen Teuvo.** Self- Organizing Maps. 3rd edition. - Springer, 2001. - 501p.
3. **Паклин Н. Б., Орешков В. И.** Бизнес-аналитика: от данных к знаниям. – СПб.: Питер, 2009. ISBN 978-5-49807-257-9.

Proceedings of 5th International Workshop ITELMS'2010

Study of Nanodot Structure Fabrication While Using Au/Cr Self-Assembled Clusters as an Etch Mask

R. Kaliasas, M. Mikolajunas, D. Virzonis

Faculty of Technologies, Kaunas University of Technology Panevezys Institute Daukanto str. 12, LT-35212 Panevezys, Lithuania, e-mail: remigijus.kaliasas@ktu.lt; marius.mikolajunas@ktu.lt; darius.virzonis@ktu.lt

Abstract

Nanodot and nanopillar structures are of great interest to the common nanoelectronic devices, such as photonic crystals and surface plasmon resonance instruments. During the fabrication proceses of the nanodot structures, self-organized clusters of the gold and cromium species were deposited to serve as etch masks for etching the features down to the substrate. Then reactive ion etching (RIE) was used to form the nanopillars. The feasibility of this technology was investigated in terms of achievable etching aspect ratio with different etching regimes and gas mixtures.
KEY WORDS: *nanodot, sef-assembled, Au/Cr clusters.*

1. Introduction

Quantum heterostructures, such as nanodots, nanovires and nanopillars are of particular interest to photonics, photovoltaics and photocatalysis. Generally this interest is determined by the possibility of photo-active surface modification, enabling fine-tuning and justification of physical properties. Applicability and photoactivity of these heterostructures depend on the material which they are made of, physical properties of surrounding medium and geometrical dimensions of the structures. Vertically organized nanopillars are the most common structures in photoactive devices due their favorable orientation [1-5]. There are several physical characteristics of the nanopillars which can influence the photoactivity positively: a) increased area and light absorption ability of the photoactive surface; b) bandgap variations those different for bulk and nanostructured material; c) periodicity of the structure, enabling surface plasmon resonance effects. Diameter, periodicity and height of the pillars can be varied as is generally known in the art in order to form a device that can couple with light of a specific wavelength or specified wavelength range. State of the art techniques of periodic nanostructures fabrication are electron beam lithography and focused ion beam milling with the possibility of nanoimprint templates fabrication. However, practical applications are requiring more productivity and cost-efficiency of the fabrication process. Therefore variety of nanostructuring methods based on the bottom-up nanostructuring approach, such as self-organizing masks and templates are being researched. Nanosphere lithography [6-9] and anodized aluminum templates [3, 9, 10] are the predominant techniques. However, due the low controllability of the mask or template fabrication processes, these approaches still limit minimum size of the fabricated features at values more than 50 nm, which is still large if compared even with contemporary photolithography capabilities [11] and limit induction of quantum effects such as surface plasmon resonance at shorter wavelengths. Self-organized cluster fabrication and application as an etch masks is another alternative for the nanopillar fabrication and has a potential of masking the areas of less than 10 nm [12]. However, self-organized clusters of that dimension range suffer from stability issues, which require additional research [13]. Sub-monolayers of titanium and chromium are widely used to improve metal nanocluster adhesion [14]. However, since the chromium and titanium produce chemical bonds with silicon and silicon dioxide, they tend to form monolayers even at very low equivalent thickness [15]. Method of combining two metals of different adhesion/coalescence properties to form metal nanoclusters of improved stability is described by V. Ovchinnikov, A. Malining et. al. [4, 5]. Authors report few nanometer gold/chromium film depositions, followed by rapid thermal annealing to produce well organized gold-chromium nanodot masks for RIE silicon nanopillar fabrication. However this research was limited by comparatively large structures (tens and hundreds of nanometers) fabrication, presumably due the lack of well established deposition control. Limiting factor for successful nanopillar RIE etching when fabricated Au/Cr agglomerates are used as an etch mask, is sputtering away of the agglomerates during the etch process by accelerated atoms and ions, and this is critical in the case of few nanometer sized agglomerates. However, etching recipes can be specifically tuned to preserve the etch mask long enough to etch the nanopillars of required aspect ratio. Therefore we aimed our research as follows: a) explore the limitations of gold/chromium agglomeration and masking properties in the range of ten and less nanometers; b) improve etching recipes for nanopillar dimensions of 10 nm and less; c) explore periodicity and lateral size repeatability of fabricated nanopillars.

2. Experiment

Gold and chromium thin films were deposited in sequence by the electron beam evaporation in AVAC HVC600 at 3e-7 mBar base pressure without interrupting the vacuum. Single crystal boron doped silicon (100) substrates underwent full standard cleaning procedure (10 min in H_2O_2:NH_4OH:H_2O at 80 °C, 30 s HF dip, 10 min in

H_2O_2:HCL:H_2O at 80 °C) just before placing them to the deposition tool. Quarz crystal microbalance deposition monitoring system with resolution of 0.1 nm was used to control the deposition.

The next sample preparation step was the rapid thermal annealing (RTA), done in STEAG SHS 100M tool. Samples were heated at 900 °C in the nitrogen atmosphere for 5 s with additional 1 s temperature ramping time.

Prepared samples were evaluated by the scanning electron microscopy (SEM, Raith e-LiNe) and scanning probe microscopy (Nanosurf EasyScan 2). During SEM examination of nanopillars, samples were tilted at 70 degrees to the horizontal line. Statistical evaluation of the agglomerates size distribution was done by applying circular measurement model to each of the agglomerate visible in the SEM image. Each case was measured in 1×1 μm region of the interest.

Pillars were etched with parallel plate 300 mm diameter Advanced Vacuum Vission 320-RIE reactor with 13.56 MHz radio frequency (RF). Flow rates of etch gases, RF power and chamber pressure were stabilized during process. An anisotropic etching process based on CF_4 gases was used for silicon etching. The etching experiments were performed at a flow rate of 30 sccm and a pressure of 10–100 mTorr. The RF power was varied from 70 W, which included a self-bias on the cathode of -190 V, to 150 W (self-bias -310 V).

3. Results and Discussion

It was prepared four samples with different thickness, where the Au and Cr coatings were respectively in 1.3 nm, 1.0 nm, 0.5 nm and 0.3 nm.

Fig. 1 shows SEM and AFM images of a samples surface after annealing. Obviously that after annealing on the surface formed chaotic arrangement of particles. Observed in various diameters conglomerates.

Fig. 2 shows distribution of Au/Cr islands size dependence of coating thickness.

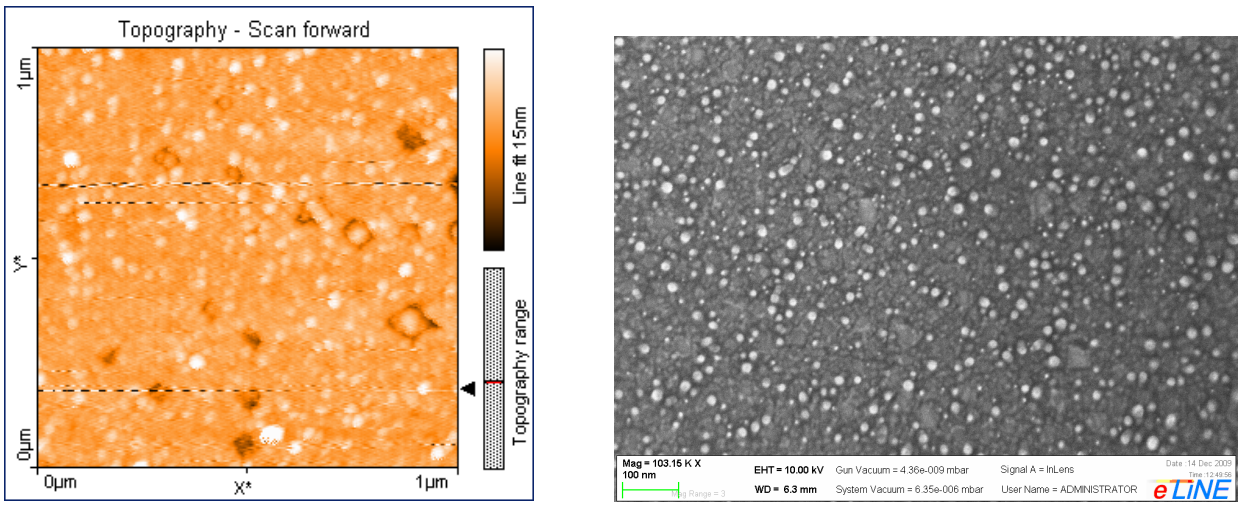

a b

Fig. 1. AFM (a) and SEM (b) images of gold-chromium particles prepared from film with thickness: Au – 1.3 nm and Cr – 1.3 nm

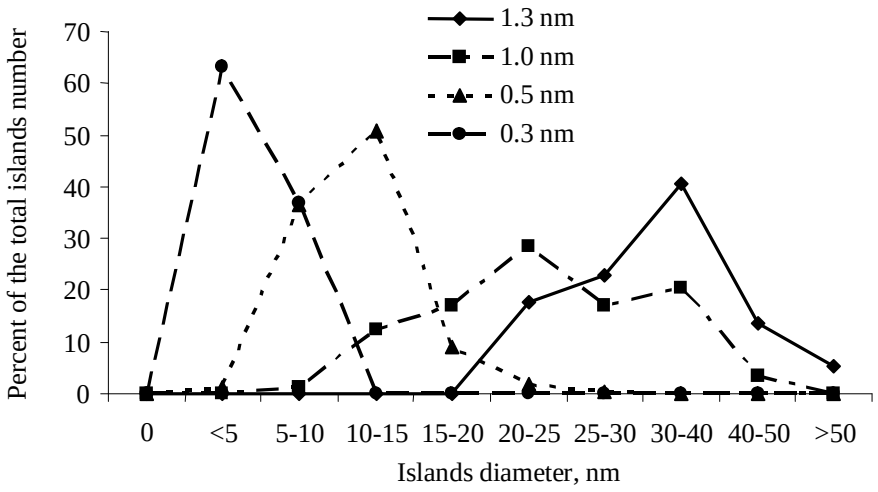

Fig. 2. Size distribution of gold-chromium islands

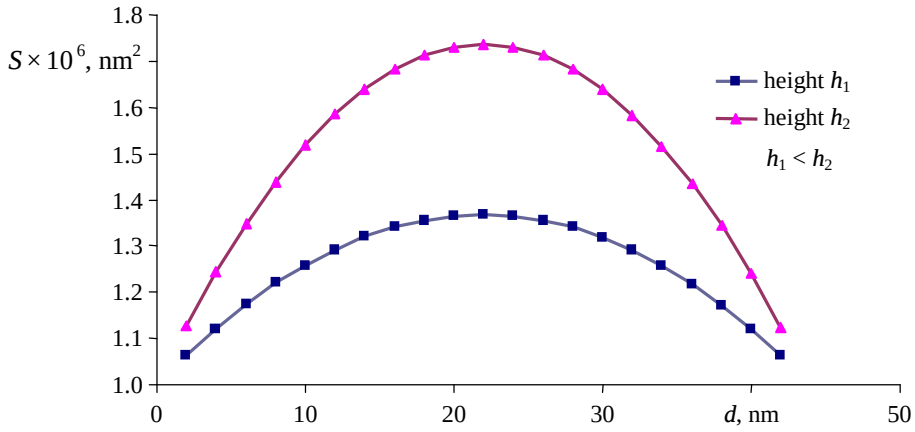

Fig. 3. Usable area dependence on islands diameter

As shown in Fig. 2, the thicker films produce the bigger islands. We observe that 0.5 and 0.3 Au/Cr film cases give better repeatability of the lateral dimensions of agglomerates, which are of 11 nm ±4 nm in the case of 0.5 nm and 5 nm ± 2.5 nm in the case of 0.3 nm (evaluated as mean ± |standard deviation|).

As can be seen from Fig.2, there exists Gaussian distribution. This distribution allowed make a mathematical model for find most useful surface. It is assumed that the etching formed a high cylindrical columns. Dependence of usable area per square micrometer, on diameter of islands at different column heights, shown in Fig. 3.

As shown in Fig. 3 the maximum of usable area we get when diameter of columns will be equal to 22 nm. It is logical that the higher the column height the usable area is greater. However, the column height can only be a certain size, because etching with RIE are a large agglomerates (islands) erosion.

All samples for the erosion experiments were prepared from one 4“ with 1,0 nm Au/Cr film thickness wafer and were etched during 5 and 10 min.. We found etching pressure and plasma power affecting erosion level at most. Results of erosion level investigation are shown in the Fig. 4.

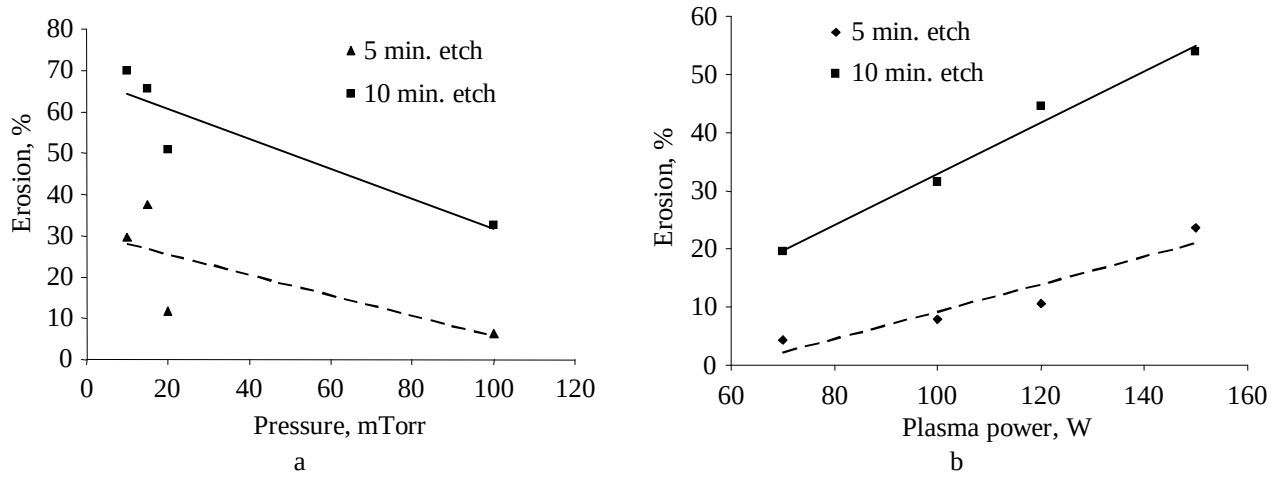

Fig. 4. Agglomerate islands erosion investigation; a – erosion dependence on the etching pressure (plasma power 150 W); b – erosion dependence on the plasma power (pressure 20 mTorr)

It is well-known that CF_4 gas allows anisotropic silicon etching [8, 9], related to polymer deposition on the sidewalls of the pillars, which inhibit undercut of the mask. However, the anisotropic etching depends on the pressure, the plasma power and flow rate of gas, too. The SEM images of the samples after RIE are shown in Fig. 5. As can be seen from the SEM micrographs, there are three different pillar shapes: straight sidewalls, conical and overcutting.

4. Conclusions

1.3, 1.0, 0.5 and 0.3 nm thick Au/Cr film samples were deposited, and agglomerates of correspondingly decreasing dimensions were found in all cases except of 0.3 nm film, which was evaluated to have lower-than-boundary conditions for agglomeration. By controlling the pressure, plasma power and gas flow can be formed in different nanopillar. Highly anisotropic etching was achived, when using CF_4 plasma, thus resulting in 10 nm and sub-10 nm nanopillars with 1:10 aspect ratio.

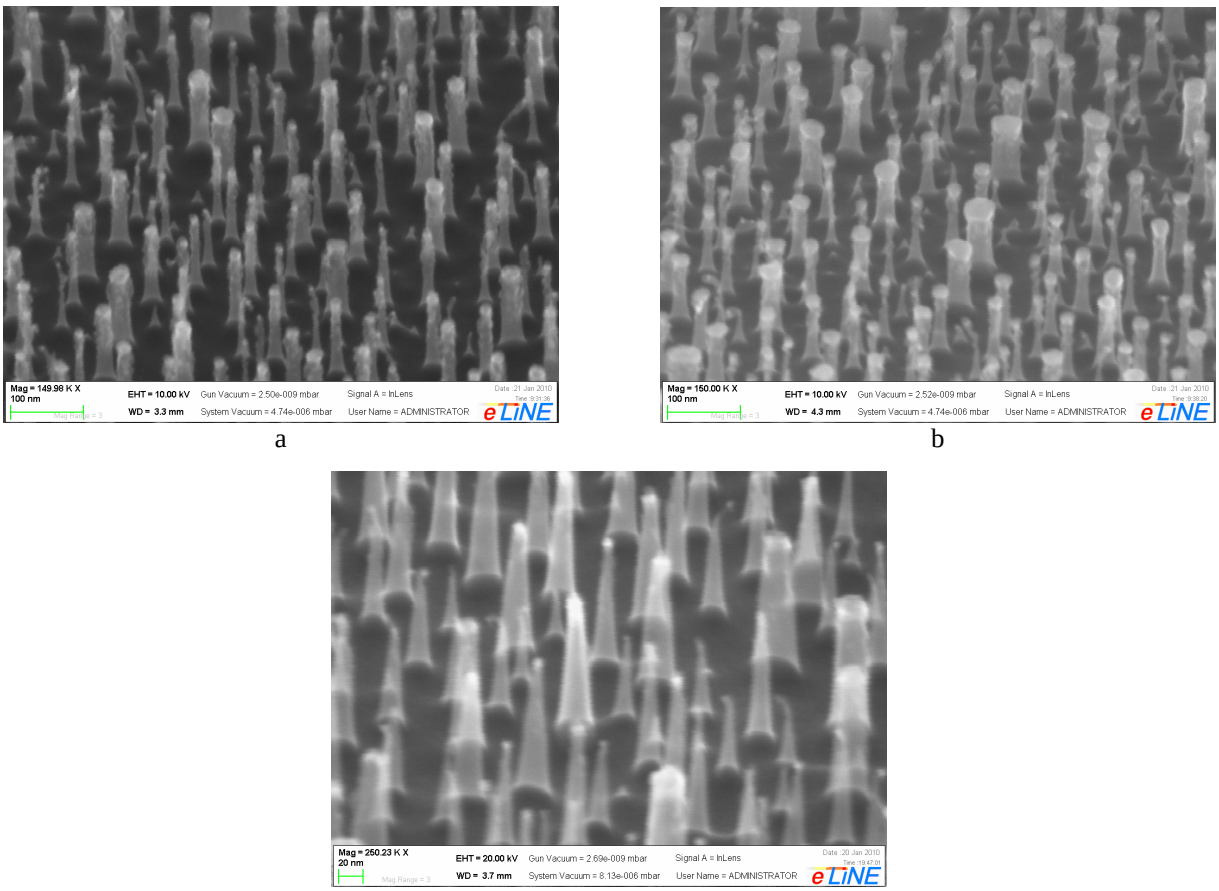

5 Fig. Different pillar shapes obtained after RIE through gold– chromium mask: a – straight walls; b – overcutting; c – cones. Tilt angle 70°. Etching time 10 min

References

1. **Fan Z., Ruebusch D. J., Rathore A. A., Kapadia R., Ergen O., Leu P. W., Javey A.** Nano Res. 2/11 (2009) 829.
2. **Dong X., Tao J., Li Y., Zhu H.** Applied Surface Science 256/8 2532.
3. **Fan Z., Razavi H., Do J.-W., Moriwaki A., Ergen O., Chueh Y.-L., Leu P. W., Ho J. C., Takahashi T., Reichertz L. A., Neale S., Yu K., Wu M., Ager J. W., Javey A.** Nat Mater 8/8 (2009) 648.
4. **Malinin A., Ovchinnikov V., Novikov S., Tuovinen C., Hovinen A.** Materials Science and Engineering B 74/1-3 (2000) 32.
5. **Ovchinnikov V., Malinin A., Novikov S., Tuovinen C.** Materials Science and Engineering B 69-70 (2000) 459.
6. **Xu H., Lu N., Qi D., Gao L., Hao J., Wang Y., Chi L.** Microelectronic Engineering 86/4-6 850.
7. **Gang Z., Dayang W.** Chemistry - An Asian Journal 4/2 (2009) 236.
8. **Kang Y. H., Oh S. S., Kim Y.-S., Choi C.-G.** Microelectronic Engineering 87/2 125.
9. **Krishna M. G., Kumar P., Waqar A., Mark J. J.** Emerging Nanotechnologies for Manufacturing, William Andrew Publishing, Boston, p. 93.
10. **Rahman S., Yang H.** Nano Letters 3/4 (2003) 439.
11. **Holmes J. S., Mitchell H. P., Hakey C. M.** Manufacturing with DUV lithography : Optical lithography, International Business Machines, Armonk, NY, ETATS-UNIS, 1997.
12. **Lee T., Liu J., Chen N.-P., Andres R. P., Janes D. B., Reifenberger R.** Journal of Nanoparticle Research 2/4 (2000) 345.
13. **Morris J. E., Rudraraju N.** High Density packaging and Microsystem Integration, 2007. HDP '07. International Symposium on, 2007, p. 1.
14. **Sexton B. A., Feltis B. N., Davis T. J.** Sensors and Actuators A: Physical 141/2 (2008) 471.
15. **Jukna T., Baltrusaitis J., Sinkevicius V., Virzonis D.** Thin Solid Films 516/10 (2008) 2943.

Proceedings of 5th International Workshop ITELMS'2010

Moisture Motion Kinetics in Concrete

J. Kaupienė, T. Pakėnaitė, M. Navardauskaitė

Kaunas University of Technology, Daukanto str. 12, 44556, Panevėžys, Lithuania, E-mail: jovita.kaupiene@ktu.lt; eddelwise@gmail.com; unreal196@gmail.com

Abstract

The paper presents an investigation of water absorption and content in concrete cubes, it‘s dependence on composition of concrete, methods of moisture measurement in concrete, concrete‘s protection from moisture.
KEY WORDS: *concrete, moisture, motion, porosity, protection, waterproofing, structure.*

1. Introduction

Experience of building construction and exploitation, field and laboratory tests shows that gradual decay of constructions and materials depends on moisture affection and temperature variation. Most difficult to assess and mostly connected with stability of building parts is environmental moisture affection.

Concrete is the material, obtained by mixing cement, large and small aggregate and water together. Also there could be added additives, if needed [3]. Concrete's necessary characteristics are formed during cement's hydration. Physical and mechanical properties of concrete depend on many factors. One of them is the concrete's structure. It constantly changes over time and is divided into few levels: sub-microstructure, microstructure, meso-structure, macrostructure, mega-structure. In sub-microstructure's level, while cement hardens, chemical and physical processes are going on. Microstructure is a level of cement structure. Macrostructure is a level of fine part structure. Mega-structure is a level of large aggregates in concrete [4].

Since structure of concrete pores changes during cement's hydration, it could be said that it affects processes of adsorption and desorption. In moisture adsorption from the environment, liquid, which is exposed by capillary pressure forces, falls into micro-cracks.

2. Moisture Measurement in Concrete

Moisture in concrete is measured by various methods, using various measuring instruments. Equipment must be enough stable and accurate, correspond to other requirements.

1. The gravimetric method

The most accurate measurement is the gravimetric method. Samples are removed from the investigated body and weighed in the moist state, dried and weighed in the dry state. Data tables are filled with the information and moisture is calculated.

However, it is not always possible to take undisturbed samples, so usage of this method is limited [1].

2. Measurement of dielectric constant

Water's dielectric constant is measured by the capacitance of a capacitor embedded in concrete. For this measurement bridge and oscillatory circuits are used. There are high frequencies for measurements in concrete recommended, because of the dielectric losses. Usage of high frequencies keeps dielectric losses small. Frequency must be permanent. Also the direct contact between the electrodes and the concrete has to be avoided (they can be covered with the conductive rubber).

Dissolved salts have no substantial influence on dielectric constant, but binding energy of adsorbed water has.

In connection with capacitance measurements it has to be noted that moisture layers parallel to the capacitor electrode surfaces produce erroneous measurements [1].

3. Measurement of electric conductivity

While measuring electrical conductivity it is not recommended to put electrodes directly on the concrete, because the transfer resistance between the concrete and electrodes may occur. So reference bodies are used those, which equilibrium moisture adjust to the surrounding concrete: gypsum, mortar, glass fiber cloth, ceramic. Glass fiber cloth and ceramics are suitable for long time measurements, because they don't change under the influence of water.

There are ions, arising from dissolved salts, whose concentration may undergo changes and could be hard to determine, so, when using contact sensors it is needed to consider the danger of an additional, undesired conductivity.

In order to sensor will not have direct contact with the concrete, they are positioned into hollow spaces within the concrete body. In these spaces the moisture content adjusts to prevailing air humidity [1].

4. Measurement of microwave absorption

This is a relatively sensitive method, but some difficulties while measuring concrete may occur, because electromagnetic waves partially depend on outer concrete body surface. If the specimen is encased in the form or insulation material, the moisture, that form or insulator contain, is added to the measurement.

At lower frequencies, dissolved salts cause an additional adsorption [1].

5. Measurement of microwave resonance frequency

The resonance frequency in a cavity resonator depends on the dielectric constant, which depends on the moisture content. This method has a high accuracy [1].

6. Measurement of thermalized neutrons

This method is considered as the best non-destructive method for determination of water content.

Usually measurements are done on the outer surface of the concrete body. Fast neutrons emitted by a radioactive isotope enter into the concrete test body. By collision with light nuclei, the neutrons lose their kinetic energy. Detector, which registers only thermal neutrons, measures an index for the hydrogen concentration and thus the moisture content in the concrete [1].

3. Investigation of Concrete Structure

Concrete's structural characteristics can be seen from it's structural indicators. The main structural characteristic is porosity. Concrete's structural characteristics are: effective porosity, total porosity, porous space reserve, relative pore and capillary wall thickness, structural singleness distortion rate. Effective porosity describes the pore cavity, which during the test is filled with water. Total porosity describes the pore and capillary cavity in specimen. Porous space reserve is the space, which is not filled with water in the beginning, but during the test slowly fills in [2].

Compositions of concrete cubes tested in laboratory, are presented in Table 1.

Table 1

The composition of investigated concrete cubes

Materials	Units	Content in 1m^3 of concrete mixture		
		C25/30 (D1 series)	C35/45 (D2 series)	C/35/45 (D3series)
Content of cement	kg	366	457	457
Content of water	l	205	160	160
Content of dolomite aggregate	kg	1171	1157	1157
Content of sand	kg	601	656,14	656,14
V/C	-	0,56	0,35	0,36
Flormix plasticizer	ml	-	-	90
Mobility	mm	7 (S2)	-	9 (S2)
Vebe rate	s	-	32 (V0)	-

Concrete cubes were hardened in accordance with the requirements, specified in LST EN 12390-2:2003. 28 days cubes were kept in water in constant temperature. After 28 days, compressive strength of concrete was measured. Measured values were: D1 series – 32.43 MPa, D2 series – 43.28 MPa, D3 series – 45.62 MPa.

For measuring water penetration into concrete cubes a following system was constructed. There was a vessel, where dry and weighed before cubes were placed in. After that, the vessel was closed, air from it was taken out and vacuum created. Cubes were left in vacuum for an hour and then water was made to flow into the vessel, until it reached concrete surface from the below or until cubes were all in the water, that depended on the test, that was made. After some time vessel was opened and cubes weighed in the moist state. Also there were made similar tests, just not in the vacuum, but in the natural conditions.

After tests concrete's structural indicators were calculated according to the following formulas [2]:

$$W_E = \frac{m_0}{V} = \frac{m_1 - m_0}{m_0} \cdot 100\%; \qquad W_R = \frac{m_0}{V} \cdot \frac{m_4 - m_0}{m_0} \cdot 100\%;$$

$$R = \left(1 - \frac{W_E}{W_R}\right) \cdot 100\%; \qquad D = \frac{100 - W_R}{W_R} \cdot 100\%; \qquad N = \frac{h_{max} - h_{min}}{h_{min}}$$

where: W_E – effective porosity, %; W_R – total porosity, %; R – porous space reserve, %; D – relative pore and capillary wall thickness, %; m_0 – weight of dry specimen, g; m_1 – weight of moist specimen, soaked in natural conditions, g; m_4 – weight of moist specimen, soaked in vacuum, g; V – volume of specimen, determined after test of absorption in vacuum, cm^3; h_{max} – maximum value of moisture capillary rise, mm; h_{min} – minimum value of moisture capillary rise, mm.

Calculated values of structural indicators are shown in Fig. 1.

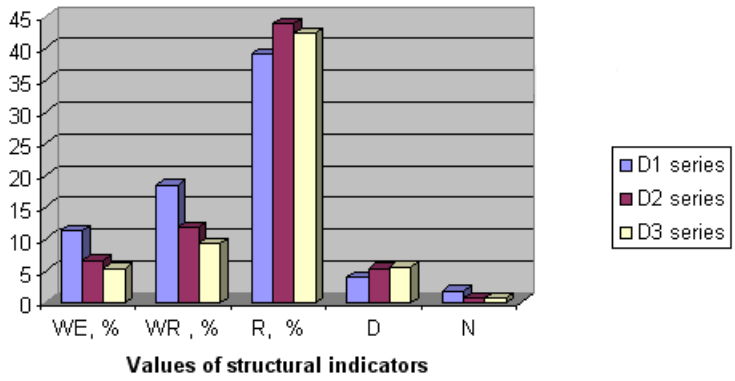

Fig. 1. Values of structural indicators of investigated concrete cubes

4. Concrete's Protection from Moisture

Concrete is leaking because of capillary, cracks and cavity. Also, conduction channels may appear, because of increased loads and heating – freezing cycles during the exploitation period. To waterproof and protect concrete constructions from affection of aggressive chemical materials are used various materials. The main property of those materials is ability to induce the formation of insoluble crystals in pores and capillary of concrete. So concrete became not leaking.

Why is it worth to use materials for waterproofing and protection of concrete?

1. Concrete became not leaking, because crystals of those materials fill in all pores and capillary and there are no places left that water could flow through.
2. Concrete could "breathe". After placing waterproof materials an concrete's surface, there is new structure formed. In this formed structure spaces are too small for water molecules, but big enough to let vapor through. So vapor does not condense and concrete remains dry.
3. Protect reinforcement in concrete. Penetration of water and harmful materials into the concrete is stopped, so reinforcement is protected from corrosion.
4. Concrete became resistant to affection of heating and freezing cycles. In heating and freezing cycles water goes from one state to other, so its volume changes and forces, that disturb concrete, appear. Waterproof materials do not allow water into the concrete, so protects from harmful affection.
5. Increases the compressive strength of concrete.
6. Concrete became resistant to affection of aggressive environment.

5. Conclusions

1. Filling on of the porous space depends on method of water uptake.
2. Usage of plasticizers affects moisture motion in concretes with the same composition, comparing with concrete without them.
3. If effective porosity, total porosity, structural singleness distortion have a maximum values, then porous space reserve and relative pore and capillary wall thickness has minimum values, because in specimens like this there are many big, opened and connected to each other pores and capillary. It depends on composition of concrete – size of large aggregate is the biggest and quantities of components are small.
4. If effective porosity, total porosity, structural singleness distortion have a minimum values, then porous space reserve and relative pore and capillary wall thickness have maximum values, because in specimens like this there is small quantity of small, connected to each other or not, pores and capillary, so hollow cavity of specimen is not big. It also depends on composition of concrete – size of large aggregate is the smallest and quantities of components are bigger.
5. Water has a harmful affection to concrete, so it is recommended to use waterproofing and protecting materials.

References

1. **Hundt J., Buschmann J.** Moisture measurement in concrete.
2. **Nagrockienė D., Žurauskienė R., Mačiulaitis R., Kičaitė A., Ravnialičevas V.** Medžiagų mokslas. Metodikos nurodymai laboratoriniams darbams atlikti. – Vilnius: Technika, 2005. p. 51-56.
3. **Makalauskas M.** Gelžbetoninių gaminių technologija. – Vilnius: Mokslas, 1990. p. 39-43.
4. **Deltuva J., Gailius A., Gumuliauskas A., Kulikauskas L., Malakauskas M., Martynaitis M.** Statybinės medžiagos. – Vilnius: Mokslas, 1982. 219 p.

Proceedings of 5th International Workshop ITELMS'2010

Development of Public Transport and Housing in Lithuania

J. Kaupienė, A. Simonaitytė, R. Stankaitis

Kaunas University of Technology, Daukanto str.12, LT-35212, Panevėžys, Lithuania, E-mail: jovita.kaupiene@ktu.lt; phibi_lost@yahoo.com; remyx_lt@yahoo.com

Abstract

In this work observes historical and cognitive facts of development of public transport and housing in Lithuania that depended on each other and was affected by economical, social factors and landscape. Post-chases were first conveyance used for public and international transport. Later when the communication system became more advanced it was replaced by trains and busses. Nowadays public transport is less popular because of increased individual transport.
KEY WORDS: *housing, house types, villages, public transport, roads, communication.*

1. Intruduction

Knowledge about lodgments, shelters and houses in the territory of Lithuania begins in very old times. Geographical conditions, social structures, and traditions influenced a building type during ages. Buildings were various: over ground (built simply on the ground), log constructions, oval, rectangular, with a different length ant etc. In the center and corners building had balks dug into the ground witch helped to keep stability of the construction. Most of houses had two accommodations and a roof consisted of 2-3 slopes [1]. Settlements were formed and transformed depending on people activities, social and economical conditions, surrounding nature and thickness of residents.

Wars with Teutonic Order negatively affected the development of Lithuanian cities during the 13th – 15th centuries, but it was not stopped absolutely. The major cities such as Vilnius, Kernavė, Kaunas and Merkinė grew up near castles. There lived craftsmen, tradesmen and husbandmen. Since the 16th Vilnius, the capital of The Great Duchy of Lithuania became a crossroad not only between duchy cities, but between abroad cities such Riga (Latvia), Lida (Belarus), Pskov (Russia), Viciebsk (Belarus) and others, too.

Stable trade connections and post-chases had a big importance to a formation of the roads web in Lithuania. The connections between major cities become essential in 16th century by starting to use post-chases for an international consignments from Vilnius and Kaunas to Vienna, Venice and Krakow. Technical roads level was not very high. Construction of land roads were made only by using natural soil without any strengthening elements. Mounds were constructed only in swampy places and a surface of causeways was strengthened with wooden boards. Fords were usual and popular road element during that time. Depending on growth of cities in Lithuania the roads web also became wider. Rail ways and rivers also were used as a part of the public transport in the country. When intensity of the land transport grew up, was decided to find a more modern road construction. Macadam roads solve that problem and influenced a progress of public roads in Lithuania.

2. Houses and Communication in Old Days

According researchers and archeologists first houses in the territory of Lithuania were 7-10 meters of length and 4-6 meters of width. The roof had 2 or 4 slopes. Construction was simple: piles dug into the ground, gaps filled with moss, bark, stones and a roof was made by using reeds, braches and pine barks.

In about 1000 BC husbandry went to upper level and progress of civilization growth began. Harvest was bigger than before; people had more food products and needed to protect them from wild animals and other tribes. They started to live in settlements with a castle built on a mound. Mound was steep and strengthened by using balks, stones and clay. In the middle territory in Lithuania fortress such as castles in Kernavė and Merkinė had rather stronger fortifications (Fig. 1 and 2). Area on the mound was not big enough and houses were built near each other as much as possible. So latter people lent on a base of the mound and extended their living place into one or few new villages. The castle still left as a defense point. There lived husbandmen, warriors, craftsmen. Settlement had its fortifications and entrances [2]. Bigger villages had some sections witch was disjoin by using a street web and walls. It was a rudiment of a city structure [3].

There is not much known about wooden castles, because most of them did not remain till our days. Only mounds left. In the 16th century stone castles were built by Germanic craftsmen. These castles were expensive and required a lot of people not only to build it but defend, too. Medieval castles were strongest fortifications during that time.

To communicate with other tribes Lithuanian progenitors used rivers and sea ways. Pretty good in navigation was Curonian tribe. They even organized retaliatory campaign against North men (Vikings). The fact that Lithuanians used the biggest rivers Nemunas and Nėris for navigation is proved by Pope Innocent IV in his bull written in 1254.

Fig. 1. Kernavė. The reconstruction of King Mindaugas' Throne Castle and Mound according R. Kulikauskienė and architect A. Sazanovas

Fig. 2. Kernavė. Castle and settlement according R. Sidris

As a material for boats and ships Lithuanian tribes used oaks. Rivers did not require big recourses to tend it and it was the faster and safer way to travel, get some food, weapons or other things than using land ways, especially in the spring or autumn when ground was wet.

3. House Types

In the 10th century a primitive Lithuanian house had a place for fire inside. In one side of the house lived people and in other side they kept animals. The house had no windows only small gaps in the wall. Entrance was on the back side. Roof was made of straws, without chimney and had 2-4 slopes. Ceilings were only above the place where people kept fire to protect a roof from sparks. All walls were made of horizontally laid logs. House measurements were about 7×13 meters.

In the 16th century in Lithuania were formed three ethnographical house types: Samogitian, Upper Lithuanian and Suvalkija's houses. Each type came from very old times and had building traditions witch makes them different and interesting [4]. Common for all houses were a furnace made from clay and the main entrance to a house always on the side of the house. As construction materials people used wooden logs and roof was made of straws and canes.

Upper Lithuanian house was called "pirkia" (Fig. 3). A prototype was a small and cramped house with a furnace made of clay inside. Later houses became much bigger and roomy. Upper Lithuanian house had three parts: a porch in the center, living place with the furnace in one side and sitting room in other side of the house. Sitting room

Fig. 3. Upper Lithuanian house

Fig. 4. Samogitian house

Fig. 5. Suvalkija's house

was called “seklyčia“. There people celebrated major events. While rich people had two sides in the house poor people had only one. The porch had not ceiling and it was only way to a loft in the house. Roof was with two slopes. The main entrance and window-blinds was graced with painted flowers, fretworks or some ornaments.

Samogitian houses were massive (Fig. 4) and had various kinds of rooms. The house was called “troba”; it usually had from three to ten rooms. The main different between Samogitian house and others ethnographical types of house is that “troba” had separate accommodations for guests and residents to live and sleep. A working place was on the east part of the house, family rooms on the west part, a porch, kitchen, guest rooms and sitting-room in the middle part of the house.

Suvalkija’s houses (Fig. 5) took some attributes from both Samogitian and Upper Lithuanian houses. House was called “stuba”. A planning of the house was almost the same as in Samogitia. But few things were very interesting. Most of the houses had a distinctive handmade furnace and chimney system. People used this system to smoke-dry meat. Suvalkija’s people were first in Lithuania who started use tiles made from clay to cover up the roof and wooden cleats to batten outside walls.

4. Village Types in Lithuania

Old Lithuanian villages are divided into three groups depending on houses and streets placing:

- *One street villages*. Features: houses situated regularly, with a back side to the only street or road through the village (Fig. 6).
- *Desultory villages*. Features: poor planning-houses situated chaotically, a wide web of small streets or few small streets in and one bigger near the village (Fig. 7).
- *Detached granges*. Features: situated near major roads about few kilometers from each other.

In the beginning only landscape affected formation of new villages. Later more important became social and economical factors.

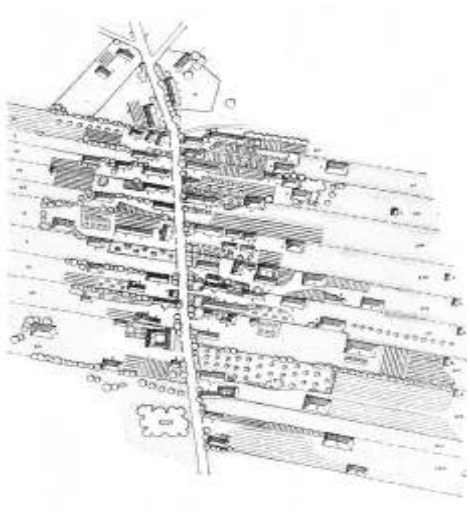

Fig. 6. Planning of one street village

Fig. 7. Planning of desultory village

Desultory villages were formed in the 10th century. These villages were different than primary settlements because they were not situated near mounds or castles. Houses were located freely and people had problems with their territory borders, especially husbandmen, because a tillable plot often crossed neighboring plots. Till the 16th century most of settlements were such as this type. Desultory villages outspread in Suvalkija, Northern Lithuania, Samogitia and other regions during the19th century. Nowadays this kind of villages can be found in Western Lithuania and in the region of Klaipėda.

Villages by one street are known from writings written by scouts of Teutonic Order in the 14th century. Such villages were mostly established in 16th century when agricultural reforms were made in The Great Duchy of Lithuania. In time these villages grew up into bigger ones with more streets.

Detached granges are mentioned from the 13th century, but must of them were established later in the 19th century when Lithuanian agriculture was reformed by government of The Russian Empire [5]. Reforms stopped with the beginning of World War I. The last distribution of villages into detached granges was made in 1922.

5. Development of Towns and Communication

From XVII century town-planning was developed over all country, considering to West Europe models and inciting rectangular plan structures. Usually it was designed a market-square that use to have social importance to community, and there was built a town-hall in the center of it. A square was usually surrounded by cook-shops, taprooms, trading premises and townspeople houses. At the end off XVII century towns and small towns were situated

every 17.4 km. Further development of them was stopped by social disasters such as wars with Russian and Sweden, plague, famine, pillages by foreign soldiery and especially fires that wiped some of the towns out.

Since long-ago towns' growth and development was stimulated by transportation and routes building. In XVI century there has been quite dense network of overland routes in Lithuania already, but the routes have not been surfaced by hard covering yet. The tracks that were used as post ways were the most important routes at those days. Every 15-20 km along a post track there was a wagon, harnessed by 4-6 horses, where were seated up to 15 passengers. In order to guaranty the traffic of passengers and loads there was necessary to keep many horses at the post stations. In 1850 60 horses were kept at the post station in Kaunas, 84 – in Ukmergė, and other stations usually had about 48 horses. According to post traffic system it is known it were took 34.9 thousands passengers over the highroad of Kaunas, 11.1 – over the highroad of Tauragė, 9.1 – over the post track of Ukmergė – Šiauliai and 3.3 – over the post track of Kaunas – Raseiniai – Tauragė.

In XIX century development of towns was impelled by highroads building. At the middle of XIX century there were about 686 km of highroads over all country. It was started to develop the industry that was very increased after railways building. In 1857-1858 it was prepared a project of railway of Daugpilis - Gardinas and Lentvaris - Virbalis, constructions were started in 1858 in Vilnius area. In the first exploiting years the traffic by railway was very small, it was running barely two pairs of passenger trains and a pair of goods trains per day, and the traffic Vilniaus - Varšuva direction was still smaller – two pairs of passenger trains and a pair of goods trains per week.

Excluding broad-gauge lines, at the end of XIX century there was built narrow-gauge lines. Because of smaller overall dimensions of equipment, narrow-gauge lines required simpler specification and less expense. They were being built by arterial lines as access roads to passengers and goods from distant areas.

Train was grave concurrent to overland and waterborne transportation as it was faster, more comfortable, secure and steady for regular transit. As a result after railways building the importance of highroads decreased.

Vilnius and Kaunas (less Šiauliai and Panevėžys) became the industrial centers and the communities of the cities were changing and adapting to the new living conditions. Villages were built up near railway stations (Naujoji Vilnia, Pabradė, Švenčionėliai, Kaišiadorys, Mažeikiai). Old towns (Varniai, Merkinė, Punia, Žiežmariai) that were situated further from arterial traffic declined and transformed into small villages. In 7-10 decades townspeople population increased twice as much. Towns and cities were connected by telegraph and telephone lines, there were electricity supply and sewerage installed. From the times of Czarist Russian occupation living houses were planned and equipped quite primitively, but there was a lack even of such housing after a war. That motivated to provide new housing that were very modest, mostly from wood at first and comfortable, hygienic, good-looking and bricked some time later.

In independence period radical village's reformation was in progress because of economical and cultural increase, advancement and agrarian reform. It was taking care of buildings and granges development and the country was awarded for the models of outhouses and plans of granges. Because of fires and deforestation it was necessary to change wood to incombustible building materials. In 1938 it was prepared a plan of bricked constructions development by V. Juodeika and V. Švilpa but it was built very few buildings until World War II.

During the war it was destroyed over 26500 houses in Lithuania. Because of strong lack of the housing in 1944 it was established building trusts, urbanism and architecture designing offices for rebuilding. In 1955 it was started to produce reinforced concrete slabs and silicate blocks to accelerate constructions in the country. Building materials manufacturing increased and cities' engineering infrastructure such as thermofication, gasification, electrification and water supply was developing.

In 1985 mostly it was building bocks of flats that 75% comprised buildings of large slabs, 21% - bricked walls with sectioned slabs and 4% - monolith of reinforced concrete. Until 1965 blocks of flats were building of 5 floors, and later - of 9, 12, 16 floors. Bricked houses were constructing variously but by typical projects. Initially the flats were very small. Later the layout was improved and it was started to build using blocks-sections.

Large-slabs house was dominating block of flats type that was being built since 1959. It was constantly improved by building on loggias, reorganizing interior structure and plans of flats with larger kitchens, higher rooms and better proportions.

Monolith blocks of flats were being built from 1972 using expanded clay concrete that was pouring into sectional forms. This type of dwelling was usually constructed up to 16 floors designing individual forms.

Blocks of expanded clay concrete slabs were manufactured at the factories of Vievis and Palemonas (in Kaunas), using a large-slabs houses construction system from room-size products. This type of housing was unpopular because of low outside walls heat insulation.

Constructions were controlled by the Soviets. It was urgent to solve a problem of lacking living space; as a result constructions were of quite low quality. It revealed such problems as strong heat wastes and poor esthetical view.

After Independence declaration housing politic in Lithuania was changed. It was refused of market control and started privatization. Duration of intensively exploiting sectioned dwellings was prolonged.

The dominating type of house was block of flats that comprised 80% of living place. After 1990 the Government was prompting individual houses building by exempting private constructions. Individual houses were being built according to past standards and their owners' requests, as a result new buildings were very large and uneconomical – waste of heat was enormous. Because of increase of construction prices and decrease of living conditions to complete many constructions was impossible.

There was big change of constructions after new standards and normative acceptation in 1992. After changed demands of customers bricked dwellings constructions was increased. It was impelling more economy and energy-saving constructions of individual houses for one family and it was decreased capacities and heights in blocks of flats building.

Since 1994 the prices of housing were constantly increasing. Rapid privatization of immovable property and increasing inflation and banks crisis determined that prices of housing grew into nearly 150% to 1999. In 2004 – 2007 constructions were booming and housing market outlived a golden age. Increased economics and incoming of habitants, an entry to European Union, advantageous credit terms conditioned a big jump in immovable property market – the prices increased over 3 times during this period. At the beginning of 2008 the prices tend to decline in all country as a result of world-wide financial crisis. From the highest point in December of 2007 to June of 20098 prices decreased nearly 31.5% and gradually tend to stabilize.

New constructions are organizing differently from the past when it was formatting living areas and building blocks of flats complexes. Currently detached plots are built up by living houses, but it is not considering to free spaces for car parks, playgrounds, preschools and schools territories reserving.

6. Towns' Public Transport

For a long time all exploited transportation was simple wagon pulled by horses. At the beginning of XIX century for people communication and goods transit was using wagonettes teamed by two horses or simple peasants' wagons harnessed by a horse. Richer towns' dwellers were riding by horses or by carriages pulled by two, three or more horses (Fig. 8). That kind of transportation was sufficient while population in towns was not extensive and life was not very intensive.

After railways building it was necessary to organize regular passengers' communication inside towns. In the next half of XIX century growing the towns and expanding the network of transport it was required more improved transportation. In larger cities – Vilnius and Kaunas – it was popular to travel by post-coaches pulled by four horses that could transport up to 10 passengers. The wooden wheels were changed to rubber tyres to make transport faster and reduce the noise.

The next conveyance was omnibus. It was defined rules of the road, the rights and duties of drivers, payment rights, hours of attendance and courses. At the end of XIX century post-coaches and omnibuses were outrivaled by horsy tram, so-called *konkė*. In 1893 there was built about 10 km lines for trams. In 1909 *konkės* were used by over 2.6 millions passengers that means one citizen of Vilnius used it approximately 14 times a year. In 1905 *konkės* conveyed about 1.6 millions passengers in Kaunas city.

The first cars upstarted at the beginning of XX century in Lithuania. In 1905 in VIlnius there was driving few cars already. Starting the 3rd decade there was expanding communication by buses, but their exploiting was very short because of coarse surface of the streets. In 1928 there was coursing only 8 buses in Klaipėda and there was 39 courses of buses in 1931 in Kaunas. Transportation by buses increased when narrow-gauge was liquidated and surface of streets was improved (Fig. 9, 10 and 11).

Fig. 8. A carriage et a street. Vilnius, 1905

Fig. 9. Public tranport. Vilnius, 1935

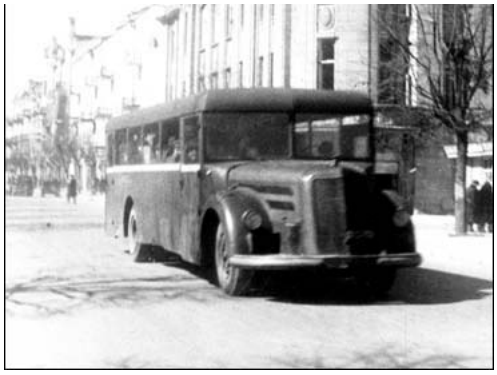

Fig. 10. A passenger bus in Gediminoas prospecte. Vilnius, 1946. A picture of E. Šiškas

Fig. 11. A trolleybus in Žvėrynas area. Vilnius, 1961. A picture of Šestokovas

7. Development of Panevėžys

The city is situated in convenient geographical position where crosses the main country's highroads and international highway *Via Baltica,* that connects two capitals of Baltic States – Vilnius and Ryga, passes by. There are a railway station and two working aerodromes exploiting for local use.

Panevėžys has no worth architectural heritage because of historical circumstances. In established city were dominated wooden constructions and many buildings was destroyed through the years. However the net of the streets is considered to have urbanistic and architectural worth as usable and sensible set.

As well as in many expanding cities air pollution is an issue in Panevėžys. It could be reduced by prompting the use of public transport. However statistics revealed that supply off public transport is decreasing every year.

UAB "Panevėžio autobusų parkas" is a single company providing social conveyance services and conveying about 70% of all citizens of Panevėžys. As a result of increased popularity of individual transport, the amount of passengers is constantly reducing every year – since 1994 it is serviced 16,2% of clients less (Fig. 12). As a result of reduced demand of public transport, the courses of buses were decreased as well. Since 1991 21 courses of buses decreased to 15 (Fig. 13). Economical decline complicated the wrong state of conveyers – since 2009 the work of "Panevėžio autobusų parkas" companys is loss-making.

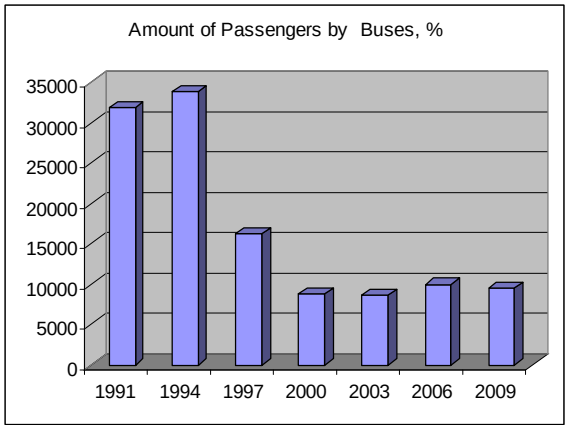

Fig. 12. Passengers of busses decrease

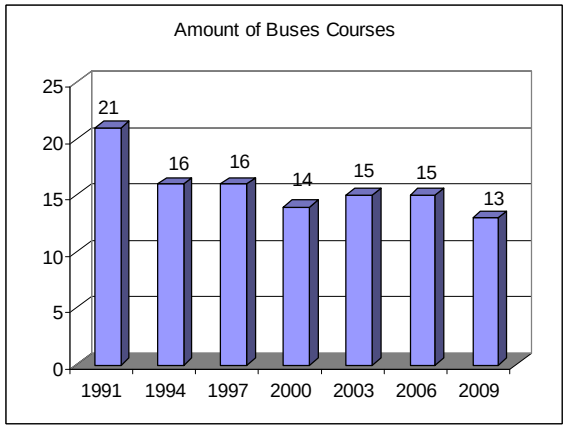

Fig. 13. Reduction of buses courses

8. Conclusions

Heritage of Lithuanian past buildings is not wide and many of buildings were destroyed during the ages. That was a result of expanded wooden constructions and wars. Some of remained buildings are included in the World and Europe cultural heritage lists.

Housing was developing according to ages, social and political circumstances. Entirety of it comprises a nowadays urbanistic face.

Transport and routes developing had important means between towns' communications. During recent decade public transport popularity is decreasing every year.

References

1. **Girininkas A., Kretuonas.** Vidurinis ir vėlyvasis neolitas. Lietuvos archeologija. – Vilnius, 1990, t. 7, 111 p.
2. **Kulikauskienė R.** Ką slepia Kernavės piliakalniai // Mokslas ir gyvenimas, Nr. 3, 1984. 14 p.
3. Publikacija: Vitkūnas J. Kernavė : vadovas po Kernavę ir Kernavės archeologijos ir istorijos muziejų-rezervatą. Kernavė : A Guide to Kernavė and the Museum of Archaeology and History. – Vilnius, 1999. p. 36-37. pav. 28.
4. **Vaitekūnas S.** Lietuvos gyventojai per du tūkstantmečius. Mokslo ir enciklopedijų leidybos institutas. – Vilnius, 2006, 163 p.
5. Tarybų Lietuvos enciklopedija. Kaimas., T. 2 (Grūdas-Marvelės). – Vilnius, Vyriausioji enciklopedijų redakcija, 1986, 170-171 p.
6. **Bertašiūtė R.** Medinė architektūra: išsaugojimo ir plėtros galimybės. Lietuvos muziejai, 2004.
7. **Bertašiūtė R., Vasilaiskaitė V., Žumbakienė G.** Rytų Aukštaitijos tradicinė kaimo architektūra. Vilnius, 2009.
8. **Baublys A., Vasilis Vasiliauskas A.** Transporto infrastruktūra. – Vilnius: Technika, 2005.
9. Lietuvos automobilių kelių direkcijos informacinis leidinys, 2005.
10. **Inytė V.** Pašto karietos. (straipsnis iš "Laikinoji sostinė"), 2008.

Proceedings of 5th International Workshop ITELMS'2010

The Clay Wall – New Way of Ecological Construction

S. Klimanskis, T. Kličius, S. Sušinskas

Kaunas University of Technology, S. Daukanto str. 12, 35212, Panevėžys, Lithuania, E-mail: simonas.klimanskis@stud.ktu.lt; simonas.klimanskis@gmail.com; tomaskliciusr@yahoo.lt; saulius.susinskas@ktu.lt

Abstract

The paper presents a description of use of clay wall and its types in ecological construction. Structure, main integrate materials and way of such construction were described.
KEY WORDS: *clay wall, clay, construct, pounded, swab matter, branch, straw, brick.*

1. Introduction

After bondage cancellation, homestead was dissolving, new constructions became active and requirements for construction materials were rising. In the end of XIX c., clay construction was spreading because of deforestation and the cost of wood had gone up. In most of Lithuania, this type of construction was known and used since the year of dot, especially with the free peasant's and gentleman's homesteads. In the end of XIX c., it became popular in North Lithuania. The clay construction is recommended because it is cheap, ecological, practical and a good match for architectural landscape [6].

In the XX c. and third decade, the clay construction was spreading across all Lithuania. It was determined by relocation of residents and to weave over their traditions with local living and working conditions [4].

Clay as a qualitative construction material was widely used in construction of interior equipment spaces, dirt floors, chimneys, stoves, foundations and walls, as well as in manufacture of bricks [1, 2, 3, 4, 5, 6]. Even in these times, the clay construction is popular. Many tourists arriving to Lithuania like to choose such a rural tour of our homestead, which consists of clay walled house and or clay also being used other parts of the home structure. Moreover, the clay house is very popular among Lithuanian people and they still like to choose this style because of its ecology and economy.

In this paper, the clay wall and its construction technology are described. In conclusions, these walls are generalized briefly in underlining advantages and disadvantages.

2. Clay Wall

In places where there is a lot of clay, it is possible to construct clay walls. Rationally, such walls are sufficiently hygienic.

Many decisions were made in regard to clay wall construction and sofinally, several types of clay wall construction were discovered, such as:

1) pounded clay wall;
2) clay wall with swab matter;
3) clay – branch wall;
4) clay squirted straw wall;
5) unburnt (clay with straw) brick wall;
6) clay wall with wood framework.

2.1. Pounded Clay Wall

By constructing such walls, it is needed to dig the clay, pound it efficiently and use while it is naturally wet. Any clay is suitable for such walls, if it is not too fat or lean. If the clay is too fat, many gaps may emerge in drying the wall. If the clay is too lean, the wall becomes too weak in our conditions for Lithuania.

Usually it is possible to know if the clay is fat or lean. To test the clay, it is need to lay some small brick and dry it. Wide gaps will be in the brick made from fat clay, narrow gaps – from not very fat clay and without gaps will be the brick made from lean clay. When a wet piece of fat clay will be thrown down, it will not break like, for example, rather, like a wet a piece of sand, it will just change its form.

Pounded clay walls are constructing in the following way: hydro isolation layer is paving on the prepared base and the form is to be put on that.

Forms are handmade. They are about 300 mm height. It is made following way: wood poles are for digging during a temporary time at the corners and along the walls, and planks to form walls are to be put from the internal side (see Fig. 1).

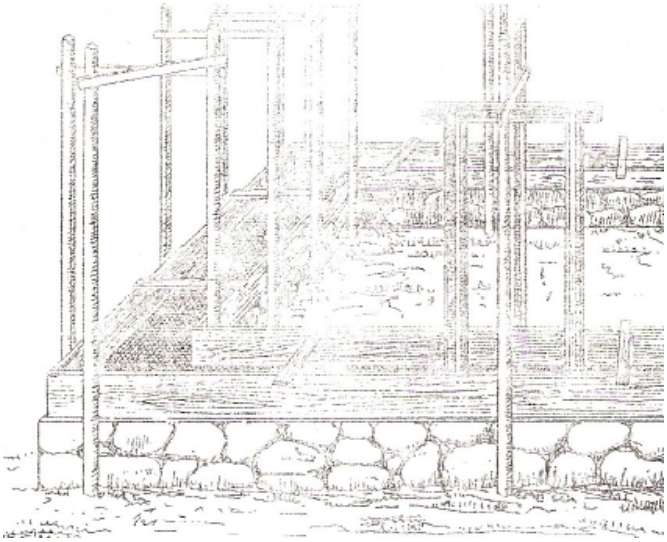

Fig. 1. The handmade form to put clay

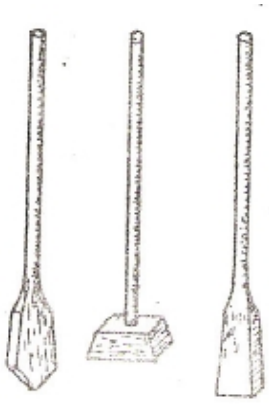

Fig. 2. Pounders: a – to pound main wall volume; b – to pound by form's wall; c – to smooth the surface

When forms are made, clay is dug out (upper layer does not need because it is too dry), and then it is brought to be put to the form. Subsequently, it needs to be pounded with 10 kg weight pounder (see Fig. 1, 2). Clay is pounding in layers of 100 mm weight while the form will be filled (300 mm height).

The clay walls are not constructed in fat layers because of their need for drying. The drying takes 2–3 days, i.e. it is enough time for the bricklayer to come around to all constructing the building. After that, the bricklayer paves next layer (row) and, in same way, continuing his job without break until the constructing of walls will come to an end.
These walls are constructed with an air gap or without it. The air gaps are formed in using wood cartridges, which have been mounted together with forms.

While the work is underway, the walls must be concealed from the rain and so, before night fall and the possible rain, the work must be covered with straw (also, weigh it down for protection from strong wind). Moreover, the walls could be covered with roofing paper and planks.

As it is already understood, the drying clay reduces its volume, for that reason, the walls will subside. Therefore, bricking of window and door openings becomes difficult, as well as processing with burnt bricks of windows and doors that decorates the home and strengthen it. The wall subsides not only because of drying clay but also because of pressure of upper layer.

The horizontal wall pressure in level with the sill and wall plane in places where windows are more and less than in places without it (because of a thicker clay layer pressures here at this point). Because of that reason, the walls between windows like to subside more frequently than under windows. The resulting effects cause gaps to emerge in the wall. Walls that are constructed without any openings may later after the drying process have such openings cut out. On the other hand, such openings can be cut out while the wall is being constructed but will need to be weighted appropriately in comparison with the weight of the wall.

Clay is too weak a material to make arcs over door and window just from it. Therefore, these openings are covered with thick planks or concrete beam (such beams are being used to construct walls from bricks) which endings have been fixed in the wall. If the openings are cut out latter, however, in constructing the walls, it will be needed to put planks at the required height to protect window's openings. In mounting casings, it is important and needed to follow that casing so taht it will not disturb or allow the wall to subside. For that purpose, free space over casings is left to put hard.

The sides of windows and doors are processing with planks that they will be more beautiful and stronger. The side that contacts with the clay wall must be hydro isolated.

The gap left between corners bricked in with burnt bricks and clay walls chinking when the walls have subsided. Otherwise, gaps could emerge between clay and bricks.

It requires a thick wood plank or slab under the endings of ceiling beams that beams the pressure and distribute it to the major area. Brick-balks to support joists fix on the endings of beam (see Fig. 3).

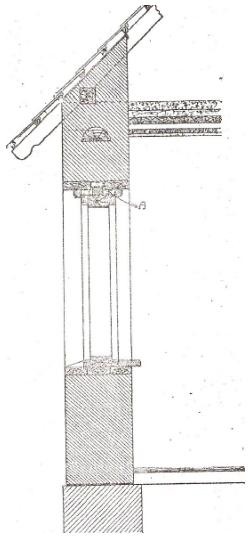

Fig. 3. The layer of clay pounded wall

The vtop of the wall needs to be covered with hydro isolating material, best – roofing paper that water would not dampen the wall. The walls dumped on the top are very disapproving.

Soil can be put on the ceiling and cover the roof, just after one month of waiting since the completion of wall construction.

This time period allows the wall to cure and strengthen. The walls must be saved from the rain by covering with roofing paper or straw while roof has not been constructed.

The clay walls must be dried until freezing temperatures, because if the the walls freeze and gone a cry, they could disintegrate in the time of thawing. Because of that reason, the clay walls should start to be constructed early in spring.

Walls from untrammeled down clay are weak frequently because clay has been dug from various concistinsy.

When it has started to dry in the wall, tensions become unequal.

If clay is without any binding matter, it is processing in following way: it is trampling down, infuse it with water, sometimes, if clay is very fat – sand. The clay is trampling down by horses. For that purpose, the clay is putting to a circular layer, which is 250 mm of thickness and diameter 15 m. One people stands in the center of that layer and encourages horses to run on the clay. The second one waters the material that is trampling down. When the clay is trampled down, it needs to be put into heaps to dry and finally, put to the wall.

For a better processing, the clay is dug and put into heaps of 60 cm of height in autumn. The clay is caching a chill in winter but it becomes fragile in spring.

2.2. Clay Wall with Swab Matter

However processed and unprocessed clay walls are weak and mainly more perviuos to warm. Swab matter, i.e. straw, heath, hard etc, is mixed to clay to eliminate this disadvantage mentioned before. Straw and clay are mixing in trampling down by horses.

For that purpose, on the clay put according to the way mentioned before, is paving a fat layer or straw (about 15–20 kg of straw for 1 m^3 of clay) and is let to walk for horses while the mixture becomes smooth.

In kneading clay, water needs to be squirted from funnel. After that the clay is putting to heaps to eliminate unnesscessary water. Later it is suitable to use.

To save the clay heaps from rain wash, it is recommended to cover with straw and dig a ditch around. It is better to store clay in shed.

In this case, same forms like clay pounded walls are suitable to construct these walls. As well as clay wall with swab matter is pounded.

When swab matter is mixed with clay walls become warmer and stronger.

It is reccommeded to construct walls of 60 cm weight for a normal living house.

All other construction parts of this wall are same like clay pounded walls. Therefore, they will not be mentioned. It is important that 1 m^3 of such wall needs 1 m^3 of clay, 15–36 kg of straw or there swab matter. To dig 1 m^3 of clay, to process it and finally, to pound wall take 1.5 work day.

2.3. Clay – Branch Wall

Clay – branch walls, as called, are made from clay and branches.

Any kind of clay can be used but it should be lean enough. The clay can be directly taken from ground if composition is homogeneous. Then it has to be moistened. If extracted clay is heterogeneous it has to be strongly pounded. Some additions like straw and hard are recommended.

Tree branches can be used such as conifer and or timber, especially pine branches. Birch and alder branches are strictly not recommended, that material will rot away.

The best season for cutting is winter. Other seasons are available for preparation then: cutting into smaller pieces – up to 70 cm. The suitable thickness of branch should be not smaller than finger but not bigger than wrist. 1 cubic meter wall requires 0.9 – 1.1 cub m extracted clay and 0.7 – 0.9 cub m branches.

The main walls for living houses are made 60 cm thick; horizontal and vertical air-shafts are included. The same framework displayed in Fig. 1 is used.

Working steps: surface of base is to be formed (usually base is up to 10 cm *wider* than wall), insulated. The triangle prism is laid down, as displayed in Fig. 4.

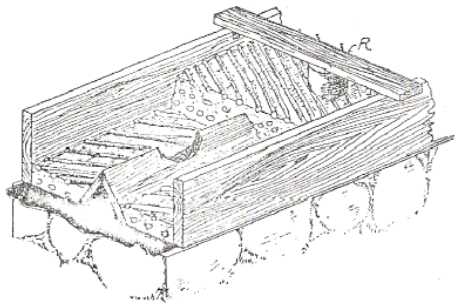

Fig. 4. The base prepared to construct clay-branch wall

Then the planks of the form (mold) are installed. After mold work wall formation is started – first layer of clay is put down, and then pounded. Next layer comes out of branches, then another layer of clay, that is also pounded. During the wall formation vertical air-shafts are being installed – distance between channels is 0.8 – 1.0 m. Vertical channels are connected to the horizontal channel (triangle prism). Sometimes during the formation process beam is installed but later is taken away – this is the alternative for horizontal tubeless air-shaft.

The clay layer between branches layers is about 10 cm thickness; every second layer of branches has to be crossed.

Areas for windows and doors are constructed in same way as described in paragraph 2.1. In space over the windows and doors another air channel has to be done. The upper horizontal air-shaft is connected to chimney, the lower horizontal air-shaft is connected to rooms or basement. Finishing works are made in the same way as described earlier.

These walls dry quickly, subsidence is small. This type has big advantages and is especially suitable for living houses.

2.4 Clay Squirted Straw Wall

Straw are put to wall's types written previously but not more. It has just a promoting significance.

This type of walls is a bit different. Straw is main material and clay is a secondary one, works only as glue. This type is promoted by agriculturalist Krasauskas.

The preparation works are the same as described earlier (see Fig. 1). The main attention is paid to edge reinforcements.

Shaved planks should be used for mold work – then the surface of formed wall will be smooth, weight of the framework will be smaller also.

Preparation work includes making clay consistence ready. For that purpose, two pits are dug. Pits are filled with clay. Water should be added, the mush is being mixed until gets consistence of sour cream. Preparation of clay mush is continuous process – first in one pit, later in other.

When straw is delivered, wall forming is to begin. Straw, best from rye, must be trodden by workers in the molds. The layer of pounded straw is about 10 cm. Then the clay is squirted on straw. After that other layer of straw is added and the process is continued. Eventually the molds have to be lifted.

Straw and fluid clay compose strong structure, no technological pauses are necessary during work.

In the places for windows thick planks are temporary installed – those have to be at least 60 cm wider than window (planks are removed after solidification). About 10 cm space is left for subsidence. Similar technology is for doors – the framework for doors and windows should be done before wall formation.

1 cub m such wall requires 60 – 80 kg straw and about 1/3 cub m clay.

But for the best result it demands plenty of workers simultaneously. So group of 20 workers can build all walls of one average living house.

Usually walls for living houses are 50 – 55 cm thick. If built correctly walls could stand firm and for a long time; those walls are resistant against mice.

2.5. Unburnt (Clay with Straw) Brick Wall

Clay with straw brick is made much bigger than normal burnt brick, for instance, 400×200×150 mm. They are handmade; the same construction site could be area for production as well, it is a good way to avoid long distance of transportation.

The main tool for production is formation box (see Fig. 5). Size of brick depends on size of the formation box.

The material for bricks is the same as for pounded clay walls; sometimes it includes granulated straw or hard.

Production of bricks contains following steps: inside walls of the formation box are moistened and small amount of sand is poured – walls and base of form; clay is added into form; wooden knife is used to form a brick; brick is removed from form.

All bricks are made this way. One side dries a bit, then bricks are turned over and left for drying again. For final drying bricks are piled up into stockpile.

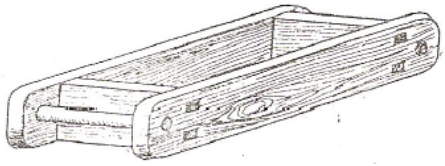

Fig. 5. Form to make unburnt clay brick

The technology of mason work is the same as masonry with burnt bricks. Principles of work are the same. Clay is used as grout, but the layer should be tiny, so wall does not moisten too much. Work with areas for windows and doors are made carefully, similar way as in other technologies for clay walls.

These walls dry quite well and quickly. Usually the process lasts two summers – one is for brick production, other is for masonry. This sort of walls is known as strong and lasting structure; also installation of air-shafts is easy.

Usually thickness of the wall is 50 – 60 cm.

2.6. Clay Wall with Wood Framework

Clay walls with wooden framework need a lot of forest wood but thin balks are enough.

The following deeds are made considering this type of wall: in the beginning thin balks are composed into wall framework – there are big spaces left between balks, that structures a firm circle; then the layer of clayey straw (macerated in fluid clay) is laid down on framework; next layer is again from wooden framework (circle) and so forth. The surface of formed walls has to be tooled and covered with smooth layer of fluid clay. This type of walls is quite strong, stable and cheap.

The wooden framework could be done out of round beams as well then the wall requires two parallel beam rows. Building work is similar as work with simple wooden framework, as seen below (see Fig. 6).

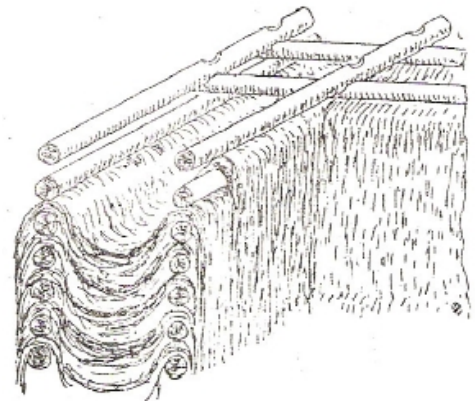

Fig. 6. The fragment of clay wall with wood framework

This technology is usually used in constructing buildings with no heating systems (non living houses), such as barns and sheds. The main framework includes columns, beams, facadee uprights.

If these walls are used in constructing living houses, there must be solid foundation, inside walls that includes vertical columns to hold the ceiling.

Comparing usual wooden walls and clay walls with framework, the second choice is better considering economy, materials, protection against fire, mice.

The alternate materials could be used forming these walls.

3. Conclusions

In this paper, clay wall and its six types were described. Main attention dedicated to the construction technology of this wall. To sum it up, it is possible to say that clay construction could be used alternative in constructing a passive house.

In comparing with modern construction, clay construction seems old-fashioned. However, this construction is based on ecological materials, its economical and is Lithuania's tradition that is has been fostered since the end of XX century and is also interesting to foreigners.

References

1. **Bertašiūtė R., Vasiliauskaitė V., Žumbakienė G., Bortkūnas R., Norvaišaitė N.** Rytų aukštaitijos tradicinė kaimo architektūra. Leidinys. – Vilnius: Etninės kultūros globos tarybos sekretoriatas, 2009. 20–23 p.
2. **Purvinas M.** Mažosios Lietuvos tradicinė kaimo architektūra. Leidinys. – Vilnius: Etninės kultūros globos tarybos sekretoriatas, 2008. 8–35, 37 p.
3. **Bomblauskas J., Burinskaitė I., Žumbakienė G.** Žemaitijos tradicinė kaimo architektūra. Leidinys. – Vilnius: Etninės kultūros globos tarybos sekretoriatas, 2008. 40–41 p.
4. **Kačinskaitė I., Baltrušaitis V., Burinskaitė I., Žumbakienė G.** Suvalkijos (Sūduvos) tradicinė kaimo architektūra. Leidinys. – Vilnius: Etninės kultūros globos tarybos sekretoriatas, 2008. 11, 40–41, 91 p.
5. **Andriušytė A., Baltrušaitis V., Burinskaitė I., Žumbakienė G.** Dzūkijos tradicinė kaimo architektūra. Leidinys. – Vilnius: Etninės kultūros globos tarybos sekretoriatas, 2008. 16–18 p.
6. **Bertašiūtė R., Baltrušaitis V., Burinskaitė I., Žumbakienė G.** Vakarų Aukštaitijos tradicinė kaimo architektūra. Leidinys. – Vilnius: Etninės kultūros globos tarybos sekretoriatas, 2008. 23–24, 90 p.

Proceedings of 5th International Workshop ITELMS'2010

Research on Noise Pollution Emitted by Transportation in Panevėžys

A. Tautkus

Kaunas University of Technology, Klaipedos str. 1, LT-35209 Panevėžys, Lithuania, E-mail: arunas.tautkus@ktu.lt

Abstract

The level of noise pollution, landscape and other nature factors has been changing very fast. During the last decade noise pollution has increased for approximately 0.5 – 1 dB per year and in some towns even for 10 – 12 dB per year. Analysing these changes it is necessary to know that the increase of noise pressure for 10 dB means the double increase for a human [1].

Noise pollution directly influences on human's health as well as on the quality of life and relaxation environment. Many people in towns suffer from noise pollution emitted by transportation. It is the main source of noise and makes 60 – 80 per cent of all noise sources in towns.

Recently the scientists of KTU Panevėžys Institute have made research on noise pollution emitted by transportation in Panevėžys.

KEY WORDS: *transportation, noise pollution, vibration.*

1. Introduction

Transportation as well as industry, municipal economy, energetics is one of the biggest environment polluters. About 40 – 60 per cent of air pollution and up to 80 per cent of noise pollution in the biggest Lithuanian cities comes from transportation. Comparing industry and energetics, transportation has some specific features. The most important are following:

- increasing amount of traffic in towns, countries and resorts;
- big car, as pollution source, concentration in small areas, difficulties limiting traffic;
- transportation is a dynamic pollution source;
- little possibilities to limit the influence on the environment in the nearest future perspectives;
- the road development falling behind the motoring growth.

Most people consider the bad impact on the environment with air pollution, because this problem has been mostly discussed. Big attention is paid to it during technical inspection of vehicles, too. But in many West Europe countries noise pollution is being evaluated during car technical inspection as well. On June 25, 2002 Europe Parliament and Council Board made a directive 2002/49/EB for noise pollution evaluation and management. It is the first document in Europe legally regulating noise pollution. Lithuania had to make responsibilities to reduce noise pollution, too.

A car is a complex noise source, because noise comes from the different car aggregates – engine, wheels, tailpipe, load, road surface. The dependence of noise pollution emitted by transportation from the different factors has been described in Fig. 1.

Analysing noise pollution emitted by traffic flow it is considered that a vehicle is a spot of a noise source, therefore the acoustic characteristics have been estimated during the experiment. The aim of the research is to estimate the noise level in the main crossroads in Panevėžys and to define the main sources of noise as well as to analyse the impact of noise pollution on people and environment and to offer the means of its reduction.

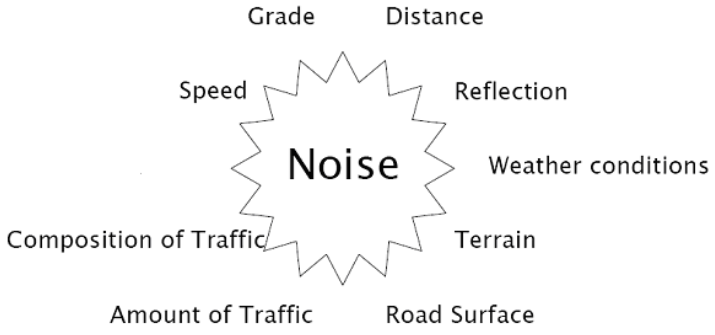

Fig.1. Factors influencing on noise pollution emitted by transportation

2. Noise Pollution and Its Classification. The Influence of Noise Pollution on Health

Noise – is a sound of any kind we hear, but disrupts the balance of human health or creates the obsessive sense of obstruction. Noise can be made of loud as well as of quiet, lower tone sounds. It influence depends on many subjective factors: intonation, health, state, age, and distance from the noise source. All the EU countries use the same classification system of the sources of noise. According to the different human activities all the sources of noise can be put into these main categories:

- road transportation;
- rail transportation;
- air transportation;
- industry;
- civil engineering and constructional activities;
- outside equipments.

The influence of noise pollution on human‘s health can be defined as specific (hearing organ – ear – injury) and unspecific, when other organs are injured. Ear injury caused by noise pollution is called the inflammation of hearing nerve – hearing neuritis or hearing neuropathy. When a human is affected by low unsafe level noise, hearing is being injured slowly and insensibly. Usually seared hearing is noticed only in 10-20 years' time of daily noise affection. In some cases even full deafness can appear. Nerve system is mostly injured – headache, head swim, tiredness, weakness, irritability, insomnia, sensitiveness can appear, consideration and memory can become weaker, neurosis can develop. Noise frustrates, disorganizes working, especially creativity and headwork. Heartbeat can become more rapid and a patient feels heart-failure or pain. Blood pressure increases, blood circulatory becomes weaker especially in limbs, digestive system disimproves. People can become ill hepatic illnesses. Noise affected for a long time can cause many illnesses.

3. Research on Noise Pollution Emitted by Transportation in Panevėžys

In order to estimate the noise level in the crossroads in Panevėžys the noise measurement has been made. The measurement was made in the four biggest crossroads in Panevėžys:

- Basanavičiaus str. – Vilniaus str.;
- Klaipėdos str. – Nemuno str.;
- Nemuno str. – Parko str.;
- Pušaloto str. – S. Kerbedžio str. – Nemuno str. roundabout.

Three day measurements were made at 7.00 – 8.00, at 16.00 – 18.00, and at 19.00 – 20.00 in every crossroad and three measurements in the different crossroad places. The following methodology was used for this measurement: The regulation No.51 of the Economical Commission for Europe of the United Nations - Uniform provisions concerning the approval of motor vehicles having at least four wheels with regard to their noise emissions.

To estimate the reciprocal noise level emitted by transport flow in the crossroads, the measurements were made in the distance of 7.5 m from the first road lane axis and in 1,2 m height from the ground, approximately in the same level as the there is human's ear in the street. In order to avoid noise reflection from the building walls, the measurement was made not less that 1 m from the building facades [2]. The results of the survey were compared with the norms of the Lithuanian Hygiene standard HN 33-2007 [2]. Marginal noise levels *Lday, Levening* were used to estimate the noise cartographer results in the surrounding environment (urban and public areas).

The example of the results of one measurement in one of the main crossroads in Panevėžys - Basanavičiaus str. – Vilniaus str. is shown in Fig.2. This crossroad is in the central part of the town and joins two Lithuanian road arterials A9 and A2.

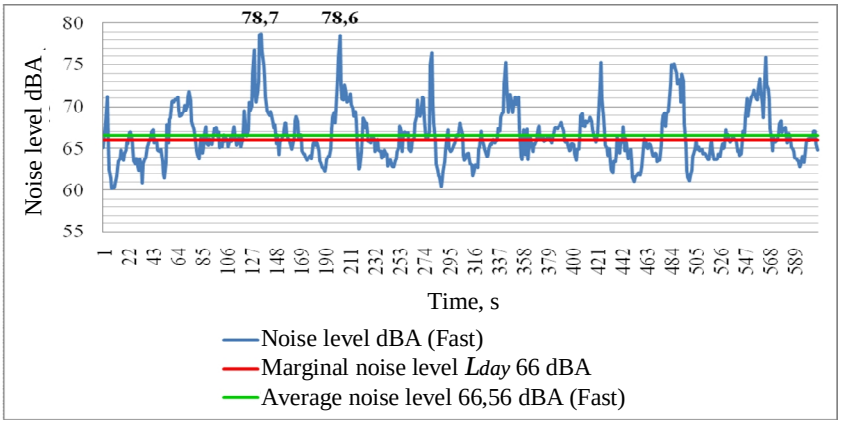

Fig.2. The results of the noise level in the crossroad of Basanavičiaus str. – Vilniaus str. (Friday 7.00)

The noise level was measured in Basanavičiaus str. – Vilniaus str. crossroad on Friday at 7:00. At daytime the reciprocal noise level *Lday* 66 dBA exceeded the hygiene norms HN 33-2007 for 3-12.6 dBA [2]. This exceeded noise norms were made mainly by the public buses with diesel engines. At this time the traffic flow intensity is not big, but the average noise level exceeded the hygiene *Lday* norms for 0,56 dBA.

During the survey the noise level was estimated in all mentioned crossroads of the town. The results are shown in Fig. 3-5. In the given diagrams it can be seen what crossroads are the noisiest at the different time of the day.

The result comparison of the noise level survey in four different crossroads is shown in Fig. 3. According to the diagram it can be seen that the biggest noise level on Tuesday and Friday morning was in the Klaipėdos str. – Nemuno str. crossroad – 71.3 and 72.5 dBA, what exceeded the standard of hygiene norms HN 33: 2007 for 8 per cent.

The results of the noise level survey in four crossroads on Friday and Saturday daytime are shown in Fig. 4 and comparing them with the normative value *Lday* it is seen that they exceed it from 5 to 17 per cent on Friday and from 1 to 4 per cent on Saturday.

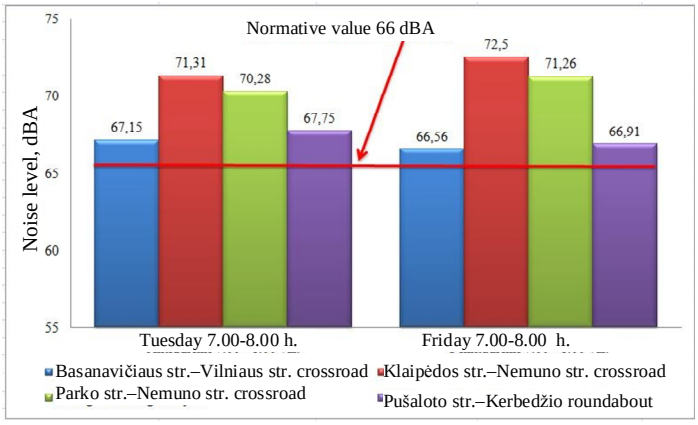

Fig. 3. The results of the noise level in the crossroads in Panevėžys during the morning rush hours on Tuesday and Friday

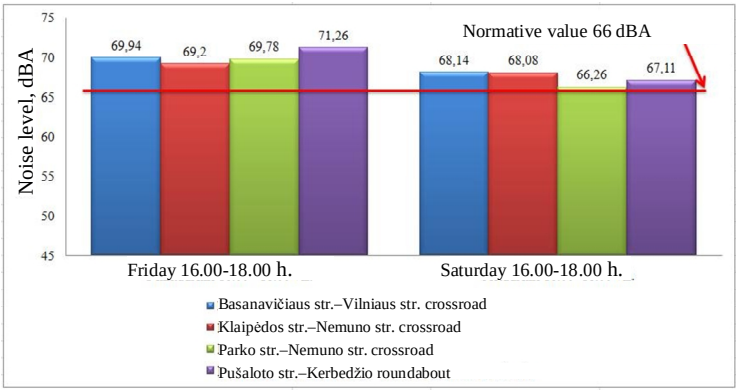

Fig. 4. The results of the noise level in the crossroads in Panevėžys during the evening rush hours on Friday and Saturday

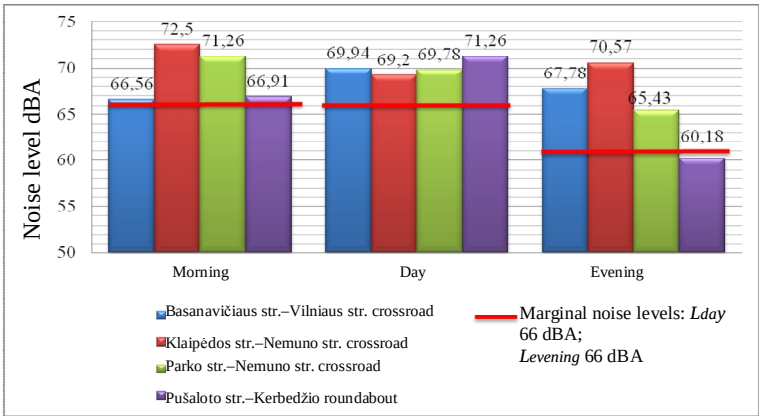

Fig. 5. The results of the noise level in the crossroads in Panevėžys during the daytime

During the daytime (16:00 – 18:00) the noise level in all crossroads is the same. At this time transport flow is the same in all crossroads. A big flow of trucks, lorries, trackers go in Pušaloto str. – S. Kerbedžio str. – Nemuno str. roundabout. They make even bigger noise pollution going on bumpy road surface. In the evening time (19:00 – 20:00) a flow in this roundabout decreases to 250 cars/h, therefore the noise level does not exceed the limitation of hygiene standards.

4. The Means of Noise Reduction

Three possible ways of noise reduction are following:

- reduction of noise level near its source: engine, friction of wheels and road surface;
- separation of noise source from its impact zone by noise-spread barriers;
- reduction of resolved noise in the particular place.

The main means of noise reduction:

- the standards of car pollution and emission;
- planning (for example, to design housing development further from the high level noise zones);
- facility means (noise barriers, tunnels, isolation, etc.);
- operative procedures (speed reduction, usage of quieter equipment, etc.);
- research and new technologies;
- information and teaching [3].

5. Conclusions

1. Having estimated the results of the survey on noise pollution level in four biggest crossroads of Panevėžys it can be claimed that the most polluted crossroads are Basanavičiaus str. – Vilniaus str. and Klaipėdos str. – Nemuno str. The noise level in these crossroads exceeds the noise norms for 8 – 18 per cent.
2. During the survey the noise level has changed from 66.56 to 72.5 dBA in the morning, from 66.26 to 71.26 dBA in the afternoon, and from 60.18 to 71.44 dBA in the evening. Maximum noise level was from 81 to 89 dBA.
3. In order to decrease the noise level some mean should be applied. The most popular and useful are smooth and isolated noise composite walls or screens, often used plantations and dikes, however they cannot be used in the centre of the town, because they restrain the visibility and make road safety problems. The most efficient mean in such crossroads is traffic control – the evaluation of traffic flows and the change of traffic light regulation cycles.
4. Most of the means to decrease the noise cannot be implemented at once, because they need much time and resources.

References

1. **Klibavicius A.** Transporto neigiamo poveikio aplinkai vertinimas: mokomoji knyga. Vilnius: Technika, 2009. 70 p.
2. HN 33:2007. Akustinis triukšmas. Triukšmo ribiniai dydžiai gyvenamuosiuose ir visuomeninės paskirties pastatuose bei ju aplinkoje. Patvirtinta Lietuvos Respublikos sveikatos apsaugos ministro 2007 m. liepos 2 d. įsakymu Nr. V-555. Vilnius, 2007.
3. Handbook of noise and vibration edited by Malcolm J. Crocker. New Jersey : John Wiley & Sons, Inc., 2007, 1569 p.

Proceedings of 5th International Workshop ITELMS'2010

Investigation of Scanning Probe Microscope Electromechanical System Dynamics

I. Morkvėnaitė-Vilkončienė, D. Virzonis

Kaunas University of Technology Panevėžys Institute, Daukanto str. 12, 36212, Panevėžys, Lithuania, E-mail: inga.vilkonciene@ktu.lt; darius.virzonis@ktu.lt

Abstract

In-depth knowledge of scanning probe microscopy (SPM) dynamics is necessary when interpreting obtained images and especially when the sources of artifacts are to be identified. The aim of this research was to build and test the dynamic model of SPM electromechanical system. For simplicity reasons only atomic force microscopy (AFM) contact mode dynamics was explored. Experimental validation of the model has shown the necessity of including additional components to the model description.
KEY WORDS: *scanning microscope, electromechanical system dynamics, model of the cantilever.*

1. Introduction

Atomic force microscopy (AFM) is a class scanning probe microscopy (SPM) and is applied in a variety of surface studies including atomic scale friction [1], elasticity [2] and surface forces [3]. However, this technique is mainly used for high resolution surface topography imaging. The imaging process is based on the AFM tip, having curvature radius of tens to few nanometers, deflection monitoring. The tip deflection is caused by its interaction with the surface; typically imaging is done under conditions that minimize the force between the tip and the surface atoms.

One of the drawbacks of AFM imaging is limited imaging speed, which typically is slower than one frame per several minutes. This is caused by multiple dynamic factors, related to the sensory part of an AFM and also to the data transfer and processing capabilities. Attempts to increase the scanning speed inevitably leads to impaired image quality and dynamic errors-induced artifacts. Moreover, different surface properties require different scanning strategies, which are not obvious until several try and mistake attempts are made. All this still prevents AFM technique from being widely used for quality assurance and parameter control in industry, keeping this technique solely suitable for research.

In this work we aimed creating and exploring the computer model of AFM sensory part and use it to predict limiting factors of selected imaging mode.

2. Description of a Simulink Model

The sensor part of AFM electromechanical system, most affecting the image quality, is subjected by the following forces: cantilever spring force, friction force, inertia and the force of interaction with the sample:

$$F_{inertia} + F_{spring} + F_{friction} = F(z) \tag{1}$$

The simplest approach, which nevertheless leads to a realistic description of most tip movements, is to start with Newton's equation of motion [2, 4]:

$$m\frac{\mathrm{d}^2 z}{\mathrm{d}t^2} + g\,\frac{\mathrm{d}z}{\mathrm{d}t} + kz = F(z) \tag{2}$$

where m – the effective mass of the cantilever; k – the spring constant of the cantilever, and $g = 2\sqrt{k/m}$ – the dissipation term.

Linear second order differential equation is written as [5]:

$$\frac{\mathrm{d}^2 z}{\mathrm{d}t^2} + 2\,x\,w_n\,\frac{\mathrm{d}z}{\mathrm{d}t} + w_n^2\,z = w_n^2\,x \tag{3}$$

where $w_n = \sqrt{k/m}$ is the undamped angular frequency of the cantilever and x is a constant called the damping ratio.

The transfer function of (3) is [5]:

$$\frac{Z(s)}{X(s)} = \frac{w^2{}_n}{s^2 + 2x\ w_n s + w^2{}_n} \tag{4}$$

From (1), (2), (3) and (4), we obtain the transfer function, from which a model of Matlab/Simulink model was created (Fig. 1).

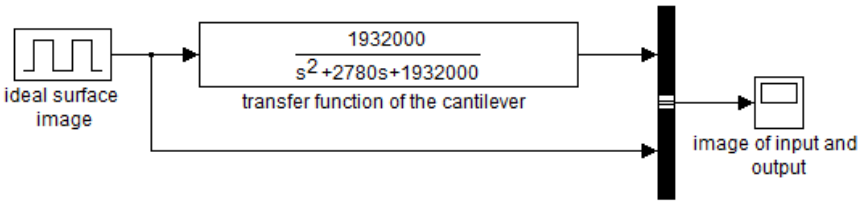

Fig. 1. Simulink model of the cantilever movement

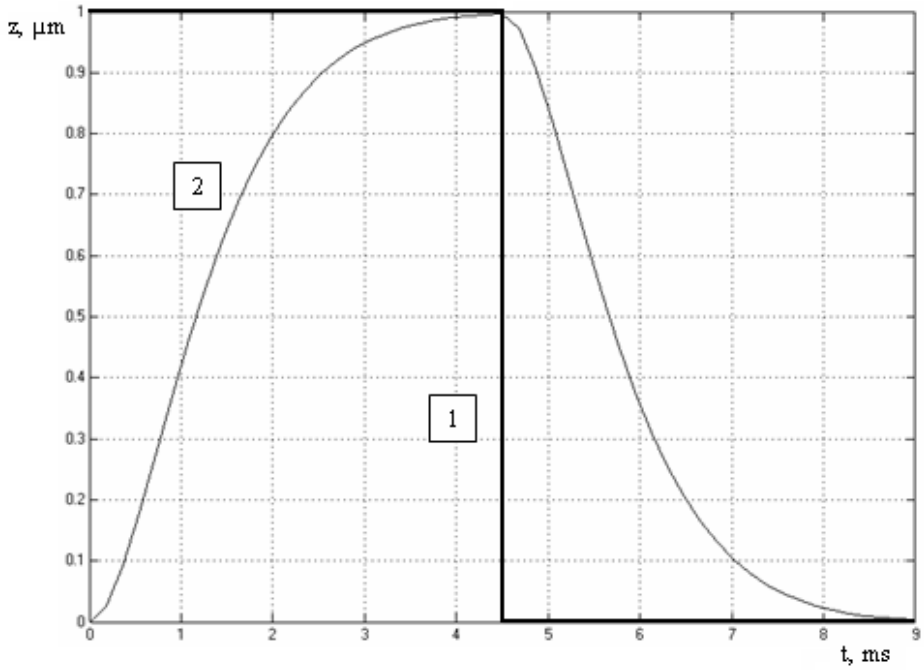

Fig. 2. Simulation of profile scan: 1– ideal surface image, 2 – the obtained image

Rectangular 5 ms 1 µm hight pulses simulate the ideal surface profile. Coefficients were obtained by the manufacturer‘s data available on the Nanosurf EasyScan 2 SPM, working with CONTR cantilever. Coefficients obtained for a contact mode have following values: spring constant k = 0.2 N/m, width, thickness and length: 50 µm, 2 µm and 450 µm. On the Fig. 2 the system output is compared with an input. Dynamic errors can be explicitly observed.

3. Comparision of Experimental Data with Model Output

For experimental validation of developed model we prepared a sample with 1 µm hight periodic (50 µm period) polymer (PMMA) features over the silicon substrate. The features were fabricated using electron beam lithography. Such a features were chosen for maximum controlability and adequacy with simulated conditions. For experiments we choosed the monocrystal silicon cantilever with the tip radius of 10 nm. Cantilever dimensions: width, thickness and length: 50 µm, 2 µm and 450 µm. For better representation of the sensory part dynamics the duration of the single line scan was variated from 0.1 s to 1.5 s with 0.1 s with constant scanning distance of 75 µm. Then the single line scan duration was re-calculated to the scanning speed by dividing scanning distance by the single line scan duration. To obtain additional information about the interaction between the surface and the cantilever tip, contact force was varied from 10 nN to 40 nN in 10 nN increments.

In Fig. 3 the single line scans obtained at 750 µm/s speed within described conditions are shown. It can be observed that higher surface-tip interaction force give more adequate profile of the scan. Decreasing of the interaction causes false information, to be evaluated as artifacts to appear. For example, the valley at 50 – 60 µm is not anymore represented by the scan data, if the tip-surface interaction force is decreased to 10 nN.

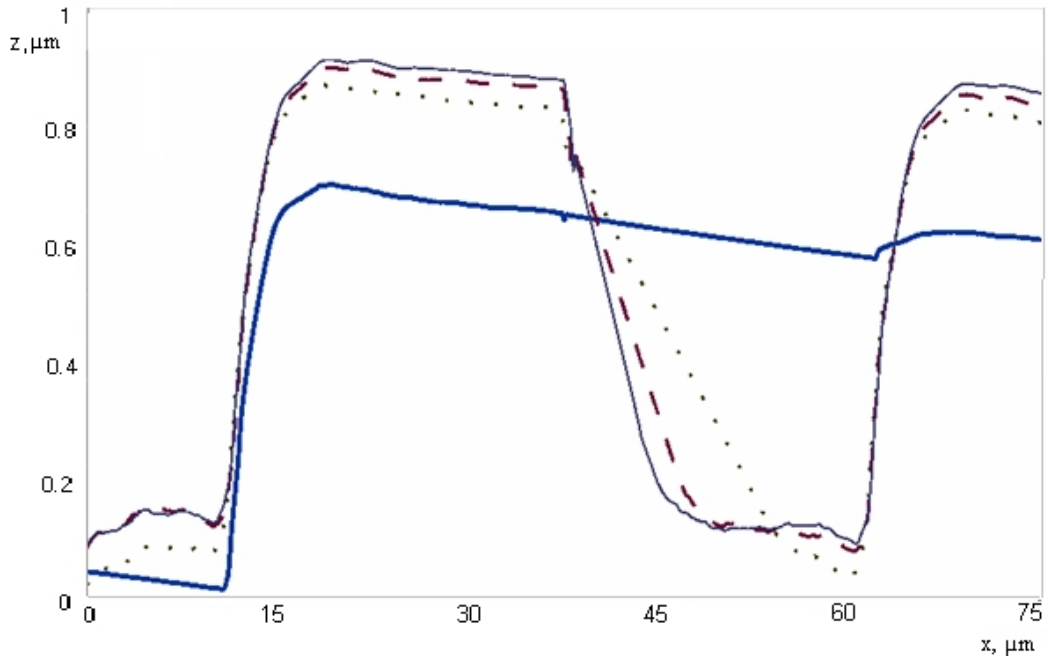

Fig. 3 Single line AFM scan of 1 µm high periodic (50 µm) PMMA structure obtained by 750 µm/s scanning speed and different surface-tip interaction forces. Thick solid line: 10 nN; points: 20 nN; dashed line: 30 nN; thin line: 40 nN.

When compared described experimental data with simulation results presented in Fig. 2, it can be seen that transitional rise to maximum process of 4.5 ms obtained during simulation is not far from the corresponding value obtained experimentally, which can be estimated within the range of 6 to 7 ms.

4. Conclusions

Output of developed Simulink model of the AFM sensory part essentially represents the tip-surface interaction dynamics, which was confirmed by experimental data. However the update of the system model, introducing additional system components such as surface-tip interaction and more detailed sensory part mechanics simulation is needed to make present model more representatives when taking in to account more variables of tip-surface interaction. This is to be done within the next stages of this work.

References

1. **Mate C. M., McClelland G. M., Erlandsson R., Chiang S.** ibid. 59, 1942 (1987).
2. **Butt H. J., Cappella B., Kappl M.** Force measurements with the atomic force microscope: technique, interpretation and applications. Surface Science Reports 59 (2005) 1–152.
3. **Burnham N. A., Colton R. J., Vac J.** Sci. Technol. A7, 2906 (1989).
4. **Sarid D.** Scanning Force Microscopy: With Applications to Electric, Magnetic, and Atomic Forces (Oxford Series in Optical and Imaging Sciences). ISBN-10: 0-19-509204-X. Hardcover, 1994. – 288 p.
5. **Januševičius V. S.** Automatinis valdymas. ISBN: 9955-09-316-1. – Kaunas: Technologija, 2003. – 556 p.

Proceedings of 5th International Workshop ITELMS'2010

Application of Scientific Approaches for Evaluation of Quality of Learning Objects in eQNet Project

E. Kurilovas[1,2], S. Serikoviene[1,3]

[1] Vilnius University, Institute of Mathematics and Informatics, Akademijos str. 4, 08663 Vilnius, Lithuania
2 Vilnius Gediminas Technical University, Saulėtekio av. 11, 10223 Vilnius, Lithuania
3 Kaunas University of Technology, Klaipėdos str. 1, 35209 Panevėžys, Lithuania
e-mail: eugenijus.kurilovas@itc.smm.lt; silvija.serikoviene@gmail.com

Abstract

The paper is aimed to analyse the application of several scientific approaches, methods, and principles for evaluation of quality of learning objects for Mathematics subject. The authors analyse the following approaches to minimise subjectivity level in expert evaluation of the quality of learning objects, namely: (1) principles of multiple criteria decision analysis for identification of quality criteria, (2) technological quality criteria classification principle, (3) fuzzy group decision making theory to obtain evaluation measures, (4) normalisation requirement for criteria weights, and (5) scalarisation method for learning objects quality optimisation. The applied approaches have been used practically for evaluation of learning objects while implementing European Lifelong Learning programme's eQNet project in Lithuanian comprehensive schools in winter and spring 2010.
KEY WORDS: *learning object, multiple criteria decision analysis, optimisation methods, expert evaluation, quality criteria.*

1. Introduction

eQNet is a three-year (September 2009-2012) Comenius Multilateral Network [3] funded under the European Commission's Lifelong Learning programme. The project is coordinated by European Schoolnet (EUN) and involves 9 Ministries of Education or agencies nominated to act of their behalf. The primary aim is to improve the quality of learning objects (LOs) in European Schoolnet's Learning Resource Exchange (LRE) [8] which currently offers almost 130,000 LOs and assets from over 25 providers. As a pan-European service, the LRE particularly seeks to identify LOs that "travel well" (i.e., reusable) across national borders and can be used in a cultural and linguistic context different from the one in which they were created [3].

eQNet will do this by establishing a network consisting of researchers, policy makers and practitioners (teachers) that will develop and apply "travel well" quality criteria to both existing LRE content as well as that to be selected in future from national repositories. The vision driving the LRE is that a significant percentage of high quality LOs developed in different countries, in different languages and to meet the needs of different curricula can be re-used at European level.

eQNet will provide a forum for joint reflection and co-operation related to the exchange and re-use of educational content and allow network members to: (1) better share information and expertise particularly related to "travel well" quality criteria (pedagogical, technical and intellectual property rights (IPR) factors); (2) develop new frameworks to improve the quality of LOs and metadata in both national repositories and the LRE, including the growing volume of user-generated content and metadata, as well as to improve the multilinguality of LRE content as a result of the translation of metadata, making use, where appropriate, of automatic metadata translation approaches and technologies; (3) enable schools to participate in a Community of Practice related to the use LOs at European level.

Major results will include: the development of "travel well" quality criteria to more easily identify LOs with the potential for cross-border use (this work package is coordinated by Lithuanian partner, in particular by the author of the paper); the practical application by teachers of these criteria to >3,500 LOs in the LRE; 'showcases' of the best of these LOs in a "travel well" section of the LRE portal; where necessary, the enrichment of selected LOs with new or better metadata; a Community of Practice for teachers around these LOs [3].

2. Methodology of the Research

One of the main features achieving the high LOs effectiveness and efficiency level is LOs reusability. The need for reusability of LOs has at least three elements: (1) interoperability: LO is interoperable and can be used in different platforms; (2) flexibility in terms of pedagogic situations: LO can fit into a variety of pedagogic situations, and (3) modifiability to suit a particular teacher's or student's needs: LO can be made more appropriate to a pedagogic situation by modifying it to suit a particular teacher's or student's needs [4].

Reusability of LOs (or their ability to "travel well" between different contexts and education systems) is considered by the authors as a part of the overall quality of LOs. This means that any high quality LO has some reusability level (or potential to "travel well"), but this does not mean that any reusable LO is quality one.

The main problem analysed in the paper is how to establish (1) a 'proper' set of LOs "travel well" quality evaluation criteria which should reflect the objective scientific principles of construction a model (criteria tree) for LOs "travel well" quality evaluation, and also (2) a 'proper' method for evaluation of LOs quality.

Expert evaluation is referred here as the multiple criteria evaluation of LOs aimed at selection of the best alternatives (i.e., LOs) based on score-ranking results [6]. If the set of decision alternatives (LOs) is assumed to be predefined, fixed and finite, then the decision problem is to choose the optimal alternative or, maybe, to rank them. But usually the experts have to deal with the problem of optimal decision in the multiple criteria situation where the objectives are often conflicting. In this case, an optimal decision is the one that maximises the expert's utility. These principles of identification of quality evaluation criteria have been analysed in multiple criteria decision analysis (MCDA) theory related research works, e.g., [2].

Evaluation of LOs quality is a typical case where the criteria are conflicting, i.e., LOs could be very qualitative against several criteria, and not qualitative against the other ones, and vice versa. Therefore, the authors propose to use MCDA approach for creation of LOs quality evaluation model and method.

LOs multiple criteria evaluation method is referred here as the experts' additive utility function represented by formula (1) below including LOs evaluation criteria, their ratings (values) and weights [6]. This method is well-known in the theory of optimisation methods and is named "scalarisation method". A possible decision here could be to transform multi-criteria task into one-criterion task obtained by adding all criteria together with their weights. It is valid from the point of view of the optimisation theory, and a special theorem exists for this case [6].

Therefore, here we have the experts' additive utility function:

$$f(X) = \sum_{i=1}^{m} a_i f_i(X); \quad \sum_{i=1}^{m} a_i = 1; \quad a_i > 0 \tag{1}$$

where $f_i(X_j)$ is the rating (i.e., non-fuzzy value) of the criterion i for the each of the examined LOs alternatives X_j. The weights here should be 'normalised' according to the 'normalisation' requirement

$$\sum_{i=1}^{m} a_i = 1; \quad a_i > 0 \tag{2}$$

The major is the meaning of the utility function (1) the better LOs meet the quality requirements in comparison with the ideal (i.e., 100%) quality.

3. Literature Analysis and Research Results

This section is aimed (1) to apply the aforementioned scientific approaches to propose a suitable scientific model and method for evaluation of quality of LOs, and (2) to present experimental evaluation results.

3.1. Learning Objects Quality Evaluation Model

The following principles of identification of quality evaluation criteria are relevant to all MCDA approaches: (1) value relevance; (2) understandability; (3) measurability; (4) non-redundancy; (5) judgmental independence; (6) balancing completeness and conciseness; (7) operationality; (8) simplicity versus complexity [2].

On the other hand, according to the technological quality criteria classification principle, we can divide technological quality criteria into 'internal quality' and 'quality in use' criteria of the educational software such as LOs. 'Internal quality' is a descriptive characteristic that describes the quality of software independently from any particular context of its use, while 'quality in use' is evaluative characteristic of software obtained by making a judgment based on criteria that determine the worthiness of software for a particular project. Any LOs quality evaluation model (set of criteria) should provide the experts (decision makers) the clear instrumentality who (i.e., what kind of experts) should analyse what kind of LOs quality criteria in order to select the best LOs suitable for their needs. According to aforementioned principle, 'internal quality' criteria should be mainly the area of interest of the software engineers, and 'quality in use' criteria should be mostly analysed by the programmers and users taking into account the users' feedback on the usability of software [6].

The authors have applied these two principles in their papers [5], [6] on technological evaluation of the learning software, and thus have identified a number of LOs technological quality evaluation criteria presented in the technological part of the LOs quality evaluation model presented in Fig. 1.

On the other hand, the authors have analysed a number of existing models (sets of quality evaluation criteria) for evaluation of pedagogical quality of LOs, e.g., [1], [7], [9], [10], and [12]. The suitable criteria based on MCDA principles [2] are: (1) interactivity, strong visual structure (animations, images and short videos are travelling best); (2) language independence or low language dependence (easily translatable) or multilinguality; (3) ease of use, intuitiveness. Intellectual property rights (IPR) criterion should also be considered here [5].

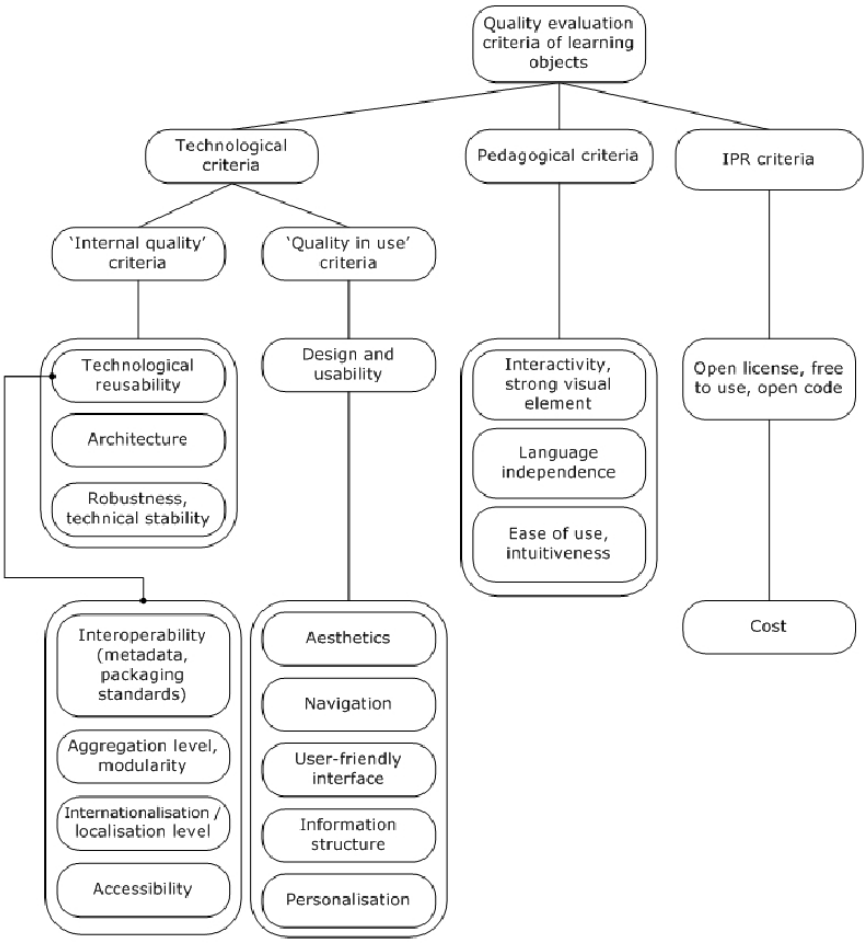

Fig. 1. LOs quality evaluation model (criteria tree)

Therefore, the authors propose to construct the LOs quality evaluation model (see Fig. 1) based on the literature analysis, MCDA principles of identification of quality evaluation criteria, and technological quality criteria classification principle.

3.2. Learning Objects Quality Evaluation Method

The widely used measurement criteria of the decision attributes' quality are mainly qualitative and subjective. Decisions in this context are often expressed in natural language, and evaluators are unable to assign exact numerical values to the different criteria. Assessment can be often performed by linguistic variables: 'bad', 'poor', 'fair', 'good' and 'excellent'. These values are imprecise and uncertain: they are commonly called 'fuzzy values'. Integrating these different judgments to obtain a final evaluation is not evident. Therefore, the authors have proposed to use fuzzy group decision making theory to obtain final assessment measures [11]. Linguistic variables conversion into non-fuzzy values of the evaluation criteria is as follows: 'excellent'=0.850; 'good'=0.675; 'fair'=0.500; 'poor'=0.325; 'bad'=0.150 [6].

The weight of the evaluation criterion reflects the experts' opinion on the criterion's importance level in comparison with the other criteria for the particular needs. For example, for the most simple (general) case, when all LOs evaluation criteria are of equal importance (i.e., we pay no especial attention to LOs reusability criteria), the experts could consider the equal weights ai = 0.125 according to the normalisation requirement (2). But if we pay especial attention to LOs reusability criteria, we can, e.g., consider the increased weights for the 1st and 6th LOs quality evaluation criteria (see Fig. 1 and Table 1), because these criteria deal with LOs reusability mostly. In this case these increased weights could be, e.g., twice higher in comparison with the other ones – 0.2, and all other criteria weights according to normalisation requirement (2) should be equal 0.1.

Lithuanian Mathematics expert teacher (the co-author of the paper) has applied the presented evaluation model and method in eQNet project (see Table 1). A number of probably qualitative reusable LOs have been identified in Lithuanian LOs repositories and evaluated against the aforementioned model and method (see formula (1). There are three examples of these LOs presented in Table 1:

LO1: "Coordinate Method" (available online at <http://mkp.emokykla.lt/imo/lt/mo/250/>);
LO2: "Polygon area" (available online at <http://mkp.emokykla.lt/imo/lt/mo/431/>);
LO3: "Interval Method" (available online at <http://mkp.emokykla.lt/imo/lt/mo/316/>).

Table 1

Results of experimental evaluation of LOs general quality (q) and "travel well" quality (twq)

LOs evaluation criteria	MO_1q	MO_2q	MO_3q	MO_1twq	MO_2twq	MO_3twq
Technological criteria:						
1. Technological reusability	0.675	0.850	0.675	0.1350	0.1700	0.1350
2. Design and usability	0.675	0.850	0.850	0.0675	0.0850	0.0850
3. Working stability	0.675	0.500	0.675	0.0675	0.0500	0.0675
4. Architecture	0.675	0.500	0.500	0.0675	0.0500	0.0500
Pedagogical criteria:						
5. Interactivity level	0.850	0.500	0.325	0.0850	0.0500	0.0325
6. Language independence	0.675	0.850	0.325	0.1350	0.1700	0.0650
7. Ease of use, intuitiveness	0.850	0.850	0.500	0.0850	0.0850	0.0500
IPR criteria:						
8. Open licence, cost	0.850	0.850	0.850	0.0850	0.0850	0.0850
Evaluation results:	0.7406	0.7188	0.5875	0.7275	0.7450	0.5700

These results mean that LO1 meets 74.06% general quality (q) in comparison with the ideal, LO2 – 71.88%, and LO3 – 58.75%. They also mean that LO1 meets 72.75% "travel well" quality (twq) in comparison with the ideal, LO2 – 74.50%, and LO3 – 57.00%. Therefore, LO1 is the best alternative (among the evaluated) from general quality point of view, but LO2 is the best from "travel well" quality point of view.

4. Conclusion and Recommendations

The presented research results show that MCDA approach-based LOs evaluation model presented in Fig. 1 and method represented by formula (1) are applicable in real life situations when education institutions have to decide on purchase of LOs for their education needs in the market. The proposed approaches are quite objective, exact and simply to use for choosing the qualitative LOs alternatives.

On the other hand, the proposed LOs "travel well" quality evaluation approach is applicable for the aims of eQNet project in order to select "travel well" LOs from LRE or elsewhere to use them in the other education contexts and countries.

References

1. Becta: Quality principles for digital learning resources (2007).
2. **Belton V., Stewart T.J.** Multiple criteria decision analysis: an integrated approach. Kluwer Academic Publishers (2002).
3. eQNet: Quality Network for a European Learning Resource Exchange project website, http://eqnet.eun.org (2010).
4. **Kurilovas E.** Interoperability, Standards and Metadata for e-Learning. In: G.A. Papadopoulos and C. Badica (Eds.): Intelligent Distributed Computing III, Studies in Computational Intelligence 237, pp. 121--130. Springer-Verlag Berlin Heidelberg (2009).
5. **Kurilovas E., Dagiene V.** Learning Objects and Virtual Learning Environments Technical Evaluation Criteria. Electronic Journal of e-Learning, Vol. 7, Issue 2, pp. 127–136 (2009).
6. **Kurilovas E., Serikoviene S.** Learning Content and Software Evaluation and Personalisation Problems. Informatics in Education, Vol. 9 (1), pp. 91–114 (2010).
7. **Leacock T. L., Nesbit J. C.** A Framework for Evaluating the Quality of Multimedia Learning Resources. Educational Technology & Society, 10 (2), pp. 44–59 (2007).
8. LRE: European Learning Resource Exchange service for schools web site, http://lreforschools.eun.org/LRE-Portal/Index.iface (2010).
9. MELT: EU eContentplus programme's Metadata Ecology for Learning and Teaching project web site, http://melt-project.eun.org (2008).
10. **Paulsson F., Naeve A.** Establishing technical quality criteria for Learning Objects, http://www.frepa.org/wp/wp-content/files/Paulsson-Establ-Tech-Qual_finalv1.pdf (2006).
11. **Ounaies H. Z., Jamoussi Y., Ben Ghezala H. H.** Evaluation framework based on fuzzy measured method in adaptive learning system. Themes in Science and Technology Education, Vol. 1, Nr. 1, pp. 49–58 (2009).
12. **Vargo J., Nesbit J. C., Belfer K., Archambault A.** Learning object evaluation: Computer mediated collaboration and inter–rater reliability. International Journal of Computers and Applications, Vol. 25 (3), pp 198–205 (2003).

Proceedings of 5th International Workshop ITELMS'2010

Substantiation of Highway Infrastructure Development: Socio-Economic Point of View

Z. Bazaras, D. Micevičienė

Kaunas University of Technology Panevėžys Institute, Klaipėdos str. 3, 35209, Panevėžys, Lithuania, E-mail: Zilvinas.Bazaras@ktu.lt; Diana.Miceviciene@ktu.lt

Abstract

The paper generally raises the aspects of the validity of investment in highwayt infrastructure development in terms of socio- economic point of view. The pilot analysis based on modern assumptions as well as empirical data allowed to state that travel costs change as the initial generator of socio-economic effects in the result of highway infrastructure development might be questioned.
KEY WORDS: *highway, infrastructure, development, socio-economic, travel time, costs.*

1. Introduction

The linkage between transport and economy itself is a highly contentious issue which has generated considerable debate and an abundant in scientific literature. There is firmly-held belief among politicians that investment in transport infrastructure contributes to large economic effects, however this belief is not borne out by academic analysis which wood seem to indicate that the impact of this type of investment remains limited. The channels and mechanisms by which improvements in transport network generates economic effects is still a "black box" despite the fact that experts agree on the initial impulse of the impacts causing impulse – change in travel costs. To begin the analysis of public investments, infrastructure and socio-economic development is a literature survey that focuses on how public investments in water, sewer, highway or mass transportation lead to economic growth; which economic sectors rely on various infrastructure systems; and what other factors are needed to complement. However, practice show, that a single type of infrastructure is unlikely to induce widespread private investment without the others. The detailed literature review [1, 2, 3, 4] allows to state, that inadequate infrastructure can deter investments when public works suffer from deferred maintenance or are used significantly over capacity. Intensive state investment in large-scale objects must be well substantiated for public resources are limited. Thus, transparent decision-choice funding of projects or programs must be strictly prioritized seeking to allocate the resources optimally. State must intervene into the economy only in case when a market failure can not be removed by other, less competition distortive measures. Public support should be an appropriate policy tool to align the interests of many groups of interest. The prevalence of unsatisfactory public systems may contribute to disinvestment, discourage local expansions and lead to a general climate of economic decline. Ironically, a vibrant economy, as we have seen in this region over the past decade, places unexpected stress on infrastructure systems. If maintenance is deferred during "boom" years, costly investments to upgrade a deteriorating public capital plant may be required while the economy is stagnating in order to prevent a long term decline [1].

So the *objective* of the article is to overlook the main effects generated by highway networks and empirically test if the initial impuls generate the impact sprawl. The *theoretical arguments* linking transportation infrastructure and economic development possesses both logical and intuitive appeal *based on systematic comparative and logical analysis.*

2. Investigation of Interaction between Highway Infrastructure Development and Socio-Economic Effects: Literature Review

The beginnings of analysis into the impact of transport infrastructure on economic development are considered to be an academic discussion on the quantitative assessment of the impact initiated by USA scientists in 1950s. The pioneers in analyzing the impact of transport infrastructure on economic development and growth are A. Hirschman (1958) and H. Mohring (1961); individual aspects of the issue were also investigated by P.Rosenstein-Rodan (1961). Until the beginning of 1970s, rather little attention was paid to topic and it was researched under other economic and managerial issues narrowly and in a generalized way. The essential change in this attitude was scientific works published in 1980s, introducing methodological principles to assess the impact of transport infrastructure on economic development and regional regeneration. The works also emphasized the significance of roads or highways on economic now [3-12].

The topic of the significance of transport infrastructure as the whole in socio-economic environment was escalated in scientific literature when the European Union started to form the Trans-European Transport Network (TEN-Tr.). The development of the corridors was evaluated as one of the factors that guarantee competitiveness and economic advance of countries. The issues of variety and quality of services of transport infrastructure and purposeful state intervention spheres when choosing and adapting efficient models of infrastructure development were especially emphasized. However, exclusively the impact highway has not been virtually analyzed in scientific studies using the methods of cost-benefit analysis, modified production function approach and correlation-regression analysis was

assessed in general terms [6-20]. While the need to justify investments into transport infrastructure developed in Europe, Asia and Africa was increasing, scientific literature started to pay more attention to the impact of exploitable transport infrastructure on economic growth mechanism. The analysis of the phenomenon, however, is still narrow, fragmentary, focusing on the aims of specialized studies that the authors perform. The organization of studies suffers from the lack of more general criteria of the analyzed impact analysis and assessment. There is a need for a more methodologically grounded model that would integrate the complex analysis of the impact of road ors highways infrastructure that would enable to distinguish the study principles of the analyzed impact as established in terms of travel cost change. Present experience of experts is to be treated rudiment.

Many economists agree [2-15] that transport infrastructure generally generate large developmental payoffs throughout society. However, as the authors of the paper noticed, *how* those effects come about is not readily understood. Variables such as the state of the transportation network, the region's stage of economic development, the competitive structure of the region's markets, and technological and institutional changes in transportation, communication, and production systems all affect improvements and the changes they generate, as well as how the overall economy responds. As these contexts vary, so do underlying forces of change, and the consequent social and economic effects, as it was noticed. Taking into account that the criteria of possible classification of the effects in the academic press are still equivocal, that authors of the paper suggest to accept the following presented below.

Table 1

Effects Highway infrastructure development

Over time		
Short term ‘ ’	***Long Term*** ‘ ’	***Very long term***
Reduction of congestion Rise in demand and firm's output Logistical reorganization Consumer Surplus Gain in productivity Opening greater markets	Local and regional growth Export expansion Entry and exit of firms Regional/national integration Structural effects	Promotion of globalization processes Global distribution and production Global flows of goods, services, capital and knowledge
2. Geographic		
Local	***Regional***	***National/Supranational***
Growing specialization of firms Reducing the monopoly power Changes in prices of products and production factors	Expansion of markets Growing competitiveness Growing migration Formation of clusters Expansion of interregional relationship	Growing output Growing employment rates Expansion of import Social and economic cohesion
3. Benefit getters		
Infrastructure user	***Third party involved***	***General public***
Consumer surplus Greater accessibility Economies of scale Places of work Wide market with many niches Income(from fares, user remuneration)	Ground rent Lower priced consumer goods Greater supply of goods Stimulation of consumption	Network forming function Creation ties between regions Lower concentration in towns Raising the rate of innovation Fulfilling basic needs Growing economic welfare

Analyzing the academic literature, the authors of the paper may conclude, that efforts to establish the sequence and the causing relationship between the infrastructure and economic performance or social bust must be impelled. For the sake of empirical adequacy of modeling the mechanism enabling understand the impact of the developed highway infrastructure on socio-economic environment, authors present one more significant detail, often discussed in most of the studies examined. Seeking to determine the impact sprawl and present more defined manner, we do recommend separate the direct and indirect effects. As most of experts conclude, *direct network effects* (reduced travel times, improved capacity of network, improved connectivity, and increased activity of network users) relate to changes in demand over links and/or modes that arise on the network. *The indirect network effects* (sustainable transport, regional development) are connected to strategic policy objectives on regional development, land-use and sustainable transport are also referred to as spill over effects. The principal interaction between the two is presented in the Fig. 1, which is explained in detail in the next chapter of the paper.

3. The Mechanism of the Impact Sprawl

The fact that there is no compromise on the economic benefits arising from well developed transport networks, because of the practical difficulty made by transport-*using* firms can generate economy-wide adjustments and redistributions over the long run.

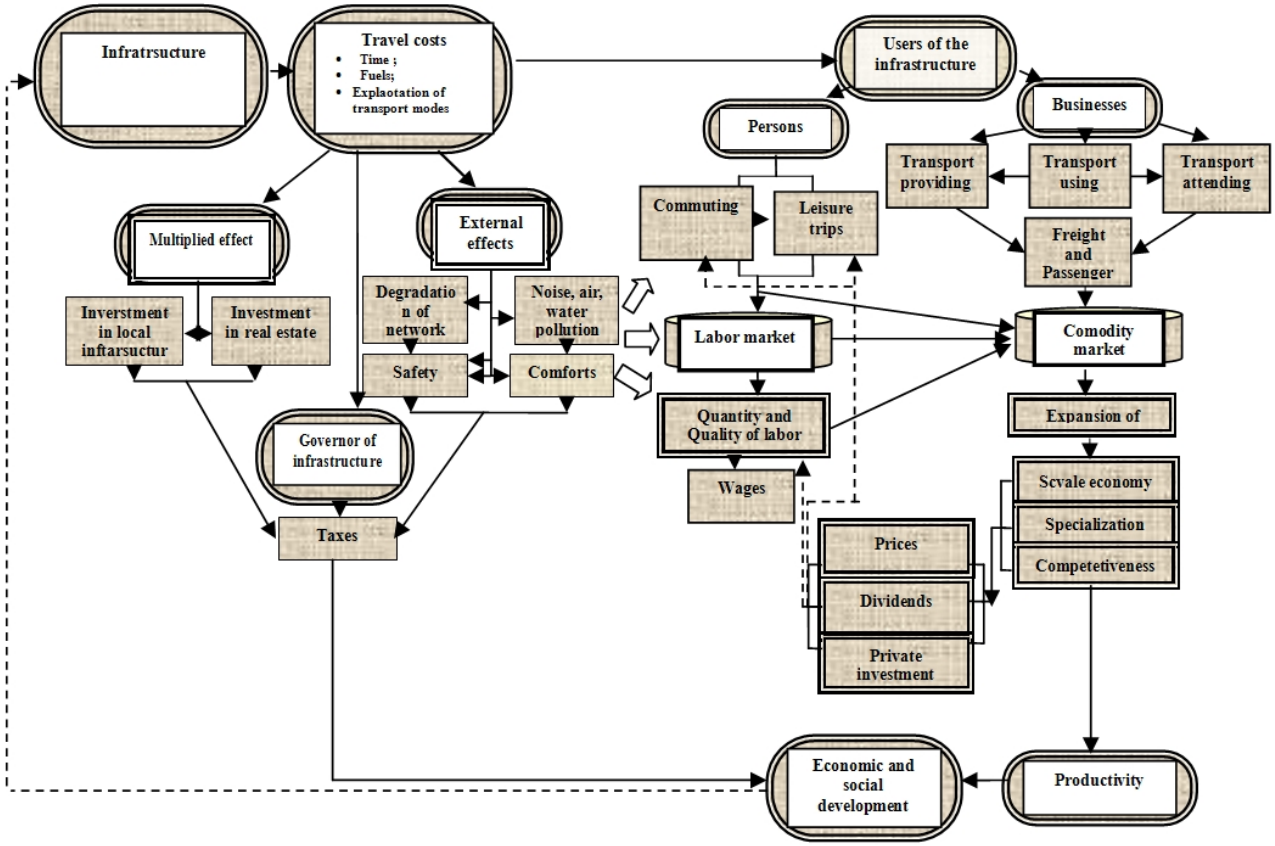

Fig. 1. Interrelationship between transport infrastructure development and socio-economic performance

Typical highway infrastructure improvements reduce effective distances between origins and destinations by reducing congestion, thereby lowering travel times. Travelers gain directly from travel time savings and lowered vehicle-operating costs. Companies enjoy direct efficiency gains from cheaper and more reliable freight services and reduced assembly and delivery costs. Cheaper and better transportation services provide incentives for firms to reorganize and reduce their inventories, sometimes to just-in-time levels. The advantages of scale economies occur as firms consolidate production and distribution sites and increase outputs. Assessments of short-term effects from improved transportation typically focus on benefits to and adjustments in transport-*providing* firms, but the changes made by transport-*using* firms can generate economy-wide adjustments and redistributions over the long run.

As the improvements lower costs and increase accessibility among various market actors (input suppliers, labor, and customers), market expansion and integration follow. The economy is constantly being restructured as firms enter and leave, making for leaner production processes, lower production costs, and higher productivity. Third, lowered transport costs and increased accessibility enlarge markets for labor and other inputs. Firms are able to draw labor from broader areas and with wider ranges of attributes, improving labor supply and lowering its costs. Similar effects occur when transport improvements open up new land for economic activities. Cumulating processes reinforce the clustering, and regional specialization develops.

Sustained transportation improvements can also lead to major shifts in technology, new production structures, a dual structural shift: a new social and technical environment or a new set of economic opportunities emerges, and the pattern of relationships between the environment and social actors changes. Improvements in transport technology and infrastructure have promoted major structural changes in national economies. They continue to facilitate globalization processes in contemporary times, much as they did in earlier eras, lead to major shifts in technology, new production structures, and a dual structural shift: a new social and technical environment or a new set of economic opportunities emerges, and the pattern of relationships between the environment and social actor's changes. Improvements in transport technology and infrastructure have promoted major structural changes in national economies and regional regeneration. *However, the question arises does this mechanism works in practice?* At present the transport economists in Denmark [21] work on the validation of the initial part of the model presented in Fig. 1. The investigation of so popular attitude among the politician concerning direct impact of the developed transport networks on one of the major elements of transport costs – travel time – still remains in controversy. *The problem of substantiation of federal investment* in highway infrastructure hoping reduce travel times and initiate the above analyzed processes arises as an open ground for the scientific discussion. Deeper economic analysis of the authors based on the transport corridor I, presented in the following chapter allows to state that cost-benefit analysis in not sufficient instrument for the effect evaluation.

4. Travel Time Changes in the Result of Highway Infrastructure Development: Empirical Evidence

Aiming to reveal whether the highways infrastructure improvement significantly affect travel time changes and generate the theoretical effects described in former chapters of the paper, the analysis of the changes of the development of the 1st European transport corridor *Via Baltica* was performed. The investigation was based on the data of Lithuanian Transport and Road Research Institute and Lithuanian Department of Statistics in the year 2004 – 2008. The results of the research are summarized in the Table 2.

Table 2

Travel time saving of private travelers

Variable	Value	Variable	Value	Variable	Value
1. Average number of cars		*2. Commuting*		*3. Travel time economy*	
1.1. Average number of transport means in the fleet, cars/day	10493	2.1. Commuting percent	59	3.1. Travel time economy, percent	4.5
1.2. Average number of cars in the fleet, percent	64	2.2. Average number of cars cars/day	6716	3.2. Average travel time economy hours/ day	66
1.3. Average number of cars means in the fleet, cars/day	6716	2.3. Commuting by cars	3962	3.3. Travel time economy of the commuting by cars, hours/days	38.9

To this end, basing on the analysis of traffic flow patterns in the corridor, it was found that average number of cars per single transport stream corridor (Table 2). It was found that in 2004 – 2008 corridor used by an average of 6 715 cars. Secondly it was determined the number of the commuting. Basing on the data presented by Lithuanian Department of Statistics to the Government of the Republic of Lithuania about the structure of local tourism it was carried out that 59 percent. Of the transport means are traveling on business purposes. It was found that development or reinforcement of the corridors infrastructure decreased the travel duration 4.5 percent (Table 2). Commuting time decreased 38.9 hours per day for all individual corridor users. While the daily time savings *per vehicle,* was not great.

The lack of data and limitations h of cost-benefit approach did not allowed determining the value of save travel time of the private corridor users in monetary terms. To achieve this required accurate data on traffic structure, the number of passenger car, destination, an average of different professions, peoples attitude or willingness to pay for better transport conditions as well as alternatives to use the saved time. The terms of observation, questioning techniques of the information received would provide a more complete, and in particular, received a minor indicator of travel time savings in economic terms. But the conclusion is clear – the impact was not significant.

Investigating corridor reconstruction on business travel costs, it was determined that in 2004-2008 *time savings* per day were also *very low* (Table 3).

Table 3

Travel time saving of business users

Variable	Value	Variable	Value
1. Average number of business vehicles		*2. Travel time economy*	
1.1. Average number of transport means, cars/day	10493	2.1. Travel time economy, percent	4.5
1.2. Average number of busses, trucks and minivans, percent	27	2.2. Average travel time economy, hours/ day	66
1.3. Average number of business cars in the fleed, cars/day	2833	2.3. Average travel time economy of business users, hours/ day	17.8

In the absence of better data, and the data presented in the Table 3 was under the assumption that business traffic represents only trucks, buses and minibuses. The international freight traffic in the corridor, according the Transport and Road Research Institutes data, in this period amounted to 26 percent.

The pilot investigation of the phenomenon demonstrated that in the period 2004-2008 Ist European transport corridor road reconstruction allowed to obtain the travel time economy but in was not significant as most authors declare. The investigation even of several fragments of so complex interaction between the highway infrastructure development and possible spread of its effects in the socio-economic environment allows to state that the phenomenon requires more in-depth, long-term and more specialized studies and allows to question the validity of huge investment amounts in the projects that are not well substantiated firstly socially and economically as sustainable development issues.

3. Conclusions

The research has shown that highway infrastructure as a research subject is not sufficiently investigated.

This article advances several essential ideas. First, the economic effects of the infrastructure improvements must be treated as significant benefits spreading in local, regional, national and supranational dimensions. Second, these economic outcomes vary according the state of the preexisting transport network, the state of economic and social

development and finally, competition in regions. This suggests that socio-economic assessments of highway infrastructure development must incorporate a broader range of interrelationships.

History teaches that sustained improvements in transportation, going hand in hand with parallel improvements in information and production technologies and institutional structures, cause structural and developmental transformations.

Determining the overall impact of infrastructure development in academic press remains fraught with uncertainty, so this paper has been focused on an analysis of some of the mechanism by which developed transport infrastructure we insisted, contribute as catalyst to economic performance. The mechanism relate to good market, the other – to labor market (the main "nodes" of impact analyzed are considered to be labor and commodity markets, the impact object – costs of the trip, the impact subjects – private persons and businesses).

Basing on the distinct principles of the cost-benefit analysis and using the data of Lithuanian Transport and Road Research Institute and Lithuanian Department of Statistics furthermore on restrictive assumptions, assessing the possible impact of the 1st European transport corridor (*Via Baltica*) on Lithuanian socio-economic environment in terms of travel cost change allowed to establish that in the period analyzed (2004-2008) improved quality of transport corridor road infrastructure allowed business users and individuals save travel time but the impact was not significant.

References

1. **Artis M., Nixson F.** (eds.) *The Economics of the European Union. Policy and Analysis* (4rd edition). Oxford: Oxford University Press, 2007. 436 p. ISBN 978-0-19-929896-9.
2. **Aschauer A.** Is infrastructure productive? *Journal of Monetary Economics*, March, 1989, vol. 23 (2), p.177-200.
3. **Baum H., Korte J.** Infuence of Economic Growth on Transport Infrastructure. *Transport and Economic Development.* Report of the hundred and ninth round table of transport economics. March 29-30, 2001, Paris, p. 5-50.
4. **Berechman J.** Transport, Investment and the Economic Development. Is There a Link? *Transport and economic development.* Report of the hundred and ninth round table of transport economics. March 29-30, 2001, Paris, p. 103-132.
5. **Blum I., Dudley L.** Transportation, Location and Growth. *Transport and Economic Development.* Report of the hundred and ninth round table of transport economics. March 29-30, 2001, Paris, p. 51-85.
6. **Boarnet M.G.** Infrastructure Services and the Productivity of Public capital: the Case of Streets and Highways. *National Tax Journal*, 1999, vol. 50, no 1, p. 39-57.
7. **Brathen S. Hervik A.** Strait Crossings and Economic Development. *Transport policy*, vol. 4(4), p. 193-200.
8. **Button K. J., Henser A. D.** Handbook of Transport Geography and Spatial Systems. Elsewier LTD, 2004, 672 p. ISBN 0-008-044108-4.
9. **Exel J.** et al. EU involvement in TEN development: Network Effects and European Value Added. *Transport policy*, October, 2002, vol. 9, no 4, p. 299-311.
10. **Forkenbrock D. J., Weisborg G. E.** Guidebook for Assessing the Social and Economic Effects of Transportation Projects. NCITRP report 456: National Academy Press, 2001. 141 p. ISBN 0-309-06703-0.
11. **Fourracre P., Turner J.** Women and Transport in Developing Countries. In *Transport Reviews,* 1995, vol. 15, no. 1, p. 77-96.
12. **Goddwin E.** Transport, Infrastructure and the Economy. European federation for transport and environment, *T&E*, 00/6, December 2000.
13. **Hook I.** Transport Sector Implications of Planned Accession by Central Europe into the European Union. A Report for German Marshall Fund from the Environmental Fellowship, May, 1996, 75 p.
14. **Laird J. J.** et al. Network Effects and Total Economic Impacts in Transport Appraisal. *Transport policy*, 2005, vol.12 (6), p. 537-544.
15. **Liou K.T.** Handbook of Economic development. Marcel Dekker, 1998. 604 p. ISBN 0- 82-47-0181-X.
16. **Mercenier J., Sruiivasan N.** Applied General Equilibrium and Economic Development. Michigan University Press, 2001. 360 p. ISBN 0-472-10382-2.
17. **Munnel A. H.** How does the transport infrastructure affect regional economic performance? New England Economic review (September/October), p.11-32.
18. **Prudhomme R.** Transport and the Economic Development. Report of the hundred and ninth round table of transport economics. March 29-30, 2001, Paris, p.81-102.
19. **Reynaud C.** The Concept of Corridors and Networks in Developing pan-European Infrastructure. *Transport infrastructure development for a wider Europe*, November 27-28, Paris, 2003, 32 p.
20. **Rodrigue P.** The Geography of Transport Systems. New York: Routledge, 2009. 352 p. ISBN 978-0-415-48324-7.
21. **Shade W.** et al. Analysis of the Contribution of Transport Policies to the Competitiveness of the EU Economy and Sicheldschmidt, H. The EU Programme Trans-European Networks – a Critical assessment. *Transport Policy,* July 1999, vol. 6, no 3, p. 169-181.
22. **Vickerman R. W.** The regional impacts of Trans-European networks. In *Regional science Springer,* 2001. p. 237-254.
23. **Wood D. F., Murphy P. R.** International Logistics. Second Editon. 2002. 527 p. ISBN 0-8144-0666-1.
24. **Fosgerau M.** et al. Travel time variability, definition and valuation. DTU Transport, 2008, p 82. ISBN 978-87-7327-174-2.

Proceedings of 5th International Conference ITELMS'2010

Investigation of Split-Platform Automated Storage/Retrieval System Performance

V.V. Janilionis, Z. Bazaras

Kaunas University of Technology, Donelaičio str. 73, 44029, Kaunas, Lithuania, E-mail: vytautas.janilionis@stud.ktu.lt; zilvinas.bazaras@ktu.lt

Abstract

The purpose of this reserach is to identify factors which have the most significant impact on the performance of the split-platform automated storage/retrieval system. The effect of dwell point, input/output point location, storage and retrieval policy, elevator control policy and rack type to performance measure - average total travel time of the storage and retrieval transactions were investigated. Simulation modeling techniques and multi-factor ANOVA were used in this research. The best factor combinations for performance measure were identified.
KEY WORDS: *split-platform automated storage/retrieval system, automatic warehouse, logistics, simulation, multi-factor ANVOA.*

1. Introduction

This paper analyses the split-platform automated storage and retrieval system (AS/RS), which is a relatively new system compared to standard AS/RS [1]. In split-platform AS/RS system the load handling process is split between vertically moving elevator and horizontally moving shuttle, which operate independently from each other, while in standard AS/RS, vertical and horizontal moves are performed by a single stacker crane. The standard AS/RS were analysed by many researches, but only a few papers can be found about analysis of split-platform systems [2].

Some previous researches considered split-platform systems only for containers and pallets [3, 4]. In this research the split-platform system handles smaller than the pallet loads and operates on perfect sequencing rules. The perfect sequencing performs partial or none sequencing on the arriving loads, and uses a strict sequencing rule on the leaving loads: the loads enter system in any order, but they leave the system in strict specified order. In practice perfect sequencing is widely used in robotic palletizing systems where robots have to pick loads in specific order which cannot be violated [5, 6]. The factor list which might affect the total travel time (TTT) of the load in the system was extended compared to the previous research [7] and includes dwell point, input/output point location, storage and retrieval policy, elevator control policy and rack type factors.

Analytical models for investigating AS/RS systems are only applicable to simple systems, which do not include the large combination of control policies [8, 9, 10]. For complex system model development and analysis, simulation techniques have to be used [11]. Simulation modeling techniques and multi-factor ANOVA [12] were used in this research to identify the best factor combination for the performance measure. Therefore, for the simulation model development and result analysis the Automod software [13] was integrated with the statistical analysis software SPSS [14].

2. System description

The purpose of the split-platform AS/RS is to link warehouse bulk storage with functions like picking, order assembly and sequencing. Fig.1 shows the investigated split-platform AS/RS.

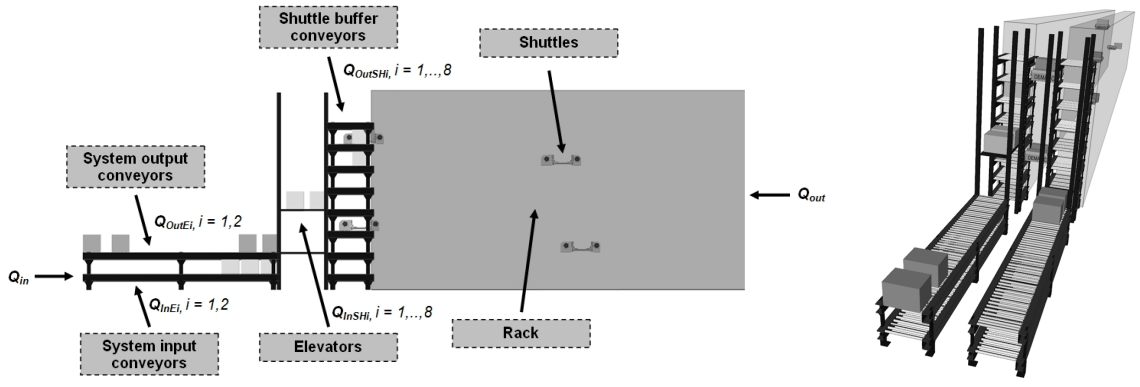

a b

Fig.1. Split-platform AS/RS: a – side view; b – perspective front view

The functionality of the system can be characterized by storage and retrieval operations. In this research, the split-platform AS/RS operates on perfect sequencing rules.

For the storage operation, loads arrive to the system in any order from the other system in the warehouse and are put to the input queue Q_{in} before entering system input conveyors. If the required system input conveyor queue Q_{InEi} has enough remaining capacity, the load is put on the conveyor and travels to elevator, otherwise it stays in queue Q_{in}. At the end of the system input conveyor load is assigned a destination level x_i using discrete uniform distribution. If required shuttle buffer conveyor queue Q_{InSHi} at the level x_i, i = 1, …, 8 has enough remaining capacity, the load claims elevator resource and waits for the pickup, otherwise, depending on the control logic, it either stays in queue Q_{InEi} or looks for another destination level which has capacity available. Elevator picks up a load and transports it to destination level x_i. Elevator handles storage requests using FIFO rule. The load is put to the shuttle buffer conveyor queue Q_{InSHi}, where it is assigned a destination rack location y_j on level x_i using discrete uniform distribution, and claims shuttle resource. Shuttle picks up the load and transports it to destination location y_j and completes the storage operation.

During retrieval operation, a load is generated in space and put to the invisible output queue Q_{out}, where it is assigned a rack level x_i depending on the control logic, and rack location y_j on level x_i using discrete uniform distribution. The load is also assigned a unique increasing number label l_k, which is used as a sequencing criterion. If the required shuttle buffer conveyor queue Q_{OutSHi} has enough remaining capacity, the load is put to the rack and claims the shuttle resource, otherwise it stays in queue Q_{out}. Shuttle picks up the loads using FIFO rule and transports to the shuttle buffer conveyor, where loads are put in queue Q_{OutSHi} and claim the elevator resource if system output conveyor queue Q_{OutEi} has enough remaining capacity. Elevator handles retrieval requests in perfect sequence order: loads are picked according to the their label l_k in increasing order l_1, l_2, …, l_k, l_{k+1}, …. Elevator picks up a load and transports it to the system output conveyor, where the loads are transported to the end of the conveyor and complete the retrieval operation.

3. Simulation model

The simulation model of the split-platform AS/RS considered in this research has the following structure: 1 aisle, 8 levels, 2 system input conveyors, 2 system output conveyors, 8 shuttle input buffer conveyors, 8 shuttle output buffer conveyors, 2 elevators, 8 shuttles (1 per level) and rack with 960 storage locations. A simulation model was used to estimate the total travel time (TTT) of the load in the system with different equipment parameters, control algorithms and loads input and output rates.

The simulation of the system was carried out using Automod simulation software. The Automod software allows constructing models of any size and complexity that can be used for planning and design, for day-to-day operations analysis, and for controls development and testing. The built models are highly accurate and use three dimensional true to scale virtual reality graphics.

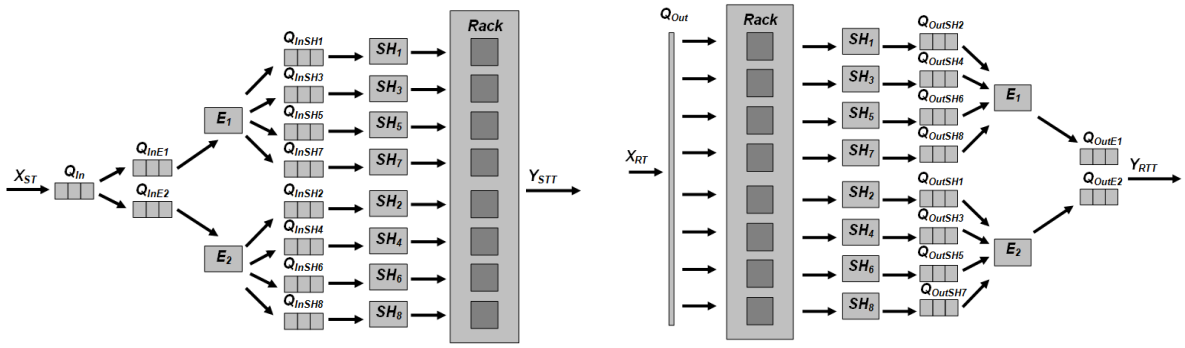

Fig. 2. Model flow diagram: a – storage operation; b – retrieval operation

Fig.2 shows a flow diagram of the split-platform AS/RS simulation model with the following parameters:

- X_{ST} and X_{RT} – average system input and output rates of loads (loads/h) - both interarrival times between loads have the uniform distribution;
- Y_{STT} – time of the storage operation, s – this is time interval from load entering queue Q_{in} to being put to the rack location (x_i, y_j);
- Y_{RTT} – time of the retrieval operation, s – this is time interval from creating a load retrieval request in the rack location (x_i, y_j) to leaving the system; $TTT = Y_{STT} + Y_{RTT}$;
- Q_{In} – input queue with infinity capacity, where the storage load enters system;
- Q_{Out} – output queue with infinity capacity, where the retrieval load enters system;
- Q_{InEi} – queues of size 10 before the elevator, where loads wait until being picked by the elevator, i = 1, 2;
- Q_{OutEi} – queues of size 10 after the elevator, where loads wait until they leave the system, i = 1, 2;

- E_i – elevator resource, which can achieve the maximum speed of 2 m/s and handles up to 2 storage or retrieval loads at a time;
- Q_{InSHi} – queues of size 2 before the shuttle, where loads wait until being picked by the shuttle, i = 1, …, 8;
- Q_{OutSHi} – queues of size 2 after the shuttle, where loads wait until they are picked by the elevator, i = 1, …, 8;
- SH_i – shuttle resource, which can achieve the maximum speed of 2 m/s and handles 1 storage or retrieval request at a time.

The accuracy of the simulation model developed in this research can be improved by adding more parameters to the model such as transport equipment acceleration and deceleration, physical load storage in the rack, etc. In this paper, only parameters which are significant to the total travel time of the load in the system are included.

The purpose of this research is to identify effect of five factors (X1_IO - I/O location, X2_DP - dwell point, X3_SR - storage and retrieval policy, X4_RT – rack type and X5_EC - elevator control policy) on the average total travel time (TTT) of the storage and retrieval transactions.

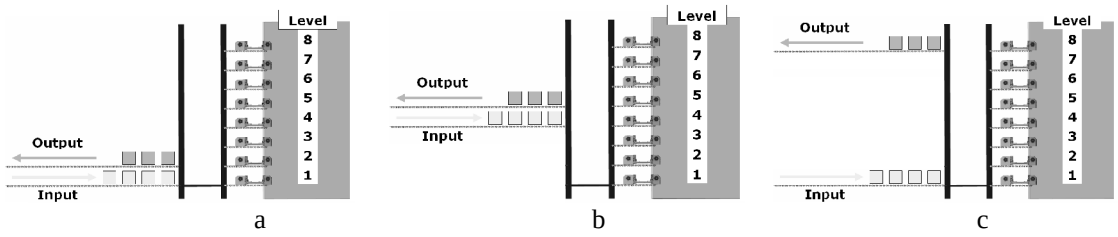

Fig. 3. I/O location factor levels

I/O location factor (X1_IO) defines the position of the system input and output conveyors and has the following levels: (1) bottom, co-located (Fig.3, a); (2) middle, co-located (Fig.3, b); (3) separated (Fig.3, c).

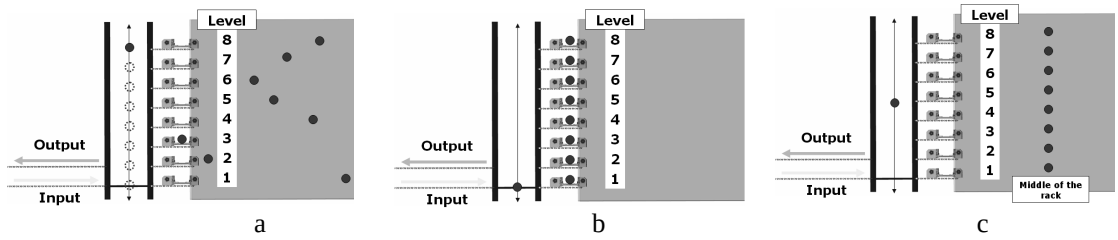

Fig. 4. Dwell point factor levels

Dwell point factor (X2_DP) defines the elevator and shuttle stopping positions when they become idle. The following factor levels are considered in this research: (1) stay dwell (Fig.4, a) – the elevator and the shuttle stay idle in the position of the last request completion until next request; (2) return to start (Fig.4, b) – the elevator returns to the system input conveyor level and the shuttle to the front of the rack and stay there until next request; (3) return to middle (Fig.4, c) – the elevator returns to the middle level and the shuttle to the middle of the rack and stay there until next request.

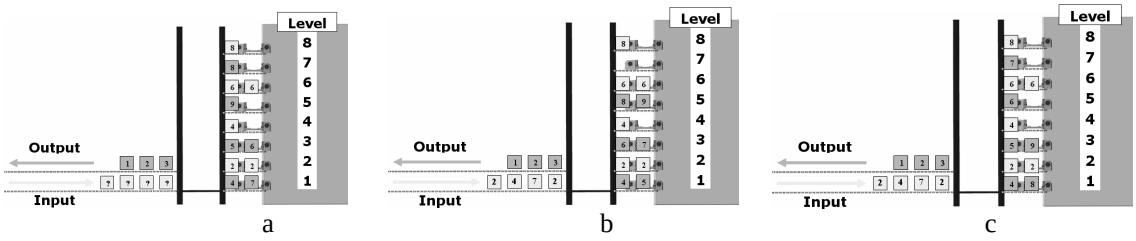

Fig. 5. Storage/Retrieval factor levels (Note: labels on input loads refer storage level, on output loads – perfect sequence label)

Storage/Retrieval factor (X3_SR) defines the storage and retrieval location selection strategies. The following factor levels are considered in this research: (1) random – arriving loads are stored in any level and retrieved in perfect sequence order from any random level (Fig.5, a); (2) paired round-robin – arriving loads are stored in a specific level and two adjacent loads in the perfect sequence are retrieved from the same level (Fig.5, b); (3) round-robin - arriving loads are stored in a specific level and two adjacent loads in the perfect sequence are retrieved from the adjacent levels (Fig.5, c).

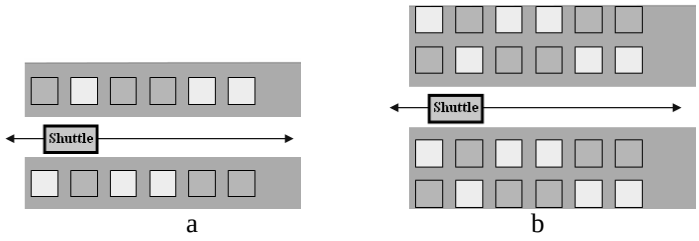

Fig. 6. Rack type factor levels

Rack type factor (X4_RT) defines the structure of the rack in the following levels: (1) single deep rack – each rack position can store only 1 load (Fig.6, a); (3) double deep rack – each rack position can store up to 2 loads (Fig.6, b); (3) 50% single deep and 50% double deep rack is a mixed type of rack. The double deep rack has the same amount of storage locations as the single deep but it is 2 times shorter. However, 50% of the time the required load will be stored in the second position and blocked by the load in front. In such case the reshuffling is needed: the shuttle picks the first blocking load and transports it to any empty rack location and then returns to pick up the required load.

Elevator control factor (X5_EC) defines the elevator requests selection priorities and has the following levels: (1) retrieval priority – elevator firstly looks for a retrieval request and secondly for the storage request; (2) storage priority – is the opposite of the retrieval priority; (3) random priority – elevator selects between retrieval and storage priorities randomly.

4. Experimental results

Results presented in this paper were generated by performing independent simulation runs with equal average system input X_{ST} and output X_{RT} rates, $X_{ST} = X_{RT} = l$, where $l \in \{400, 525, 550, \ldots, 575\}$ loads/h, interarrival times between loads have the uniform distribution, elevators run at speed $V_E = 2$ m/s, shuttles – $V_{SH} = 2$ m/s. The SPSS [14] software was used for analysis of simulation results and development of multi-factor ANOVA models.

The Fisher-test (F-test) was applied to evaluate the significance of main factors effects X1_IO, X2_DP, X3_SR, X4_RT, X5_EC and factors interactions effects. The all significant factors and their interactions ($p<0.05$) for input and output rates $l = 525$, loads/h are presented in Table 1. To be able to interpret ANOVA results, the model adequacy should be verified. Hypothesis about normality of residuals and homogeneity of variances were tested for all models. Test results indicated that for all models, residuals are normally distributed and conditional variance of the residuals is a constant (homoscedastic). The results for testing the normality of residuals for $l = 525$, loads/h are presented in Fig. 7 (Kolmogorov-Smirnov test, $p > 0.05$).

Table 1

ANOVA results for total travel time (TTT), $l = 525$, loads/h

Source	Type III Sum of Squares	Mean Square	F	P-value.
Corrected Model	312237.8	1939.366	99.6	.000
Intercept	23752063.1	23752063.1	1220932.4	.000
X1_IO	10651.207	5325.6	273.7	,000
X2_DP	6806.710	3403.3	174.9	.000
X3_SR	185955.837	185955.8	9558.7	.000
X4_RT	92866.503	46433.2	2386.8	.000
X5_EC	10116.619	5058.3	260.0	.000
X1_IO * X2_DP	509.898	127.4	6.5	.000
X1_IO * X4_RT	188.218	47.0	2.4	.048
X2_DP * X4_RT	446.846	111.7	5.7	.000
X3_SR * X4_RT	180.729	90.364	4.6	.010
X1_IO * X5_EC	809.833	202.458	10.4	.000
X2_DP * X5_EC	454.328	113.582	5.8	.000
X1_IO * X2_DP * X5_EC	387.477	48.435	2.4	.012
X4_RT * X5_EC	728.035	182.009	9.3	.000

Table 1 shows that $p < 0.05$ for all the main effects X1_IO, X2_DP, X3_SR, X4_RT and X5_EC. It should be noted that all main factors are significant, but the most significant factors that affects mean of response TTT are X3_SR

and X4_RT, because they have the largest F-value. Similar results were obtained for the other input and output rates considered in this research.

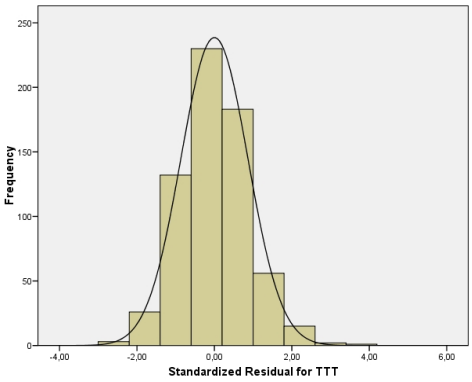

One-Sample Kolmogorov-Smirnov Test

		ZRE_1
N		648
Normal Parameters [a,b]	Mean	,0000
	Std. Deviation	,86669
Most Extreme Differences	Absolute	,033
	Positive	,033
	Negative	-,022
Kolmogorov-Smirnov Z		,834
Asymp. Sig. (2-tailed)		,490

a. Test distribution is Normal.

b. Calculated from data.

Fig. 7. Results of testing normality of residuals l = 525, loads/h

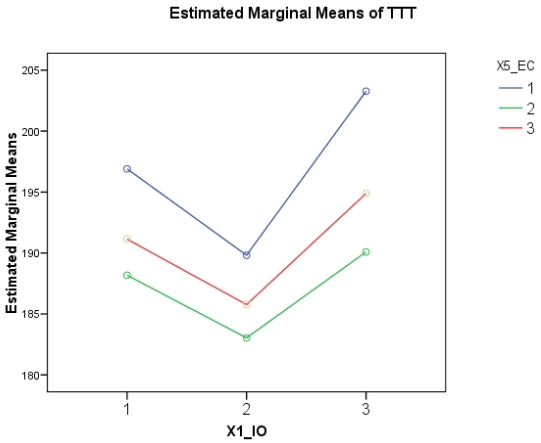

Fig. 8. X1_IO and X5_EC interaction effects

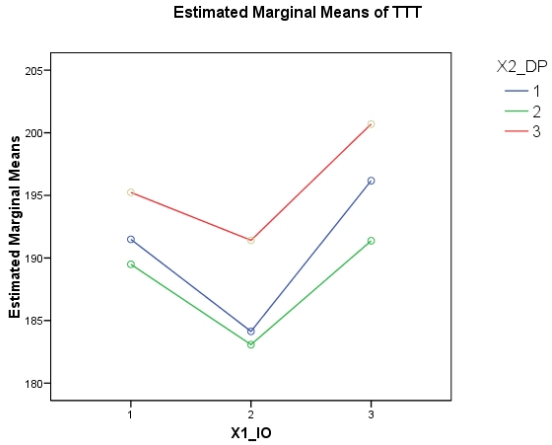

Fig. 9. X1_IO and X2_DP interaction effects

Interaction occurs when effects of one factor vary according to levels of the other factor. Fig.8-9 show X1_IO*X5_EC and X1_IO*X2_DP interactions effects. According to the results in Table 1, seven two-way interactions X1_IO*X2_DP, X1_IO*X4_RT, X2_DP*X4_RT, X3_SR*X4_RT, X1_IO*X5_EC, X2_DP*X5_EC, X4_RT*X5_EC are significant ($p<0.05$) and only one three-way interaction X1_IO * X2_DP * X5_EC are significant for the TTT. The four-way and five-way interactions are not significant.

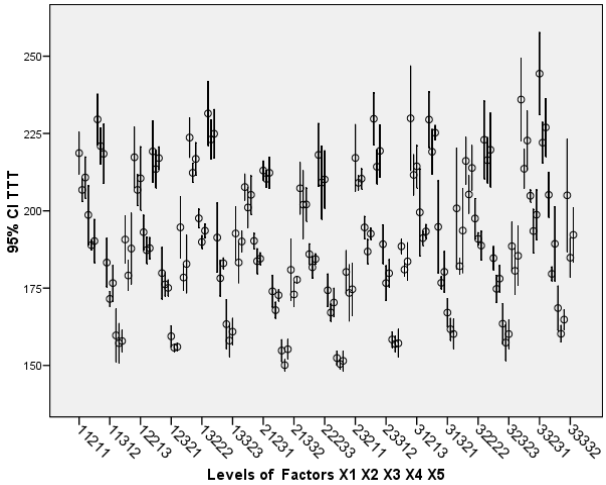

Fig. 10. 95 % confidence interval of total transfer time mean for different factors levels combinations l = 525, loads/h

Tukey's test was applied to find out the homogeneous groups of factor levels for different load input/output rates. It is an all pair-wise comparison test which compares the mean of each treatment to every other treatment, and

identifies where the difference between two means is significant. We performed a Tukey's test for each combination of five factors when input/output rates were from 400 to 575 (loads/h). Assumptions of Tukey's test (the observations are independent, the means are from normally distributed populations, equal variation across observations (homoscedasticity)) were satisfied.

Fig. 10 presents the 95% confidence interval for the mean of total travel time (TTT) for different combinations of factors' levels. Table 2 shows a sorted list of combinations in decreasing order in terms of TTT. In each homogenous group of factors' levels, the value of average TTT does not differ statistically significant. As a result from the best group, we conclude that the best response (minimum TTT) is obtained when factors' levels are X3_SR=3 and X4_RT=2 and worst (maximum TTT) when X3_SR=2 and X4_RT=3. Results also showed that for load input/output rates from 400 to 575, loads/h, optimal combinations of factors' levels reduce the average TTT 1.3-7 times.

Table 2

Homogeneous subsets of factors levels combinations, Tukey HSD

	l = 400		l = 525		l = 550		l = 575	
	Levels of factors $X_1 X_2 X_3 X_4 X_5$	**Mean TTT**	**Levels of factors** $X_1 X_2 X_3 X_4 X_5$	**Mean TTT**	**Levels of factors** $X_1 X_2 X_3 X_4 X_5$	**Mean TTT**	**Levels of factors** $X_1 X_2 X_3 X_4 X_5$	**Mean TTT**
Best group	22323	115.35	21322	150.10	22322	166.30	22322	194.72
	22322	115.56	22322	150.47	21322	167.35	21322	209.09
	22321	115.88	22323	151.49	21323	168.82	23322	209.43
	21322	116.22	22321	152.41	22323	169.17	22323	211.93
	21323	116.52	21321	154.82	23322	171.23	22312	224.69
	21321	116.55	21323	155.25	22321	172.01	21323	225.16
	12321	117.24	12322	155.72	21321	173.75	21312	230.57
	32323	117.32	12323	156.02	23323	174.52	23323	233.53
	12323	117.36	23322	156.96	11322	176.11	21321	234.29
	12322	117.37	23323	157.18	32322	177.91	22223	248.63
	32322	117.58	11322	157.21	12323	180.07	22321	249.81
	11323	117.66	32322	157.38	13322	181.50	13322	252.88
	…	…	…	…	…	…	…	…
	…	…	…	…	…	…	…	…
Worst group	…	…	…	…	…	…	…	…
	33232	161.88	11231	229.56	31231	397.32	32232	1560.97
	13211	161.98	23231	229.74	12232	400.74	13232	1589.26
	33212	162.01	31211	229.92	11232	397.32	11232	1605.88
	33233	162.12	13231	231.48	33231	441.61	33231	1724.82
	33213	162.50	33211	235.97	31232	488.49	31232	1725.28
	33231	162.57	33231	244.35	33232	496.40	33232	1835.07

5. Conclusions

By using Automod software, the simulation model of split-platform AS/RS system was developed, which allowed testing the effects on the system's performance for different load input/output rates, equipment parameters and control strategies.

Multi-factor ANOVA results showed that the all main factors I/O location, Dwell point, Storage/Retrieval, Rack type, Elevator control had a significant effect on the total travel time. Factors Storage/Retrieval and Rack type had the strongest effect on the average total travel time. Some factors interactions e.g. (I/O location)*(Elevator control) also showed a significant effect on the average total travel time.

Tukey's test was employed to find out the homogeneous groups of factors' levels for different load input/output rates. The optimal combinations of factors' levels for the performance measure were identified. Analysis results also showed that for load input/output rates from 400 to 575 (loads/h), optimal combinations of factors' levels reduce the average total travel time significantly (1.3-7 times).

References

1. **Hu Y. H., Shell Huang S. Y., Chen C., Hsu W. J., Toh A. C., Loh C. K., Song T.** Travel time analysis of a new automated storage and retrieval system. Computers & Operations Research, 32 (2005), pp. 1515–1544.
2. **Roodbergen K. J., Vis I. F. A.** A survey of literature on automated storage and retrieval systems. European Journal of Operational Research, 194 (2009), pp. 343 – 362.
3. **Vasili M., Hong T.S., Homayouni S. M., Ismail N.** A Statistical model for expected cycle time of SP-AS/RS: An application of Monte-Carlo simulation. Applied Artificial Intelligence, 22 (2008), pp. 824-840.

4. **Kuo P. H., Krishnamurthy A., Malmborg C. J.** Design models for unit load storage and retrieval systems using autonomous vehicle technology and resource conserving storage and dwell point policies. Applied Mathematical Modelling, 31(10), 2007, pp. 2332–2346.
5. **Janilionis V. V., Janilionis V.** Regression models for predicting loads transfer time in automatic warehouse palletizing system. – Proceedings of 4th International Conference Intelligent Technologies in Logistics and Mechatronics Systems. 2009, pp. 108-113.
6. **Dallari F., Marchet G., Melacini M.** Design of order picking system, The International Journal of Advanced Manufacturing Technology, 2009, 42(1-2) , pp. 1-12.
7. **Ekren B. Y., Heragu S. S., Krishnamurthy A, Malmborg C. J.** Simulation based experimental design to identify factors affecting performance of AVS/RS. Computers & Industrial Engineering, 58 (2010), pp. 175–185.
8. **Lerher T., Sraml M., Kramberger J., Potrc I., Borovinsek M., Zmazek B.** Analytical travel time models for multi aisle automated storage and retrieval systems. The International Journal of Advanced Manufacturing Technology, 2006, 30 (3-4), pp. 340-356.
9. **Vasili M. R., Tang S. H., Homayouni S. M., Ismail N.** Comparison of different dwell point policies for split-platform automated storage and retrieval system. International Journal of Engineering and Technology, Vol. 3, No. 1, 2006, pp. 91-106.
10. **Fukunari M., Malmborg C. J.** An efficient cycle time model for autonomous vehicle storage and retrieval systems. International Journal of Production Research, Vol. 46, No. 12, 2008, pp. 3167–3184.
11. **Rohrer M. W.** Maximizing simulation ROI with Automod. - Proceedings of the 2003 Winter Simulation conference. 2003, vol. 1, pp. 201 – 209.
12. **Johnson R. J., Wichern D. W.** Applied Multivariate statistical analysis.- Prentice Hall, 1992.-642pp.
13. Applied AutoMod 12.2.1.-Santa Clara:-Applied Materials Inc., 2008, 1076 p.
14. **Norušis M. J.** SPSS 15.0 Advanced Statistical Procedures Companion.- Prentice Hall, 2007, 432 p.

Authors Index

INTELLIGENT TECHNOLOGIES IN LOGISTICS AND MECHATRONICS SYSTEMS (ITELMS'10). Proceedings of the 5th International Conference. Held on June 4-5, 2010, Panevezys, Lithuania.

INTELEKTUALIOS TECHNOLOGIJOS LOGISTIKOJE IR MECHATRONINĖSE SISTEMOSE (ITELMS'10). 5-os tarptautinės konferencijos, įvykusios Panevėžyje 2010 m. birželio 4-5 d., pranešimų medžiaga (anglų kalba).

Maketavo D. Vaičiulis